Diversity dynamics and ecology of small mammals in relation to the Neogene tectonic and climate history of western North America

by

Tara Magnolia Smiley

A dissertation submitted in partial fulfillment
of the requirements for the degree of
Doctor of Philosophy
(Geology)
in the University of Michigan
2016

Doctoral Committee:

Associate Professor Catherine Badgley, Chair
Professor Daniel C. Fisher
Associate Professor Nathan A. Niemi
Assistant Professor Daniel L. Rabosky
Associate Professor Nathan D. Sheldon

DEDICATION

To Tom Kunas
for leading me to my first fossil &
revealing the beauty in science

ACKNOWLEDGMENTS

The National Science Foundation Graduate Research Fellowship Program, the University of Michigan Rackham Predoctoral Fellowship and the Earth and Environmental Sciences Department supported this research. Funding from the Society of Vertebrate Paleontology Patterson Award, the Earth and Environmental Sciences Turner Award, the Inter-university Training for Continental-scale Ecology Research-in-Residence Award, and the Rackham Graduate School made fieldwork and laboratory analyses possible.

I would like to acknowledge my collaborators and co-authors, without whom this research would not have been possible. I thank Jennifer Cotton and Ethan Hyland for assistance in the field, during sample analysis, and in manuscript preparation. Great appreciation goes to Bob Reynolds for introducing me to my field area and providing boundless enthusiasm and guidance in all things Mojave related. Thank you to Thure Cerling for teaching me so much about stable isotopes and supporting my research at the University of Utah. Several undergraduate students have helped with this research; in particular, Molly Moroz and Laura McQuarter have contributed greatly to data collection of modern and fossil heteromyids.

I would also like to thank my dissertation committee members: Dan Fisher, Nathan Niemi, Dan Rabosky, and Nathan Sheldon. Their input throughout my graduate studies improved the research presented in this dissertation, pushed me to explore new and challenging concepts, and expanded my scientific scope. I would especially like to thank my advisor and chair, Catherine Badgley. Catherine's wealth of knowledge, intellectual curiousity, devotion to thoughtful and well-constructed science, and passion for teaching, outreach, and conservation

has inspired me from day one and will continue to influence me positively for the rest of my career. She has always been available to guide and support me through any task, and has done so with much warmth, encouragement, and a strong push when needed. Thank you, Catherine, for helping me to develop into the scientist I am today.

Thank you to my fellow graduate students and the folks at the Museum of Paleontology, in particular Miriam Zelditch. I would especially like to thank the members of the Badgley Lab over the years, Rachel Cable, Mairin Balisi, Soledad Domingo, Katharine Loughney, and Jeff Shi for their company, assistant, and support from the office to the field. I would also like to thank my writing group, Susan Cheng, Lauren Cline, and Alison Gould for endless encouragement. Thank you to my friends in the Geology Department, especially Carli Arendt, Clay Tabor, Petr Yakovlev, Meghan Taylor, and Rich Fiorella for making my time here so enjoyable. A warm thanks goes to my friends outside of Michigan, Tiffany Blair, Amy Groesbeck, Lindsay Wahlborg, Manuela Molzan, and in particular Mama Hawa, Hawa, and Muku for helping me maintain an important sense of perspective throughout this journey.

I would also like to express my graditude to my family. Thank you to my Mom for inspiring me to be adventurous and always optimistic. Thank you to my Dad for fueling my curiosity from a young age and challenging me to always ask more questions. I thank both of my parents for instilling in me a deep love of the natural world and my brother, Sam, for making grand outdoor adventures happen today. Thank you to my Grandma Judy for being my support here in Michigan. I am also appreciative of the love and encouragement I have received from Maria, Greg, Kurt, and Gretchen throughout my education. Finally, I am extraordinarily grateful to Pascal Title. Merci beaucoup for your constant love, support, patience, and encouragement – you have enriched my life in countless ways.

TABLE OF CONTENTS

LIST OF FIGURES

LIST OF TABLES

ABSTRACT

The middle Miocene from 17 to 14 Ma was a time of elevated mammalian diversity in western North America that coincided with regional tectonic extension, the development of topographic complexity, and the last major warming interval of the Neogene, the Miocene Climatic Optimum (MCO). Multiple processes govern species richness from local to regional scales, including community assembly, speciation, extinction, and immigration. This research centers on understanding these processes in relation to landscape and climate change and characterizing the properties of the middle Miocene diversity peak across spatial scales. I focus on rodents, which represent much of the extant and Neogene diversity in western North America.

Chapter 1 presents the conceptual framework and major questions of this dissertation. In Chapter 2, I used stable isotopes in two modern heteromyid species to develop diet-isotope models across environmental and climate gradients in western North America. Rodent isotopes reliably track vegetation and climate variation and can be used for paleoecological inference. In Chapter 3, I generated a multi-proxy record from the Crowder and Cajon Valley formations in the Mojave to compare local paleoenvironmental change with faunal diversity during the MCO. These formations document the earliest evidence of C_4 grass in the region, increased aridity during the MCO, and heterogeneous vegetation and moisture conditions. High species diversity within each basin and low faunal similarity across basins indicate that peak mammal diversity during the middle Miocene involved high local diversity and spatial turnover. In Chapter 4, using dental metrics and isotopic composition of fossil-rodent teeth, I evaluated corresponding changes

in species dietary ecology. Within each basin, rodent dietary ecology was remarkably stable; however, over longer timescales, rodents consumed more C_4-grass resources, implying a shift in their diets during the MCO. Rodents recorded finer-scale spatial and temporal variation in vegetation than did other proxies, thus providing unique paleoenvironmental information. In Chapter 5, I assessed the influence of variable preservation history through the Neogene on estimates of diversification rates in relation to tectonic activity. Simulating fossil records under several preservation scenarios, I determined that preservation alone is unlikely to produce the middle Miocene peak in mammalian diversity.

CHAPTER 1

Introduction

One of the primary goals in paleobiology is to explain the origin and maintenance of species diversity across space and through geologic time. Biodiversity patterns and the processes that generate them have been a longstanding topic of fascination and scientific debate that relies on the synthesis of ideas and data across biological and geological sciences (e.g., Fritz et al. 2013). For example, a striking gradient in species diversity in relation to areas of high elevation and topographic complexity has been demonstrated for birds, mammals, and vascular plants, with mountains emerging as global biodiversity hotspots today (Myers et al. 2000, Barthlott et al. 2005, Ruggiero and Hawkins 2008, Badgley 2010). In North America, mammal species richness per unit area rises steeply from the low-relief Great Plains to the topographically complex intermontane west (Fig. 1.1; Simpson 1964, Badgley and Fox 2000). Although clear patterns have emerged, various hypotheses to explain the underlying mechanisms for increased diversity in montane regions remain unresolved.

The fundamental processes that govern species diversity are both ecological and evolutionary in nature. Topographically and environmentally complex regions promote high faunal turnover across diverse habitats and steep altitudinal bioclimatic zones, thereby supporting elevated regional species richness (Kerr and Packer 1997, Coblentz and Riitters 2004). Tectonic and climate histories stimulate or dampen diversification processes and geographic-range shifts, contributing to broad-scale patterns in the distribution of species over deep time (Cracraft 1985,

Vrba 1992, Badgley 2010). The Cenozoic fossil record of mammals in North America reveals a dynamic and intermittent topographic diversity gradient, suggesting that changes in species diversity reflect complex connections among abiotic factors, biogeographic processes, and species ecology and evolution (Barnosky and Carrasco 2002, Finarelli and Badgley 2010).

The central goal of my research is to link regional-scale biogeographic processes with local-scale ecological dynamics in small-mammal faunas over the Neogene, and specifically during the middle Miocene interval of high diversity in western North America. The strong topographic diversity gradient during this time coincided with a global warming period known as the Miocene Climatic Optimum (MCO) and an interval of intense tectonic extension that generated the complex topography found in the Basin and Range Province today. My primary research questions are as follows: (1) Does species ecology vary predictably in relation to climate and vegetation changes across space and through time? (2) How did local ecosystems change through the MCO warming? (3) Did species richness, composition, and ecology respond to changes in local environments during this time? (4) Is high species richness during the middle Miocene facilitated by increases in local species diversity or high species turnover across space? (5) How do changes in fossil preservation impact our ability to reliably infer diversification dynamics for the fossil record? By focusing on evolutionary and ecological processes operating across spatial scales in the past, this research contributes to our understanding of the relative roles of these processes shaping diversity patterns over deep time.

To address these questions, I couple studies of the fossil record with modern ecology and biogeography over broad temporal and spatial scales and integrate methods spanning stable-isotope ecology, tooth-shape analysis, and diversification simulations. I focus on the taxonomically and ecologically diverse heteromyid rodents (kangaroo rats and pocket mice) and

on ecosystems in the intermontane west, specifically within the Mojave Desert region of southern California. In this chapter, I describe the conceptual framework for my research, introduce the geologic context and my primary study group, and present a preview of the upcoming chapters in this dissertation.

Conceptual framework

The topographic diversity gradient (TDG) for mammals is a prominent feature across all major continents today. In North America, species boundaries align strongly with topographic barriers in the intermontane west compared to the low-relief Great Plains (Fig. 1.1). Ecological explanations for diversity gradients across the modern landscape point to compelling correlations between species richness and climate and physical factors, such as topographic roughness, habitat heterogeneity, and specific climate variables (Kerr and Packer 1997, Badgley and Fox 2000, Coblentz and Riitters 2004). However, these correlations do not provide direct evidence of the underlying evolutionary dynamics that generate and maintain the TDG, nor do they incorporate the influence of tectonic and climate history over deep time (e.g., Jablonski et al. 2006). Paleontological perspectives on mammalian diversification in North America demonstrate that diversity and diversification rates vary over space and through time, with diversification pulses corresponding to the development of topographic complexity and climate warming in the middle Miocene from ~17 to 14 Ma (Barnosky and Carrasco 2002, Davis 2005, Finarelli and Badgley 2010). Phylogenetic and phylogeographic approaches using extant taxa additionally reveal that clade history, including the timing and rates of diversification and the genetic structure of populations, is related to the presence and formation of geographic barriers (e.g.,

Riddle and Hafner 2006, Hoorn et al. 2010). These correlations motivate further research into the evolutionary, ecological, and geological underpinnings of the TDG across spatial scales.

Large-scale patterns of biodiversity are driven by three processes over geologic time: origination, extinction, and changes in geographic distribution (often referred to as immigration). All three processes vary over time and space, leading to significant net changes in diversity (Jablonski et al. 2006, Lomolino et al. 2010). Tectonic activity, volcanism, and erosion drive changes in topographic complexity, creating elevational gradients and habitat heterogeneity, and thereby decrease the continuity of bioclimatic zones, impose barriers to dispersal, and fragment species geographic ranges (Kerr and Packer 1997, Coblentz and Riitters 2004). Isolation of populations, in combination with processes such as genetic drift and ecological adaptation to local environmental conditions, can promote allopatric speciation (Coyne and Orr 2004, Badgley 2010). Additionally, in the case of extensional tectonic regions like the Basin and Range Province, area gain from landscape broadening and increasing elevational gradients can increase speciation due to expanding biome area and increased likelihood of barrier formation (Rosenzweig 1995, Atwater and Stock 1998, McQuarrie and Wernicke 2005).

Changes in global and regional climate introduce novel environmental conditions, steepen or reduce elevational gradients, and influence the distribution of resources across the landscape, impacting the overall suitability, extent, and connectivity of mammalian habitats (Badgley 2010). Climate change can promote diversification by fragmenting and isolating populations and shifting species geographic ranges as they track their preferred habitats (Vrba 1992, Barnosky 2001). Warming also dampens the magnitude of the thermal lapse rate along both latitudinal and elevational gradients (Poulsen and Jeffery 2011, Pound et al. 2012), broadening elevation zones, and reducing habitat area and continuity at high latitudes and elevations. Figure 1.2 illustrates

how these factors interact over geologic time to influence mammal diversity in intermontane, or topographically complex, regions. The dynamic nature of regional species diversity has important implications for the processes governing community assembly in relation to species-environment and ecological interactions (Ricklefs 1987, Mittelbach and Schemske 2015). The TDG today and in the past reflects the combined outcome of these processes operating over local to regional scales.

Geologic context

North America's geophysical template is the ideal testing ground for evaluating the roles of interacting tectonic and climate drivers on species diversification: the tectonically active and topographically complex western region lies adjacent to the tectonically quiescent and low-relief Great Plains region (Fig. 1.3). From the Oligocene (since ~30 Ma) to the present, tectonic extension west of the Rocky Mountains increased overall habitat area by ~400,000 km^2 and generated a topographic fabric of alternating isolated mountain ranges and basins (Atwater and Stock 1998, Dickinson 2013). Kinematic models have generated details of the timing and physical extent of major topographic change in the Basin and Range Province (McQuarrie and Wernicke 2005). Paleotopography and relief have also been constrained by paleoaltimetry isotopic signatures and physical models (Horton and Chamberlain 2006, Herold et al. 2008, 2011, Mix et al. 2011). Features of global climate history are known from deep-sea isotopic records (Zachos et al. 2008, Tipple et al. 2010), while paleoclimate models and proxy data have produced Neogene environmental data layers that elucidate variation in temperature, precipitation, and seasonal variables across different regions of North America (Herold et al. 2009, Feng et al. 2013, Goldner et al. 2014).

Coinciding with the interval of greatest tectonic extension was the last major global warming period, the middle Miocene Climatic Optimum, or MCO (Zachos et al. 2008). Contemporaneous changes in regional vegetation and the development of modern biomes in western North America added complexity to the changing nature of the regional landscape (e.g., Fox and Koch 2003, Strömberg 2011, Pound et al. 2012). The expansion of grasslands, and eventually desert ecosystems, during the Neogene had significant implications for mammalian habitats and dietary resources (e.g., Janis et al. 2004, Edwards et al. 2010, Jardine et al. 2012). Although tectonic, climatic, and vegetation datasets vary in their geographic and temporal resolution, they provide important context for evaluating the role of landscape history in alternative diversification models for generating the TDG.

The most complete continental fossil record spanning the MCO within western North America occurs in the Mojave Desert of southern California (Fig. 1.4). Work over several decades has generated a rich fossil record from this region, including abundant small-mammal remains from three primarily middle Miocene formations. The Barstow, Crowder, and Cajon Valley formations are temporally well constrained through biochronological, radiometric, and paleomagnetic dating methods (Weldon 1984, Liu 1990, MacFadden et al. 1990). These formations record local processes within the larger Basin and Range Province. Each basin is an archive of the influences of tectonic activity and climate change on mammal diversification and paleoecology at the local scale. In addition, paleoenvironmental data from paleosol units in the Crowder and Cajon Valley formations serve to illuminate local-scale environmental changes and habitat heterogeneity during the MCO. Continuous stratigraphic coverage among formations in the Mojave during the interval of intensified tectonic activity and climate change represents a

critical record for the diversification history of mammals that is poorly represented elsewhere in the Basin and Range Province.

Focal group, the Heteromyidae

The rodent family Heteromyidae is an evolutionary radiation within western North America with a high diversity of species (~60 extant taxa) and ecological specializations, especially within desert ecosystems, such as the Mojave, today (Genoways and Brown 1993, Wilson and Reeder 2005). Commonly known as kangaroo rats and pocket mice, the group consists of primarily seed-eating, burrowing species with life histories and habits closely tied to local vegetation and habitat. Studies of heteromyids span several decades and include topics such as ecological competition, physiology, historical biogeography, and distribution changes in response to current climate warming and habitat transformation (e.g., Brown and Lieberman 1973, Price and Brown 1982, Kolter and Brown 1988, Rowe et al. 2011, Terry et al. 2011). Molecular-phylogenetic analyses reveal ancient divergence times among the major lineages of heteromyids, dating back to the MCO (Riddle 1996, Hafner et al. 2007). Since the earliest record of the clade at ~30 Ma in North America, close to 120 fossil species have been identified (Korth 1994, Korth and Samuels 2015). Peak diversity in the heteromyid fossil record coincided with the MCO during an interval of extension and mountain building that generated complex topography, fragmenting geographic ranges for small mammals and potentially stimulating the formation of new species via geographic isolation (Wahlert 1993, Korth 1994, Smiley et al. *in prep*). Given this rich history of ecological and evolutionary research, heteromyids are a compelling group for testing hypotheses about diversification and ecological responses to landscape change.

Chapter preview

Ecological attributes of species, such as diet, habitat use, and climatic tolerances, can be understood on the basis of morphological adaptations and stable-isotopic composition of their tissues. However, these approaches must be validated in modern ecosystems before application to the fossil record. In Chapter 2, I examined geographic variation in the carbon, nitrogen, oxygen and hydrogen isotopic signatures of two modern heteromyid species across western North America. Spatial variation in isotopic composition reflected diets that covaried with seasonal temperature and precipitation gradients and accurately predicted the distribution of C_3 (cool, mesic-adapted) and C_4 (warm, arid-adapted) grasses (Smiley et al. 2015). Furthermore, I found significant differences in carbon isotopic niches between species along these environmental gradients. These results indicate that the isotopic composition of small mammals reliably records the local environment, resource use, and interspecific niche differences and can be used to evaluate species ecology and environments in the past.

The fossil record indicates that peak mammal diversity in the Miocene of western North America coincided with the interval of global warming and mountain building 17–14 million years ago (Finarelli and Badgley 2010, Badgley et al. 2014). In Chapter 3, I investigated how this regional pattern was recorded within two sedimentary basins at the edge of the Basin and Range Province. Combining fieldwork and a variety of laboratory analyses, including phytolith, carbon isotopic, and elemental chemistry analysis of fossil soils, I assessed local environmental conditions and faunal composition within the fossil record of the Crowder and Cajon Valley formations in the Mojave Desert, California (Smiley et al. *in review*). I found the earliest evidence of C_4 vegetation in the region, evidence for a forested and mesic (~800 $mmyr^{-1}$ of precipitation) ecosystem, and locally diverse large and small-mammal faunas. Exceptionally low

faunal similarity across the Crowder, Cajon Valley, and nearby Barstow formations indicates that high turnover in species composition across space contributed to elevated diversity during the middle Miocene.

Evidence for corresponding changes in environmental conditions and mammal diversity over space and time documented in Chapter 3 led me to investigate the ecological responses of small-mammal individuals, species, and assemblages from the Crowder and Cajon Valley formations during the MCO. In Chapter 4, I evaluated the isotopic composition of small-mammal fossils. They recorded greater vegetation heterogeneity than did soil organic matter and phytolith assemblages. Based on enamel isotopic composition and dental morphology, I found little ecological differentiation among small mammals during this warm, mesic interval compared to differentiation among coexisting rodents in modern desert ecosystems. Co-occurring Miocene species overlapped significantly in their carbon isotopic composition, hypsodonty index, and tooth area throughout the record. Furthermore, species dietary ecology within basins was stable over time, while significant differences in isotopic composition between basins implied a longer-term response during the MCO.

In Chapter 5, I returned to regional-scale diversity dynamics. Because fossil productivity has been shown to covary with diversity in the Basin and Range Province during the Neogene (e.g., Badgley et al. 2014, 2015), I assessed whether or not we can correctly infer shifts in diversification rates under variable degrees of preservation. Based on data from the North American fossil and continental rock records, I simulated fossil records under several diversification and preservation scenarios. I then examined how well the simulations captured origination, extinction, and diversification rates with an imperfectly sampled fossil record. While variation in preservation rates distorted diversification patterns in certain scenarios, the effects

were mild and shifts in diversification rates were generally recovered. These results increase our confidence that the high origination rates inferred from the North American fossil record represent actual changes in diversity during the middle Miocene interval of significant landscape and climate change.

Finally, in Chapter 6, I synthesize these findings and summarize diversity patterns and paleoecological response to climate and landscape change during the MCO across spatial scales in the Basin and Range Province. I conclude by discussing how my research outcomes can be used to guide further research into the factors that influence the topographic diversity gradient.

REFERENCES

Atwater, T., Stock, J., 1998. Pacific-North America plate tectonics of the Neogene southwestern United States: an update. International Geology Review 40, 375–402.

Axen, G.J., Taylor, W.J., Bartley, J.M., 1993. Space-time patterns and tectonic controls of Tertiary extension and magmatism in the Great Basin of the western United States. Geological Society of America Bulletin 105, 56–76.

Badgley, C., 2010. Tectonics, topography, and mammalian diversity. Ecography 33, 220–231.

Badgley, C., Fox, D.L., 2000. Ecological biogeography of North American mammals: species density and ecological structure in relation to environmental gradients. Journal of Biogeography 27, 1437–1467.

Badgley, C., Smiley, T.M., Finarelli, J.A., 2014. Great Basin mammal diversity in relation to landscape history. Journal of Mammalogy 95, 1090–1106.

Badgley, C., Smiley, T.M., Loughney, K., 2015. Miocene mammal diversity of the Mojave region in the context of Great Basin mammal history. Desert Symposium Proceedings, 34–43.

Barnosky, A.D. 2001. Distinguishing the effects of the Red Queen and Court Jester on Miocene mammal evolution in the northern Rocky Mountains. Journal of Vertebrate Paleontology 21, 172–185.

Barnosky, A.D., Carrasco, M.A., 2002. Effects of Oligo-Miocene global climate changes on mammalian species richness in the northwestern quarter of the USA. Evolutionary Ecology Research 4, 811–841.

Barthlott, W., Mutke, J., Rafiqpoor, D., Kier, G., Kreft, H., 2005. Global centers of vascular plant diversity. Nova Acta Leopoldina NF 92, 61–83.

Brown, J.H., Lieberman, G.A., 1973. Resource utilization and coexistence of seed-eating desert rodents in sand dune habitats. Ecology 54, 788–797.

Cerling, T.E., Harris, J.M., MacFadden, B.J., Leakey, M.G., Quade, J., Eisenmann, V., Ehleringer, J.R., 1997. Global vegetation change through the Miocene/Pliocene boundary. Nature 389, 153–158.

Chamberlain, C.P., Mix, H.T., Mulch, A., Hren, M.T., Kent-Corson, M.L., Davis, S.J., Horton, T.W., Graham, S.A., 2012. The Cenozoic climatic and topographic evolution of the western North American Cordillera. American Journal of Science 312, 213–262.

Chapin, C.E., 2008. Interplay of oceanographic and paleoclimate events with tectonism during middle to late Miocene sedimentation across the southwestern USA. Geosphere 4, 976–991.

Coblentz, D.D., Riitters, K.H., 2004. Topographic controls on the regional-scale biodiversity of the south-western USA. Journal of Biogeography 31, 1125–1138.

Coyne, J.A., Orr, H.A., 2004. Speciation (Vol. 37). Sinauer Associates, Sunderland, Massachusetts.

Cracraft, J., 1985. Biological diversification and its causes. Annals of the Missouri Botanical Garden 72, 794–822.

Dickinson, W.R., 2002. The Basin and Range Province as a composite extensional domain. International Geology Review 44, 1–38.

Dickinson, W.R., 2006. Geotectonic evolution of the Great Basin. Geosphere 2, 353–368.

Dickinson, W.R., 2013. Phanerozoic palinspastic reconstructions of Great Basin geotectonics (Nevada-Utah, USA). Geosphere 9, 1384–1396.

Davis, E.B., 2005. Mammalian beta diversity in the Great Basin, western USA: Palaeontological data suggest deep origin of modern macroecological structure. Global Ecology and Biogeography 14, 479–490.

Edwards, E.J., Osborne, C.P., Stromberg, C.A.E., Smith, S.A., Bond, W.J., Christin, P.A., Cousins, A.B., Duvall, M.R., Fox, D.L., Freckleton, R.P., Ghannoum, O., Hartwell, J., Huang, Y., Janis, C.M., Keeley, J.E., Kellogg, E.A., Knapp, A.K., Leakey, A.D.B., Nelson, D.M., Saarela, J.M., Sage, R.F., Sala, O.E., Salamin, N., Still, C.J., Tipple, B., 2010. The origins of C_4 grasslands: integrating evolutionary and ecosystem science. Science 328, 587–591.

Feng, R., Poulsen, C.J., Werner, M., Chamberlain, C.P., Mix, H.T., Mulch, A., 2013. Early Cenozoic evolution of topography, climate, and stable isotopes in precipitation in the North American Cordillera. American Journal of Science 313, 613–648.

Finarelli, J.A., Badgley, C., 2010. Diversity dynamics of Miocene mammals in relation to the history of tectonism and climate. Proceedings of the Royal Society B: Biological Sciences 277, 2721–2726.

Fox, D.L., Koch, P.L., 2003. Tertiary history of C_4 biomass in the Great Plains, USA. Geology 31, 809–812.

Fritz, S.A., Schnitzler, J., Eronen, J.T., Hof, C., Böhning-Gaese, K., Graham, C.H., 2013. Diversity in time and space: wanted dead and alive. Trends in Ecology & Evolution 28, 509–516.

Genoways, H.H., Brown, J. H., 1993. Biology of Heteromyidae. Special Publication No. 10, The American Society of Mammalogists.

Goldner, A., Herold, N., Huber, M., 2014. The challenge of simulating the warmth of the mid-Miocene Climatic Optimum in CESM1. Climate of the Past 10, 523–536.

Hafner, J.C., Light, J.E., Hafner, D.J., Hafner, M.S., Reddington, E., Rogers, D.S., Riddle, B.R., 2007. Basal clades and molecular systematics of heteromyid rodents. Journal of Mammalogy 88, 1129–1145.

Hoorn, C., Wesselingh, F.P., ter Steege, H., Bermudez, M.A., Mora, A., Sevink, J., Sanmartin, I., Sanchez-Meseguer, A., Anderson, C.L., Figueiredo, J.P., Jaramillo, C., Riff, D., Negri, F.R., Hooghiemstra, H., Lundberg, J., Stadler, T., Sarkinen, T., Antonelli, A., 2010. Amazonia through time: Andean uplift, climate change, landscape evolution, and biodiversity. Science 330, 927–931.

Herold, N., Seton, M., Müller, R.D., You, Y., Huber, M., 2008. Middle Miocene tectonic boundary conditions for use in climate models. Geochemistry, Geophysics, Geosystems 9, 1–10.

Herold, N., You, Y., Müller, R.D., Seton, M., 2009. Climate model sensitivity to changes in Miocene paleotopography. Australian Journal of Earth Sciences 56, 1049–1059.

Herold, N., Huber, M., Müller, R.D., 2011. Modeling the Miocene Climatic Optimum. Part I: land and atmosphere. Journal of Climate 24, 6353–6372.

Horton, T.W., Chamberlain, C.P., 2006. Stable isotopic evidence for Neogene surface downdrop in the central Basin and Range Province. Geological Society of America Bulletin 118, 475–490.

Korth, W.K., 1994. The Tertiary record of rodents in North America. Plenum Press, New York City, NY.

Korth, W.W., Samuels, J.X., 2015. New rodent material from the John Day Formation (Arikareean, Middle Oligocene to Early Miocene) of Oregon. Annals of Carnegie Museum 83, 19–84.

Jablonski, D., Roy, K., Valentine, J.W., 2006. Out of the tropics: evolutionary dynamics of the latitudinal diversity gradient. Science 314, 102–106.

Janis, C.M., Damuth, J., Theodor, J.M., 2004. The species richness of Miocene browsers, and implications for habitat type and primary productivity in the North American grassland biome. Palaeogeography, Palaeoclimatology, Palaeoecology 207, 371–398.

Jardine, P.E., Janis, C.M., Sahney, S., Benton, M.J., 2012. Grit not grass: concordant patterns of early origin of hypsodonty in Great Plains ungulates and Glires. Palaeogeography, Palaeoclimatology, Palaeoecology 365–366, 1–10.

Kerr, J.T., Packer, L., 1997. Habitat heterogeneity as a determinant of mammal species richness in high-energy regions. Nature 385, 252–254.

Kotler, B.P., Brown, J.S., 1988. Environmental heterogeneity and the coexistence of desert rodents. Annual Review of Ecology and Systematics 19, 281–307.

Liu, W., 1990. Paleomagnetism of Miocene sedimentary rocks in the Transverse ranges: the implications for tectonic history. Dissertation, California Institute of Technology.

Lomolino, M.V., Riddle, B.R., Whittaker, R.J., Brown, J.H., 2010. Biogeography, 4th Edition. Sinauer Associates, Inc., Sunderland, MA.

Mittelbach, G.G., Schemske, D.W., 2015. Ecological and evolutionary perspectives on community assembly. Trends in Ecology and Evolution 30, 241–247.

MacFadden, B.J., Swisher, C.C., Opdyke, N.D., Woodburne, M.O., 1990. Paleomagnetism, geochronology, and possible tectonic rotation of the middle Miocene Barstow Formation, Mojave Desert, south California. Geological Society of America Bulletin 102, 478-493.

McQuarrie, N., Wernicke, B.P., 2005. An animated tectonic reconstruction of southwestern North America since 36 Ma. Geosphere 1, 147–172.

Mix, H.T., Mulch, A., Kent-Corson, M.L., Chamberlain, C.P., 2011. Cenozoic migration of topography in the North American Cordillera. Geology 39, 87–90.

Myers, N., Mittermeier, R.A., Mittermeier, C.G., 2000. Biodiversity hotspots for conservation priorities. Nature 403, 853–858.

Patterson, B.D., Ceballos, G., Sechrest, W., Tognelli, M.F., Brooks, T., Luna, L., Ortega, P., Salazar, I., Young, B.E., 2007. Digital distribution maps of the mammals of the Western Hemisphere, version 3.0. NatureServe, Arlington, Virginia, USA.

Poulsen, C.J., Jeffery, M.L., 2011. Climate change imprinting on stable isotopic compositions of high-elevation meteoric water cloaks past surface elevations of major orogens. Geology 39, 595–598.

Pound, M.J., Haywood, A.M., Salzmann, U., Riding, J.B., 2012. Global vegetation dynamics and latitudinal temperature gradients during the Mid to Late Miocene (15.97–5.33Ma). Earth Science Reviews 112, 1–22.

Price, M.V., Brown, J.H., 1982. Patterns of morphology and resource use in North American desert rodent communities. Great Basin Naturalist Memoirs 7, 117–134.

Ricklefs, R.E., 1987. Community diversity: relative roles of local and regional processes. Science 235, 167–171.

Riddle, B.R.,1996. The molecular phylogeographic bridge between deep and shallow history in continental biotas. Trends in Ecology and Evolution 11, 207–211.

Riddle, B.R., Hafner, D., 2006. Phylogeography in historical biogeography: investigating the biogeographic histories of populations, species, and young biotas. Biogeography in a Changing World, 161–176.

Rosenzweig, M.L., 1995. Species diversity in space and time. Cambridge University Press, New York City, NY.

Rowe, R.J., Terry, R.C., Rickart, E.A., 2011. Environmental change and declining resource availability for small-mammal communities in the Great Basin. Ecology 92, 1366–1375.

Ruggiero, A., Hawkins, B.A., 2008. Why do mountains support so many species of birds? Ecography 31, 306–315.

Simpson, G.G., 1964. Species density of North American recent mammals. Systematic Zoology 13, 57–73.

Smiley, T.M., Cotton, J.M., Badgley, C., Cerling, T.E., 2015. Small-mammal isotope ecology tracks climate and vegetation gradients across western North America. *Oikos* doi: 10.1111/oik.02722.

Smiley, T.M., Hyland, E.G., Cotton, J.M., Reynolds, R.E., *in review*. Early evidence of C_4 grasses, precipitation variability, and faunal response during the Miocene Climatic Optimum in the Mojave region.

Sonder, L.J., Jones, C.H., 1999. Western United States extension: how the west was widened. Annual Review of Earth and Planetary Sciences 27, 417–462.

Strömberg, C.A.E., 2011. Evolution of grasses and grassland ecosystems. Annual Reviews of Earth and Planetary Sciences 39, 517–544.

Terry, R.C., Li, C.L., Hadly, E.A., 2011. Predicting small-mammal responses to climatic warming: autecology, geographic range, and the Holocene fossil record. Global Change Biology 17, 3019–3034.

Tipple, B.J., Meyers, S.R., Pagani, M., 2010. Carbon isotope ratio of Cenozoic CO_2: A comparative evaluation of available geochemical proxies. Paleoceanography 25, 1–11.

Wahlert, J.H., 1993. The Fossil Record, in Genoways, H.H., Brown, J.H. (Eds.) Biology of Heteromyidae. The American Society of Mammalogists, pp. 1–37.

Weldon, R.J. 1984. Implications of the age and distribution of the late Cenozoic stratigraphy in Cajon Pass, Southern California, in Hester, R.L., Hallinger, D.E. (Eds.), San Andreas Fault–Cajon Pass. Wrightwood American Association of Petroleum Geologists, pp. 9–16.

Wilson, D.E., Reeder, D.M. 2005. Mammal species of the World. Johns Hopkins University Press, Baltimore, MD.

Wing, S.L., 1998. Tertiary vegetation of North America as a context for mammalian evolution, in Janis, C.M., Scott, K.M., (Eds.), Evolution of Tertiary mammals of North America. Cambridge University Press, New York, NY, pp. 3–65

Vrba, E.S., 1992. Mammals as a key to evolutionary theory. Journal of Mammalogy 73, 1–28.

Zoback, M.L., Mckee, E.H., Blakely, R.J., Thompson, G.A., 1994. The northern Nevada rift: regional tectono-magmatic relations and middle Miocene stress direction. Geological Society of America Bulletin 106, 371–382.

Zachos, J.C., Dickens, G.R., Zeebe, R.E., 2008. An early Cenozoic perspective on greenhouse warming and carbon-cycle dynamics. Nature 451, 279–283.

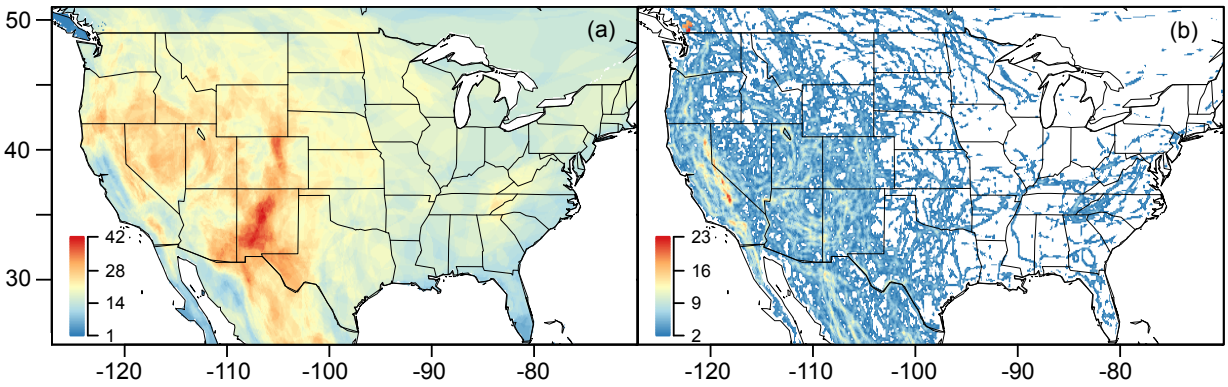

Figure 1.1 (a) Species richness of extant rodents and (b) distribution of overlapping range boundaries for two or more species, based on species ranges compiled at 0.1-degree resolution. Geographic-range data are from NatureServe (Patterson et al. 2007). Today, both species density and spatial turnover are greater in the region of recent tectonic activity and high topographic complexity. (Figure from Badgley, Smiley, et al., *in review*).

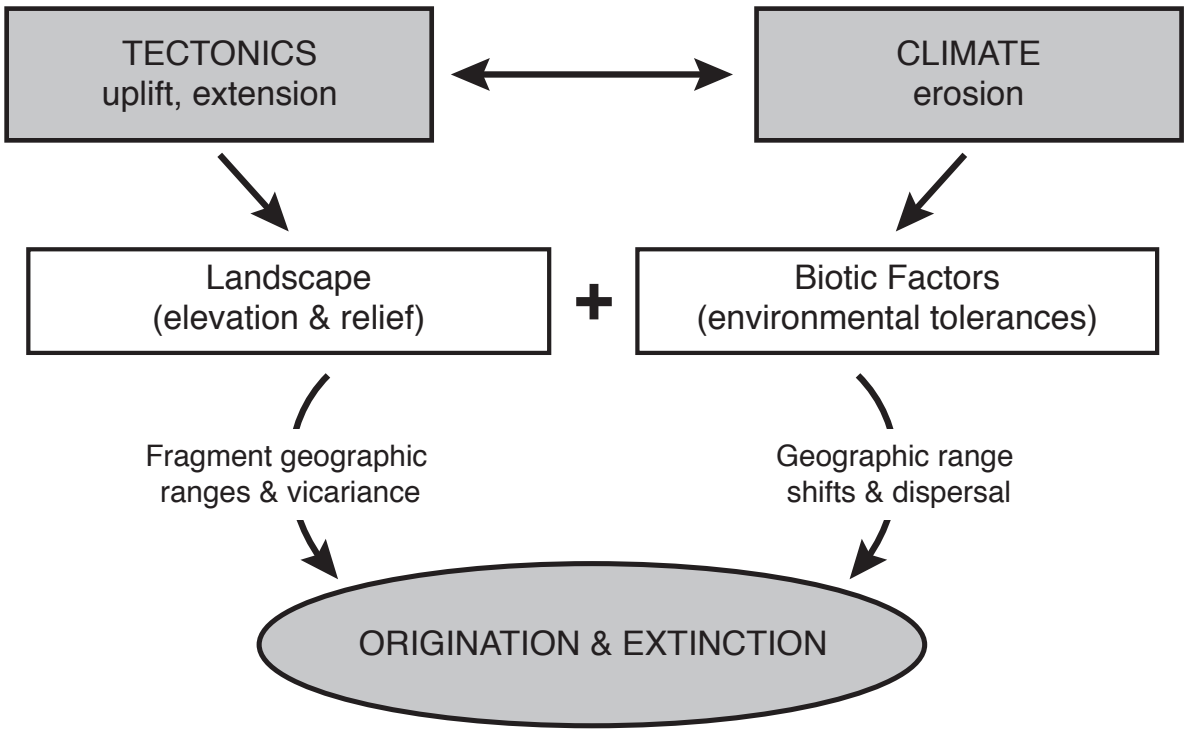

Figure 1.2 Conceptual diagram that links the tectonic and climatic processes shaping regional landscapes, environmental conditions, and species diversity over geologic timescales. Within topographically and climatically complex regions, biogeographic processes include dispersal, geographic-range shifts, and fragmentation of species ranges. These processes can influence origination and extinction in various ways; geographic differences in origination and extinction rates in tectonically active versus passive regions can generate the topographic diversity gradient. (Figure from Badgley, Smiley and Cable, *in press*).

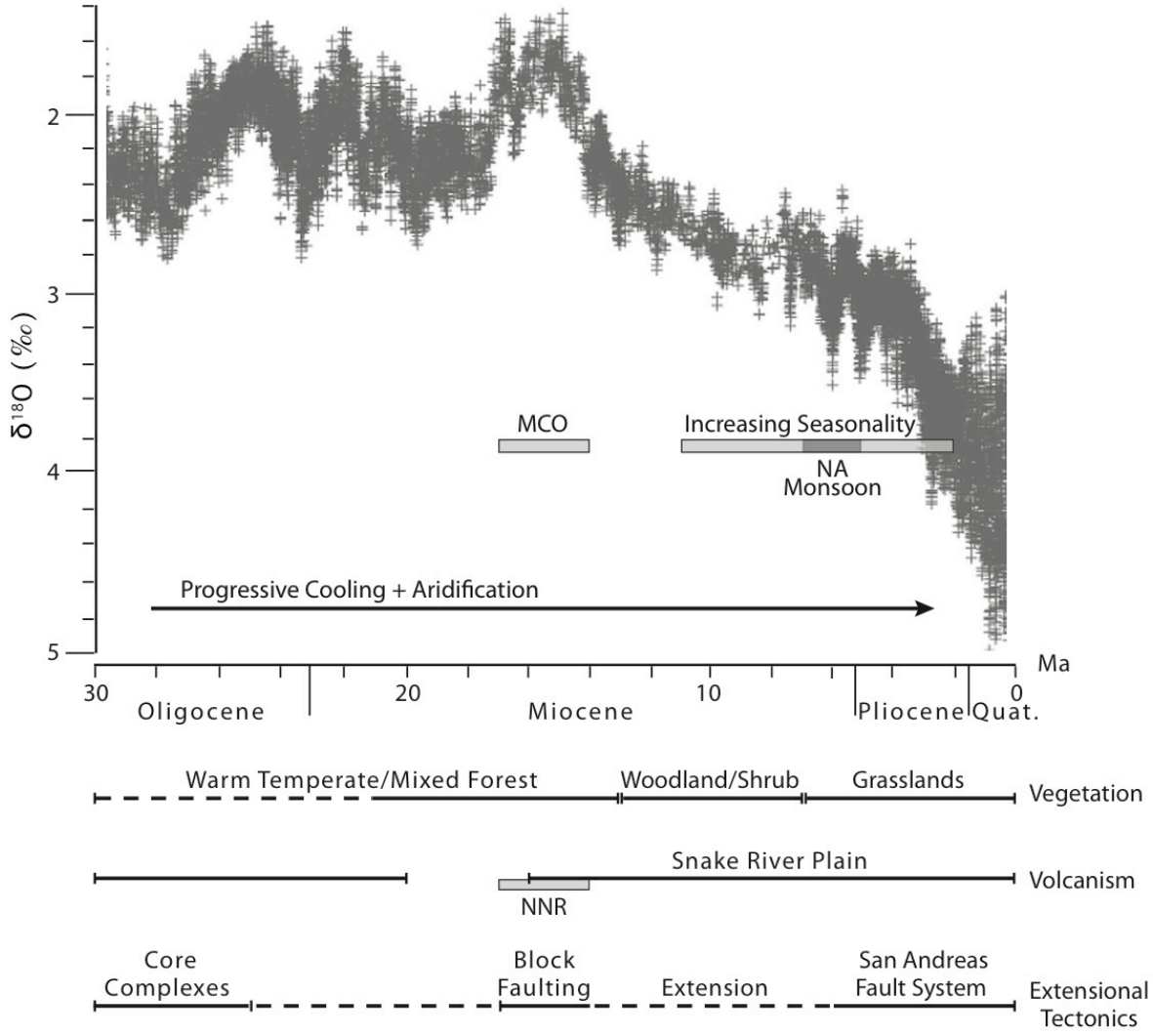

Figure 1.3 Neogene tectonic, climatic, and landscape history in western North America (Atwater and Stock 1998, Axen et al. 1993, Barnosky and Carrasco 2002, Cerling et al. 1997, Chamberlain et al. 2012, Chapin 2008, Dickinson 2002, Dickinson, 2006, Horton and Chamberlain 2006, McQuarrie and Wernicke 2005, Pound et al. 2012, Sonder and Jones 1999, Wing 1998, Zoback et al. 1994). The deep-sea oxygen-isotope curve (modified from Zachos et al. 2008) is a temperature-dependent record that serves as a proxy for Cenozoic climate change. While tectonic and climate events occurred continuously in western North America throughout the Neogene, a significant episode of synchronous tectonic and climatic change lasted from approximately 17 to 14 Ma. MCO, Miocene Climatic Optimum; NNR, Northern Nevada Rift; NA Monsoon, North American Monsoon. (Figure from Badgley, Smiley and Finarelli 2014).

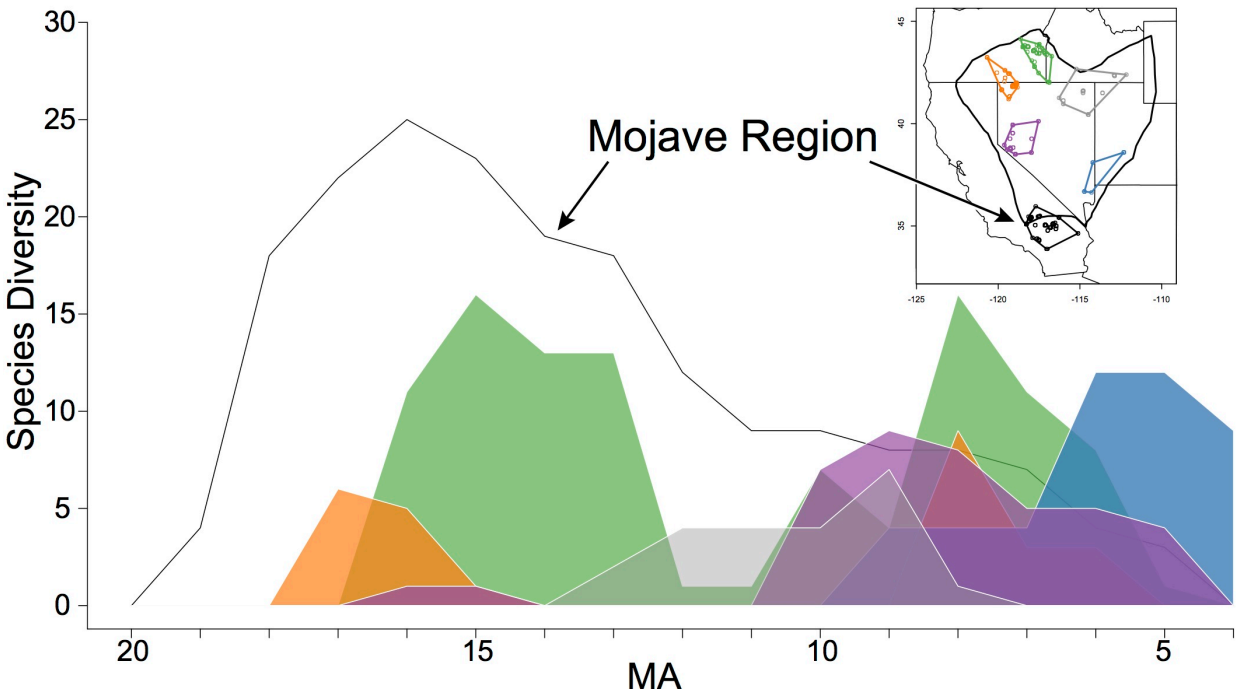

Figure 1.4 Overlapping species diversity of rodents for the six regions shown in the Great Basin inset, with the highest richness peak in the Mojave region during the Miocene Climatic Optimum. (Figure from Badgley, Smiley and Loughney 2015).

CHAPTER 2

Small-mammal isotope ecology tracks climate and vegetation gradients across western North America[1]

ABSTRACT

Stable carbon, nitrogen, hydrogen, and oxygen isotopes have been used to infer aspects of species ecology and environment in both modern ecosystems and the fossil record. Compared to large mammals, stable isotopic studies of small-mammal ecology are limited; however, high species and ecological diversity within small mammals presents several advantages for quantifying resource use and organism-environment interactions using stable isotopes over various spatial and temporal scales. We analyzed the isotopic composition of hair from two heteromyid rodent species, *Dipodomys ordii* and *Perognathus parvus*, from localities across western North America in order to characterize dietary variation in relation to vegetation and climatic gradients. Significant correlations between the carbon isotopic composition ($\delta^{13}C$) of these species and several climatic variables imply that seasonal temperature and precipitation control the composition and distribution of dietary resources (grass seeds). Our results also suggest a moisture influence on the nitrogen isotopic composition ($\delta^{15}N$) of heteromyid diets. Population- and species-level variation in $\delta^{13}C$ and $\delta^{15}N$ values record fine-scale habitat heterogeneity and significant differences in resource use between species. Using classification

[1] Smiley, T.M., Cotton, J.M., Badgley, C., Cerling, T.E., 2015. Small-mammal isotope ecology tracks climate and vegetation gradients across western North America. Oikos.

and regression-tree techniques, we modeled the geographic variation in heteromyid $\delta^{13}C_{diet}$ values based on 10 climatic variables and generated an isotope landscape model ('isoscape'). The isoscape predictions for $\delta^{13}C_{diet}$ differ from expectations based on observed C_4 distributions and instead indicate that *D. ordii* and *P. parvus* record seasonally abundant grass resources, with additional model deviations potentially attributed to geographic variation in dietary selection. The oxygen and hydrogen isotopic composition of *D. ordii* is enriched relative to local meteoric water and suggests that individuals rely on highly evaporated water sources, such as seed moisture. Based on the climatic influences on vegetation and diet documented in this study, the isotopic composition of small mammals has high potential for recording ecological responses to environmental changes over short and long time scales.

INTRODUCTION

Stable isotopes have become a significant tool for ecologists and paleoecologists alike for investigating relationships among resource use and availability and with environmental conditions across a variety of temporal and spatial scales (e.g., Koch 1998, Cerling et al. 2003). Stable isotopes preserved in fossil enamel and bone have provided the basis for dietary inferences of extinct species and documented major vegetation and climatic shifts from the local to the regional scale (e.g., Lee-Thorp and van der Merwe 1987, Bryant et al. 1996, Cerling et al. 1997). Applications to modern mammals include tracking of migration patterns and foraging ecology in the context of recent climate change and quantification of the isotopic niche in individual- to community-level comparisons (e.g., Koch 2007, Newsome et al. 2007). Small mammals, which are abundant and diverse in both modern and ancient ecosystems, have emerged as useful indicators of local environmental conditions with fine-scale variation in their stable isotopes recording aspects of habitat heterogeneity (Hynek et al. 2012, Gehler et al. 2012)

and of niche partitioning over evolutionary timescales (Kimura et al. 2013). However, large gaps in our knowledge of isotope ecology remain across broad spatial scales, seasonal climates, and complex landscapes. Small mammals, studied along geographic and climatic gradients, offer promising insights about local and regional processes influencing mammalian isotopic composition and underlying variation in vegetation and climatic conditions.

Here, we investigate stable isotopes of carbon, nitrogen, oxygen, and hydrogen in hair of two modern heteromyid rodents, *Dipodomys ordii* and *Peroganthus parvus*, in order to document their dietary ecology and resource use in relation to vegetation and climatic gradients across 25 localities in western North America (Fig. 2.1). The geographic distributions of these two wide-ranging species encompass diverse environmental conditions and significant habitat heterogeneity, including Great Plains grasslands, the southwestern deserts, and the Great Basin. The rodent family Heteromyidae is a mammal radiation within western North America with high species and ecological diversity. The Heteromyidae have been studied as a model system to analyze ecological processes such as sympatric niche differentiation (Brown and Lieberman 1973) and the role of landscape history and biogeography in shaping regional diversity (Kelt 1999). *D. ordii* and *P. parvus* have small home ranges (less than 1 ha and 0.4 ha, respectively), forage on the ground, collect grass seeds in their cheek pouches for long-term storage in underground caches, and have highly efficient water-use strategies to conserve moisture in desert environments (MacMillen and Hinds 1983). The larger, bipedal individuals of *D. ordii* prefer less vegetated microhabitats and incur greater physiological costs due to water loss while foraging in the summer, whereas the smaller, quadrupedal individuals of *P. parvus* tend to forage beneath and around vegetation and can enter torpor during the cold season (Brown and Lieberman 1973, Price 1978). Differences in body size, locomotion, microhabitat selection, and

seasonal foraging ability provide a basis for differences in spatial and temporal resource use and microhabitat selection. Strong gradients in temperature, precipitation, and seasonal climate conditions across western North America provide the landscape context for evaluating the isotope ecology of these small mammals.

For herbivorous mammals, such as heteromyids, carbon isotope values, expressed as $\delta^{13}C$, of body tissues reflect the isotopic composition of vegetation ingested during formation of those tissues, thereby reflecting diet as well as the types of vegetation available for consumption (DeNiro and Epstein 1978, Hynek et al. 2012). Cool-season C_3 grasses and warm-season C_4 grasses fractionate carbon from the atmosphere through distinct photosynthetic pathways, resulting in average $\delta^{13}C$ values of *ca.* -26.5‰ and -12.5‰, respectively, under pre-industrial atmospheric CO_2 conditions (Farquhar et al. 1989, Cerling et al. 1997). Through differences in photosynthetic pathway and plant physiology, climate acts as a primary control on the distribution and abundance of C_3 and C_4 grasses and on large-scale variation in $\delta^{13}C$ values of vegetation across the modern landscape, as documented by observations as well as statistical and mechanistic models (Teeri and Stowe 1976, Ehleringer et al. 1991, Tieszen et al. 1997).

While nitrogen isotopic composition often signifies animal trophic position, $\delta^{15}N$ values can also vary among individuals from the same primary-consumer level due to differences in local environment and isotopic composition of vegetation consumed (DeNiro and Epstein 1981, Ambrose 1991). Factors that influence the nitrogen isotopic composition of the local ecosystem (i.e., 10s of km^2 or less) include prior land use, species-level differences in plant $\delta^{15}N$, mycorrhizal associations, and climate (Evans 2001, Pardo and Nadelhoffer 2010). Although global and regional analyses document significant negative correlations between mean annual rainfall and plant $\delta^{15}N$, this relationship exhibits considerable variation around the general trend

(Handley et al. 1999, Amundson et al. 2003) and is often masked by regional to local soil heterogeneity, processes of N-deposition and loss, and plant nutrient utilization (Prado and Nadelhoffer 2010).

Oxygen and hydrogen isotope ratios, expressed as $\delta^{18}O$ and $\delta^{2}H$, record the isotopic composition of water sources consumed by animals, which indirectly reflect the isotopic composition of local meteoric water (Bryant et al. 1996). The isotopic composition of meteoric water is determined by latitude, elevation, temperature, and distance from coast, leading to predictable spatial patterns (Dansgaard 1964, Rozanski et al. 1993, Bowen 2010). The relationship between $\delta^{18}O$ and $\delta^{2}H$ in precipitation at the global scale is expressed by the global meteoric water line; the slope and intercept of this line at the local scale vary with changes in atmospheric humidity (Gat 1996, Kendall and Coplen 2001). Sources of oxygen and hydrogen that influence the isotopic composition in tissues of herbivorous mammals include drinking water and plant water, which are subject to fractionation processes such as evaporation in relation to aridity of the local environment, and atmospheric O_2 from respiration (Kohn 1996).

In this study, we compared geographic variation in heteromyid isotopic composition with climatic variables important for heteromyid ecology, grass productivity, and water fractionation processes over a broad spatial scale. Utilizing $\delta^{13}C$ and $\delta^{15}N$ records of dietary composition, we tested for significant differences in resource use between *D. ordii* and *P. parvus* in local ecosystems and over climate and vegetation gradients. We performed a novel application of classification and regression-tree (CART) methods to isotopic data to evaluate the relative importance of 10 climatic variables for predicting $\delta^{13}C$ values. We utilized the CART model to predict a carbon isoscape of heteromyid diet, which provided the basis for predicting C_3 and C_4 grass abundance across the landscape. In order to test the validity of rodent $\delta^{13}C$ composition as

a vegetation proxy, we evaluated the isoscape model with our observed $\delta^{13}C$ values and proportions of C_4 grasses in local grass floras (Paruelo and Lauenroth 1996). Finally, we compared $\delta^{18}O$ and $\delta^{2}H$ of *D. ordii* with the isotopic composition of local meteoric water to infer water resource use. Our results enabled us to evaluate the potential for vegetation reconstruction, climate inference, and assessment of resource use based on rodent isotopic composition.

MATERIALS AND METHODS

Collection and Analyses

Hair samples were collected from 158 museum specimens of *D. ordii* (n = 89) and *P. parvus* (*n* = 69) from the University of Michigan Museum of Zoology and the Natural History Museum of Utah. Specimens were selected to represent a wide geographic distribution of localities (*n* = 25; Fig. 2.1) and a minimum of four adult individuals per species per locality (Table S2.1). Most individuals from each locality were collected within the same month and year, thereby representing a population sample of co-occurring individuals. Approximately 5 mg of hair per individual were collected and analyzed for the isotopic composition of the individual's diet since the last molt. Because the timing and frequency of molting varies geographically, and molting intervals for localities in this study are unknown, the isotopic composition of heteromyid hair samples may represent average seasonal to annual diet (Desha 1967, Speth 1969). Hair samples were rinsed with a 2:1 chloroform:methanol mixture to remove any surface contaminants and then homogenized, and samples for oxygen and hydrogen analysis were equilibrated with local atmospheric conditions prior to analysis. Samples were analyzed for carbon and nitrogen by a Carlo Erba Elemental Analyzer (EA), interfaced with a continuous-flow ThermoFinnigan Delta Plus XL Isotope Ratio Mass Spectrometer (IRMS). For oxygen and

hydrogen analysis, samples were pyrolyzed with a Thermo Temperature Conversion/EA and analyzed on a continuous-flow ThermoFinnigan Delta Plus XL IRMS. All analyses were preformed at the Stable Isotope Ratio Facility for Environmental Research Laboratory at the University of Utah. Isotope values are expressed as δ values, $\delta x = 1000\ (R_{sample}/R_{standard} - 1)$, where x is ^{13}C, ^{15}N, ^{2}H and ^{18}O, and R_{sample} and $R_{standard}$ are the molar ratios of the heavy to light isotopes (e.g., $^{13}C/^{12}C$) for the sample and standard. δx is expressed in per mil (‰) relative to international standards: Vienna Pee Dee Belemnite for carbon, atmosphere for nitrogen, and Vienna Standard Mean Ocean Water for oxygen and hydrogen. Measurement standard deviations for $\delta^{13}C$ and $\delta^{15}N$ were ≤ 0.2‰ for standards and average errors were 0.1‰ for samples under replicate analyses. Analytical precision for $\delta^{2}H$ was ≤ 1.5‰ and for $\delta^{18}O$ was ≤ 0.2‰.

The carbon isotopic values of museum specimens collected from 1922 to 1968 were corrected for changes in the $\delta^{13}C$ value of atmospheric CO_2 based on the year of collection (Leuenberger 2007). For each locality, 10 climatic variables were extracted from the WorldClim dataset (Hijmans et al. 2005), using the geostatistical raster package (Hijmans 2015), in R version 3.1.2. Temperature and precipitation data represent annual means as well as seasonal and extreme variations (e.g., mean annual precipitation and maximum temperature during the warmest month), composite variables (e.g., mean temperature during the wettest/driest quarter and precipitation during the warmest/coldest quarter), and mean diurnal range (calculated as the mean of monthly maximum minus minimum temperatures). The 10 climatic variables were selected because they exhibit strong spatial gradients across western North America (Fig. S2.1), are biologically meaningful (e.g., physiological costs for heteromyids from seasonal extremes in temperature, strong effect of moisture on primary productivity and availability of seed resources), and overall, have low to moderate correlations. Precipitation variables were the most

strongly correlated; however, because of significant variation in seasonal precipitation across the localities, it was important to include these variables.

Statistical Analyses

We analyzed geographic variation in heteromyid isotopic composition in relation to latitude and longitude using Pearson's correlation tests. Utilizing the Student's *t*-test and the *F*-test, we assessed differences in mean and variance in the isotopic composition of *D. ordii* and *P. parvus* samples among and within localities where the two species co-occur. Because climate values across the heteromyid localities are not normally distributed, we used Spearman's rank correlation analysis to assess significant relationships between the 10 climatic variables and each isotope ratio. Using CART machine learning techniques, we additionally examined the relative importance of each climatic variable for heteromyid carbon isotopic composition by conducting conditional forest analysis of 1000 decision trees through the party package in R (Strobl et al. 2008). CART and random forest analyses are useful tools for non-parametric regression and prediction, and can test the relative importance of a large number of predictor variables while accounting for multivariate interactions (Breiman 2001, Strobl et al. 2009). Conditional forest analysis has the additional advantage of being able to cope with correlated predictor variables by calculating the conditional permutation importance of each variable, which takes into consideration importance contingent on other variables (Strobl et al. 2008). We produced a heteromyid-diet isoscape for western North America based on the variable importance outcome of the conditional forest analysis and bioclimatic layers using the raster package (Hijmans et al. 2005, Hijmans 2015). The isoscape was adjusted to reflect an isotopic enrichment of 3.2‰ from diet to hair (Sponheimer et al. 2003). However, a range of enrichment values has been

documented for small mammals based on taxon, diet consumed, and other factors and the use of a different value would uniformly shift the predicted diet isoscape up or down accordingly. The isoscape was restricted to the combined geographic range of the two species studied. Model $\delta^{13}C$ predictions based on all individuals were then compared to the average isotopic composition of population samples at each locality to assess local fit. We then converted the modeled carbon isotopic values to relative abundances of C_4 grasses using a two-component mixing model, with pure C_3 and pure C_4 end-member values of -26.7‰ and -12.5‰, respectively (average pre-industrial grass $\delta^{13}C$ values; Cerling et al. 1997). Predicted C_4 grass abundances based on heteromyid diets were then compared with observed proportions of C_4 grasses within local grass floras (Table S2.3), calculated from data compiled by Paruelo and Lauenroth (1996).

Finally, we evaluated the oxygen and hydrogen isotopic composition of *D. ordii* in comparison to the isotopic composition of local precipitation across a subset of localities spanning a steep gradient in isotopic composition of local water sources (Bowen 2010; localities = 8, individuals = 39). We tested for significant correlation between the oxygen and hydrogen isotopic composition of *D. ordii* using a Pearson's correlation test, and regressed $\delta^{2}H_{hair}$ on $\delta^{18}O_{hair}$. We compared results from the regression analysis to global and local meteoric water lines from Coplen and Kendall (2000) in order to evaluate the isotopic offset between local water sources and *D. ordii* hair, as well as the overall similarity in the trends of these two datasets. We performed all analyses using the R software environment for statistical computing, version 3.1.2.

RESULTS

Variation in $\delta^{13}C$ and $\delta^{15}N$ between species and in relation to climatic gradients

The carbon isotopic composition of the two wide-ranging heteromyid species, *D. ordii* and *P. parvus*, varies from -23.4‰ to -7.3‰ across western North America (Table S2.2). Assuming a carbon isotopic enrichment of 3.2‰ between diet and hair (Sponheimer et al. 2003), this range corresponds to individual diets composed of exclusively C_4 vegetation, diets of mixed vegetation, and diets of primarily C_3 vegetation (Fig. 2.2a). We found that $\delta^{13}C_{diet}$ is negatively correlated with latitude (r = -0.45, $P < 0.001$) and positively correlated with longitude (r = 0.37, $P < 0.001$), tracking expected geographic variation in C_3 and C_4 vegetation (Teeri and Stowe 1976, Paruelo and Lauenroth 1996) and implying a greater contribution of C_4 grasses to the heteromyid diets of more southern and eastern populations. There are significant differences in $\delta^{13}C_{diet}$ of *D. ordii* and *P. parvus* (across all localities: $P < 0.001$; within localities: $P = 0.014$) and in isotopic variance within population samples ($P < 0.001$). Across the sites, *D. ordii* individuals are enriched in ^{13}C relative to *P. parvus* (with one exception: Ekker's Ranch, UT), and *D. ordii* has greater variability within population samples than *P. parvus* (Fig. 2.2a).

We evaluated the relationship between $\delta^{13}C_{diet}$ and climatic variables for *D. ordii* and *P. parvus* individually as well as in combination, and found significant correlations between carbon isotopic composition and several climatic variables (Table 2.1). $\delta^{13}C_{diet}$ tends to be positively correlated with temperature variables and negatively correlated with precipitation variables across the sample sets. The highest correlation coefficients correspond to seasonal variables that represent interactions between temperature and precipitation, such as mean temperature during the wettest quarter (i.e., rainy season temperature) and precipitation during the coldest quarter. Seasonal variables have strong trends in relation to longitude (e.g., Fig. S2.1) and contrast localities with warm rainy seasons in the east vs. localities with cold rainy seasons in the west. These composite variables encompass both temperature (e.g., cross-over temperature, Ehleringer

1978) and precipitation (e.g., precipitation minimum, Still et al. 2003) thresholds that are important for C_4 grass dominance during the growing season.

The nitrogen isotopic composition of *D. ordii* and *P. parvus* varies by 15.4‰ across localities and up to 9‰ within population samples (Fig. 2.2b). Correlation coefficients for the relationship between $\delta^{15}N_{hair}$ and latitude and longitude are both non-significant. While differences between *D. ordii* and *P. parvus* are significant ($P < 0.001$), their $\delta^{15}N$ values overlap somewhat and samples of co-occurring species do not exhibit a consistent offset in isotopic composition. Correlations between climatic variables and $\delta^{15}N$ values are generally weaker than with $\delta^{13}C$ values (Table 2.1). All significant correlations between $\delta^{15}N$ and precipitation variables are negative, suggesting a moisture control on nitrogen isotopic composition of these rodents.

Isoscape and C_4 grass abundance based on heteromyid $\delta^{13}C$

Using CART conditional forest analysis, we assessed the relative importance of interacting climatic variables in predicting the isotopic composition of heteromyid diets across western North America (Table S2.4). Our model explains 69.7% of the variance in the data, and has an average error of ±2.23‰ on the validation (out-of-bag) dataset. Precipitation during the coldest quarter and mean temperature during the wettest quarter had the highest variable importance scores (> 1.5) in our model. Although these two variables are significantly correlated, both were included in the analysis because winter precipitation contributes to long-term soil moisture, whereas temperature during the rainy season reflects growing season conditions. Mean diurnal range of temperature also had relatively high variable importance (1.09). Several other climatic variables had intermediate variable importance scores (> 0.39), while mean annual

precipitation and warmest quarter precipitation had the lowest variable importance in our model (< 0.16).

Using the CART model, we generated a heteromyid-diet isoscape and compared the predicted values for $\delta^{13}C_{diet}$ against the sample average $\delta^{13}C_{diet}$ measured for each locality (Fig. 2.3a). For most localities, measured minus predicted $\delta^{13}C_{diet}$ values fell within analytical error of our model. Localities that exceed the error range (±2.23‰) tend to have large variance and are in areas of high topographic and climatic complexity. The CART model paired with an isotope mixing model predicts a high to low longitudinal gradient in C_4 grass abundance according to heteromyid diet from the Great Plains to the Pacific Northwest (Fig. 2.3b). This geographic trend compares well with measured percent C_4 grasses within the total grass flora calculated from Paruelo and Lauenroth (1996); however, model predictions of C_4 grasses based on heteromyid isotopic composition tend to predict greater C_4 abundance compared to measured values with two notable exceptions: Arizona and the eastern edge of *D. ordii*'s geographic range.

δ^2H and $\delta^{18}O$ in relation to climate and local water sources

The hydrogen and oxygen isotopic composition of *D. ordii* individuals (n = 39) from eight localities in the southwest (Fig. 2.2c-d) are negatively correlated with latitude (δ^2H: r = -0.41, $P < 0.01$; $\delta^{18}O$: r = -0.41, $P < 0.01$) and longitude ($\delta^{18}O$: r = -0.36, $P < 0.03$). δ^2H and $\delta^{18}O$ values are positively correlated with mean temperature during the wettest quarter (Table 2.1) and decrease from western to eastern, inland localities, matching expected climate influences and spatial patterns (Dansgaard 1964, Rozanski et al. 1993, Bowen 2010). However, due to the small number of localities and high within-sample variability (e.g., up to 50‰ for δ^2H), correlations between climatic variables and δ^2H and $\delta^{18}O$ of *D. ordii* are generally non-significant.

D. ordii δ^2H and $\delta^{18}O$ values were significantly correlated ($r = 0.56$, $P < 0.001$) and assessed by linear regression ($r^2 = 0.31$, $P < 0.001$) in order to compare with the global meteoric water line (GMWL) and local meteoric water lines (LMWL), which document the influence of evaporative processes in arid western states (Fig. 2.4). The low slope of the linear regression (4.71) suggests that *D. ordii* is utilizing water sources that have been further evaporated from local water sources, such as leaf-derived seed moisture. The high variance around this relationship and an average isotopic enrichment from meteoric water to heteromyid hair of ~25‰ for $\delta^{18}O$ and ~30‰ for δ^2H likely reflects the combined isotopic composition of ingested food, water, and inspired air, and biological fractionation during metabolism and assimilation into tissue.

DISCUSSION

This study spans a diversity of biomes, physiographic configurations, and environmental conditions, ranging from the topographically complex high-desert biome of the Basin and Range Province to the low-relief Great Plains grassland biome. Spatial variation in the isotopic composition of granivorous small mammals from study localities records differences in diet and water sources and reflects the associated variation in isotopic signatures of local vegetation and precipitation across the landscape. For *D. ordii* and *P. parvus*, much of this variation is correlated with geographic and climatic gradients. The more enriched carbon isotopic composition of samples from southern and eastern localities indicates a greater contribution of C_4 grasses to the diet and therefore a greater presence of C_4 on the landscape in these regions. The $\delta^{13}C_{diet}$ values of several *D. ordii* individuals in southern localities overlap with the average $\delta^{13}C$ of C_4 grasses. In contrast, $\delta^{13}C_{diet}$ values for some *P. parvus* individuals in the northern most

localities imply a pure C_3 diet. The carbon isotopic composition of most *D. ordii* and *P. parvus* individuals reflects a diet of mixed C_3 and C_4 grass seeds with variation in the relative contribution of these two dietary resources between species and across their geographic ranges.

A significant positive correlation between rainy season temperature and $\delta^{13}C_{diet}$ ($r = 0.57$, $P < 0.001$) implies that localities with a warm growing season show an increased contribution of C_4 grasses to heteromyid diets. A significant negative correlation between precipitation during the cold quarter and $\delta^{13}C_{diet}$ ($r = -0.62$, $P < 0.001$) implies greater C_3 grass within the diets of heteromyids from localities with higher winter precipitation and a spring growing season due to snow melt (e.g., eastern Washington). Compared to mean or extreme temperature and precipitation variables, the strong significant correlations and high relative importance of these composite climatic variables (Table 2.1) likely signify that heteromyid carbon isotopes track seasonal differences in the availability of C_3 and C_4 biomass for consumption and mirror the $\delta^{13}C$ value of more abundant growing-season resources rather than the mean annual value. Temporal separation of cool-season C_3 and warm-season C_4 grass production occurs across the temperate grasslands of North America, changing resource availability for these small herbivores seasonally (Collatz et al. 1998, Still et al. 2003). In addition to seed abundance, foraging behavior of heteromyids is also influenced by factors such as seed moisture content and air temperature (Brown and Lieberman 1973, Price 1978). Therefore, seeds collected and stored for year-round consumption may not represent the annual average proportion of C_3 or C_4 grasses.

The dietary signal from $\delta^{15}N$ varies by more than 15‰ across the landscape, and unlike $\delta^{13}C$, is not correlated with geographic gradients (Fig. 2.2b). Isotopic variation of up to 9‰ within single localities is better explained by local differences in vegetation composition and growth habits (including rooting depth, nutritional strategies, and fungal associations), moisture

levels, and N-deposition than by differences in trophic position (Evans 2001, Pardo and Nadelhoffer 2010). Physiological mechanisms, such as catabolism, lactation, and increasing urea concentration as a water-conserving strategy, could additionally contribute to some of the variation among individuals from the same locality (e.g., Koch 2007). At the regional scale, we found significant negative correlations between heteromyid $\delta^{15}N$ values and both mean annual and seasonal precipitation variables (Table 2.1). These correlations follow global patterns attributed to greater N-losses (N lost through volatilization, denitrification, and leaching is typically depleted in ^{15}N) at drier sites, leading to ^{15}N-enrichment of residual soil and plant nitrogen pools (Handley 1999, Amundson et al. 2003). However, there is considerable variability associated with this relationship in both global studies and within our data, suggesting that microhabitat conditions and local processes leading to spatial heterogeneity in soil and foliar $\delta^{15}N$ can overprint this pattern (Bowen 2010, Pardo and Nadelhoffer 2010).

While large-scale spatial patterns in $\delta^{13}C$ and $\delta^{15}N$ of *D. ordii* and *P. parvus* can be broadly attributed to environmental and climatic gradients, significant differences in isotopic composition between the species suggest that species diverge in their resource and microhabitat use. Across the localities sampled, *P. parvus* generally consumes a greater proportion of C_3 grasses than *D. ordii*, while differences in diet inferred from $\delta^{15}N$ composition could relate to microhabitat selection across an isotopically heterogeneous local landscape (Flaherty and Ben-David 2010). Signficant isotopic niche differentiation between co-occuring *D. ordii* and *P. parvus* conforms to documented resource and microhabitat partitioning among heteromyid species with differences in body size, locomator modes, and foraging behavior (Brown and Lieberman 1973, Price 1978). Within-species variance can additionally serve as a proxy for isotopic niche width (Newsome et al. 2007), and significantly greater $\delta^{13}C$ variablity in *D. ordii*

suggests that the larger kangaroo rat is a more generalist feeder, sampling both C_3 and C_4 grasses within their local ecosystems to a greater degree than in *P. parvus*.

Individuals from the same population with diets dominated by either C_3 or C_4 grasses also document the proximity of these two vegetation types within the local environment. High within-locality variation in isotopic composition implies that small mammals present several advantages over large mammals for recording local habitat heterogeneity. Whereas large mammals represent a temporally and spatially averaged isotopic signal from the landscape, small mammals with relatively small home ranges (e.g., 1 ha or less) can provide fine-scale estimates of the spatial and seasonal variation in vegetation (Hynek et al. 2012). Additionally, through consumption of small amounts of biomass and rapid rates of metabolism and tissue formation, there is little time for dietary mixing and a high probability of recording isotopic end-members within the rodent diet (Podelsak et al. 2008). Population-level analyses of rodent assemblages can be ideal for capturing spatial and temporal heterogeneity in resources, such as C_3 and C_4 grasses, for ecological and paleoecological studies. However, high within-locality variability in heteromyid $\delta^{13}C_{diet}$ and potential species-level dietary selection also suggests that it may be necessary to sample several individuals and species in order to accurately reconstruct the relative abundance of C_3 and C_4 grasses in an ecosystem.

The modeled $\delta^{13}C_{diet}$ isoscape shows strong geographic and topographic gradients, high isotopic heterogeneity in the intermontane west, and agrees, within error, with the average isotopic composition of samples from most localities (Fig. 2.3a). High within-site variability in carbon isotopic composition at Desert Range, UT ($\delta^{13}C_{diet}$ range = 8‰) could explain relatively poor model predictions at this site (residual = 5.7‰). The C_4 grass-abundance map generated from the heteromyid-diet isoscape mirrors trends in C_4 grass abundance documented by

observations (Paruelo and Lauenroth 1996) and predicted by plant physiology (Ehleringer 1978). Across most of the geographic range of *D. ordii* and *P. parvus*, our model tends to predict slightly higher C_4 grass abundance than observed in the total grass flora. One plausible explanation for this pattern is based on our assigned isotopic end-member values; due to relatively low mean annual precipitation (less than 600 $mmyr^{-1}$) across localities, an arid-C_3 end-member value may be more appropriate (Diefendorf et al. 2010), which would systematically lower C_4 estimates. Alternatively, the greater C_4 grass abundance predicted in our model could reflect higher seasonal abundance compared to mean annual abundance of C_4 grasses, suggesting the need for temporally dynamic models of resource isotopic composition. In two regions, Arizona and the eastern edge of *D. ordii*'s geographic distribution, our model predicts lower C_4 grass abundance than observed. The southwestern desert and Great Plains biomes tend to receive most of their rainfall in the summer, whereas the majority of localities used to generate this model receive higher winter rainfall. More complete geographic sampling and a greater diversity of heteromyid species should improve the model and more accurately characterize C_4 grass distributions across a variety of seasonal temperature and precipitation conditions.

While model construction and assumptions may explain the apparent departure of predicted $\delta^{13}C_{diet}$ and C_4 distribution from measured values within certain regions, differences in dietary preference among species and land-use history are also compatible with the observed patterns. In general, the isoscape model supports the importance of seasonally available grass resources to the heteromyid diet. However, in low-resource environments, such as the desert southwest, isotopic composition may additionally reflect variation in the degree of dietary selection across a species range. Results from this analysis demonstrate a potential strategy for distinguishing resource availability (influenced by climate and habitat characteristics) from

resource use (influenced by ecological interactions and microhabitat selection). The long history of land-use, and in particular rangeland disturbance, across much of western North America is also relevant. As all sites are within or near publicly managed or protected lands (Bureau of Land Management and United States Forest Service), the indirect influence of grazing or direct influence of introduced grass species could potentially be a confounding factor at some localities and should be the subject of its own study in the future.

In order to characterize spatial variation in water resource use by heteromyids, we evaluated δ^2H and $\delta^{18}O$ for *D. ordii* only to control for any fractionation differences due to body size and physiology when ingested water and inspired air are assimilated into animal tissue (Fig. 2.4; Bryant and Froelich 1995, Kohn 1996). Warm and arid *D. ordii* localities tend to have higher rates of surface-water evaporation and plant transpiration, increasing the δ^2H and $\delta^{18}O$ values of water and plant matter that a small mammal may ingest (Helliker and Ehleringer 2002). LMWLs in arid ecosystems of New Mexico, Utah, Colorado, and Texas document the effect of low relative humidity, with slopes ranging from 6.3 to 7.5 (Coplen and Kendall 2000). The low slope (4.71) of the linear regression line for δ^2H_{hair} and $\delta^{18}O_{hair}$ suggests that highly evaporated water sources, such as plant moisture stored in seeds, are utilized by *D. ordii* and recorded in their isotopic composition. From these results, in addition to significant positive correlations between both δ^2H and $\delta^{18}O$ in *D. ordii* and mean temperature during the rainy season, we infer that the hydrogen and oxygen isotopic composition of small mammals can track climatic gradients and water sources across the modern landscape. However, high variability in the isotopic composition of *D. ordii* and taxon-specific enrichment values limit their application to paleoenvironmental studies until more work is done to sample a greater variety of climatic

conditions and improve our understanding of the unique physiology of these desert-adapted rodents (Podlesak et al. 2008, Gehler et al. 2012).

CONCLUSIONS

The carbon isotopic composition of two herbivorous rodents, *D. ordii* and *P. parvus*, is influenced by climate and vegetation gradients across western North America. Seasonal temperature and precipitation variables are the strongest correlates with $\delta^{13}C_{diet}$ in these species and can be used to predict variation in carbon isotopic composition and C_4 grass distributions according to heteromyid diet across the landscape. Significant negative correlations between $\delta^{15}N_{hair}$ and precipitation variables suggest a moisture control on the nitrogen isotopic composition of dietary resources and environment. The differences in $\delta^{13}C$ and $\delta^{15}N$ values between *D. ordii* and *P. parvus* imply differences in resource and possibly microhabitat use, with *D. ordii* consuming a higher proportion of C_4 grasses than co-occurring *P. parvus*. In general, the oxygen and hydrogen isotopic composition of *D. ordii* is positively correlated with temperature variables and negatively correlated with precipitation variables. In comparison to LMWLs, the slope of the relationship between $\delta^{18}O$ and $\delta^{2}H$ in *D. ordii* suggests these rodents are acquiring water from highly evaporated moisture sources, such as seeds.

This study assesses small-mammal isotopic composition over broad geographic and climatic gradients, and highlights the potential for small mammals, such as heteromyids, to record changes in vegetation and water sources across the landscape. The stable isotope ecology of small mammals can be used to assess dietary selection, local habitat heterogeneity, seasonal variation in resource availability, and environmental moisture conditions. Results from this study have several implications for studying the fossil record of small mammals, including quantifying

differences in resource use among fossil species and fine-scale variation in vegetation that may not be captured by records from large mammals, preserved soil organic matter, and carbonates. However, due to high individual variation in isotopic composition, moderate sample sizes of small mammals ($n \geq 4$) are needed to accurately assess the average composition of dietary and water sources. Just as modern heteromyid rodents track spatial variation in resources and climate across the modern landscape, fossil heteromyids should also record changing resource use, vegetation composition, and climate through geologic time.

ACKNOWLEDGMENTS

This work was supported by the National Science Foundation (NSF - 1137336, Inter-university Training for Continental-scale Ecology) and analyses were done in the SIRFER lab at the University of Utah. We thank Chris Still at Oregon State University for guidance with CART methods. We thank Eric Rickart and Cody Thompson for assistance, and the Natural History Museum of Utah and the University of Michigan Museum of Zoology for making specimens available for study. Three anonymous reviewers provided useful comments that improved the manuscript.

REFERENCES

Ambrose, S.H., 1991. Effects of diet, climate and physiology on nitrogen isotope abundances in terrestrial foodwebs. Journal of Archaeological Sciences 18, 293–317.

Amundson, R., Austin, A.T., Schuur, E.A.G., Yoo, K., Matzek, V., Kendall, C., Uebersax, A., Brenner, D., Baisden, W.T., 2003. Global patterns of the isotopic composition of soil and plant nitrogen. Global Biogeochemical Cycles 17, 1031.

Bowen, G.J., 2010. Isoscapes: spatial pattern in isotopic biogeochemistry. Annual Review of Earth and Planetary Sciences 38, 161–187.

Breiman, L., 2001. Random forests. Machine Learning 45, 5–32.

Brown, J. H., Lieberman, G.A., 1973. Resource utilization and coexistence of seed-eating desert rodents in sand dune habitats. Ecology 54, 788–797.

Bryant, J.D., Froelich, P.N., 1995. A model of oxygen isotope fractionation in body water of large mammals. Geochimica et Cosmochimica Acta 59, 4523–4537.

Bryant, J.D., Froelich, P.N., Showers, W.J., Genna, B.J., 1996. Biologic and climatic signals in the oxygen isotopic composition of Eocene-Oligocene equid enamel phosphate. Palaeogeography, Palaeoclimatology, Palaeoecology 126, 75–89.

Cerling, T.E., Harris, J.M., MacFadden, B.J., Leakey, M.G., Quade, J., Eisenmann, V., Ehleringer, J.R., 1997. Global vegetation change through the Miocene/Pliocene boundary. Nature 389, 153–158.

Cerling, T.E., Harris, J.M., Passey, B.H., 2003. Diets of East African Bovidae based on stable isotope analysis. Journal of Mammalogy 84: 456–470.

Collatz, G.J., Berry, J.A., Clark, J.S., 1998. Effects of climate and atmospheric CO_2 partial pressure on the global distribution of C_4 grasses: present, past, and future. Oecologia 114, 441–454.

Coplen, T.B., Kendall, C., 2000. Stable hydrogen and oxygen isotope ratios for selected sites of the U.S. Geological Survey's NASQAN and Benchmark surface-water networks. US Geological Survey Open-File Report 00-160, pp. 424.

Dansgaard, W., 1964. Stable isotopes in precipitation. Tellus 16, 436–468.

DeNiro, M.J., Epstein, S., 1978. Influence of diet on the distribution of carbon isotopes in animals. Geochimica et Cosmochimica Acta 42, 495–506.

DeNiro, M.J., Epstein, S., 1981. Influence of diet on the distribution of nitrogen isotopes in animals. Geochimica et Cosmochimica Acta 45, 341–351.

Desha, P.G., 1967. Variation in a population of kangaroo rats, *Dipodomys ordii medius* (Rodentia: Heteromyidae) from the high plains of Texas. Southwestern Naturalist 12, 275–289.

Diefendorf, A.F., Mueller, K.E., Wing, S.L., Koch, P.L., Freeman, K.H., 2010. Global patterns in leaf ^{13}C discrimination and implications for studies of past and future climate. Proceedings of the National Academy Sciences 107, 5738–5743.

Ehleringer, J.R., 1978. Implications of quantum yield differences on the distributions of C_3 and C_4 Grasses. Oecologia 31, 255–267.

Ehleringer, J.R., Sage, R.F., Flanagan, L.B., Pearcy, R.W., 1991. Climate change and the evolution of C_4 photosynthesis. Trends in Ecology and Evolution 6, 95–99.

Evans, R.D., 2001. Physiological mechanisms influencing plant nitrogen isotope composition. Trends in Plant Science 6, 121–126.

Farquhar, G.D., Ehleringer, J.R., Hubick, K.T., 1989. Carbon isotope discrimination and photosynthesis. Annual Review of Plant Biology 40, 503–537.

Flaherty, E.A., Ben-David, M., 2010. Overlap and partitioning of the ecological and isotopic niches. Oikos 119, 1409–1416.

Gat, J.R., 1996. Oxygen and hydrogen isotopes in the hydrologic cycle. Annual Review of Earth and Planetary Science 24, 225–262.

Gehler, A., Tütken, T., Pack, A., 2012. Oxygen and carbon isotope variations in a modern rodent community – implications for palaeoenvironmental reconstructions. PLoS ONE 7, e49531.

Handley, L.L., Austin, A.T., Robinson, D., Scrimgeour, C.M., Raven, J.A., Heaton, T.H.E., Schmidt, S., Stewart, G.R., 1999. The ^{15}N natural abundance ($\delta^{15}N$) of ecosystem samples reflects measures of water availability. Australian Journal of Plant Physiology 26, 185–199.

Helliker, B.R., Ehleringer, J.R., 2002. Differential ^{18}O enrichment of leaf cellulose in C_3 versus C_4 grasses. Functional Plant Biology 29, 435–442.

Hijmans, R.J. 2015. raster: Geographic data analysis and modeling. R package version 2.3-24.

Hijmans, R.J., Cameron, S.E., Parra, J.L., Jones, P.G., Jarvis, A., 2005. Very high resolution interpolated climate surfaces for global land areas. International Journal of Climatology 25, 1965–1978.

Hynek, S.A., Passey, B.H., Prado, J.L., Brown, F.H., Cerling, T.E., Quade, J., 2012. Small mammal carbon isotope ecology across the Miocene–Pliocene boundary, Northwestern Argentina. Earth and Planetary Science Letters 321, 177–188.

Kelt, D.A., 1999. On the relative importance of history and ecology in structuring communities of desert small mammals. Ecography 22, 123–137.

Kendall, C., Coplen, T.B., 2001. Distribution of oxygen-18 and deuterium in river waters across the United States. Hydrological Processes 15, 1363–1393.

Kimura, Y., Jacobs, L.L., Cerling, T.E., Uno, K.T., Ferguson, K.M., Flynn, L.J., Patnaik, R., 2013. Fossil mice and rates show isotopic evidence of niche partitioning and dental ecomorphology related to dietary shifts in Late Miocene of Pakistan. PloS ONE 8, e69308.

Koch, P.L., 1998. Isotopic reconstruction of past continental environments. Annual Review of Earth and Planetary Sciences 26, 573–613.

Koch, P.L., 2007. Isotopic study of the biology of modern and fossil vertebrates, in: Lajtha, K., Michener, R. (Eds.), Stable isotopes in ecology and environmental science. Blackwell, Oxford, pp. 99–154.

Kohn, M.J., 1996. Predicting animal $\delta^{18}O$: Accounting for diet and physiological adaptation. Geochimica et Cosmochimica Acta 60, 4811–4829.

Lee-Thorp, J.A., van der Merwe, N.J., 1987. Carbon isotope analysis of fossil bone apatite. South African Journal of Science 83, 71–74.

Leuenberger, M., 2007. To what extent can ice core data contribute to the understanding of plant ecological developments of the past? in: Dawson, T., Siegwolf, R. (Eds.), Stable Isotopes as Indicators of Ecological Change. Academic Press, London, pp. 211–233.

MacMillen, R.E., Hinds, D.S., 1983. Water regulatory efficiency in heteromyid rodents: a model and its application. Ecology 64:,152–164.

Newsome, S.D., del Rio, C.M., Bearhop, S., Phillips, D.L., 2007. A niche for isotopic ecology. Frontiers in Ecology and the Environment 5, 429–436.

Pardo, L.H., Nadelhoffer, K.J., 2010. Using nitrogen isotope ratios to assess terrestrial ecosystems at regional and global scales, in: West, J.B., Bowen, G.J., Dawson, T.E., Tu, K.P. (Eds.), Isoscapes: Understanding Movement, Pattern, and Process on Earth Through Isotope Mapping. Springer, New York, pp. 221–249.

Paruelo, J.M., Lauenroth, W.K., 1996. Relative abundance of plant functional types in grasslands and shrublands of North America. Ecological Applications 6, 1212–1224.

Podlesak, D.W., Torregrossa, A.-M., ehleringer, J.R., Dearing, M.D., Passey, B.H., Cerling, T.E., 2008. Turnover of oxygen and hydrogen isotopes in the body water, CO_2, hair, and enamel of a small mammal. Geochimica et Cosmochimica Acta 72, 19–35.

Price, M.V., 1978. The role of microhabitat in structuring desert rodent communities. Ecology 59, 910–921.

Rozanski, K., Araguás-Araguás, L., Gonfiantini, R., 1993. Isotopic patterns in modern global precipitation. Geophysical Monograph 78: 1–36.

Speth, R.L., 1969. Patterns and sequences of molts in the Great Basin pocket mouse, *Perognathus parvus*. Journal of Mammalogy 50, 284–290.

Sponheimer, M., Robinson, T., Ayliffe, L., Passey, B., Roeder, B., Shipley, L., Lopez, E., Cerling, T., Dearing, D., Ehleringer, J., 2003. An experimental study of carbon-isotope fractionation between diet, hair, and feces of mammalian herbivores. – Canadian Journal of Zoology 81, 871–876.

Still, C.J., Berry, J.A., Collatz, G.J., DeFries, R.S. 2003. Global distribution of C_3 and C_4 vegetation: carbon cycle implications. Global Biogeochemical Cycles 17, 1006.

Strobl, C., Boulesteix, A.-L., Kneib, T., Augustin, T., Zeileis, A., 2008. Conditional variable importance for random forests. BMC Bioinformatics 9, 307.

Strobl, C., Malley, J., Tutz, G., 2009. An introduction to recursive partitioning: rationale, application, and characteristics of classification and regression trees, bagging, and random forests. Psychologyical Methods 14, 323–348.

Teeri, J.A., Stowe, L.G., 1976. Climatic patterns and the distribution of C_4 grasses in North America. Oecologia 23, 1–12.

Tieszen, L.L., Reed, B.C., Bliss, N.B., Wylie, B.K., DeJong, D.D., 1997. NDVI, C_3 and C_4 production, and distributions in Great Plains grassland land cover classes. Ecological Applications 7, 59–78.

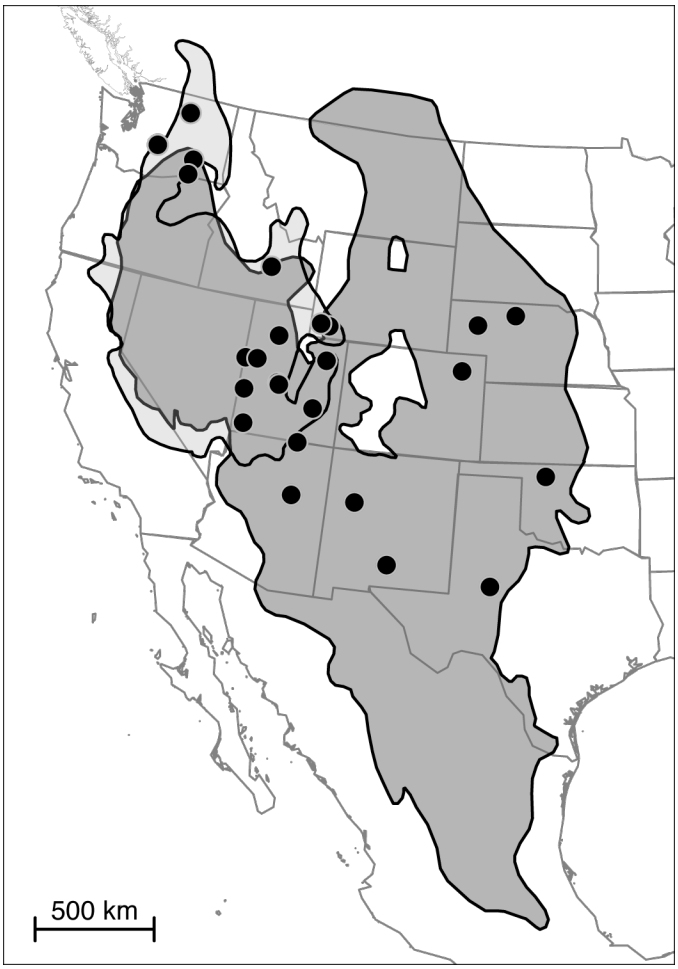

Figure 2.1 Geographic ranges of *Dipodomys ordii* and *Perognathus parvus* are shown in dark and light gray, respectively, with sample localities as black circles (n = 25).

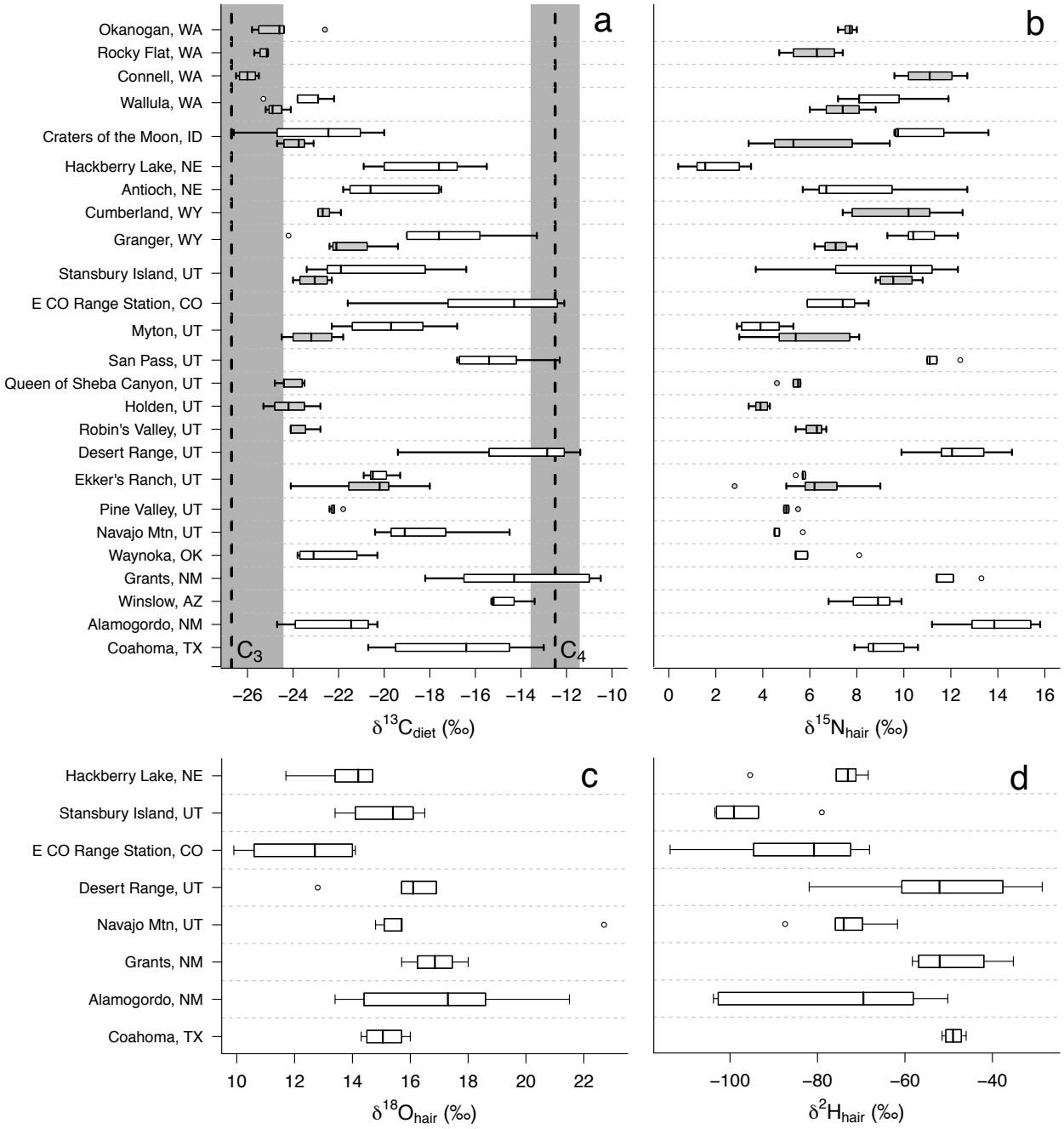

Figure 2.2 Isotopic composition of heteromyid samples. (a) Carbon isotopic composition of diet ($\varepsilon^*_{\text{hair-diet}}$ = 3.2 ‰ from Sponheimer et al. 2003) with average (vertical dashed lines) ± 1 standard deviation (gray bands) isotopic composition of C_3 and C_4 grasses (Cerling et al. 1997) and (b) nitrogen isotopic composition of hair, with *D. ordii* samples (n = 89) shown in white and *P. parvus* samples (n = 69) shown in light gray for 25 localities, listed from higher to lower latitude. (c) Oxygen and (d) hydrogen isotopic composition of *D. ordii* samples (n = 39) from eight localities, listed from higher to lower latitude.

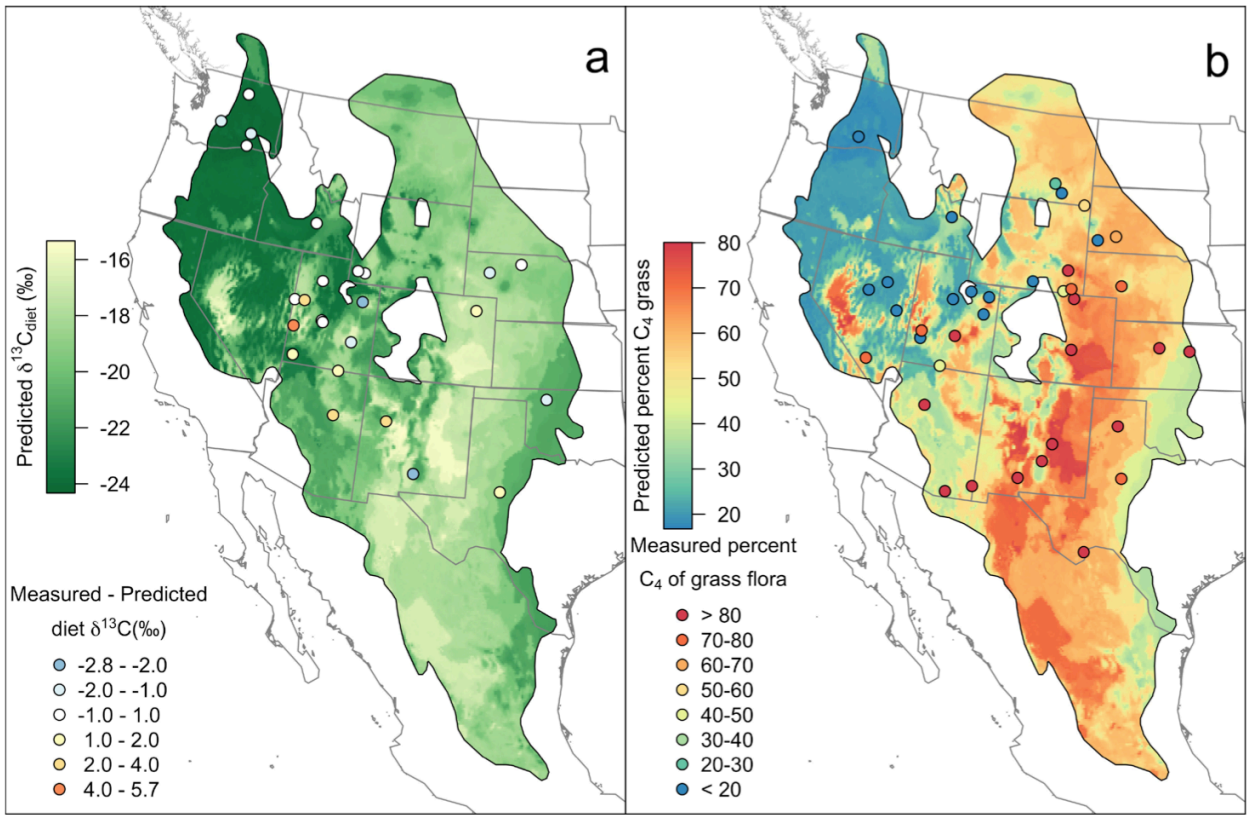

Figure 2.3 (a) Geographic variation in the carbon isotopic composition (isoscape) of *D. ordii* and *P. parvus* diets across their combined geographic range. $\delta^{13}C_{diet}$ values are predicted based on a conditional forest model, and the color of the filled circles represents the difference between measured and predicted $\delta^{13}C_{diet}$ values. (b) Percent C_4 grass abundance within the grass flora derived from the modeled isoscape, with the color of the filled circles representing the measured percent C_4 of the grass flora calculated from Paruelo and Lauenroth (1996).

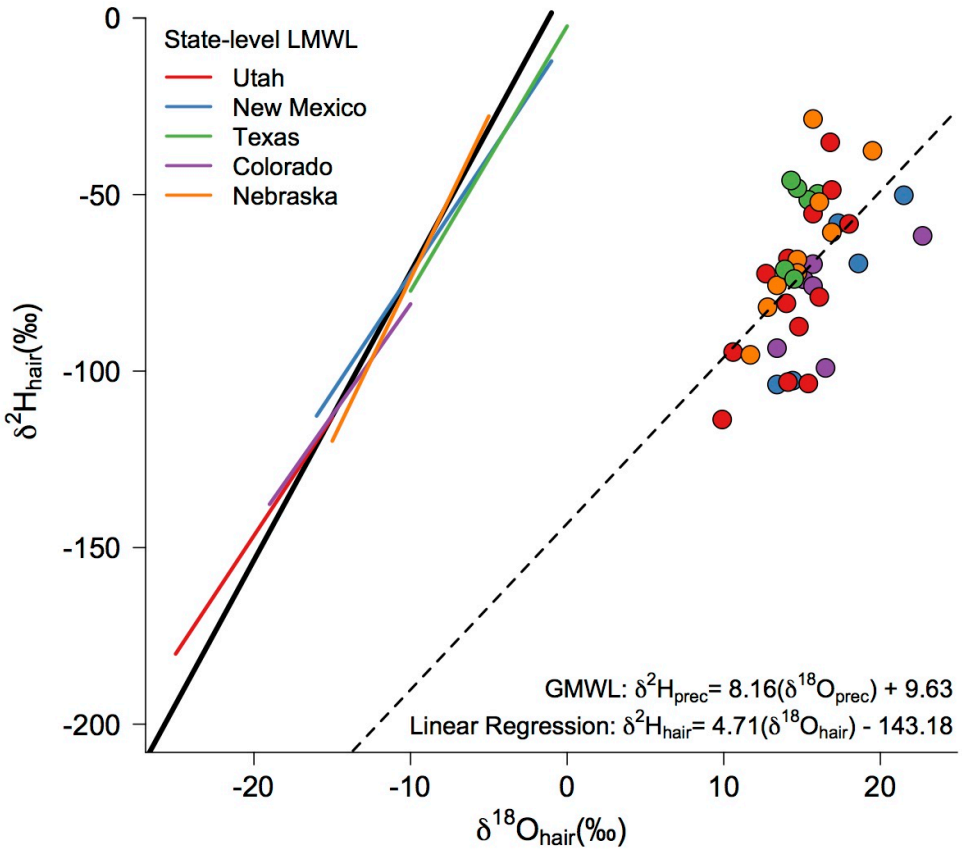

Figure 2.4 Oxygen and hydrogen isotopic composition of *D. ordii* specimens (n = 39) and corresponding global meteoric water line (GMWL: black solid line) and local meteoric water lines (LMWL) from Coplen and Kendall (2000). The relationship between δ^2H and $\delta^{18}O$ in *D. ordii* is expressed as a linear regression (black dashed line).

Table 2.1 Spearman's correlation coefficients (*r*) of isotopic variables with 10 climatic variables, T = temperature, P = precipitation; bold values are significant at $P < 0.05$, *$P < 0.01$, **$P < 0.001$.

Variable	$\delta^{13}C_{hair}$ *r*			$\delta^{15}N_{hair}$ *r*			$\delta^{2}H_{hair}$ *r*	$\delta^{18}O_{hair}$ *r*
	D. ordii (n = 89)	*P. parvus* (n = 65)	Combined (n = 154)	*D. ordii* (n = 89)	*P. parvus* (n = 65)	Combined (n = 154)	*D. ordii* (n = 39)	*D. ordii* (n = 39)
Mean diurnal range	**0.40****	**0.25**	**0.31****	**0.41****	**-0.46****	0.12	**0.43***	0.20
T seasonality	-0.01	**0.44****	**0.21***	**-0.56****	0.10	**-0.30****	**-0.48***	**-0.45***
Maximum T, warmest month	-0.04	0.13	**0.33****	0.17	0.13	**0.25***	0.14	0.22
Minimum T, coldest month	-0.15	-0.24	-0.01	0.18	**0.26***	**0.25***	-0.18	**0.40**
Mean T, wettest quarter	0.13	**0.54****	**0.57****	-0.03	0.04	0.07	**0.50***	**0.37**
Mean T, driest quarter	**-0.28***	**-0.44****	**-0.37****	0.18	0.20	0.08	-0.17	**0.43***
Mean annual precipitation	**-0.26**	-0.18	-0.19	-0.17	**-0.34***	**-0.21***	-0.14	**-0.53****
P, driest quarter	-0.09	0.00	**-0.30****	-0.06	**-0.41****	**-0.28****	0.13	0.13
P, warmest quarter	-0.07	**0.25**	0.16	-0.19	**-0.31***	-0.12	-0.07	**-0.51***
P, coldest quarter	**-0.44****	**-0.37***	**-0.62****	0.06	**-0.27***	-0.14	-0.02	**0.37**

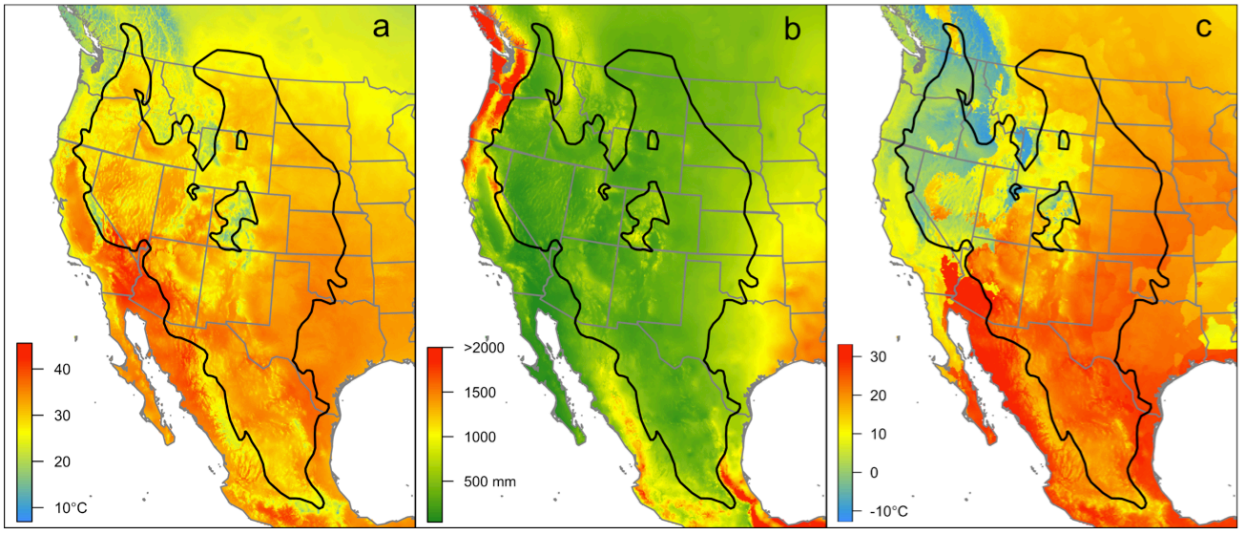

Figure S2.1 Representative climate gradients: (a) maximum temperature during the warmest month (°C); (b) mean annual precipitation (mm); and, (c) mean temperature during the wettest quarter (°C). Climate data were acquired from the WorldClim Dataset (Hijmans et al. 2005). The black outline represents the combined geographic range of *D. ordii* and *P. parvus*.

SUPPLEMENTARY TABLES

Table S2.1 Locality data for heteromyid samples.

ID	Locality	Latitude	Longitude	Elevation (ft)	n	Species Sampled
1	Coahoma, TX	32.361	-101.234	2350	5	*D. ordii*
2	Alamogordo, NM	32.8703025	-105.9496891	4000	6	*D. ordii*
3	Winslow, AZ	35.0242	-110.6967	4850	3	*D. ordii*
4	Grants, NM	35.072542	-107.739941	6300	5	*D. ordii*
5	Waynoka, OK	36.582	-98.879	1500	5	*D. ordii*
6	Navajo Mtn, UT	37.00833	-110.795136	6000	5	*D. ordii*
7	Pine Valley, UT	37.39185	-113.50456	6000	5	*P. parvus*
8	Ekker's Ranch, UT	38.34884	-110.31461	6000	16	*D. ordii, P. parvus*
9	Desert Range Exp Station, UT	38.662	-113.765	5250	10	*D. ordii*
10	Robin's Valley, UT	39.03329	-112.12577	8000	3	*P. parvus*
11	Holden, UT	39.09992	-112.1981	6400	5	*P. parvus*
12	Queen of Sheba Canyon, UT	39.818	-113.9725	8000	5	*P. parvus*
13	Sand Pass, UT	39.86078	-113.39526	4760	5	*D. ordii*
14	Myton, UT	40.19566	-109.98653	5080	10	*D. ordii, P. parvus*
15	E Colorado Range Station, CO	40.36433	-103.21438	4350	5	*D. ordii*
16	Stansbury Island, UT	40.8451	-112.5264	4300	9	*D. ordii, P. parvus*
17	Granger, WY	41.49115	-110.10454	6640	8	*D. ordii, P. parvus*
18	Cumberland, WY	41.544676	-110.531574	6700	5	*P. parvus*
19	Antioch, NE	42.1231	-102.5802	3865	5	*D. ordii*
20	Hackberry Lake, NE	42.5622	-100.67344	3000	6	*D. ordii*
21	Craters of the Moon, ID	43.3391	-113.5293	5500	10	*D. ordii, P. parvus*
22	Wallula, WA	46.856	-118.9042	400	8	*D. ordii, P. parvus*
23	Connell, WA	46.6636	-118.81794	910	4	*P. parvus*
24	Rocky Flat, WA[a]	46.8797	-120.9056	3850	4	*P. parvus*
25	Okanogan, WA	48.3614	-119.5822	840	6	*P. parvus*

[a]Rocky Flat, WA was removed from isotope-climate correlation analyses and isoscape modeling; due to extremely high precipitation values, this westernmost locality was considered an outlier with regard to climatic trends within the dataset.

Table S2.2 Raw isotopic data for *D. ordii* and *P. parvus* samples (i.e., not corrected for carbon isotopic changes in atmospheric CO_2). Replicate measurements are indicated in gray text.

Locality ID	Collection	Museum. no.	Species	Collected	$\delta^{15}N_{AIR}$ (‰)	$\delta^{13}C_{VPDB}$ (‰)	$\delta^{2}H_{SMOW}$ (‰)	$\delta^{18}O_{SMOW}$ (‰)
1	UMMZ	78074	*Dipodomys ordii*	Mar-1936	10.0	-10.3	-49.8	16.0
1	UMMZ	78075	*Dipodomys ordii*	Mar-1936	8.7	-13.6	-51.5	15.4
1	UMMZ	78076	*Dipodomys ordii*	Feb-1936	8.5	-16.7	-48.2	14.7
1	UMMZ	78077	*Dipodomys ordii*	Feb-1936	7.9	-18.0	-46.0	14.3
1	UMMZ	78078	*Dipodomys ordii*	Feb-1936	10.6	-11.7	na	na
2	UMMZ	58325	*Dipodomys ordii*	Jul-1927	15.4	-18.0	na	na
2	UMMZ	58335	*Dipodomys ordii*	Jul-1927	14.0	-19.3	-50.2	21.5
2	UMMZ	58358	*Dipodomys ordii*	Jul-1927	13.7	-17.8	-58.1	17.3
2	UMMZ	58361	*Dipodomys ordii*	Jul-1927	15.8	-17.5	-69.5	18.6
2	UMMZ	58376	*Dipodomys ordii*	Jul-1927	11.2	-21.1	-103.8	13.4
2	UMMZ	58377	*Dipodomys ordii*	Jul-1927	12.9	-21.8	-102.7	14.4
3	UMMZ	66044	*Dipodomys ordii*	Jul-1932	6.8	-12.5	na	na
3	UMMZ	66046	*Dipodomys ordii*	Jul-1932	8.9	-12.5	na	na
3	UMMZ	66047	*Dipodomys ordii*	Jul-1932	9.9	-10.7	na	na
4	UMMZ	82061	*Dipodomys ordii*	May-1939	13.3	-13.8	-55.4	15.7
4	UMMZ	82062	*Dipodomys ordii*	May-1939	12.1	-15.5	-58.3	18
4	UMMZ	82063	*Dipodomys ordii*	May-1939	11.4	-7.8	-35.2	16.8
4	UMMZ	82064	*Dipodomys ordii*	May-1939	9.6	-8.3	na	na
4	UMMZ	82065	*Dipodomys ordii*	May-1939	11.4	-11.6	-48.7	16.9
5	UMMZ	76023	*Dipodomys ordii*	Jun-1936	8.1	-20.9	na	na
5	UMMZ	76024	*Dipodomys ordii*	Jun-1936	5.4	-20.3	na	na
5	UMMZ	76025	*Dipodomys ordii*	Jun-1936	5.4	-21.1	na	na
5	UMMZ	76030	*Dipodomys ordii*	Jun-1936	5.9	-18.5	na	na
5	UMMZ	76031	*Dipodomys ordii*	Jun-1936	4.1	-17.6	na	na
6	NHMU	11551	*Dipodomys ordii*	Sep-1955	4.7	-16.4	-74.0	15.1
6	NHMU	11552	*Dipodomys ordii*	Sep-1955	5.7	-14.6	-69.7	15.7

6	NHMU	11554	*Dipodomys ordii*	Sep-1955	4.5	-11.8	-61.7	22.7
6	NHMU	11555	*Dipodomys ordii*	Sep-1955	4.5	-17.7	-75.9	15.7
6	NHMU	11556	*Dipodomys ordii*	Sep-1955	3.8	-17.0	-87.4	14.8
7	NHMU	21150	*Perognathus parvus*	Jul-1963	5.5	-19.7	na	na
7	NHMU	21151	*Perognathus parvus*	Jul-1963	5.0	-19.6	na	na
7	NHMU	21153	*Perognathus parvus*	Jun-1963	4.6	-19.6	na	na
7	NHMU	21155	*Perognathus parvus*	Jul-1963	4.9	-19.8	na	na
7	NHMU	21158	*Perognathus parvus*	Jul-1963	5.1	-19.2	na	na
8	NHMU	8766	*Perognathus parvus*	May-1951	7.0	-18.5	na	na
8	NHMU	8769	*Perognathus parvus*	May-1951	2.8	-19.8	na	na
8	NHMU	8769	*Perognathus parvus*	May-1951	2.8	-19.7	na	na
8	NHMU	8770	*Perognathus parvus*	May-1951	7.3	-19.2	na	na
8	NHMU	8770	*Perognathus parvus*	May-1951	7.2	-19.4	na	na
8	NHMU	8776	*Perognathus parvus*	May-1951	9.0	-17.4	na	na
8	NHMU	8788	*Perognathus parvus*	May-1951	6.3	-17.4	na	na
8	NHMU	21343	*Perognathus parvus*	May-1965	5.9	-17.8	na	na
8	NHMU	21345	*Perognathus parvus*	May-1965	6.2	-17.1	na	na
8	NHMU	21349	*Perognathus parvus*	May-1965	5.9	-15.5	na	na
8	NHMU	21356	*Perognathus parvus*	May-1965	5.7	-16.5	na	na
8	NHMU	21357	*Perognathus parvus*	May-1965	5.0	-17.7	na	na
8	NHMU	21360	*Perognathus parvus*	May-1965	7.9	-21.6	na	na
8	NHMU	21381	*Dipodomys ordii*	May-1965	5.5	-18.3	na	na
8	NHMU	21381	*Dipodomys ordii*	May-1965	5.3	-18.5	na	na
8	NHMU	21382	*Dipodomys ordii*	May-1965	6.0	-18.0	na	na
8	NHMU	21384	*Dipodomys ordii*	May-1965	5.7	-17.3	na	na
8	NHMU	21384	*Dipodomys ordii*	May-1965	5.6	-17.5	na	na
8	NHMU	21386	*Dipodomys ordii*	May-1965	5.6	-18.0	na	na
8	NHMU	21386	*Dipodomys ordii*	May-1965	5.9	-18.0	na	na
8	NHMU	21387	*Dipodomys ordii*	May-1965	6.0	-16.7	na	na
8	NHMU	21387	*Dipodomys ordii*	May-1965	5.7	-16.9	na	na
9	NHMU	3834	*Dipodomys ordii*	Jul-1940	11.6	-9.1	-28.6	15.7

9	NHMU	3863	*Dipodomys ordii*	Jul-1940	13.5	-8.7	-81.9	12.8
9	NHMU	3894	*Dipodomys ordii*	Jul-1940	14.6	-9.6	-60.7	16.9
9	NHMU	3905	*Dipodomys ordii*	Jul-1940	9.9	-16.4	-52.1	16.1
9	NHMU	3918	*Dipodomys ordii*	Jul-1940	12.0	-9.3	-37.6	19.5
9	NHMU	24106	*Dipodomys ordii*	May-1968	13.4	-10.7	na	na
9	NHMU	24107	*Dipodomys ordii*	May-1968	12.5	-17.1	na	na
9	NHMU	24107	*Dipodomys ordii*	May-1968	12.5	-17.0	na	na
9	NHMU	24122	*Dipodomys ordii*	May-1968	12.0	-13.0	na	na
9	NHMU	24195	*Dipodomys ordii*	May-1968	12.1	-11.3	na	na
9	NHMU	24196	*Dipodomys ordii*	May-1968	11.5	-10.2	na	na
10	NHMU	17066	*Perognathus parvus*	Aug-1959	6.3	-21.4	na	na
10	NHMU	17068	*Perognathus parvus*	Aug-1959	6.7	-20.2	na	na
10	NHMU	17074	*Perognathus parvus*	Aug-1959	5.4	-21.5	na	na
11	NHMU	17055	*Perognathus parvus*	Jun-1959	4.2	-20.9	na	na
11	NHMU	17057	*Perognathus parvus*	Jun-1959	3.7	-20.2	na	na
11	NHMU	17059	*Perognathus parvus*	Jun-1959	3.4	-22.2	na	na
11	NHMU	17060	*Perognathus parvus*	Jun-1959	3.9	-21.6	na	na
11	NHMU	17061	*Perognathus parvus*	Jun-1959	4.3	-22.7	na	na
12	NHMU	3768	*Perognathus parvus*	Jun-1940	5.6	-21.7	na	na
12	NHMU	3802	*Perognathus parvus*	Jun-1940	4.6	-20.8	na	na
12	NHMU	3803	*Perognathus parvus*	Jun-1940	6.2	-21.7	na	na
12	NHMU	3804	*Perognathus parvus*	Jun-1940	5.5	-20.8	na	na
12	NHMU	3804	*Perognathus parvus*	Jun-1940	5.5	-20.9	na	na
12	NHMU	3805	*Perognathus parvus*	Jun-1940	5.3	-22.1	na	na
13	NHMU	25176	*Dipodomys ordii*	May-1963	11.1	-14.2	na	na
13	NHMU	25176	*Dipodomys ordii*	May-1963	11.1	-14.2	na	na
13	NHMU	25177	*Dipodomys ordii*	May-1963	12.4	-9.7	na	na
13	NHMU	25178	*Dipodomys ordii*	May-1963	9.5	-12.8	na	na
13	NHMU	25179	*Dipodomys ordii*	May-1963	11.4	-11.7	na	na
13	NHMU	25180	*Dipodomys ordii*	May-1963	11.2	-14.1	na	na
13	NHMU	25180	*Dipodomys ordii*	May-1963	10.9	-14.2	na	na

14	NHMU	24160	*Dipodomys ordii*	May-1968	3.0	-19.8	na	na
14	NHMU	24160	*Dipodomys ordii*	May-1968	2.9	-19.9	na	na
14	NHMU	24162	*Dipodomys ordii*	May-1968	4.7	-15.8	na	na
14	NHMU	24163	*Dipodomys ordii*	May-1968	5.3	-14.4	na	na
14	NHMU	24192	*Dipodomys ordii*	May-1968	3.1	-19.0	na	na
14	NHMU	24204	*Dipodomys ordii*	May-1968	3.9	-17.3	na	na
14	NHMU	25124	*Perognathus parvus*	May-1968	8.1	-20.8	na	na
14	NHMU	25281	*Perognathus parvus*	May-1968	7.7	-22.0	na	na
14	NHMU	25281	*Perognathus parvus*	May-1968	7.7	-22.2	na	na
14	NHMU	25282	*Perognathus parvus*	May-1968	3.0	-21.6	na	na
14	NHMU	25285	*Perognathus parvus*	May-1968	4.7	-19.2	na	na
14	NHMU	25285	*Perognathus parvus*	May-1968	4.7	-19.5	na	na
14	NHMU	27996	*Perognathus parvus*	Jun-1968	5.5	-19.9	na	na
14	NHMU	27996	*Perognathus parvus*	Jun-1968	5.3	-19.9	na	na
15	NHMU	17678	*Dipodomys ordii*	Mar-1959	7.9	-9.5	-72.4	12.7
15	NHMU	17680	*Dipodomys ordii*	Mar-1959	5.9	-9.8	-68.1	14.1
15	NHMU	17682	*Dipodomys ordii*	Jun-1959	7.4	-14.6	-94.6	10.6
15	NHMU	17684	*Dipodomys ordii*	Jul-1959	5.9	-11.7	-80.8	14.0
15	NHMU	17686	*Dipodomys ordii*	Jun-1959	8.5	-19.0	-113.7	9.9
16	NHMU	11429	*Perognathus parvus*	May-1954	8.8	-21.3	na	na
16	NHMU	13523	*Perognathus parvus*	May-1954	10.8	-19.7	na	na
16	NHMU	13524	*Perognathus parvus*	May-1954	9.2	-20.7	na	na
16	NHMU	13526	*Perognathus parvus*	May-1954	9.9	-20.1	na	na
16	NHMU	14186	*Dipodomys ordii*	May-1954	12.3	-19.8	-103.1	14.1
16	NHMU	14187	*Dipodomys ordii*	May-1954	7.1	-15.5	-79.0	16.1
16	NHMU	14200	*Dipodomys ordii*	May-1954	3.7	-20.8	-103.5	15.4
16	NHMU	14206	*Dipodomys ordii*	May-1954	11.2	-13.7	-93.5	13.4
16	NHMU	14488	*Dipodomys ordii*	May-1954	10.3	-19.3	-99.1	16.5
17	UMMZ	87489	*Dipodomys ordii*	Aug-1942	12.3	-14.8	na	na
17	UMMZ	87492	*Dipodomys ordii*	Aug-1942	11.3	-13.1	na	na
17	UMMZ	87493	*Dipodomys ordii*	Aug-1942	9.3	-21.4	na	na

17	UMMZ	87495	*Dipodomys ordii*	Aug-1942	10.4	-10.6	na	na
17	UMMZ	87499	*Dipodomys ordii*	Aug-1942	10.2	-16.2	na	na
17	UMMZ	87508	*Perognathus parvus*	Aug-1942	6.2	-19.3	na	na
17	UMMZ	87510	*Perognathus parvus*	Aug-1942	8.0	-19.6	na	na
17	UMMZ	87511	*Perognathus parvus*	Aug-1942	7.1	-16.7	na	na
18	NHMU	27978	*Perognathus parvus*	Aug-1955	10.2	-19.7	na	na
18	NHMU	27979	*Perognathus parvus*	Aug-1955	12.5	-20.2	na	na
18	NHMU	27979	*Perognathus parvus*	Aug-1955	12.5	-20.4	na	na
18	NHMU	27980	*Perognathus parvus*	Aug-1955	7.8	-20.0	na	na
18	NHMU	27981	*Perognathus parvus*	Aug-1955	11.1	-20.3	na	na
18	NHMU	27982	*Perognathus parvus*	Aug-1955	7.4	-19.2	na	na
19	UMMZ	75536	*Dipodomys ordii*	Jul-1935	9.5	-14.8	na	na
19	UMMZ	75537	*Dipodomys ordii*	Jul-1935	6.4	-14.8	na	na
19	UMMZ	75538	*Dipodomys ordii*	Jul-1935	6.7	-19.0	na	na
19	UMMZ	75539	*Dipodomys ordii*	Jul-1935	5.7	-17.9	na	na
19	UMMZ	75541	*Dipodomys ordii*	Jul-1935	12.7	-18.7	na	na
20	UMMZ	68239	*Dipodomys ordii*	Jul-1933	1.8	-12.7	-68.4	14.7
20	UMMZ	68242	*Dipodomys ordii*	Jul-1933	3.5	-18.1	-95.4	11.7
20	UMMZ	68244	*Dipodomys ordii*	Jul-1933	0.4	-15.0	-75.7	13.4
20	UMMZ	68245	*Dipodomys ordii*	Jul-1933	1.2	-14.6	-72.2	14.7
20	UMMZ	68247	*Dipodomys ordii*	Jul-1933	1.3	-14.1	-71.2	13.9
20	UMMZ	68248	*Dipodomys ordii*	Jul-1933	3.0	-17.2	-73.9	14.5
21	UMMZ	78098	*Dipodomys ordii*	Oct-1936	9.7	-17.3	na	na
21	UMMZ	78099	*Dipodomys ordii*	Oct-1936	9.8	-19.3	na	na
21	UMMZ	78101	*Dipodomys ordii*	Oct-1936	9.6	-20.0	na	na
21	UMMZ	78140	*Perognathus parvus*	Sept-1936	5.7	-20.3	na	na
21	UMMZ	78144	*Perognathus parvus*	Sept-1936	4.9	-21.0	na	na
21	UMMZ	78155	*Perognathus parvus*	Sept-1936	3.4	-21.9	na	na
21	UMMZ	78157	*Perognathus parvus*	Sept-1936	4.5	-20.7	na	na
21	UMMZ	78182	*Perognathus parvus*	Oct-1936	7.8	-21.6	na	na
21	UMMZ	78183	*Perognathus parvus*	Oct-1936	9.4	-20.9	na	na

21	UMMZ	78859	*Dipodomys ordii*	Oct-1936	13.6	-12.5	na	na
22	UMMZ	54736	*Dipodomys ordii*	May-1922	7.2	-20.0	na	na
22	UMMZ	54737	*Dipodomys ordii*	May-1922	8.1	-22.5	na	na
22	UMMZ	54740	*Dipodomys ordii*	Jun-1922	9.8	-20.1	na	na
22	UMMZ	54741	*Dipodomys ordii*	Jun-1922	11.9	-21.0	na	na
22	UMMZ	168368	*Dipodomys ordii*	May-1922	8.1	-19.6	na	na
22	UMMZ	54746	*Perognathus parvus*	June-1922	7.4	-21.2	na	na
22	UMMZ	54748	*Perognathus parvus*	June-1922	8.8	-22.0	na	na
22	UMMZ	54750	*Perognathus parvus*	June-1922	6.0	-22.4	na	na
23	UMMZ	86569	*Perognathus parvus*	Sep-1940	9.6	-23.7	na	na
23	UMMZ	86570	*Perognathus parvus*	Sep-1940	10.8	-22.8	na	na
23	UMMZ	86571	*Perognathus parvus*	Sep-1940	12.7	-23.5	na	na
23	UMMZ	86572	*Perognathus parvus*	Sep-1940	11.4	-23.0	na	na
24	UMMZ	95979	*Perognathus parvus*	Sep-1947	7.4	-22.4	na	na
24	UMMZ	95980	*Perognathus parvus*	Sep-1947	6.7	-22.4	na	na
24	UMMZ	95981	*Perognathus parvus*	Oct-1947	5.9	-22.6	na	na
24	UMMZ	95982	*Perognathus parvus*	Oct-1947	4.7	-23.0	na	na
25	UMMZ	68045	*Perognathus parvus*	Jul-1933	8.0	-19.9	na	na
25	UMMZ	68047	*Perognathus parvus*	Jul-1933	7.7	-21.6	na	na
25	UMMZ	68055	*Perognathus parvus*	Jul-1933	7.7	-21.9	na	na
25	UMMZ	68056	*Perognathus parvus*	Jul-1933	7.8	-22.7	na	na
25	UMMZ	68057	*Perognathus parvus*	Jul-1933	7.2	-23.0	na	na
25	UMMZ	68079	*Perognathus parvus*	Jul-1933	7.5	-21.8	na	na

Table S2.3 Calculated proportion of C_4 grass within the total grass flora, locality data, and source references for vegetation abundance measurements from Paruelo and Lauenroth (1996).

Site ID	Town	State	Latitude	Longitude	Prop C_4	Source Reference
21	Appleton-Whittel Research Ranch	AZ	31.6	-110.5	1	Bock et al. 1984
26	Portal	AZ	32	-109.12	1	Chew 1982
37	Coconino County	AZ	35.27	-112.35	1	Hessing et al. 1982
10	CPER	CO	40.82	-104.6	0.90	Sims et al. 1978
36	El Paso	CO	38.55	-104.5	0.99	Kinraide 1984
17	Idaho National Engineering Laboratory	ID	43.73	-112.67	0	Anderson and Shumar 1986
6	Hays	KS	38.87	-99.38	0.97	Sims et al. 1978
71	Salina	KS	38.75	-97.62	0.92	Piper and Gernes 1988
30	Alzada	MT	45.03	-104.47	0.59	MacCracken et al. 1983
46	Kluver North	MT	45.88	-106.47	0.20	Singh et al. 1983
48	Fort Howes	MT	45.48	-106	0.03	Lauenroth et al. 1984
16	Arapaho	NE	41.55	-101.8	0.71	Barnes et al. 1983
7	Jornada	NM	32.62	-106.75	1	Sims et al. 1978
12	Fort Stanton Experimental Ranch	NM	33.48	-105.55	1	Piper et al. 1971
38	Lincoln County	NM	34.28	-105.08	1	Beavis et al. 1982
31	Grass Valley	NV	39.82	-116.75	0	Young et al. 1986
35	Lowry Spring	NV	39.16	-114.9	0	Everett and Koniak 1981
62	Elko County	NV	40.33	-115.75	0	Tueller and Eckert 1987
68	Nevada Test Site	NV	36.83	-116.08	0.71	Beatley 1975
20	Wind Cave National Park	SD	43.53	-103.45	0.17	Forde et al. 1984
27	Badlands National Park	SD	43.75	-102.33	0.70	Uresk 1990
9	Pantex	TX	35.3	-101.53	0.94	Sims et al. 1978
19	Black Gap Wildlife Management Area	TX	29.58	-102.92	1	Aide and Van Auken 1985
23	Synder	TX	32.97	-101.18	0.79	McPherson et al. 1988
28	Escalante desert	UT	38.17	-113.25	0	Germano and Lawhead 1986
29	Glen Canyon	UT	37.1	-111.87	0.47	Rasmussen and Brotherson 1986
33	Capitol Reef National Park	UT	38.52	-111.3	0.85	Player ad Urness 1982

40	Uinta Basin 2, Vernal	UT	40.45	-109.65	0	Brotherson and Brotherson 1979
43	Utah Lake Grasewood	UT	40.12	-111.75	0	Brotherson et al. 1986
54	Hill Creek	UT	39.66	-109.83	0	Brotherson and Brotherson 1979
57	Rock Creek	UT	40.58	-110.75	0	Brotherson and Brotherson 1979
60	Pine valley (Spiny hopsage)	UT	38.5	-113.25	0.78	Yorks et al. 1992
1	ALE	WA	46.4	-119.55	0	Sims et al. 1978
32	SSHA	WY	41.42	-107.17	0	Bruke et al. 1989a
63	Pole Mountain	WY	41.12	-105.28	0.43	Boutton et al. 1980
64	Cheyenne	WY	41.25	-104.82	0.79	Boutton et al. 1980
65	Wheatland	WY	42.07	-105.12	0.93	Boutton et al. 1980

Table S2.4 Results from conditional forest analysis (1000 trees) assessing the relative importance of 10 climatic variables in predicting $\delta^{13}C_{diet}$ values of *D. ordii* and *P. parvus* across 25 localities in western North America; importance score refers to the conditional permutation importance score. T = temperature, P = precipitation.

$R^2 = 0.697$ Root mean-square error = 2.23	
Variable	Importance Score
P, coldest quarter	1.80
Mean T, wettest quarter	1.59
Mean diurnal range	1.09
Min T, coldest month	0.63
Mean T, driest quarter	0.62
T seasonality	0.58
P, driest quarter	0.53
Maximum T, warmest month	0.39
Mean annual precipitation	0.15
P, warmest quarter	0.14

CHAPTER 3

Evidence of early C_4 grasses, habitat drying, and faunal response during the Miocene Climatic Optimum in the Mojave Region[1]

ABSTRACT

Major changes to landscapes, climate, and mammalian faunas occurred at the regional scale in western North America during the Miocene Climatic Optimum (MCO) from 17.0 to 14.0 Ma, but few studies have looked at how the MCO affected basin-scale environments. Paleoenvironmental reconstructions coupled with mammalian fossil assemblages from the Crowder and Cajon Valley formations in the Mojave Desert, California, contribute insights into local-scale (10s of kilometers) diversity dynamics in response to warming during the Hemingfordian and Barstovian North American land mammal ages. By integrating phytolith analyses, carbon isotopic composition of preserved soil organic matter (SOM), and elemental geochemistry of paleosols, we provide reconstructions of depositional environments, vegetation, and precipitation through the MCO. Our reconstructions indicate that the Crowder and Cajon Valley basins were stable, large-scale braided stream and floodplain systems with intermittent paleosol development and significant spatial heterogeneity in vegetation and moisture conditions. Phytolith evidence suggests that vegetation was primarily mixed C_3 forest and grassland. In the Crowder Formation, we document the earliest presence of C_4 grasses in the region at ~17.0 Ma. Based on elemental geochemistry of paleosols, mean annual precipitation

[1] Smiley, T.M., Hyland, E.G., Cotton, J.M., Reynolds, R.E. Evidence of early C_4 grasses, habitat drying, and faunal response during the Miocene Climatic Optimum in the Mojave Region. Palaeogeography, Palaeoclimatology, Palaeoecology, *in review*.

(MAP) estimates are 807 (± 182) $mmyr^{-1}$ at 17.0 Ma in the Crowder Formation and 740−800 (± 182) $mmyr^{-1}$ from 16.0−15.0 Ma in the Cajon Valley Formation. Together, phytolith assemblages and $\delta^{13}C_{SOM}$ document a significant drying trend in the Crowder Formation and an increase in grassland in the Cajon Valley Formation. Faunal turnover and declines in species diversity in the Crowder Formation correspond with local environmental responses to global warming during the MCO. High species diversity within faunal assemblages and low faunal similarity among assemblages of the Crowder, Cajon Valley, and nearby Barstow formations indicate that peak mammal diversity was accommodated at both local and regional scales during sustained tectonic activity and the MCO in western North America.

INTRODUCTION

Miocene Climatic Optimum and mammal diversity

Western North America has a complex tectonic history that overlaps with long-term climatic trends and rapid climatic shifts at both global and regional scales during the Cenozoic. From the early Miocene (~23.0 Ma) to the present, tectonic extension west of the Rocky Mountains increased overall habitat area by ~400,000 km^2 and generated a topographic fabric of alternating isolated basins and mountain ranges within the Basin and Range Province (e.g., McQuarrie and Wernicke 2005). Interactions between tectonic forces and climate change in this region have produced a landscape of high topographic complexity and habitat heterogeneity, with significant consequences for mammalian diversity, evolution, and biogeography. Peak mammal diversity in the fossil record of western North America coincides with an intensification of regional tectonic activity and the global warming interval known as the Miocene Climatic Optimum (MCO), between roughly 17.0 and 14.0 Ma (Zachos et al. 2001, Barnosky and Carrasco 2002, Finarelli

and Badgley 2010, Badgley et al. 2014). The contribution of local patterns and processes, such as basin-scale diversity, climate and environmental change, and ecological response, to the regional diversity record during the Miocene remains unresolved.

In order to evaluate mammalian diversity dynamics, evolution, and paleoecology across this interval of increased tectonic activity and substantial climate warming, a sedimentary and fossil record that captures changes in diversity before, during, and after the MCO is critical. Within North America, the most continuous continental record through the MCO occurs in the Mojave Desert and Cajon Pass regions of southern California, USA (Fig. 3.1). The well-documented Barstow Formation and the less well-studied Cajon Valley, Crowder, and Hector formations together extend over the middle Miocene from 22.9 to 12.5 Ma and preserve a diversity of small and large mammal fossils that span the mid-Hemingfordian through Barstovian North American Land Mammal Ages (NALMA; Lindsay 1972, Woodburne et al. 1990, Tedford et al. 2004, Reynolds et al. 2008).

In this study, we investigate the geological, paleoenvironmental, and faunal history of the Crowder and Cajon Valley formations in the vicinity of the Cajon Pass region during the MCO. The primary aims of this paper are to: 1) present a revised stratigraphic framework for the known mammalian faunal assemblages, 2) establish paleoenvironmental reconstructions of vegetation utilizing phytolith assemblages and the carbon isotopic composition of preserved soil organic matter, 3) estimate mean annual precipitation and infer variation in moisture conditions based on the elemental geochemistry and carbon isotopic composition of paleosols, and 4) examine variation in taxonomic richness and composition corresponding to paleoenvironmental reconstructions.

Age constraints

Fossil collection in the Crowder and Cajon Valley formations has occurred over the last five decades, with a focused effort on the recovery of small-mammal fossils. To date, 59 identified taxa of small and large mammals are known from the two formations (Woodburne and Golz 1972, Reynolds 1991, Reynolds et al. 2008). Highly fossiliferous assemblages of both large and small mammals in addition to several dated tuffs make the Barstow Formation of the western Mojave Desert a useful reference for biostratigraphic and chronostratigraphic correlation with the Crowder and Cajon Valley formations. Mammalian assemblages of the Crowder and Cajon Valley formations overlap in age with those of the Barstow Formation; however, the Crowder and Cajon Valley formations also record an older Hemingfordian fauna that coincided with early MCO warming. Age determination based on biostratigraphic correlation with NALMAs, faunal zones from the Barstow Formation, and paleomagnetic stratigraphy indicate that the Crowder Formation was deposited between 17.5 and 7.1 Ma or younger (Reynolds et al. 2008), and the Cajon Valley Formation between 18.0 and 12.7 Ma (Woodburne and Golz 1972, Winston 1985, Weldon 1986, Liu 1990, Reynolds et al. 2008).

Lithological variation in the Crowder and Cajon Valley formations is the basis for subdividing the strata into five and six, respectively, distinct and laterally extensive units (Woodburne and Golz 1972, Foster 1980). Fossils of the Hemingfordian and Barstovian NALMAs span Units 1 and 2 within the Crowder Formation and Units 3 through 5 within the Cajon Valley Formation (Woodburne and Golz 1972, Weldon 1986). Since Hemingfordian and Barstovian strata within the Crowder and Cajon Valley formations record local environmental and faunal turnover in relation to the MCO and regional tectonic change, the stratigraphy, fossil taxa, and paleoenvironment of these units are the focus of this study.

Geologic and depositional context

The Cajon Pass lies at the junction of the San Bernardino and San Gabriel Mountains of the Transverse Ranges, where the Crowder and Cajon Valley (formerly known as the Miocene Punchbowl Formation of Woodburne and Golz 1972) formations represent separate continental basins now physically adjacent due to movement along the Squaw Peak Fault (Fig. 3.1). At the time of deposition, these basins are estimated to have been separated by tens of kilometers (Meisling and Weldon 1989). Sediments of both the Crowder and Cajon Valley formations are primarily arkosic sandstones and conglomerates that were deposited unconformably over crystalline basement rocks or the Vaqueros Formation, a marine conglomerate and sandstone locally exposed below the Cajon Valley Formation (Noble 1954, Dibblee 1967, Woodburne and Golz 1972, Morton and Miller 2006). The composite section of the Crowder Formation contains 980 m of continental sandstone and conglomerate alternating with fine-grained sandstone and siltstone beds (Foster 1980, Winston 1985). The Cajon Valley Formation is approximately 2,440 m thick and primarily composed of arkosic sandstone and conglomerate with greater lithologic variation, lateral continuity, and sediment induration than the Crowder Formation (Woodburne and Golz 1972, Meisling and Weldon 1989).

Based on lithologies, clast composition, sedimentary structures, and bedforms, the depositional environments for the Crowder and Cajon Valley formations are interpreted as fluvial in nature, with features most closely resembling braided channel and floodplain systems in extensional basins (Woodburne and Golz 1972, Foster 1980, Winston 1985, Meisling and Weldon 1989). Exposures of the Crowder and Cajon Valley formations extend laterally for 35 km and 20 km, respectively, suggesting deposition in broad basins over a low-relief landscape of eroded crystalline bedrock (Noble 1954, Woodburne and Golz 1972, Weldon 1986). For both

formations, clast lithologies and cobble imbrication indicate paleocurrent directions with southward and southwestward transport of sediment from terranes in the Mojave Block and Victorville highlands to the north (Woodburne and Golz 1972, Foster 1980). Fining-upward lithologies and the presence of lignites and limestone beds in the southeastern portion of the Cajon Formation imply gradual infilling of basins over a southwest-draining paleoslope (Foster 1980, Weldon 1986, Meisling and Weldon 1989). In the Crowder and Cajon Valley formations, mammal fossils are typically associated with finer-grained sandstone and siltstone beds that often contain clays, evidence of root traces, and other pedogenic features (Winston 1985, Reynolds 1991).

Paleoenvironmental reconstructions

We integrated data from phytolith assemblages, preserved soil organic material (SOM), and elemental geochemistry of paleosols to reconstruct the vegetation and paleoclimate of the Crowder and Cajon Valley formations. Although lignites and *Celtis* seeds present in Unit 5 of the Cajon Valley Formation provide an indication of wet, forested habitats during the Barstovian (Woodburne and Golz 1972, Reynolds 1991), the plant macrofossil and phytolith records of the Cajon Valley and Crowder formations were otherwise previously unknown. Phytoliths are silica bodies formed within the cells of several vascular plant groups and are readily incorporated into soils during plant decay (Piperno 1988). Phytoliths have high preservation potential, especially in paleosols, which are often devoid of plant macrofossils and palynomorphs (Strömberg 2004), and have been the basis for recognizing major vegetation shifts in the past, such as the regional expansion of North American grassland ecosystems through the Cenozoic (e.g., Edwards et al. 2010, Strömberg and McInerney 2011). Distinct phytolith morphotypes are useful for identifying

plant sources at various taxonomic levels, and distinguishing among woody vegetation (e.g., forest), C_3-grass, and C_4-grass indicator taxa (Strömberg 2004, Piperno 2006). Representational biases have been documented in modern phytolith assemblages compared to aboveground biomass and may lead to the overestimation of grass indicators within an ecosystem. However, correction factors specific to soil type have been determined to calibrate phytolith assemblages to percent vegetation cover (Hyland et al. 2013).

The relative abundance of C_3 and C_4 vegetation in an ecosystem can also be recorded by the carbon stable isotopic composition, expressed as $\delta^{13}C$, of preserved soil organic matter (e.g., Koch 1998). In terrestrial settings, photosynthetic pathway is the dominant control on vegetation $\delta^{13}C$ values, with C_3 plants strongly discriminating against ^{13}C during CO_2 fixation relative to C_4 plants (e.g., Smith and Epstein 1971), and results in distinct, non-overlapping carbon isotopic composition for these groups (Cerling et al. 1997). Enrichment factors for C_3 and C_4 vegetation relative to atmospheric CO_2 are -19.6‰ and -4.7‰, respectively (Passey et al. 2002). A potentially confounding factor in estimating the relative proportions of C_3 and C_4 vegetation based on $\delta^{13}C_{SOM}$ can arise under changing moisture conditions. Variation around mean $\delta^{13}C_{C3}$ is related to aridity, with decreased fractionation of atmospheric CO_2 during photosynthesis under water stress (Farquhar et al. 1989, Cerling and Harris 1999, Passey et al. 2002). A significant negative relationship between foliar carbon isotopic composition and mean annual precipitation (MAP) has been documented for modern C_3 plants; therefore, within pure-C_3 ecosystems, variation in $\delta^{13}C_{SOM}$ can be used to infer relative moisture (Diefendorf et al. 2010, Kohn 2010). Together, phytolith assemblages and $\delta^{13}C_{SOM}$ data can differentiate ecosystem shifts due to changing C_4 vegetation or moisture conditions.

For comparison, quantitative paleoprecipitation (MAP) estimates can be derived from the elemental geochemistry of paleosols. Based on the relationship between the chemical index of alteration minus potassium (*CIA-K*; Maynard 1992) and mean annual precipitation in modern soils, the following transfer function has been developed (Sheldon et al. 2002):

$$\text{MAP (mmyr}^{-1}) = 221.1e^{0.0197(CIA-K)} \quad (1)$$

(SE = ±182 mm yr^{-1}, $R^2 = 0.72$).

This method has been applied broadly to Miocene paleosols (e.g., Retallack 2007), and compares well to independent paleoprecipitation estimation methods (e.g., Wilf 1997).

MATERIALS AND METHODS

Field methods

In the Crowder Formation, we measured one composite stratigraphic section (~110 m) through upper Unit 1 and Unit 2 east of Interstate 15 in Cajon Pass (Fig. 3.1). In the Cajon Valley Formation, we measured northwestern (CV-NW) and southeastern (CV-SE) sections (~850 m each) from continuous exposures of Units 3 and 5 along railroad cuts west of Interstate 15 and north and south of Highway 138, respectively (Fig. 3.1). Unit 4 occurs discontinuously or may be a lateral facies of the more widespread Unit 5 elsewhere in the formation (Woodburne and Golz 1972) and was not present in either of the measured sections. The Cajon Valley sections are approximately three kilometers apart, although at least one fault, the Cleghorn Fault, associated with the San Andreas Fault System, separates them (Morton and Miller 2006). We selected the locations of the sections to incorporate as many previously sampled San Bernardino County Museum and University of California-Riverside fossil localities as possible and to follow sections sampled in earlier paleomagnetic studies (Woodburne and Golz 1972, Winston 1985,

Weldon 1986, Liu 1990, Reynolds et al. 2008). Unit thicknesses and boundaries in measured sections are similar to the sections from which paleomagnetic data were collected, thereby enabling age inference of stratigraphic units and rock samples.

We collected samples for bulk SOM, phytoliths, and elemental geochemistry analyses from the finer-grained beds exhibiting features of paleosol development (e.g., high clay content, slickensides, root traces, carbonate development). Because the tops of paleosols typically preserve the most phytoliths (Strömberg 2002) and SOM can become enriched in ^{13}C at depth due to microbial decomposition (Wynn et al. 2005), we collected fresh samples from the most clay-rich upper paleosol horizon with the highest concentration of root traces, when present. We collected 28 samples from the Crowder section, every 4.5 m on average and ranging from 0.3 to 27.0 m apart, depending on paleosol distribution and development. From the CV-SE and CV-NW sections, we collected 34 and 42 samples, respectively. The sampling interval varied in relation to the distribution of paleosols and was on average every 23.0 m for CV-SE and 11.0 m for CV-NW. From these field samples, we selected a subset of paleosols for further laboratory analysis (n = 53) based on clay content, presence of visible SOM, absence of contaminants (e.g., modern roots), and association with fossil-bearing horizons.

Laboratory methods

We processed paleosol samples for phytolith extraction (n = 24) according to the methodology of Strömberg et al. (2007). Following disaggregation by dissolution in 10% HCl, 1–2 g of homogenized sample material were sieved at two different mesh sizes, 250 μm and 53 μm, and cleaned of organic matter using a concentrated solution of HNO_3 and KCl. We then separated the biosilica fraction of the sample via $ZnBr_2$ heavy-liquid floatation (2.38 g cm^{-3}) and

mounted the extracts on slides using Cargille Meltmount 1.539. Slides were analyzed and photographed using a Leica petrographic microscope at a range of magnifications (400-1000x). For samples yielding countable assemblages (>200 diagnostic phytoliths, $n = 22$), we categorized phytoliths by plant functional group based on morphotypes documented in modern reference collections of Strömberg (2003, 2005). Forest Indicators (FI) include dicots, conifers, woody plants (e.g., shrubs), and palms, while Grass Indicators (GI) include both C_3 grasses (e.g., pooids) and C_4 grasses (PACMAD, panicoid, and chloridoid groups).

For carbon isotopic analysis of organic matter, we selected and cleaned bulk paleosol samples ($n = 53$) in methanol to remove modern carbon and in dilute (7%) HCl to dissolve carbonates (e.g., Cotton et al. 2012). We then crushed samples to homogenize them and weighed them in tin capsules. We analyzed samples for weight percent carbon and $\delta^{13}C_{SOM}$ using a Costech elemental analyzer attached to a Finnigan Delta V+ isotope ratio mass spectrometer at the Stable Isotope Laboratory at the University of Michigan. Results are reported in units per mil relative to Vienna Pee Dee Belemnite (VPDB). International Atomic Energy Agency (IAEA) sucrose and caffeine standards were used to normalize measured values to VPDB, with a standard analytical error of less than 0.1‰. We conducted replicate analyses for >25% of the samples, resulting in an average sample standard error of ~0.5‰. We analyzed clay-rich Inceptisol samples from the Crowder and CV-SE sections ($n = 4$) for major elemental composition via X-ray fluorescence (XRF). XRF analyses of whole-rock samples were conducted at the ALS Chemex Lab in Vancouver, BC, Canada, with an average analytical uncertainty of 0.001% and a replicate standard deviation of 0.1%.

Quantitative inference

Based on countable phytolith assemblages from the Crowder (n = 8), CV-SE (n = 7), and CV-NW (n = 7) sections, we estimated the percentages of forest, C_3-grass, and C_4-grass indicators as a fraction of the total diagnostic morphotypes, with counting errors estimated via a bootstrapping program (Chen et al. 2015). Bias towards a greater abundance of grass morphotypes compared to other vegetation types has been documented in modern soils (Hyland et al. 2013); however, this bias is minor in Inceptisols (1.7%), which is the predominant paleosol type in the Cajon Valley and Crowder formations, and is generally smaller than the phytolith counting error for the paleosols examined here. Therefore, it was not necessary to apply correction factors to the phytolith counts, and we interpreted the relative proportion of grass phytoliths in these paleosol samples as the relative abundance within the local environment.

To compare paleosol $\delta^{13}C_{SOM}$ with the carbon isotopic composition of C_3 and C_4 vegetation during the middle Miocene, we adjusted the isotopic composition of end-member C_3 and C_4 values according to the average $\delta^{13}C$ composition of atmospheric CO_2 for 1-million year time bins through the MCO, based on benthic foraminifera reconstructions from Tipple et al. (2010; 3-myr moving average values). We applied a Spearman's correlation test to assess the significance of $\delta^{13}C_{SOM}$ trends in relation to stratigraphic thickness as a measurement of elapsed time. We calculated mean annual precipitation values based on the *CIA-K* proxy determined from elemental compositions of Inceptisol samples (Sheldon et al. 2002).

To compare paleoenvironmental reconstructions with mammalian faunas of the Crowder and Cajon Valley formations, we compiled fossil data from various publications, field reports, and database records from the San Bernardino County Museum (Table S3.1). Specimens had been identified to taxonomic family, and when possible to genus and species based on distinct

morphological features, typically of the dentition (Woodburne and Golz 1972, Reynolds 1991, Pagnac 2006, Reynolds et al. 2008). Local species biostratigraphic ranges were determined by the stratigraphic position of fossil localities and the assumption that species ranged through gaps in fossil preservation. Species diversity through time for the Crowder and Cajon Valley formations was tallied based on the temporal duration of species within each basin.

RESULTS

Stratigraphic framework

Sections measured in the Crowder and Cajon Valley formations span the Hemingfordian to Barstovian transition and record local environmental conditions and faunal assemblages during the MCO (Figs. 3.2 and 3.3). Unit 1 of the Crowder Formation (17.0−15.5 Ma) is primarily composed of massive and poorly sorted medium to coarse arkosic sandstone with conglomeratic lenses of heterogeneous subrounded to subangular clasts (Fig. 3.2). Sandstone beds are 2.9 m thick on average (range is 0.2−26.0 m) and persist laterally for several hundred meters. Conglomeratic lenses are typically 3.0–6.0 m across and up to 1.0 meter thick and can exhibit graded bedding, cobble imbrication, and planar and trough cross-bedding. Laterally extensive tabular beds of laminated siltstone and fine sandstone with notable clay content are a distinct feature of upper Unit 1. The tops of these thin beds are generally altered by pedogenesis, and when paleosols could be identified to soil order, features most closely matched those of Inceptisols. We interpret these thick sandstone beds with channel macroform deposits (e.g., bars and dunes) as a series of active, low-sinuosity streams (Collinson 1978, Foster 1980, Winston 1985). The contact between Units 1 and 2 is sharp (estimated ~15.5 Ma). Unit 2 is composed of arkosic wacke with a higher content of fine sandstone, sandy siltstone, and claystone than Unit 1.

Thick fine-grained beds are laterally persistent with lenses of more indurated coarse sandstone and well-rounded pebbles, as well as small-scale, cut-and-fill structures and gravel-stringer deposits. These sandstone lenses represent channel deposits incised into the lower fine-grained floodplain deposits. Sand is dispersed throughout the silty-claystones, including within lenticular clay-rich units that display red and green mottling and other pedogenic features. The transition from the sandstone-dominated Unit 1 to the silt and claystone-dominated Unit 2 represents the transition from a sandy braided-river system to a lower gradient meandering floodplain system with more interchannel sediments preserved (Collinson 1978, Foster 1980, Winston 1985). Paleosols throughout upper Unit 1 and Unit 2 represent surfaces exposed between flooding events and are the primary source of fossils recovered from the Crowder Formation.

In contrast, roughly contemporaneous Units 3 and 5 of the Cajon Valley Formation represent significantly more lithological variation over space and through time (Fig. 3.3). Unit 3 contains several sequences of well-indurated, light-colored coarse sandstones and conglomerates alternating with less resistant, reddish-brown, finer-grained sandstones and siltstones that often preserve pedogenic features. Within the measured sections, Unit 5 overlies Unit 3 and contains a sequence of heterogeneous beds. Unit 5 in the southeastern section includes mottled maroon, gray, and yellow coarse sandstones and conglomerates, green siltstones, and black mudstones with localized plant-bearing lignite beds and freshwater limestones. Unit 5 in the northwestern section is lithologically similar, but lacks the mudstone, lignite, and limestone beds (Woodburne and Golz 1972).

Approximately 850 m of sediment were deposited in the Cajon Valley Formation from ~16.5–13.7 Ma, indicating a higher rate of sediment accumulation than for the Crowder Formation. In the CV-SE section, the dominant sandstone beds are 3.7 m thick on average and

range from 0.3 to 23.0 m. In the CV-NW section, these beds are 2.9 m thick on average and range from 0.2 to 43.5 m. Tabular sandstone beds can display large-scale (up to several meters) trough cross-bedding, imbricated cobbles, and basal scouring. The tops of sandstone beds exhibit typically weak pedogenic horizons, and are noted for distinct color changes (red or mottled purple and green), greater clay content, and prominent post-depositional features, such as drab-haloed root traces. The transition from Unit 3 to Unit 5 (~15.0 Ma) is a gradual increase in the frequency of sandstone and red paleosol alternations. Unit 5 is composed of heterogeneous strata with great color variation, but few red paleosol horizons. Units 3 and 5 comprise many tabular channel units and are consistent with a bed-load dominated, braided-stream system with periodic soil development (Collinson 1978). The presence of freshwater limestones and lignites containing plant debris and diatoms in the southeastern section indicate spatial variation in depositional environments across the basin, with localized pond development in the topographic low of the basin center, compared to continuous active-channel deposits in the more marginal northwestern portion of the basin (e.g., Woodburne and Golz 1972, Foster 1980).

Mammalian faunal assemblages

The contact between Crowder Formation Units 1 and 2 is accompanied by a faunal turnover and decline in number of species within fossil assemblages (Fig. 3.2). The mammalian faunas of the Crowder Formation are dominated by small-mammal species (n = 21, including 15 rodent species) and include several exceptionally diverse assemblages (e.g., 21 species within a single paleosol at the base of the section; Table 3.1). Each paleosol horizon in the section was sampled during road construction as a single locality and screen-washed for fossils (approximately 2,700 kg of matrix were extracted and screen-washed per horizon for a total of

75,750 kg; Reynolds et al. 2008). Therefore, changes in small-mammal diversity and taxonomic composition among paleosol horizons should not be due to differential sampling effort (Reynolds 1991, Reynolds et al. 2008) and can be compared to corresponding changes in the depositional environment, vegetation, or local climate.

The faunal composition of both the southeastern and northwestern sections of the Cajon Valley Formation is dominated by large mammals, with several species of horses, including the Hemingfordian *Parapliohippus carrizoensis* and the Barstovian *Scaphohippus intermontanus* (Table 3.2). Despite high sampling effort, small-mammal taxa are less common in the Cajon Valley Formation than in the Crowder Formation, perhaps due to differences in taphonomic processes. Taxonomic richness is fairly constant throughout the measured section, with the exception of two rich localities that record the sole occurrences of several taxa, including most of the small-mammal species (Fig. 3.3).

Vegetation composition and paleoprecipitation

Phytolith assemblages (n = 8) of the Crowder Formation yielded morphotypes that include forest, C_3-grass, and C_4-grass indicators (Fig. 3.4a). Phytoliths from C_4 grasses contributed a small percentage to the overall vegetation composition (1–4%); notably, these phytoliths provide the earliest record of C_4 grasses in the Mojave Region at approximately 17.0 Ma. The phytolith assemblages contain roughly equal proportions of grass and forest morphotypes throughout the section, suggesting locally stable and mixed open-habitat vegetation during climatic warming from 17.0–15.0 Ma. Diagnostic forest indicators include six dicot morphotypes and a palm morphotype, while C_3-grass indicators comprise seven distinct morphotypes, including four pooid groups. C_4-grass morphotypes include one PACMAD, one

chloridoid, and two panicoid morphotypes. $\delta^{13}C_{SOM}$ values for the Crowder Formation range from -26.3‰ to -22.0‰ (Fig. 3.4b, Table S3.2). Using more enriched $\delta^{13}C_{CO2}$ values during the MCO (-5.85‰ to -5.27‰; Tipple et al. 2010), these values also indicate that the sequence of environments was dominated by C_3 vegetation. Given that variation in $\delta^{13}C_{SOM}$ cannot be attributed to major changes in the proportions of C_3 and C_4 phytoliths through time in the Crowder Formation, carbon isotopic shifts can instead represent changes in local moisture conditions. A significant positive trend in $\delta^{13}C_{SOM}$ indicates drying in the basin through the MCO (Spearman's $r = 0.68$, $p < 0.01$). An elemental-geochemical (*CIA-K*) estimate of MAP for the base of the section is 807 (±182) $mmyr^{-1}$, implying a relatively wet ecosystem at ~17.0 Ma (Fig. 3.4b, Table S3.3). The drying trend after 17.0 Ma is most striking during the Barstovian interval, and coincides with faunal turnover and a decline in the taxonomic richness of mammalian assemblages from the Crowder Formation (Fig. 3.2).

Phytolith samples from the southeastern section of the Cajon Valley Formation (CV-SE; $n = 7$) record a mixture of forest and C_3-grass indicator types, with a slight increase from 24% to 45% in grass indicators through the section (Fig. 3.5a). Phytolith assemblages indicate more wooded habitats in the southeastern portion of the Cajon Valley Formation, with a higher percentage of forest indicators (55–76%) than in the Crowder Formation (~50%). Phytolith assemblages from this section comprise six forest indicator morphotypes and six C_3-grass morphotypes, including three pooid groups. The carbon isotope composition of this section indicates a pure-C_3 environment, with $\delta^{13}C_{SOM}$ ranging from -28.0‰ to -23.7‰ (Fig. 3.5b, Table S3.2). These values are both more negative and more variable than the carbon isotope composition of soil organic matter from the Crowder Formation, consistent with the absence of C_4 vegetation, wetter conditions (i.e., lignites and freshwater limestones present), and greater

lithological variation. There was no significant trend in $\delta^{13}C_{SOM}$ corresponding with the increase in phytolith grass indicators through the section (Spearman's $r = 0.20$, $p = 0.44$). However, the base of the section shows a large positive shift in $\delta^{13}C_{SOM}$ (~4.0‰) around 16.0 Ma that is consistent with the $\delta^{13}C_{SOM}$ shift and drying trend in the Crowder Formation at that time. The *CIA-K* index for three late Hemingfordian Inceptisols supports an average MAP estimate of 765 (±182) $mmyr^{-1}$ for the southeastern part of the basin (Fig. 3.5b, Table S3.3).

In contrast, phytolith assemblages from the northwestern section of the Cajon Valley Formation (CV-NW; $n = 7$) record a greater proportion of forest indicators (64–84%) than in CV-SE or Crowder assemblages (Fig. 3.5a). Six forest and six C_3-grass morphotypes are present throughout the section, and individual assemblages are similar to or slightly more diverse than those from the southeastern section. $\delta^{13}C_{SOM}$ values range from -23.2‰ to -20.2‰ and do not overlap with values from the southeastern section (Fig. 3.5b, Table S3.2). Assuming an arid C_3-endmember value, $\delta^{13}C_{SOM}$ values above -22.0‰ should indicate the presence of C_4 grasses; however, these grasses are not found in the phytolith assemblages from the same paleosol samples. Therefore, $\delta^{13}C_{SOM}$ from CV-NW is likely recording a C_3 ecosystem in a more arid environment of the basin (Diefendorf et al. 2010, Kohn 2010) and the local presence in low abundance of C_4 grasses that are not preserved in the phytolith record. There was no significant trend in $\delta^{13}C_{SOM}$ over time (Spearman's $r = -0.35$, $p = 0.29$) and only a slight increase in the abundance of grass indicators (19% to 37%). The higher abundance of forest-indicator phytoliths and more enriched isotopic composition of soil organic matter in the CV-NW compared to the CV-SE section suggest the presence of a strong gradient in vegetation and water stress over at least three kilometers and C_4 grasses in the northwest of the basin.

DISCUSSION

Spatio-temporal variation in paleovegetation

The Crowder and Cajon Valley formations provide a record of paleoenvironment, vegetation distribution, and faunal assemblages during a major climate-warming interval. Independent evidence from phytolith assemblages and carbon isotope composition of soil organic matter indicate primarily C_3 ecosystems within the Crowder and Cajon Valley formations, with spatial and temporal variability in C_4-grass presence and the relative abundance of grasses in the vegetation recorded in the three sections. The consistently low abundance of PACMAD, panicoid, and chloridoid phytoliths in the Crowder Formation provides the earliest evidence of C_4 grasses in the Mojave region. Based on $\delta^{13}C_{SOM}$, we also infer a low abundance of C_4 grass in the northwest section of the Cajon Valley Formation. The vegetation of the Crowder Formation was less forested (~50% grass morphotypes) than in either section of the Cajon Valley Formation; however, both Cajon Valley sections show a slight increase in the proportion of grass morphotypes in phytolith assemblages during the MCO. An increase in grasses can imply increasing aridity, as grasses are more drought-tolerant than most arborescent angiosperms (Edwards et al. 2010). The modest shift in paleoenvironmental conditions in response to global warming through the MCO may be moderated by presence of the fluvial system itself, making the aridity response we do find more striking, or due to the coastal proximity of these basins prior to the uplift of the Transverse Ranges in the late Miocene to early Pliocene (Meisling and Weldon 1986, Vallis 2011). Differences in phytolith assemblages between the two Cajon Valley sections indicate lateral variation in vegetation with a higher proportion of forest cover in the northwestern portion of the basin. However, some phytolith morphologies are produced by both trees and woody shrubs, making the distinction between

forest and shrubland ecosystems difficult to determine (Cotton et al. 2014). Together, alternating active channel deposits and weakly-developed paleosol horizons, enriched $\delta^{13}C_{SOM}$, and higher abundances of forest-indicator phytoliths in the CV-NW section likely represent a shrubland ecosystem with a small amount of C_4 grass in an arid, well-drained environment along the basin margin. In contrast, the CV-SE section represents a poorly-drained, mixed C_3 wooded-grassland ecosystem with shallow freshwater and swamp deposits near the basin depocenter.

Although there is little plant macrofossil material known from the Crowder and Cajon Valley formations with which to evaluate floral composition further, the vegetation structure inferred from phytoliths agrees with plant fossil localities of similar age elsewhere in the Mojave Desert, including the Barstow Formation. The Barstow Formation has a sparse plant fossil record that includes both forest (palms and woody dicots, including potential pine, walnut, hackberry, and juniper species) and grassland components (Alf 1970, Reynolds and Schweich 2013, Reynolds and Schweich 2015). The presence of C_4 grasses in the Barstow Formation by 14.3 Ma is documented from the isotopic composition of ungulate tooth enamel, with equids recording up to 18% C_4 dietary composition (Feranec and Pagnac 2013). The contemporaneous Tehachapi Flora (15.5–11.8 Ma) on the western edge of the Mojave region was also a woodland, with temperate oaks, conifers, palms, and several sclerophyllous shrub taxa (Axelrod 1939, 1979).

The vegetation of the Crowder and Cajon Valley formations also corresponds with broad-scale trends in regional vegetation composition across western North America. During the middle Miocene, Basin and Range floras indicate predominantly warm-temperate evergreen and deciduous hardwood forests, while broad-leaf evergreen forests expanded to at least 45°N along the Pacific Coast of North America (Wolfe 1981, Wolfe 1985, Pound et al. 2012). After the MCO, a progressive spread of savanna, woodland, and shrubland paralleled global cooling and

regional aridification (Wolfe 1985, Leopold and Denton 1987). The Crowder and Cajon Valley records also match other paleoenvironmental reconstructions based on phytoliths in the Basin and Range Province, which indicate a mix of grassy and wooded patches throughout the early to middle Miocene and a subsequent spread of grasslands during the late Miocene (Strömberg 2005, Strömberg and McInerney 2011). The small but measurable proportion of C_4 grasses in the phytolith assemblages of the Crowder Formation and inferred from the $\delta^{13}C_{SOM}$ values of the Cajon Valley Formation (CV-NW) documents the patchy distribution of these grasses across the landscape prior to their expansion across western North America (Edwards et al. 2010, Strömberg 2011). The primary driver of C_4-grass expansion globally remains unresolved, although recent studies have documented temporal and regional variation in this expansion, suggesting that multiple factors may lead to increasing C_4 grass proportions across ecosystems (Edwards et al. 2010, Fox et al. 2012). Spatial heterogeneity of C_4 grasses between the Crowder and Cajon Valley basins supports the hypothesis that the differential expansion of C_4 ecosystems was influenced by local factors instead of global climate and CO_2 drivers (Fox and Koch 2003, Strömberg and McInerney 2011, Cotton et al. 2012, Chen et al. 2015). Integration of phytolith and $\delta^{13}C_{SOM}$ data provides a multi-proxy reconstruction of the middle Miocene Mojave vegetation, and facilitates the distinction between open, closed, and mixed C_3-dominated ecosystems, and between water-stressed C_3 vegetation and a low abundance of C_4 on the landscape.

Terrestrial paleoclimate reconstructions for the MCO

Terrestrial temperature records during the MCO indicate that mean annual temperatures were 6.8 ± 2.2°C warmer than today on average, although there is considerable variation in

paleotemperature estimates depending on geographic location and the temperature proxy used (Goldner et al. 2014). The oxygen and hydrogen isotopic composition of smectites from the Barstow Formation between 15.8 and 14.8 Ma yield average annual temperature estimates of 26.0°C, or ~8.0°C warmer than mean annual temperatures today (Mix et al. 2014). Although we did not obtain paleotemperature estimates for the Crowder and Cajon Valley formations, paleoprecipitation estimates of 807 (±182) and 765 (±182) $mmyr^{-1}$, respectively, during this warm interval agree with other regional records (Wolfe 1985, Sheldon 2006, Pound et al. 2012). Based on the composition of fossil-plant assemblages, Basin and Range Province precipitation ranged from 381-635 $mmyr^{-1}$ in temperate xerophytic shrubland (Axelrod 1939) and 760-890 $mmyr^{-1}$ in mixed-forest ecosystems (Axelrod 1995). MAP estimates derived from the elemental geochemistry (*CIA-K*) of paleosols from the Picture Gorge Basalts of central Oregon (USA) decreased from 900 to 500 $mmyr^{-1}$ during the second half of the MCO, indicating Miocene aridification in the northern Basin and Range (Sheldon 2006). Although we did not have enough Inceptisol samples throughout our sections to test for drying trends based on the *CIA-K* proxy, increasing $\delta^{13}C_{SOM}$ values in the Crowder Formation and increasing proportion of grass indicators in the Cajon Valley Formation provide additional support for a transition to drier climates and associated grassland expansion throughout the middle Miocene.

Environmental significance for mammalian faunas

Linking paleoenvironmental reconstructions with changes in taxonomic richness and composition of mammalian faunas requires dense and well-resolved records for fossil assemblages, vegetation, and paleoclimate. Changes in taxonomic richness in the Cajon Valley Formation are likely controlled by differences in fossil preservation and sampling. Two species-

rich localities near the base of Unit 3 and top of Unit 5 are the only departures from otherwise fairly constant species richness and are the source of most small-mammal taxa from the Cajon Valley Formation (Fig. 3.3). Despite this taphonomic bias, small-mammal assemblages differ significantly between Unit 3 (early Barstovian) and Unit 5 (late Barstovian), suggesting turnover in faunal composition through the MCO. Paleoenvironmental reconstructions based on the phytolith and $\delta^{13}C_{SOM}$ records of the Cajon Valley Formation indicate a warm, wet climate and a shift to more open vegetation through the depositional history of the basin (Fig. 3.5), influencing habitat conditions and dietary resources for mammalian faunas (e.g., Janis et al. 2004). Large- and small-mammal faunas contained taxa inferred to be mixed feeders that included browse and grass in their diets (e.g., equids, including *Acritohippus stylodontus*), browsers (e.g., chalicothere, *Moropus*) and small granivores (e.g., heteromyid rodents; Korth 1994, Janis et al. 2005). A braided-stream system crossing an alluvial plain in an extensional basin (e.g., Foster 1980, Weldon 1986) could have supported high faunal diversity, in particular across strong spatial gradients in vegetation and moisture from the shrublands on the more arid basin margin to the mixed wooded-grasslands in the moist, and occasionally swampy, basin center.

The Crowder Formation differs strikingly from the Cajon Valley Formation in that numerous small mammal species occur continuously over several stratigraphic levels, suggesting a fairly diverse and stable faunal composition through the Hemingfordian to early Barstovian interval of the MCO (~17.0–15.7 Ma; Fig. 3.2). The most prominent change in species composition and decline in taxonomic richness in the Crowder Formation involved small mammals at ~16.0 Ma (large-mammal fossils are rare, except in the oldest localities, perhaps due to taphonomic or sampling bias). This faunal change coincided with a notable change from predominantly active channel deposits with intermittent and weakly-developed paleosols (upper

Unit 1) to more frequent and well-developed paleosols (Unit 2) within the transition from a braided-stream system to a floodplain-dominated system (e.g., Foster 1980, Winston 1985). The faunal changes and inferred change in the depositional environment at ~16.0 Ma also correspond with a significant positive shift in the carbon isotope record (Fig. 3.4). Phytolith assemblages through the Crowder Formation consistently record a mixed forest-grassland ecosystem with a low percentage of C_4 vegetation, indicating that the carbon isotope enrichment at this time was influenced by changes in climate rather than in vegetation. Therefore, mammalian faunal turnover and decline could be linked to increasing aridity in the Crowder Basin during the MCO.

Regional mammal diversity and faunal composition

The Crowder and Cajon Valley formations document faunal and vegetation composition during the MCO, including the Hemingfordian interval that is rare elsewhere in western North America, and contribute to our understanding of biological responses to changes in the global climate and local landscape (Barnosky and Carrasco 2002, Barnosky et al. 2007, Finarelli and Badgley 2010). This record from the Mojave region provides evidence that elevated regional diversity during the MCO was composed of both high alpha- (local) and beta- (variation across space) diversity. Diverse rodent assemblages (up to 10 co-occurring species) characterize the Crowder Formation and include seven species of heteromyid rodents and six sciurid genera. Camelid and equid species are the dominant large-mammal taxa within the Crowder Formation. Small-mammal taxa of the Cajon Valley Formation belong to several rodent families, including heteromyids, sciurids, cricetids, eomyids, and geomyids (Reynolds 1991, Lindsay and Reynolds 2008, Reynolds et al. 2008). The Cajon Valley Formation fossil assemblages also contain a diverse large-mammal fauna, including four equid genera, the chalicothere *Moropus*, the

oreodont *Brachycrus*, palaeomerycids such as *Bouromeryx*, and tayassuids such as *Dyseohyus* (Woodburne and Golz 1972, Pagnac 2006, Coombs and Reynolds 2015). Taxonomic similarity is low between the two formations (15 shared taxa out of 59 total) despite significant temporal overlap (inferred ages indicate overlap from ~16.5 to 15.0 Ma), suggesting spatial variation in faunal composition over tens of kilometers. Faunal similarity between the two formations is comparable for both small and large mammals (Tables 3.1 and 3.2).

Not only do the Crowder and Cajon Valley fossil records differ from one another, contributing to high alpha- and beta-diversity, but they also differ from contemporaneous records elsewhere in the Mojave region. These formations overlap temporally with the Upper Hector Formation in the Cady Mountains and the Barstow Formation within the Mud Hills and vicinity, both of which represent more inland depositional environments (Woodburne 1991). The Hector Formation spans late Arikareean to late Hemingfordian NALMAs from ~22.9–16.0 Ma (Woodburne et al. 1974, Woodburne 1998). The youngest faunal assemblage, the Upper Cady Mountain Fauna, is late Hemingfordian in age, overlapping with the time represented in the Crowder and Cajon Valley formations (Woodburne 1991). This fauna has only ~8 species, composed of taxa shared with the Crowder and Cajon Valley Hemingfordian assemblages, such as *Proheteromys sulculus*, *Parapliohippus carrizoensis*, cf. *Merycodus* and Rhinocerotidae (Miller 1980, Woodburne 1998). However, several taxa are found in the Hector Formation but not in the Crowder or Cajon Valley formations, including the beaver cf. *Anchitheriomys* and the canid *Tomarctus*, suggesting low faunal similarity between the Hemingfordian fossil record of the Cady Mountains and that of the Crowder and Cajon Valley formations.

Faunas of the Barstow Formation contemporaneous with faunas of the Crowder and Cajon Valley formations are younger than the Upper Cady Mountain Fauna and include the Red

Division (16.7 Ma), Rak Division (16.7-16.0 Ma), Green Hills (16.0–15.3 Ma), Second Division (15.3–14.8 Ma), and lower First Division (14.8–13.4 Ma) faunas (Lindsay 1972, Woodburne et al. 1990, Pagnac 2009). Differences in small-mammal composition are especially striking. The late Hemingfordian Red Division faunal assemblage lacks a small-mammal record; however, the otherwise diverse small-mammal faunas of the Barstow Formation and Crowder Formation have a greater number of unique genera and species than they do shared species (Lindsay 1972, Lindsay 1995). Although small-mammal faunas of the Cajon Valley Formation are less diverse, they also contain species not found in the Barstow Formation, including the large-bodied heteromyid, *Harrymys maximus* (Lindsay and Reynolds 2015). Large-mammal faunas are broadly similar across the three formations, suggesting lower spatial turnover for large mammals than for small mammals in the region, as occurs today. However, the Barstow Formation has a significantly more diverse large-mammal record, including several canid, oreodont, amphicyonid, and artiodactyl species not found in the Crowder and Cajon Valley formations (Woodburne et al. 1990, Wang et al. 1999, Pagnac 2009). Low faunal similarity across these regions aligns with previous observations that the MCO was an interval of high zoogeographic provinciality in western North America, as interactions between climate change and tectonic activity intensified biogeographic and macroevolutionary processes (Tedford et al. 2004, Badgley and Finarelli 2013).

CONCLUSIONS

The middle Miocene was a significant interval of local to regional landscape and climate change, including tectonic extension and the development of topographic complexity in western North America and the Miocene Climatic Optimum warming period. Peak mammal diversity for

the entire Great Basin occurred during this interval (e.g., Badgley et al. 2014); however, the processes by which this high diversity originated and was maintained (e.g., by increased faunal turnover through time and over space in response to climate warming and increasing topographic and habitat heterogeneity) remain unresolved. By coupling paleoenvironments and faunal assemblages over space and time, this study contributes to our understanding of faunal response and the geographic structure of habitat heterogeneity and mammalian diversity during significant climate and habitat change.

The Crowder and Cajon Valley formations provide new paleoenvironmental and faunal information, most notably during the initial MCO warming for which records are currently sparse in western North America. At least 59 mammalian taxa have been collected from these formations, and three stratigraphic sections document changes in depositional environments through time. The integration of phytolith, carbon isotope composition of preserved soil organic matter, and paleosol-derived mean annual precipitation proxies provides a detailed reconstruction of spatially and temporally varying paleoenvironmental conditions. These formations record formerly mesic (MAP = ~800 $mmyr^{-1}$) ecosystems, the development of increasingly arid conditions, the opening of mixed forest-grassland ecosystems, and the earliest evidence of C_4 grasses within the Mojave Desert region and more broadly across the intermontane west.

The Crowder and Cajon Valley formations document distinct depositional environments and faunal assemblages compared to the nearby Barstow Formation. Mammalian response to environmental change is evident in the Crowder Formation, which records faunal turnover and declining diversity of small mammals in relation to a drying trend in the basin. Low faunal similarity between the Crowder, Cajon Valley, and Barstow formations imply high beta-diversity

across the landscape, while diverse assemblages, especially of small mammals, in the Crowder and Barstow formations and certain paleosol units of the Cajon Valley Formation indicate high local diversity. Both contributed to increased regional diversity and document the history of mammalian diversity during past warming and landscape change.

ACKNOWLEDGMENTS

We are grateful for the financial support of this research provided by the Society of Vertebrate Paleontology's Patterson Field Research Award and the University of Michigan's Turner Research Program. We thank Catherine Badgley for field guidance and helpful review of this manuscript. We thank Katharine Loughney, Molly Moroz, Michael Woodburne, Lora Wingate, Tim Gallagher, and Symone Bawol for support in the field and in the laboratory. We thank Eric Scott and the San Bernardino County Museum for access to museum database records, as well as William Sapp and the San Bernardino National Forest Service for providing field permits to make this work possible.

REFERENCES

Alf, R.M., 1970. A preliminary report on a Miocene flora from the Barstow Formation, Barstow, California. Bulletin of the Southern California Academy of Sciences 69, 183-189.

Axelrod, D.I., 1939. Miocene flora from the western border of the Mohave Desert. Carnegie Institute Washington Publication 516, 129pp.

Axelrod, D.I., 1979. Age and origin of Sonoran Desert vegetation. Occasional Papers of the California Academy of Sciences 132, 74pp.

Axelrod, D.I., 1995. The Miocene Purple Mountain Flora of Western Nevada. University of California Publications: Geological Sciences 139, 1-63.

Badgley, C., Finarelli, J.A., 2013. Diversity dynamics of mammals in relation to tectonic and climatic history: Comparison of three Neogene records from North America. Paleobiology 39, 373–399.

Badgley, C., Smiley, T.M., Finarelli, J.A., 2014. Great Basin mammal diversity in relation to landscape history. Journal of Mammalogy 95, 1090–1106.

Badgley, C., Smiley, T.M., Loughney, K., 2015. Miocene mammal diversity of the Mojave region in the context of Great Basin mammal history, in: Mojave Miocene, Desert Symposium Field Guide and Proceedings, pp. 119–129.

Barnosky, A.D., Carrasco, M.A., 2002. Effects of Oligo-Miocene global climate changes on mammalian species richness in the northwestern quarter of the USA. Evolutionary Ecology Research 4, 811–841.

Barnosky, A.D., Bibi, F., Hopkins, S.S.B., Nichols, R., 2007. Biostratigraphy and magnetostratigraphy of the mid-Miocene Railroad Canyon Sequence, Montana and Idaho, and age of the mid-Tertiary unconformity west of the continental divide. Journal of Vertebrate Paleontology 27, 204–224.

Cerling, T.E., Harris, J.M., MacFadden, B.J., Leakey, M.G., Quade, J., Eisenmann, V., Ehleringer, J.R., 1997. Global vegetation change through the Miocene/Pliocene boundary. Nature 389, 153–158.

Cerling, T.E., Harris, J.M., 1999. Carbon isotope fractionation between diet and bioapatite in ungulate mammals and implications for ecological and paleoecological studies. Oecologia 120, 347–363.

Chen, S.T., Smith, S.Y., Sheldon, N.D., Strömberg, C.A.E., 2015. Regional-scale variability in the spread of grasslands in the late Miocene. Palaeogeography, Palaeoclimatology, Palaeoecology 437, 42–52.

Collinson, J.D., 1978. Alluvial Sediments, in: Reading, H.G. (Ed.), Sedimentary Environments and Facies. Blackwell Scientific Publications, Oxford, England, pp. 37–82.

Coombs, M.C., Reynolds, R.E., 2015. Chalicothere material (Perissodactyla, Chalicotheriidae, Schizotherinnae) from late Hemingfordian and early Barstovian faunas of the Cajon Valley Formation in the Mojave Desert Province of southern California, in: Mojave Miocene, Desert Symposium Field Guide and Proceedings, pp. 119–129.

Cotton, J.M., Sheldon, N.D., Strömberg, C.A.E., 2012. High-resolution isotopic record of C_4 photosynthesis in a Miocene grassland. Palaeogeography, Palaeoclimatology, Palaeoecology 337-338, 88–98.

Cotton, J.M., Hyland, E.G., Sheldon, N.D., 2014. Multi-proxy evidence for tectonic control on the expansion of C_4 grasses in northwest Argentina. Earth and Planetary Science Letters 395, 41–50.

Dibblee, T.W., 1967. Areal geology of the western Mojave Desert, California. U.S. Geological Survey Professional Paper 522, 153 pp.

Diefendorf, A.F., Mueller, K.E., Wing, S.L., Koch, P.L., Freeman, K.H., 2010. Global patterns in leaf ^{13}C discrimination and implications for studies of past and future climate. Proceedings of the National Academy of Sciences 107, 5738–5743.

Edwards, E.J., Osborne, C.P., Strömberg, C.A.E., Smith, S.A., Bond, W.J., Christin, P.A., Cousins, A.B., Duvall, M.R., Fox, D.L., Freckleton, R.P., Ghannoum, O., Hartwell, J., Huang, Y., Janis, C.M., Keeley, J.E., Kellogg, E.A., Knapp, A.K., Leakey, A.D.B., Nelson, D.M., Saarela, J.M., Sage, R.F., Sala, O.E., Salamin, N., Still, C.J., Tipple, B., 2010. The origins of C_4 grasslands: Integrating evolutionary and ecosystem science. Science 328, 587–591.

Farquhar, G.D., Ehleringer, J.R., Hubick, K.T., 1989. Carbon isotope discrimination and photosynthesis. Annual Review of Plant Biology 40, 503–537.

Feranec, R.S., Pagnac, D., 2013. Stable carbon isotope evidence for the abundance of C_4 plants in the middle Miocene of southern California. Palaeogeography, Palaeoclimatology, Palaeoecology 388, 42–47.

Finarelli, J.A., Badgley, C., 2010. Diversity dynamics of Miocene mammals in relation to the history of tectonism and climate. Proceedings of the Royal Society B: Biological Sciences 277, 2721–2726.

Foster, J. F. 1980. Late Cenozoic tectonic evolution of Cajon Valley, Southern California. Ph.D. thesis, University of California Riverside, 238pp.

Fox, D.L., Koch, P.L., 2003. Tertiary history of C_4 biomass in the Great Plains, USA. Geology 31, 809–812.

Fox, D.L., Honey, J.G., Martin, R.A., Peláez-Campomanes, P., 2012. Pedogenic carbonate stable isotope record of environmental change during the Neogene in the southern Great Plains, southwest Kansas, USA: Carbon isotopes and the evolution of C_4-dominated grasslands. Geological Society of America Bulletin 124, 444–462.

Goldner, A., Herold, N., Huber, M., 2014. The challenge of simulating the warmth of the mid-Miocene climatic optimum in CESM1. Climates of the Past 10, 523–536.

Gradstein, F.M., Ogg, J.G., Smith, A.G., (Eds.), 2004. A Geologic time scale 2004. Cambridge University Press, New York, New York.

Hyland, E., Smith, S.Y., Sheldon, N.D., 2013. Representational bias in phytoliths from modern soils of central North America: Implications for paleovegetation reconstructions. Palaeogeography, Palaeoclimatology, Palaeoecology 374, 338–348.

Janis, C.M., Damuth, J., Theodor, J.M., 2004. The species richness of Miocene browsers, and implications for habitat type and primary productivity in the North American grassland biome. Palaeogeography, Palaeoclimatology, Palaeoecology 207, 371–398.

Janis, C.M., Scott, K.M., Jacobs, L.L., (Eds.), 2005. Evolution of Tertiary Mammals of North America. Cambridge University Press, Cambridge, United Kingdom.

Koch, P.L., 1998. Isotopic reconstruction of past continental environments. Annual Review in Earth and Planetary Science 26, 573–613.

Kohn, M.J., 2010. Carbon isotope compositions of terrestrial C_3 plants as indicators of (paleo) ecology and (paleo) climate. Proceedings of the National Academy of Sciences 107, 19691–19695.

Korth, W.K., 1994. The Tertiary record of rodents in North America. Plenum Press, New York, New York.

Leopold, E.B., Denton, M.F., 1987. Comparative age of grassland and steppe east and west of the northern Rocky Mountains. Annals of the Missouri Botanical Garden 74, 841–867.

Lindsay, E.H. 1972. Small mammal fossils from the Barstow Formation, California. University of California Publications in Geological Sciences 93, 1–104.

Lindsay, E.H., 1995. *Copemys* and the Barstovian/Hemingfordian Boundary. Journal of Vertebrate Paleontology 15, 357–365.

Lindsay, E.H., Reynolds, R.E., 2008. Heteromyid rodents from Miocene faunas of the Mojave Desert, Southern California, in: Wang, X., Barnes, L.G. (Eds.), Geology and Vertebrate Paleontology of Western and Southern North America, Contributions in Honor of David P. Whistler. Natural History Museum of Los Angeles County, Science Series 41, 213–235.

Lindsay, E.H., Reynolds, R.E., 2015. *Harrymys maximus* (James): new interpretation for a Miocene geomyoid rodent, in: Mojave Miocene, Desert Symposium Field Guide and Proceedings, pp. 274–280.

Liu, W., 1990. Paleomagnetism of miocene sedimentary rocks in the Transverse ranges: the implications for tectonic history. Ph.D. thesis, California Institute of Technology. 218pp.

Maynard, J.B., 1992. Chemistry of modern soils as a guide to interpreting Precambrian paleosols. Journal of Geology 100, 279–289.

McQuarrie, N., Wernicke, B.P., 2005. An animated tectonic reconstruction of southwestern North America since 36 Ma. Geosphere 1, 147–172.

Meisling, K.E., Weldon, R.J., 1989. Late Cenozoic tectonics of the northwestern San Bernardino Mountains, southern California. Geological Society of America Bulletin 101, 106–128.

Miller, S.T., 1980. Geology and mammalian biostratigraphy of a part of the northern Cady Mountains, Mojave Desert, California. United States Geological Survey Open-File Report 80-878. 127pp.

Mix, H.T., Chamberlain, C.P., 2014. Stable isotope records of hydrologic change and paleotemperature from smectite in Cenozoic western North America. Geochimica et Cosmochimica Acta 141, 532–546.

Morton, D.M., Miller, F.K., 2006. Geologic Map of the San Bernardino and Santa Ana 30′ X 60′ Quadrangles, California. US Geological Survey.

Noble, L.F., 1954. The San Andreas fault zone from Soledad Pass to Cajon Pass, California. Geology of Southern California, California Department of Resources, Division of Mines Bulletin 170, 37-48.

Pagnac, D., 2006. *Scaphohippus*, A new genus of horse (Mammalia: Equidae) from the Barstow Formation of California. Journal of Mammalian Evolution 13, 37–61.

Pagnac, D., 2009. Revised large mammal biostratigraphy and biochronology of the Barstow Formation (Middle Miocene), California. PaleoBios 29, 48–59.

Passey, B.H., Cerling, T.E., Perkins, M.E., Voorhies, M.R., Harris, J.M., Tucker, S.T., 2002. Environmental change in the Great Plains: An isotopic record from fossil horses. The Journal of Geology 110, 123–140.

Piperno, D.R., 1988. Phytolith Analysis, an Archaeological and Geological Perspective. Academic Press, San Diego, California.

Piperno, D.R., 2006. Phytoliths: A Comprehensive Guide for Archaeologists and Paleoecologists. AltaMira Press, Lanham, Maryland.

Pound, M.J., Haywood, A.M., Salzmann, U., Riding, J.B., 2012. Global vegetation dynamics and latitudinal temperature gradients during the Mid to Late Miocene (15.97–5.33Ma). Earth Science Reviews 112, 1–22.

Retallack, G.J., 2007. Cenozoic paleoclimate on land in North America. The Journal of Geology 115, 271-294.

Reynolds, R.E., 1988a. Paleontological and cultural resource mitigation, for: MCI Telecommunications Corporation Fiber Optics Cable Cajon Pass, San Bernardino, California, 97pp.

Reynolds, R.E., 1988b. Paleontological salvage, for: Williams Telecommunications Fiber Optics Cable, Cajon Pass and central Mojave Desert, San Bernardino County, California, 122pp.

Reynolds, R.E., 1990. Paleontologic mitigation program, Cajon Pass Truck Escape Ramp, Cajon Summit, San Bernardino County, California, for: San Bernardino County Museum, Redlands, California, and California Department of Transportation, District 8, 78pp.

Reynolds, R.E., 1991. Biostratigraphic relationships of Tertiary small vertebrates from Cajon Valley, San Bernardino County, California. San Bernardino County Museum Association Quarterly 38, 54–59.

Reynolds, R.E., 2015. New ursid and talpid occurrences from Hemingfordian and Barstovian units of the Cajon Valley Formation, Cajon Pass, California, in: Mojave Miocene, Desert Symposium Field Guide and Proceedings, pp. 281-283.

Reynolds, R.E., Pasenko, M.R., 2008. Paleontologic resources monitoring and mitigation program, BNSF Cajon Main Third Track Summit to Keenbrook, Cajon Pass, San Bernardino County, California, for: LSA Associates, Riverside, California and BNSF Railway Company, 33pp.

Reynolds, R.E., Reynolds, R.L., Lindsay, E.H., 2008. Biostratigraphy of the Miocene Crowder Formation, Cajon Pass, southwestern Mojave Desert, California, in: Wang, X., Barnes, L.G. (Eds.), Geology and Vertebrate Paleontology of Western and Southern North America, Contributions in Honor of David P. Whistler. Natural History Museum of Los Angeles County Science Series 41, 237–253.

Reynolds, R.E., Schweich, T.A., 2013. The Rainbow Loop Flora from the Mud Hills, in: Mojave Desert, California, Desert Symposium Field Guide and Proceedings, pp. 39-48.

Reynolds, R.E., Schweich, T.A., 2015. Additions to the floras of the Barstow Formation in the Mud Hills, Mojave Desert, California, in: Mojave Miocene, Desert Symposium Field Guide and Proceedings, pp. 119-129.

Sheldon, N.D., 2006. Using paleosols of the Picture Gorge Basalt to reconstruct the middle Miocene climatic optimum. PaleoBios 26, 27–36.

Sheldon, N.D., Retallack, G.J., Tanaka, S., 2002. Geochemical climofunctions from North American soils and application to paleosols across the Eocene-Oligocene boundary in Oregon. The Journal of Geology 110, 687–696.

Smith, B.N., Epstein, S., 1971. Two categories of $^{13}C/^{12}C$ ratios for higher plants. Plant Physiology 47, 380–384.

Strömberg, C.A.E., 2002. The origin and spread of grass-dominated ecosystems in the Late Tertiary of North America: preliminary results concerning the evolution of hypsodonty. Palaeogeography, Palaeoclimatology, Palaeoecology 177, 59–75.

Strömberg, C.A.E., 2003. The origin and spread of grass-dominated ecosystems during the Tertiary of North America and how it relates to the evolution of hypsodonty in equids. Ph.D. thesis, Department of Biology, University of California Berkeley. 779pp.

Strömberg, C.A.E., 2004. Using phytolith assemblages to reconstruct the origin and spread of grass-dominated habitats in the great plains of North America during the late Eocene to early Miocene. Palaeogeography, Palaeoclimatology, Palaeoecology 207, 239–275.

Strömberg, C.A.E., 2005. Decoupled taxonomic radiation and ecological expansion of open-habitat grasses in the Cenozoic of North America. Proceedings of the National Academy of Sciences 102, 11980–11984.

Strömberg, C.A.E., 2011. Evolution of grasses and grassland ecosystems. Annual Review of Earth and Planetary Science 39, 517–544.

Strömberg, C.A.E., Werdelin, L., Friis, E.M., Saraç, G., 2007. The spread of grass-dominated habitats in Turkey and surrounding areas during the Cenozoic: Phytolith evidence. Palaeogeography, Palaeoclimatology, Palaeoecology 250, 18–49.

Strömberg, C.A.E., McInerney, F.A., 2011. The Neogene transition from C_3 to C_4 grasslands in North America: Assemblage analysis of fossil phytoliths. Paleobiology 37, 50–71.

Tedford, R.H., Albright, L.B., Barnosky, A.D., Ferrusquia-Villafranca, I., Hunt, R.M., Storer, J.E., Swisher, C.C., Voorhies, M.R., Webb, S.D., Whistler, D.P., 2004. Mammalian biochronology of the Arikareean through Hemphillian interval (late Oligocene through early Pliocene epochs), in: Woodburne, M.O. (Ed.), Late Cretaceous and Cenozoic mammals of North America: Biostratigraphy and geochronology. Columbia University Press, New York, New York, pp. 169–231.

Tipple, B.J., Meyers, S.R., Pagani, M., 2010. Carbon isotope ratio of Cenozoic CO_2: A comparative evaluation of available geochemical proxies. Paleoceanography 25, PA3202.

Vallis, G.K., 2011. Climate and the Oceans. Princeton University Press, Princeton, New Jersey.

Wang, X., Tedford, R.H., Taylor, B.E., 1999. Phylogenetic systematics of the Borophaginae (Carnivora, Canidae). Bulletin of the American Museum of Natural History 243, 1-391.

Wagner, H.M., Reynolds, R.E., 1983. *Leptarctus ancipidens* (White) (Carnivore: Mammalia) from the Punchbowl Formation, Cajon Pass, California. Bulletin of Southern California Academy of Sciences 82, 131–137.

Weldon, R.J., 1986. The late Cenozoic geology of Cajon Pass: Implications for tectonics and sedimentation along the San Andreas fault. Ph. D. thesis, California Institute of Technology. 400pp.

Wilf, P., 1997. When are leaves good thermometers? A new case for leaf margin analysis. Paleobiology 23, 373–390.

Winston, D.S., 1985. The physical and magnetic stratigraphy of the Miocene Crowder Formation, Cajon Valley Pass, Southern California. Masters thesis, University of Southern California. 111pp.

Wolfe, J.A., 1981. A chronologic framework for Cenozoic megafossil floras of northwestern North America and its relation to marine geochronology. Geological Society of America Special Papers 184, 39–48.

Wolfe, J.A., 1985. Distribution of major vegetation types during the Tertiary, in: Sundquist, E.T., Broecker, W.S. (Eds.), The Carbon Cycle and Atmospheric CO_2: Natural Variations Archean to Present: Geophysical Monograph 32, pp. 357–377.

Woodburne, M.O. (Ed.), 1987. Cenozoic mammals of North America: geochronology and biostratigraphy. University of California Press, Berkeley, California.

Woodburne, M.O., 1991. The Mojave Desert Province. San Bernardino County Museum Association Quarterly 38, 60–77.

Woodburne, M. O., 1998. Arikareean and Hemingfordian faunas of the Cady Mountains, Mojave Desert Province, California, in: Terry, D. O., Jr., LaGarry, H. E., Hunt, R. M., Jr. (Eds.), Depositional Environments, Lithostratigraphy, and Biostratigraphy of the White River and Arikaree Groups (Late Eocene to Early Miocene, North America): Boulder, Colorado, Geological Society of America Special Paper 325, pp. 197–210.

Woodburne, M.O., Golz, D.J., 1972. Stratigraphy of the Punchbowl Formation, Cajon Valley, Southern California. University of California Publications in Geological Sciences 92, 1–73.

Woodburne, M.O., Tedford, R.H., Stevens, M.S., 1974. Early Miocene mammalian faunas, Mojave Desert, California. Journal of Paleontology 48, 6–26.

Woodburne, M.O., Tedford, R.H., Swisher, C.C., III, 1990. Lithostratigraphy, biostratigraphy, and geochronology of the Barstow Formation, Mojave Desert, southern California. Geological Society of America Bulletin 102, 459–477.

Wynn, J.G., Bird, M.I., Wong, V.N.L., 2005. Rayleigh distillation and the depth profile of $^{13}C/^{12}C$ ratios of soil organic carbon from soils of disparate texture in Iron Range National Park, Far North Queensland, Australia. Geochimica et Cosmochimica Acta 69, 1961–1973.

Zachos, J., Pagani, M., Sloan, L., Thomas, E., Billups, K., 2001. Trends, rhythms, and aberrations in global climate 65 Ma to present. Science 292, 686–693.

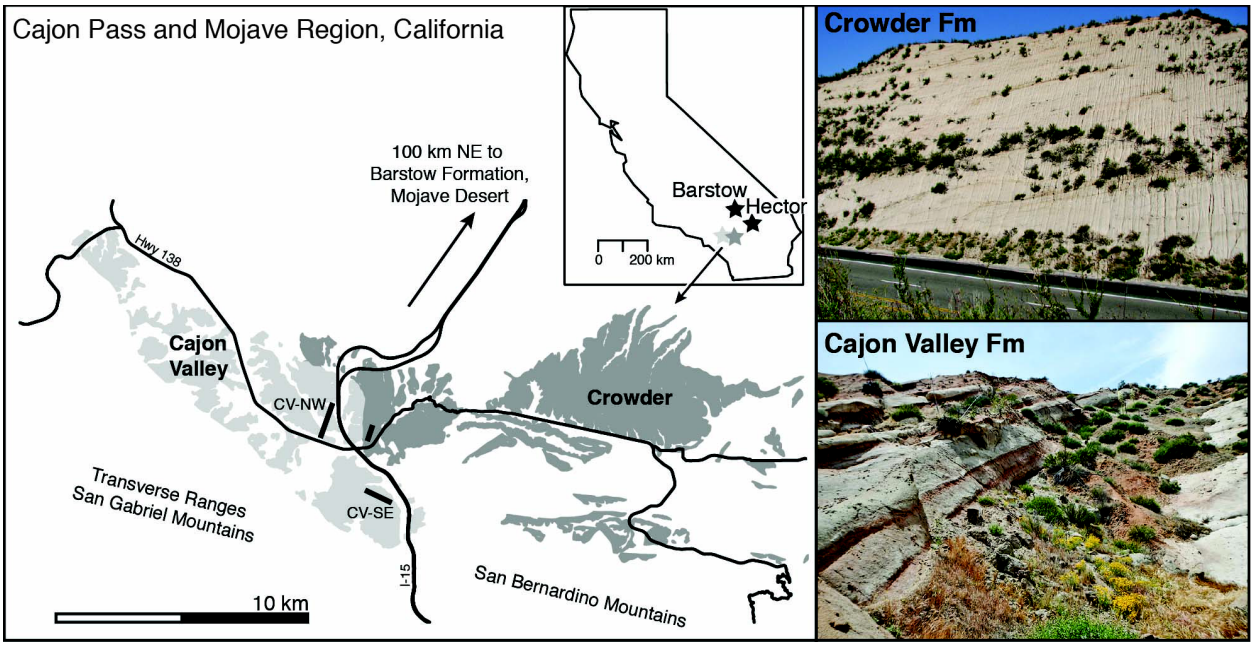

Figure 3.1 Geographic location of the study areas and field photos of paleosol units within the Crowder Formation (dark gray) and Cajon Valley Formation (light gray). Thick black bars indicate the position of the measured sections presented in this study. Map inset shows location of the middle Miocene formations in Cajon Pass and the Mojave Desert, including Crowder, Cajon Valley, Hector, and Barstow formations. Geologic map data are from Morton and Miller (2006).

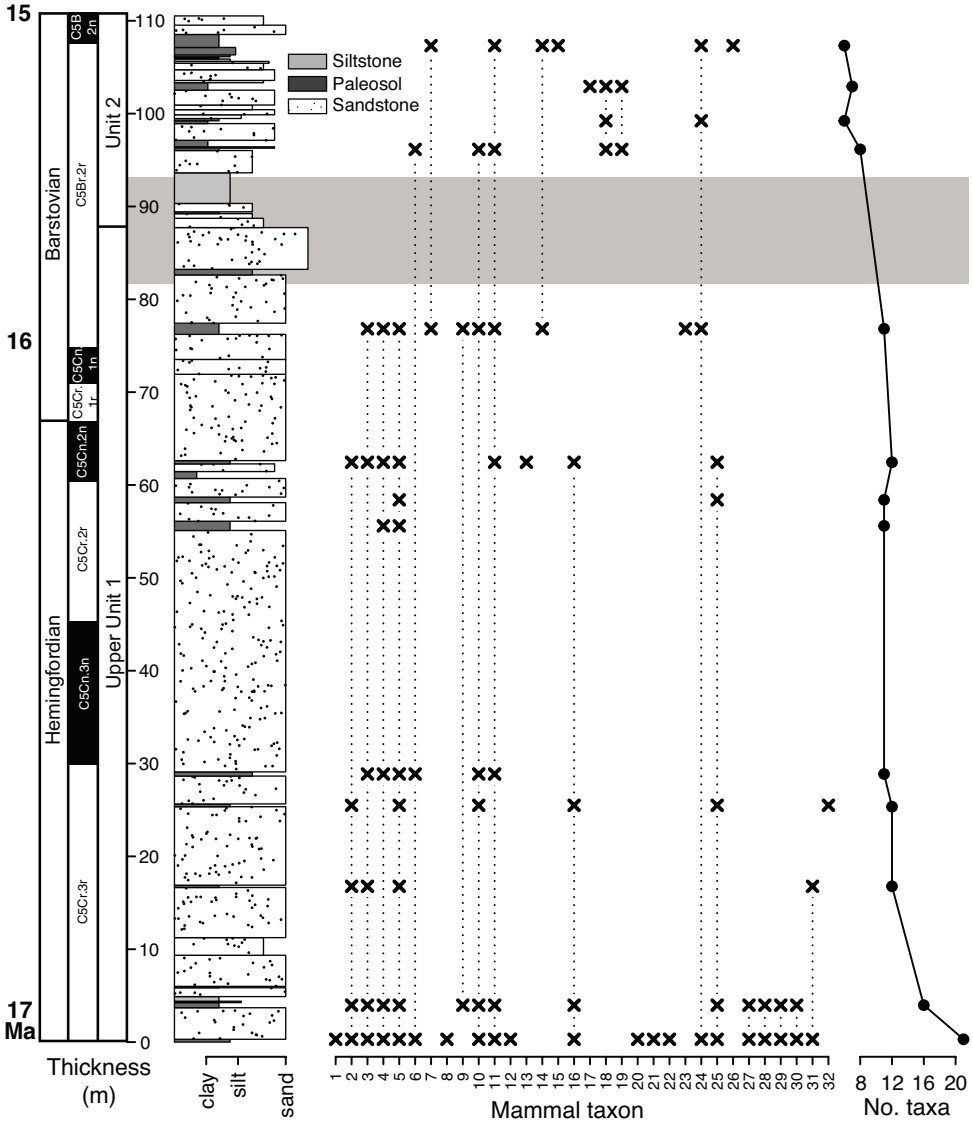

Figure 3.2 Stratigraphic section of the Crowder Formation, Upper Unit 1 and Unit 2, tied to the paleomagnetic and NALMA timescales (Woodburne, 1987; Gradstein et al., 2004), with corresponding biostratigraphic ranges of fossil mammals within the Crowder Formation (see Table 3.1 for taxon identity; x indicates fossil occurrence), and compiled mammal diversity through time (assuming lineage range-through). The horizontal gray bar indicates the interval of most pronounced environmental and faunal change. Ages of the sedimentary strata and fossil localities are inferred from paleomagnetic data in Winston (1985) and Weldon (1986), and biostratigraphy and paleomagnetic age interpretation in Reynolds et al. (2008).

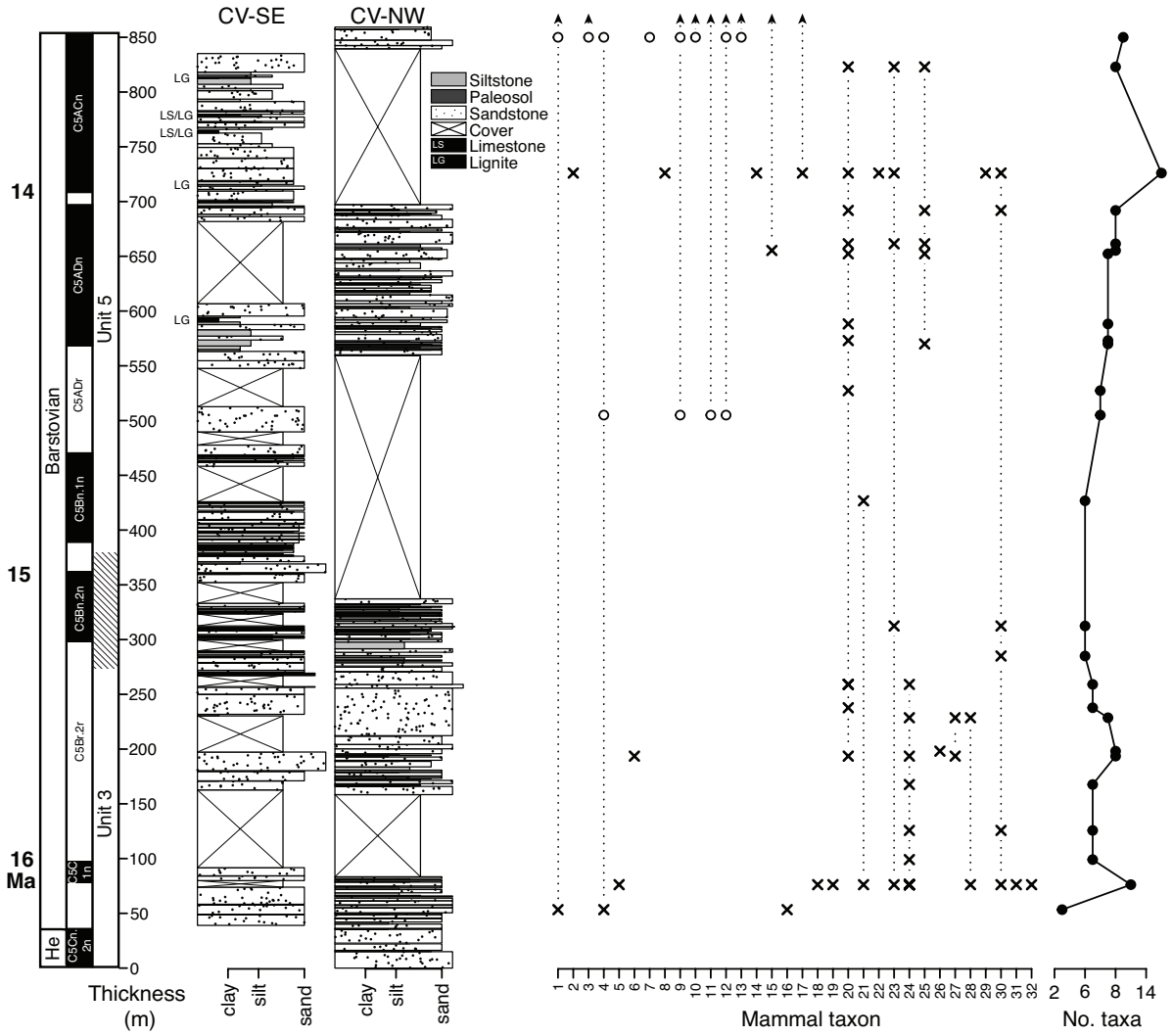

Figure 3.3 Southeastern (CV-SE) and northwestern (CV-NW) stratigraphic sections of the Cajon Valley Formation, Units 3 and 5 (gradual transition indicated by hashed lines), tied to the paleomagnetic and NALMA timescales (Woodburne, 1987; Gradstein et al., 2004), with corresponding biostratigraphic ranges of fossil taxa within the Cajon Valley Formation (see Table 3.2 for taxon identity; x and o indicate fossil occurrences of known and approximate stratigraphic position, respectively, and arrows indicate fossil occurrences stratigraphically higher than the measured section), and compiled mammal diversity through time (assuming lineage range-through). Ages of the sedimentary strata and fossil localities are based on biostratigraphy in Woodburne and Golz (1972) and from paleomagnetic data and age interpretation in Liu (1990).

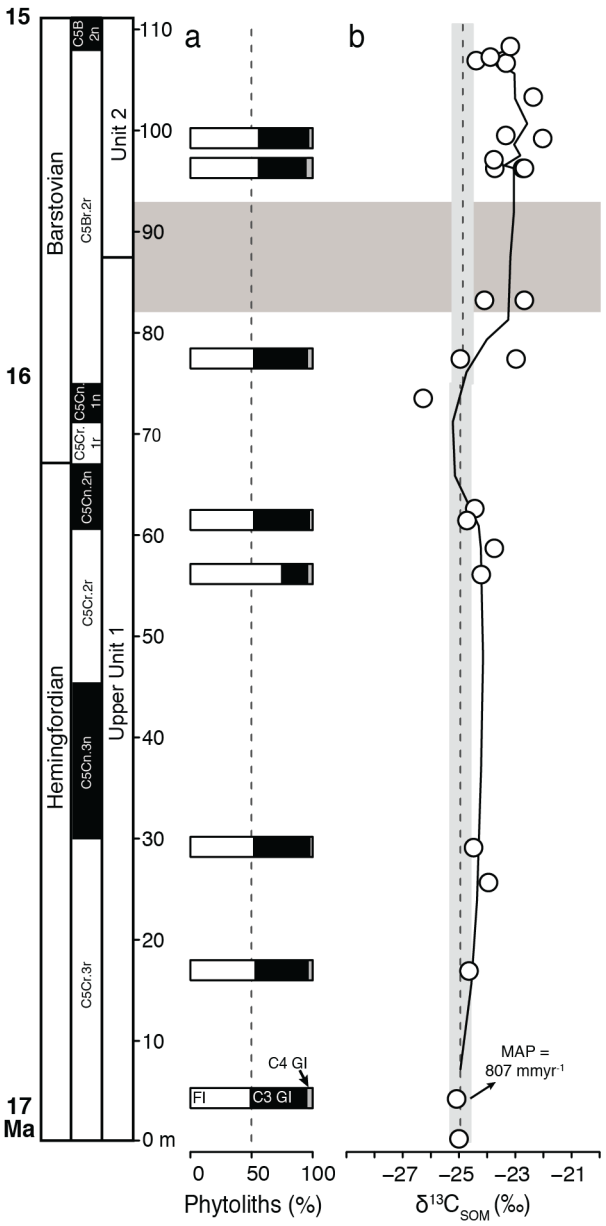

Figure 3.4 Paleoenvironmental reconstruction of the Crowder Formation during the MCO. (a) Vegetation estimates based on phytolith assemblages: % C_3-forest (white), C_3-grass (black), and C_4-grass (gray) morphotypes. (b) Carbon isotope composition of preserved soil organic matter (SOM) with mean C_3 isotopic composition under shifting average $\delta^{13}C_{CO2}$ values (black dashed line), with 90% confidence intervals (gray bars) from Tipple et al. (2010). The trend line is a 3-point moving average. MAP estimate based on *CIA-K* elemental chemistry is given where measured. The horizontal gray bar indicates the interval of most pronounced environmental and faunal change.

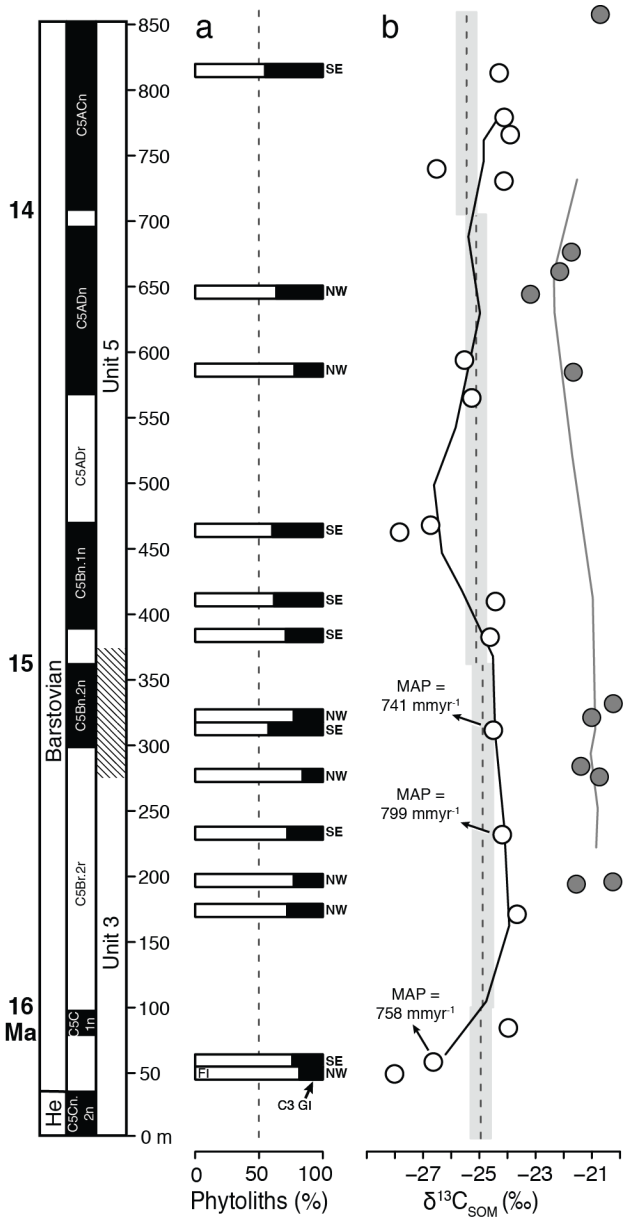

Figure 3.5 Paleoenvironmental reconstructions of the Southeastern (CV-SE) and northwestern (CV-NW) sections of the Cajon Valley Formation during the MCO. (a) Vegetation estimates based on phytolith assemblages: % C_3-forest (white) and C_3-grass (black) morphotypes. (b) Carbon isotope composition of preserved soil organic matter (SOM) with mean C_3 isotopic composition under shifting average $\delta^{13}C_{CO2}$ values (black dashed line), with 90% confidence intervals (gray bars) from Tipple et al. (2010). A 3-point moving-average trend line runs through the CV-SE (black) and CV-NW (gray) data. MAP estimates based on *CIA-K* elemental chemistry (CV-SE only) are given where measured.

Table 3.1 Mammalian faunas of the Crowder Formation.

	Small Mammals
	Heteromyidae
1	*Perognathus minutus*
2	*Paratrogomys whistleri*
3	*Mookomys "altifluminus"*
4	*Perognathus furlongi*
5	*Proheteromys sulculus*
6	*Balantiomys crowderensis*
7	*Cupidinimus halli*
	Sciuridae
8	*Protospermophilus sp.*
9	*Tamias sp.*
10	*Miospermophilus sp.*
11	*Petauristodon sp.*
	Zapodidae
12	*Megasminthus sp.*
13	*Plesiosminthus sp.*
	Cricetidae
14	*Copemys tenuis*
15	*Copemys pagei*
16	Heterosoricidae – *Paradomnina relictus*
17	Leporidae – *Hypolagus sp.*
	Ochotonidae
18	*Russellagus sp.*
19	*Hesperolagomys sp.*
	Mustelidae
20	*Miomustela sp.*
21	*Leptarctus sp.*

	Large Mammals
22	Antilocapridae – cf. *Merycodus sp.*
23	Palaeomerycidae – *Sinclairomeryx sp.*
	Equidae
24	*Archaeohippus mourningi*
25	*Parapliohippus carrizoensis*
26	"Merychippus" (large)
27	Tayassuidae – *Cynorca sp.*
	Camelidae
28	*Procamelus sp.*
29	*Michenia agatensis*
30	*Miolabis tenuis*
31	*Hesperocamelus sp.*
32	Rhinocerotidae – *Menoceras sp.*

Table 3.2 Mammalian faunas of the Cajon Valley Formation.

	Small Mammals
	Heteromyidae
1	*Cupidinimus sp.*
2	*Harrymys maximus*
3	*Perognathus furlongi*
4	*Proheteromys sulculus*
5	Sciuridae
6	*Petauristodon,* large sp.
7	*Petauristodon,* small sp.
8	*Petauristodon uphami*
	Cricetidae
9	*Copemys longidens*
10	*Copemys sp. cf. C. russelli*
11	*Copemys tenuis*
	Eomyidae
12	*Pseudadjidaumo stirtoni*
	Geomyidae
13	*Mojavemys lophatus*
14	Heterosoricidae – *Paradomnina relictus*
15	Talpidae
16	Leporidae – *Hypolagus sp.*
17	Erinaceidae – *Lanthanotherium sp.*
18	Mustelidae – *Leptarctus ancipidens*
	Large Mammals
19	Antilocapridae
20	Camelidae
21	Chalicotheriidae – *Moropus sp.*
	Equidae
22	*Acritohippus stylodontus*
23	*Archaeohippus mourningi*
24	*Parapliohippus carrizoensis*
25	*Scaphohippus intermontanus*
26	Merycoidodontidae – *Brachycrus buwaldi*
27	Moschidae – Blastomerycine
	Palaeomerycidae
28	*Bouromeryx americanus*
29	*Bouromeryx sp.*
30	Rhinocerotidae
31	Tayassuidae – *Dyseohyus sp.*
32	Ursidae – *Ursavus sp.*

Unit 6 taxa: *Cupidinimus halli*, *C. lindsayi*, *Miospermophilus*, *Spermophilus sp. cf. S. primitivus*, *Mojavemys alexandrae*, *Parapliosaccomys*, *Hypolagus fontinalis*

Unit 5, above stratigraphic section: *Aepycamelus alexandrae*, *Dyseohyus fricki*, *Scaphohippus sumani*

SUPPLEMENTARY TABLES

Table S3.1 Species and Locality Data for Figures 2 and 3; Cr = Crowder Formation, Cv = Cajon Valley Formation.

Order	Family	Taxa	Units Present	Crowder Localities*	Cajon Valley Localities*	References
Rodentia	Heteromyidae	*Perognathus minutus*	Cr1	1.103.125	-	Reynolds et al. 2008
Rodentia	Heteromyidae	*Paratrogomys whistleri*	Cr1	1.103.53 1.103.125 1.103.126	-	Reynolds et al. 2008, Lindsay and Reynolds 2008
Rodentia	Heteromyidae	*Mookomys* "altifluminus"	Cr1	1.103.53 1.103.125 1.103.126	-	Reynolds et al. 2008
Rodentia	Heteromyidae	*Perognathus furlongi*	Cr1, Cv5, Cv6	1.103.53 1.103.125 1.103.126	1.103.111 1.103.116 1.103.120	Reynolds 1990, Reynolds et al. 2008
Rodentia	Heteromyidae	*Proheteromys sulculus*	Cr1, Cv3, Cv5	1.103.53 1.103.125 1.103.126	1.103.62 1.103.105 1.103.106 1.103.112 1.103.116	Reynolds 1988a, Reynolds 1990, Reynolds 1991, Reynolds et al. 2008, Lindsay and Reynolds 2008
Rodentia	Heteromyidae	*Balantiomys crowderensis*	Cr1, Cr2	1.103.53 1.103.125 1.103.126	-	Reynolds et al. 2008, Lindsay and Reynolds 2008
Rodentia	Heteromyidae	*Cupidinimus halli*	Cr1, Cr2, Cv6	1.103.53	1.103.75	Reynolds 1991, Reynolds et al. 2008
Rodentia	Heteromyidae	*Cupidinimus sp.*	Cv3, Cv5	-	1.103.62 1.103.74 1.103.117	Reynolds 1990, Reynolds 1991

Rodentia	Heteromyidae	*Cupidinimus lindsayi*	Cv6	-	1.103.171	SBCM database records, accessed 2014
Rodentia	Heteromyidae	*Harrymys maximus*	Cv5	-	1.103.40	Lindsay and Reynolds 2015
Rodentia	Sciuridae	*Protospermophilus sp.*	Cr1	1.103.125 1.103.126	-	Reynolds et al. 2008
Rodentia	Sciuridae	*Tamias sp.*	Cr1	1.103.53	-	Reynolds et al. 2008
Rodentia	Sciuridae	*Miospermophilus sp.*	Cr1, Cr2, Cv6	1.103.53 1.103.125 1.103.126	1.103.117	Reynolds 1990, Reynolds et al. 2008
Rodentia	Sciuridae	*Petauristodon sp.*	Cr1, Cr2, Cv5	1.103.125 1.103.126	1.103.111	Reynolds 1990, Reynolds et al. 2008
Rodentia	Sciuridae	*Petauristodon sp.* (large)	Cv3	-	RV-6992	Woodburne and Golz 1972
Rodentia	Sciuridae	*Petauristodon uphami*	Cv5	-	1.103.40	Reynolds 1991, Lindsay and Reynolds 2015
Rodentia	Sciuridae	*Spermophilus sp. cf. S. primitivus*	Cv6	-	1.103.99	Reynolds 1988b
Rodentia	Zapodidae	*Megasminthus sp.*	Cr1	1.103.125 1.103.126	-	Reynolds et al. 2008
Rodentia	Zapodidae	*Plesiosminthus sp.*	Cr1	1.103.53	-	Reynolds et al. 2008
Rodentia	Cricetidae	*Copemys tenuis*	Cr1, Cr2, Cv5, Cv6	1.103.144	1.103.105 1.103.106 1.103.99	Reynolds 1988a, Reynolds 1988b, Reynolds et al. 2008
Rodentia	Cricetidae	*Copemys pagei*	Cr2	1.103.144	-	Reynolds et al. 2008
Rodentia	Cricetidae	*Copemys longidens*	Cv5, Cv6	-	1.103.105 1.103.106 1.103.111	Reynolds 1988a, Reynolds 1998b, Reynolds 1990

					1.103.99	
Rodentia	Cricetidae	*Copemys sp. cf. C. russelli*	Cv5	-	1.103.116	Reynolds 1990
Rodentia	Eomyidae	*Pseudadjidaumo stirtoni*	Cv5, Cv6	-	1.103.74 1.103.99 1.103.105 1.103.106	Reynolds 1988a, Reynolds 1988b, Reynolds 1991
Rodentia	Geomyidae	*Mojavemys lophatus*	Cv5, Cv6	-	1.103.116 1.103.117	Reynolds 1990
Rodentia	Geomyidae	*Mojavemys alexandrae*	Cv6	-	1.103.99	Reynolds 1988b
Rodentia	Geomyidae	*Parapliosaccomys sp.*	Cv6	-	1.103.99 1.103.101 1.103.102	Reynolds 1988b
Soricomorpha	Heterosoricidae	*Paradomnina relictus*	Cr1, Cv5	1.103.53	1.103.40	Reynolds 1991, Reynolds et al. 2008
Soricomorpha	Talpidae	sp. undetermined	Cv5, Cv6	-	1.103.27 1.103.99	Reynolds 1988b, Reynolds 2015
Lagomorpha	Leporidae	*Hypolagus sp.*	Cr2, Cv3	1.103.101	1.103.62	Reynolds et al. 2008, Reynolds and Pasenko 2008
Lagomorpha	Leporidae	*Hypolagus fontinalis*	Cv6	-	1.103.99	Reynolds 1988b
Lagomorpha	Ochotonidae	*Russellagus sp.*	Cr2	1.103.53	-	Reynolds et al. 2008
Lagomorpha	Ochotonidae	*Hesperolagomys sp.*	Cr2	1.103.53	-	Reynolds et al. 2008
Eulipotyphla	Erinaceidae	*Lanthanotherium sp.*	Cv5, Cv6	-	1.103.40 1.103.99	Reynolds 1988b, Reynolds 1991
Carnivora	Mustelidae	*Miomustela sp.*	Cr1	1.103.53	-	Reynolds et al. 2008

Carnivora	Mustelidae	*Leptarctus sp.*	Cr1	1.103.53	-	Reynolds et al. 2008
Carnivora	Mustelidae	*Leptarctus ancipidens*	Cr1	1.103.53	-	Wagner and Reynolds 1983, Reynolds et al. 2008
Carnivora	Ursidae	*Ursavus sp.*	Cr1, Cv3	1.103.53	1.103.8	Reynolds et al. 2008, Reynolds 2015
Artiodactyla	Antilocapridae	*cf. Merycodus sp.*	Cr1	1.103.53	-	Reynolds et al. 2008
Artiodactyla	Antilocapridae	sp. undetermined	Cv3	-	1.103.8	Reynolds and Pasenko 2008
Artiodactyla	Palaeomerycidae	*Sinclairomeryx sp.*	Cr1	1.103.53	-	Reynolds et al. 2008
Artiodactyla	Camelidae	sp. undetermined	Cr1, Cv3, Cv5	1.103.53	1.103.40 RV-6992 RV-6628 RV-6994 RV-6771 RV-6768 RV-69130 RV-7006 RV-69132 RV-7005	Woodburne and Golz 1972, Reynolds 1991, Reynolds et al. 2008
Artiodactyla	Camelidae	*Procamelus sp.*	Cr1	1.103.53	-	Reynolds et al. 2008
Artiodactyla	Camelidae	*Michenia agatensis*	Cr1	1.103.53	-	Reynolds et al. 2008
Artiodactyla	Camelidae	*Miolabis tenuis*	Cr1	1.103.53	-	Reynolds et al. 2008
Artiodactyla	Tayassuidae	*Cynorca sp.*	Cr1	1.103.53	-	Reynolds et al. 2008
Artiodactyla	Camelidae	*Hesperocamelus sp.*	Cr1	1.103.53	-	Reynolds et al. 2008
Artiodactyla	Camelidae	*Aepycamelus alexandrae*	Cv5	-	RV-7515	Pagnac 2006
Artiodactyla	Merycoidodontidae	*Brachycrus buwaldi*	Cv3	-	RV-6766	Woodburne and Golz 1972
Artiodactyla	Moschidae	Blastomerycine	Cv3	-	RV-6992	Woodburne and Golz 1972

					RV-6993	
Artiodactyla	Palaeomerycidae	*Bouromeryx americanus*	Cv3	-	RV-6993 RV-6988 1.103.8	Woodburne and Golz 1972
Artiodactyla	Palaeomerycidae	*Bouromeryx sp.*	Cv5	-	1.103.40	Reynolds 1991
Artiodactyla	Tayassuidae	*Dyseohyus sp.*	Cv3	-	1.103.8	Reynolds and Pasenko, 2008; Reynolds 2015
Artiodactyla	Tayassuidae	*Dyseohyus fricki*	Cv5	-	RV-7515	Pagnac 2006
Perissodactyl	Chalicotheriidae	*Moropus sp.*	Cv3, Cv5	-	1.103.8 1.103.59	Coombs and Reynolds 2015
Perissodactyl	Rhinocerotidae	sp. undetermined	Cr1, Cv3, Cv5	1.103.53	1.103.8 RV-6990 RV-6995 RV-7005 RV-6605 1.103.40	Woodburne and Golz 1972, Reynolds 1991, Reynolds et al. 2008, Reynolds and Pasenko 2008
Perissodactyl	Rhinocerotidae	*Menoceras sp.*	Cr1	1.103.53	-	Reynolds et al. 2008
Perissodactyl	Equidae	*Archaeohippus mourningi*	Cr1, Cr2, Cv3, Cv5	1.103.53	RV-6988 RV-6605 RV-69132 1.103.40 B-3144	Woodburne and Golz 1972, Reynolds et al. 2008

Perissodactyl	Equidae	*Parapliohippus carrizoensis*	Cr1, Cv3	1.103.53	RV-6984 RV-6985 RV-6988 RV-6989 RV-6987 RV-6990 RV-6991 RV-6992 RV-6993 RV-6994	Woodburne and Golz 1972, Reynolds et al. 2008
Perissodactyl	Equidae	"Merychippus" (large)	Cr2	1.103.53	-	Reynolds et al. 2008
Perissodactyl	Equidae	*Acritohippus stylodonus*	Cv5	-	1.103.40	Reynolds 1991
Perissodactyl	Equidae	*Scaphohippus intermontanus*	Cv5	-	RV-6770 RV-7006 RV-69132 RV-7005 B-3144	Woodburne and Golz 1972
Perissodactyl	Equidae	*Scaphohippus sumani*	Cv5	-	RV-7515	Pagnac 2006

*Unless otherwise noted, Locality Numbers refer to San Bernardino County Museum (SBCM) numbers; e.g., SBCM 1.103.53; RV- and B- localities refers to University of California, Riverside (collections now housed at the University of California Museum of Paleontology, Berkeley).

Table S3.2 Raw carbon isotopic data, carbon weight %, and atmospheric $\delta^{13}C$ used to estimate the proportion of C_4 vegetation for each sample ($\delta^{13}C_{atm}$ is based on 3-myr moving average values of benthic foraminifera reconstructions from Tipple et al., 2010). Samples were from paleosol horizons, unless an LG is noted in the Sample ID, indicating the sample was from a lignite bed. Replicate measurements are indicated in gray text.

Section	Sample ID	Height (m)	$\delta^{13}C_{VPDB}$ (‰)	C weight (%)	$\delta^{13}C_{atm}$ (‰)
Crowder	CR12-05	0.30	-25.01	0.02	-5.35
Crowder	CR12-01	4.25	-25.08	0.02	-5.35
Crowder	CR12-02	16.90	-24.64	0.01	-5.35
Crowder	CR12-03	25.65	-23.95	0.01	-5.35
Crowder	CR12-04	29.10	-25.25	0.02	-5.35
Crowder	CR12-04	29.10	-24.33	0.02	-5.35
Crowder	CR12-04	29.10	-23.86	0.04	-5.35
Crowder	CR12-10	56.10	-23.21	0.02	-5.35
Crowder	CR12-10	56.10	-23.51	0.03	-5.35
Crowder	CR12-10	56.10	-25.91	0.02	-5.35
Crowder	CR12-09	58.70	-23.71	0.03	-5.35
Crowder	CR12-09	58.70	-23.87	0.03	-5.35
Crowder	CR12-09	58.70	-23.66	0.03	-5.35
Crowder	CR12-07	61.45	-24.72	0.01	-5.35
Crowder	CR12-06	62.63	-23.95	0.02	-5.35
Crowder	CR12-06	62.63	-24.92	0.02	-5.35
Crowder	CR12-12	73.53	-26.27	0.02	-5.35
Crowder	CR12-13	77.43	-24.95	0.02	-5.27
Crowder	CR12-15	83.23	-22.25	0.02	-5.27
Crowder	CR12-15	83.23	-23.92	0.02	-5.27
Crowder	CR12-15	83.23	-26.12	0.02	-5.27
Crowder	CR12-17	96.28	-22.74	0.03	-5.27
Crowder	CR14-01	77.43	-22.97	0.02	-5.27
Crowder	CR14-02	83.23	-22.68	0.02	-5.27
Crowder	CR14-05	96.28	-23.73	0.04	-5.27
Crowder	CR14-16	96.28	-22.67	0.02	-5.27
Crowder	CR14-17	97.13	-23.76	0.03	-5.27
Crowder	CR14-14	99.23	-22.03	0.01	-5.27
Crowder	CR14-15	99.53	-23.34	0.02	-5.27
Crowder	CR14-06	103.33	-22.36	0.02	-5.27
Crowder	CR14-09	106.68	-23.32	0.03	-5.27
Crowder	CR14-10	106.93	-24.39	0.04	-5.27
Crowder	CR14-10	106.93	-23.60	0.03	-5.27
Crowder	CR14-10	106.93	-23.20	2.30	-5.27
Crowder	CR14-11	107.28	-23.89	0.04	-5.27
Crowder	CR14-13	108.33	-23.18	0.02	-5.27
CV-SE	CV12-01	49.20	-28.01	0.01	-5.35

CV-SE	CV12-02	58.30	-25.63	0.02	-5.35
CV-SE	CV12-02	58.30	-27.62	0.03	-5.35
CV-SE	CV12-02	58.30	-26.65	0.02	-5.35
CV-SE	CV12-04	84.30	-24.47	0.02	-5.35
CV-SE	CV12-04	84.30	-23.45	0.02	-5.35
CV-SE	CV12-04	84.30	-23.99	0.02	-5.35
CV-SE	CV12-05	171.00	-26.14	0.02	-5.27
CV-SE	CV12-05	171.00	-22.38	0.02	-5.27
CV-SE	CV12-05	171.00	-22.45	0.03	-5.27
CV-SE	CV12-10	231.75	-24.18	0.01	-5.27
CV-SE	CV12-20	311.45	-24.50	0.02	-5.27
CV-SE	CV12-24	382.45	-24.57	0.02	-5.51
CV-SE	CV12-24	382.45	-24.66	0.02	-5.51
CV-SE	CV12-25	409.65	-24.42	0.02	-5.51
CV-SE	CV12-27	462.55	-26.52	0.02	-5.51
CV-SE	CV12-27	462.55	-28.62	0.02	-5.51
CV-SE	CV12-27	462.55	-28.36	0.03	-5.51
CV-SE	CV12-28	467.85	-26.73	0.08	-5.51
CV-SE	CV12-29	564.95	-25.27	0.02	-5.51
CV-SE	CV12-31 (LG)	593.85	-25.59	2.17	-5.51
CV-SE	CV12-31 (LG)	593.85	-25.57	2.36	-5.51
CV-SE	CV12-31 (LG)	593.85	-25.43	1.80	-5.51
CV-SE	CVB14-07	730.45	-24.12	0.02	-5.85
CV-SE	CVB14-08	739.75	-26.51	0.01	-5.85
CV-SE	CV12-34 (LG)	765.85	-23.90	49.85	-5.85
CV-SE	CV12-37 (LG)	779.00	-24.12	27.50	-5.85
CV-SE	CV12-38 (LG)	812.95	-24.29	26.00	-5.85
CV-NW	DR14-20	194.00	-21.55	0.02	-5.27
CV-NW	DR14-21	195.75	-20.25	0.02	-5.27
CV-NW	DR14-25	275.80	-20.73	0.02	-5.27
CV-NW	DR14-26	283.90	-21.39	0.02	-5.27
CV-NW	DR14-30	321.15	-21.00	0.02	-5.27
CV-NW	DR14-31	331.70	-20.24	0.02	-5.27
CV-NW	DR14-32	584.60	-20.86	0.04	-5.51
CV-NW	DR14-32	584.60	-22.45	0.03	-5.51
CV-NW	DR14-39	644.05	-23.18	0.02	-5.51
CV-NW	DR14-40	661.35	-21.61	0.10	-5.51
CV-NW	DR14-40	661.35	-22.67	0.09	-5.51
CV-NW	DR14-41	676.25	-21.73	0.02	-5.51
CV-NW	DR14-43	857.55	-20.70	0.02	-5.85

Table S3.3 Elemental analyses.

	wt %														
Sample ID	Al_2O_3	BaO	CaO	Cr_2O_3	Fe_2O_3	K_2O	MgO	MnO	Na_2O	P_2O_5	SO_3	SiO_2	SrO	TiO_2	Total	*CIA-K*
CR-12-01	17.5	0.08	2.76	<0.01	5.87	2.77	1.85	0.14	2.48	0.28	<0.01	60.8	0.05	1.03	95.71	65.80
CR-12-03	16.3	0.07	2.65	<0.01	4.2	2.85	1.36	0.06	3.01	0.26	<0.01	65.3	0.05	0.71	96.89	62.52
CV-12-08	17.15	0.07	3.52	0.01	7.34	2.74	2.25	0.12	1.66	0.26	0.01	56.8	0.05	1.09	93.18	65.26
CV-12-20	17.5	0.1	3.52	<0.01	6.33	2.97	2.34	0.13	2.8	0.36	<0.01	58.7	0.07	1.14	96.07	61.39

$$CIA - K = 100 * (\frac{Al_{mole}}{Al_{mole} + Ca_{mole} + Na_{mole}})$$

CHAPTER 4

Ecological response to environmental change: insights from the Miocene small-mammal record[1]

ABSTRACT

Rich small-mammal assemblages from the Cenozoic of North America allow us to investigate ecological and evolutionary responses to environmental change over geologic time. We evaluated two records of small-mammal faunas from the Crowder and Cajon Valley formations, southern California, to assess how increasing temperature and aridity during the Miocene Climatic Optimum (MCO; 17–14 Ma) influenced basin-scale environmental conditions, small-mammal paleoecology, and community assembly. Using cheek teeth from these small-mammal faunas, we measured two dental metrics, hypsodonty index and occlusal area, and used *in situ* laser ablation mass spectrometry to sample the carbon and oxygen isotopic composition of tooth enamel. Dental traits and isotopic composition reflect aspects of an animal's body size and diet, allowing us to evaluate changes in small-mammal paleoecology through the MCO. Within both formations, we found stable values through time in carbon and oxygen isotopic composition, occlusal area, and hypsodonty index. These results indicate remarkable ecological stability in each basin during the MCO. In contrast, we found significant differences in isotopic composition between the Crowder (17–16 Ma) and Cajon Valley (16–13.7 Ma) faunas, implying

[1] Smiley, T.M., Moroz, M., Badgley, C., Cerling, T.E. Ecological response to warming and environmental change: insights from the Miocene small-mammal fossil record. *In prep* for Oecologia.

differences in small-mammal diets from adjacent basins over extended geologic time. The isotopic composition of rodent teeth from these formations suggests an early regional presence of C_4 grasses, with increased consumption of this resource among younger Cajon Valley faunas. With small home ranges and rapid metabolism, rodents document available vegetation at fine temporal and spatial scales and therefore provide unique information about habitat heterogeneity and the patchy presence of C_4 resources prior to C_4-grassland expansion in the late Miocene. We found little ecological differentiation among co-occurring rodents within Crowder and Cajon Valley assemblages based on isotopic composition and dental traits. This pattern contrasts with modern desert-rodent assemblages, in which heteromyid species differ significantly in isotopic composition, body size, and hypsodonty. These results imply that constraints on community assembly during the MCO differed from what we observe in western ecosystems today. Divergence among heteromyids in ecological and morphological traits following the MCO may have led to the strong interspecific differences found in present-day communities.

INTRODUCTION

The Cenozoic record of fossil mammals in North America offers an exceptional opportunity to test hypotheses about biotic response to landscape and climate change (e.g., Barnosky et al. 2003, Janis et al. 2008a, 2008b, Finarelli and Badgley 2010). In particular, rich small-mammal assemblages record notable changes in species richness, composition, and ecological dynamics during past intervals of climate-driven environmental change (Blois and Hadly 2009, Jardine et al. 2012, Badgley et al. 2014). Today, nonvolant small mammals comprise over half of North American mammal diversity and demonstrate strong gradients in ecological structure at local scales (Fox and Brown 1993, Shenbrot et al. 2012) and in species

richness at regional to continental scales (Badgley and Fox 2000, Riddle et al. 2014a). Understanding the mechanisms that contribute to changes in and maintenance of taxonomic and ecological diversity is critical not only for understanding community assembly and stability (Blois et al. 2013), but also for forecasting how species and ecosystems will respond to anthropogenic climate change and habitat transformation (Terry and Rowe 2015). This research utilizes both traditional (e.g., hypsodonty index) and novel (e.g., *in situ* laser ablation mass spectrometry) approaches to infer species ecology and community assembly during the last major global warming interval, the Miocene Climatic Optimum, thus providing a natural 'experiment' for evaluating community response to climate and environmental change (Williams and Jackson 2007, Terry 2010).

During the Miocene Climatic Optimum (MCO) from 17 to 14 Ma, terrestrial temperatures were on average 7.6 ± 2.3°C warmer than today (Zachos et al. 2001, Goldner et al. 2014). In western North America, this warming interval coincided with major tectonic extension, generating complex topography in the region. Many basins and mountain ranges were established during this time, contributing to increased habitat diversity at the regional scale and along elevational gradients. Increasing aridity and changes in vegetation distributions, including the expansion of grassland ecosystems, were underway during the Miocene in western North America (Strömberg 2005, Sheldon 2006, Strömberg 2011, Pound et al. 2012). While the rise of C_4 grasses did not occur until the late Miocene, these grasses were widespread if not ecologically dominant much earlier (Fox and Koch 2003, Strömberg et al. 2011, Chen et al. 2015). A peak in fossil mammal diversity in western North America coincided with the MCO (Barnosky and Carrasco 2002, Finarelli and Badgley 2010). Both climate and landscape drivers have been implicated for the rise in regional mammal diversity during this interval; however, their influence

on basin-scale environmental conditions, small-mammal paleoecology, and community assembly has yet to be resolved.

To evaluate local-scale responses to regional landscape changes, we analyzed two records of small-mammal faunas that span the MCO from the Crowder and Cajon Valley formations in southern California (Fig. 4.1, Table 4.1). These formations preserve rich, continuous small-mammal records from 17.5 to 12.5 Ma within a well-constrained geochronological framework. Originally deposited in geographically separate continental basins, the Crowder and Cajon Valley formations have since been juxtaposed by movement associated with the San Andreas Fault system (Meisling and Weldon 1989). The vertical and lateral distribution of lithologies in these formations indicates that deposits were formed by braided rivers and floodplains with intermittent stable surfaces and soil development (Noble 1954, Woodburne and Golz 1972, Foster 1980, Winston 1985, Weldon 1986). Integrated data from plant-phytolith assemblages, carbon isotopic composition of preserved soil organic matter, and elemental geochemical analysis of paleosols record the earliest evidence of C_4 grasses in the region at ~17.0 Ma, albeit in low abundance, and increases in aridity and the C_3-grass component on the landscape during the MCO (Smiley et al. *in review*). Spatial heterogeneity in vegetation and moisture conditions between and within basins characterized these mesic, grassy-woodland ecosystems.

Given this environmental context, we investigate the following questions: (1) Does the stable isotopic composition of rodent herbivores record similar vegetation composition as indicated by phytolith assemblages and preserved soil organic matter? (2) Does the dietary ecology and ecomorphology of rodents change through time in relation to trends in local vegetation and climate? (3) Do co-occurring species from Crowder and Cajon Valley rodent

assemblages differ in their dietary ecology? (4) How do interspecific differences in stable isotopic composition during the MCO compare with those of modern rodent communities?

We focus on small mammals, specifically herbivorous rodents, not only because they are diverse in modern and fossil ecosystems, but also because their fossil assemblages typically occur in large enough sample sizes to provide robust estimates of paleoenvironmental and community-level dynamics. Furthermore, rodent lifestyles are tightly linked with the characteristics of their local habitats, and they play critical roles (e.g., seed dispersion, prey base) in the maintenance of ecosystems in western North America and worldwide (Badgley and Fox 2000, Blois et al. 2010, Terry and Rowe 2015). Small-mammal paleoecology in relation to environmental change during the Miocene is relatively understudied compared to that of large mammals. Recent studies have noted that herbivorous rodents are early indicators of ecosystem change, with changes in their dental traits and isotope ecology preceding similar shifts within large herbivores (Jardine et al. 2012, Hynek et al. 2012).

As the primary interface between a mammal and its diet, tooth morphology reflects both evolutionary adaptation for particular dietary items and feeding ecology during an individual's lifetime (e.g., Janis et al. 2008a, 2008b, Samuels 2009). Two common metrics that utilize linear tooth measurements to infer species ecology are tooth area and hypsodonty index (Damuth and MacFadden 1990, Alroy 1998, Williams and Kay 2001). Tooth area is used to estimate body size, which in turn reflects many aspects of species life history and plays a major role in community structure and dynamics (Smith et al. 2004, Ernest 2005, McGill et al. 2006). Relative molar crown height, known as the hypsodonty index, reflects the properties of a mammal's food, with higher-crowned species consuming more abrasive material in their diet and thereby experiencing greater wear (Williams and Kay 2001, Damuth and Janis 2014). A gradual increase

in molar crown height within certain large- and small-mammal lineages (e.g., equids and heteromyids) during the Neogene corresponded with a greater reliance on grazing or seed-rich diets and the incidental incorporation of increased amounts of grit over their evolutionary history (Wahlert 1993, Korth 1994, Damuth and Janis 2011, Jardine et al. 2012).

Aspects of mammalian dietary and habitat preferences can also be inferred from the stable isotopic composition of their tissues. Carbon isotopic values ($\delta^{13}C$) of enamel reflect the isotopic composition of vegetation consumed during tooth formation, providing a basis for dietary reconstructions and vegetation estimates of the local environment (e.g, Koch 2007, Newsome et al. 2007, Cerling et al. 2015). Due to non-overlapping $\delta^{13}C$ values in C_3 (cool, wet-adapted plants) and C_4 (arid-adapted grasses and sedges) vegetation, this approach has been used to document the expansion of C_4 grasslands in the late Miocene and to differentiate browsers, mixed feeders, and grazers in ancient ecosystems (Cerling et al. 1997, 2003). Additionally, $\delta^{13}C$ values of C_3 vegetation vary in relation to environmental conditions, such as the amount of sunlight and CO_2 circulation below a forest canopy (Schoeninger et al. 1998, Cerling et al. 2004) and mean annual precipitation (Kohn 2010, Diefendorf et al. 2010). Oxygen isotopic values ($\delta^{18}O$) can be used to infer moisture regimes more directly, although the incorporation of oxygen from multiple sources—drinking water, leaf water, and respiration—often renders this record difficult to interpret (Kohn 1996, Grimes et al. 2008). Carbon and oxygen isotopes in the tooth enamel of fossil mammals have been used to reconstruct past environments and paleoecology (e.g., Koch 1998, Fricke et al. 1998, Badgley et al 2008, Domingo et al. 2013); however, the study of small-mammal isotopic composition has lagged far behind that of large mammals, primarily due to sampling challenges imposed by their small tooth size.

The development and refinement of *in situ* thermal laser ablation methods now provide the opportunity to sample the tooth enamel of small mammals (Cerling and Sharp 1996, Passey and Cerling 2006). Through stable isotopic analyses, small mammals provide valuable insight into past ecosystems (e.g., Grimes et al. 2008). With relatively small home ranges, they can provide fine-scale estimates of spatial variation in vegetation (Gehler et al. 2012, Hynek et al. 2012, Smiley et al. 2015). Additionally, rodents ingest relatively small amounts of biomass and have rapid rates of metabolism and enamel maturation, resulting in little time for dietary mixing and high probability of capturing isotopic end-member values of consumed vegetation (Passey et al. 2005, Podlesak et al. 2008). Finally, a dense fossil record enables comparisons of intra- and interspecific isotopic variation within and among assemblages, providing evidence for niche partitioning through time (e.g., Kimura et al. 2013) in some records.

MATERIALS AND METHODS

Materials

We selected fossil rodents from 11 fossil assemblages, which ranged in age from 17.0 to 15.0 Ma, from the Crowder Formation and five fossil assemblages, which ranged in age from 16.0 to ~13.0 Ma, from the Cajon Valley Formation. Fossils occurred primarily as single teeth and occasionally entire tooth rows, and genus- or species-level identifications had been made based on dental morphology (Reynolds 1991, Lindsay and Reynolds 2008, Reynolds et al. 2008). Fossils were previously collected by extensive sediment processing and screen-washing of individual paleosol units; approximately 2,700 kg of matrix were screen-washed per horizon for a total of 75,750 kg (Reynolds et al. 2008). This sampling approach produced diverse rodent assemblages in the Crowder Formation, with up to six species of heteromyids (kangaroo rats and

pocket mice) and four sciurids (squirrels) co-occurring in a single unit and several species represented continuously through the record. In contrast, the Cajon Valley Formation had fewer productive paleosol horizons, but fossils from several rodent families, including heteromyids, sciurids, cricetids (hamsters, voles, lemmings, and New World rats and mice), geomyids (gophers), and eomyids (extinct rodents related to heteromyids and geomyids), were retrieved. Small-mammal fossil localities in the Cajon Valley Formation occur along two measured sections (CV-SE and CV-NW in Fig. 4.1). Fourteen rodent species from the Crowder Formation and 16 species from the Cajon Valley Formation, represented by 191 specimens, were selected for isotopic sampling (Table 4.1). Complete teeth were measured prior to isotopic sampling.

Analytical methods

In order to document tooth size and hypsodonty index, we photographed and measured fossil rodent teeth at 20x magnification for larger rodents (e.g., sciurids) and at 40x magnification for smaller rodents (e.g., heteromyids), using a dedicated microscope camera and SPOT 5.0 software. We measured three linear dimensions per tooth: occlusal width, occlusal length, and crown height (the distance from the cervical margin to the highest point on the occlusal surface). Each linear dimension was measured three times to 1-μm precision for repeatability, and the mean value was used in subsequent analysis. The linear measurements of the first and second molars were then used to calculate two indices relevant to dietary ecology: two-dimensional occlusal surface area and hypsodonty index. We limited our analysis of tooth area and hypsodonty index to first and second molars because other tooth positions were significantly smaller in size. First and second molars are indistinguishable in tooth size for most of these rodents, and often teeth were identified as belonging in either position. We estimated

tooth area by multiplying the occlusal length by width; this measurement serves as a reasonable proxy for adult body weight (Damuth and MacFadden 1990). Hypsodonty index was calculated according to the formula determined by Williams and Kay (2001) for rodents: the crown height of a tooth divided by the square root of the occlusal area. Both occlusal area and hypsodonty index may vary with ontogenetic age or stage of tooth wear; however, few teeth exhibited signs of substantial wear, such as complete loss of enamel on the occlusal surface often observed in extant adult heteromyids.

For isotopic analysis via *in situ* laser ablation mass spectrometry, our procedures followed those established by Passey and Cerling (2006) and Kimura et al. (2013). We cleaned fossil specimens with acetone to remove glue and treated them with 2% NaOCl for one hour to remove organic contaminants. After rinsing specimens for residual NaOCl, we treated them with 0.1M sodium acetate-acetic acid buffer for approximately ten minutes to remove diagenetic carbonate minerals from the enamel surface while minimizing damage to the enamel itself and rinsed with Milli-Q ultrapure water (Kimura et al. 2013). Whole teeth were loaded into the sample chamber and laser-extraction line, designed by Sharp and Cerling (1996) and improved by Passey and Cerling (2006), at the University of Utah's Stable Isotope Laboratory. We utilized thermal laser ablation techniques to sample the tooth enamel *in situ*, ablating either the lingual or labial surface depending on tooth size and curvature. The CO_2 laser (wave length: 10.6 μm) setting ranged from 3.0 to 6.9 watts with an 8.5-ms pulse duration. We cryogenically trapped 10 to 20 nmols of CO_2 from multiple ablation pits (up to 20 depending on tooth surface area and properties) and passed the sample through a Poraplot-Q gas chromatographic column coupled with a Finnigan MAT 252 mass spectrometer via a Finnigan GP open-split interface.

We standardized our isotopic data utilizing internal CO_2 gas standards injected into the sample chamber with downstream analysis equivalent to the laser-generated CO_2. We analyzed blanks of the extraction-line He flow to correct for background CO_2 contamination using a mass-balance approach. To account for variation in laser behavior, we also regularly sampled pieces of enamel for which the isotopic composition was previously determined using conventional sampling and the phosphoric-acid method (Passey and Cerling 2006). Laser ablation isotopic data are reported in per mil (‰) units on the VPDB scale for $\delta^{13}C_{en}$ values and the SMOW scale for $\delta^{18}O_{en}$ values. The enamel standard was measured a total of 83 times across all runs, resulting in an analytical sample error of 0.66‰ for $\delta^{13}C_{en}$ and 0.91‰ for $\delta^{18}O_{en}$ during laser ablation. The mean offset for $\delta^{13}C$ values of the laser-ablated enamel standard compared to conventional H_3PO_4 sampling methods was -0.63‰. This value falls between values found by Passey and Cerling (-0.3‰; 2006) and Kimura et al. (-1.05‰; 2013) for modern tooth samples. A mean offset of -5.56‰ for $\delta^{18}O$ values was also similar to values of Passey and Cerling (~6.4‰; 2006) and Kimura et al. (-6.1‰; 2013). The offset determined for $\delta^{18}O$ values was much greater than that determined for $\delta^{13}C$ values due to the mixing of phosphate- and carbonate-bound oxygen in tooth enamel during laser ablation. Because there is ~9‰ offset between these two sources, the laser ablation method was less precise than the H_3PO_4 method, which analyzes only carbonate-derived oxygen (Iacumin et al. 1996, Passey and Cerling 2006).

Ideally, a single tooth position should be analyzed to minimize inter-tooth isotopic variation within individuals. However, due to low sample sizes at certain stratigraphic levels, we sampled all tooth positions available, including 4^{th} premolars and 1^{st}–3^{rd} molars. In order to examine inter-tooth isotopic variation, we conducted laser ablation sampling on each premolar and molar within the lower tooth rows of two modern heteromyid species, *Dipodomys ordii* (*n* =

4) and *Perognathus parvus* ($n = 4$). These species were selected because several of the fossil taxa represented in the Crowder and Cajon Valley formations are heteromyids, and the isotopic composition of these individuals was also known from their hair. Because teeth form at different times early in a mammal's life, isotopic composition across teeth within a jaw can be influenced by nursing during enamel apposition or mineralization, ontogenetic changes in dietary preference, and fine-scale temporal and spatial variability in food resources recorded during rapid turnover of rodent tissues (MacAvoy et al. 2006, Podlesak et al. 2008, Kimura et al. 2013).

We inspected each tooth under the microscope to assess whether the tooth enamel had been sampled without contamination during *in situ* laser ablation. From 251 samples (including replicate analyses), 127 reliable values were retained. We took the mean of replicate analyses to obtain one measurement per individual. Other samples had unreliable values either due to small gas sample sizes (<750 mV) or contamination by dentine during the sampling process. We identified samples that were corrupted by dentine from the characteristic black char left on the tooth surface if laser ablation passed through the enamel into the dentine or sampled a non-enamel surface such as the tooth root. To assess the impact of char on $\delta^{13}C_{en}$ values, we categorized each sample into relative char classes and performed a correlation analysis. There was a significant negative relationship ($p < 0.01$) between the level of charring and $\delta^{13}C_{en}$ values. Therefore, we removed any samples that showed notable charring. We also removed outlier values below -16.5‰ (3 samples), as these were judged unreliable given the carbon isotopic composition of the atmosphere in the middle Miocene (Tipple et al. 2010) and the rodent carbon isotopic enrichment factor ($\varepsilon^*_{en\text{-}diet} = +11.0‰$; Podlesak et al., 2008).

Quantitative inference

For comparison of isotopic values among different groups (e.g., tooth position, species, stratigraphic level), we first tested for homogeneity of variance using Levene's test and normality using a Shapiro-Wilk test. We applied the non-parametric Kruskal-Wallis test to non-normal datasets and an analysis of variance (ANOVA) to homogeneous and normal datasets (Sokal and Rohlf 2012) to evaluate isotopic and ecomorphological differences among taxonomic groups and fossil assemblages. While several comparisons met the criteria for the ANOVA test, due to small sample sizes, all *p*-values reported herein are from the more conservative Kruskal-Wallis test. We assessed the significance of correlations between two ecological traits (e.g., $\delta^{13}C_{en}$ and hypsodonty index) or a trait and stratigraphic position (as a measure of time) with Spearman's rank correlation coefficient.

The relative proportion of C_4 vegetation within a mammal's diet can be estimated by a simple linear mixing model between the mean $\delta^{13}C$ values of C_3 and C_4 plants. End-member C_3 and C_4 isotopic values vary through time in relation to the $\delta^{13}C$ value of atmospheric CO_2 (Passey et al. 2002, Fox et al. 2012). To compare enamel $\delta^{13}C$ with the carbon isotopic composition of C_3 and C_4 vegetation during the middle Miocene, we adjusted the isotopic composition of end-member C_3 and C_4 values according to the average $\delta^{13}C$ value of atmospheric CO_2 for 1-million year time bins through the MCO, based on reconstructions derived from benthic foraminifera (3-myr moving average values from Tipple et al. 2010). End-member values may additionally vary depending on local aridity and plant water stress (Farquhar et al. 1989, Cerling et al. 2003). This effect is more pronounced in C_3 plants and results in plants with more enriched (higher) $\delta^{13}C$ values in arid environments (Kohn 2010, Dienfendorf et al. 2010). Therefore, we applied two different mixing models, a mean end-member value and an

"arid" end-member value to identify a range of plausible C_4 dietary contributions (e.g., Fox et al. 2012), given inferred variation in moisture conditions within the basins through the middle Miocene.

RESULTS

To evaluate species-environment interactions through intervals of vegetation and climate change, we assessed isotopic composition and dental traits among small-mammal assemblages in the Crowder and Cajon Valley formations. Additionally, we investigated interspecific differences in dietary preferences, comparing fossil assemblages through time and fossil assemblages to modern communities. An initial test of isotopic differences in relation to tooth position was performed on tooth rows of modern species.

Inter-tooth variability

Within modern heteromyids (n = 8), we found no significant differences in isotopic composition based on tooth position within an individual tooth row, according to the Kruskal-Wallis analysis of variance (carbon: p-value = 0.80; oxygen: p-value = 0.92). Teeth within a single jaw varied by approximately 1‰; however, that variability was non-systematic and was lower than the variation among individuals (Table S4.1, Fig. S4.1). Since we did not find significant differences among tooth positions in modern jaws (Fig. S4.2), we pooled all premolars and molars in fossil comparisons in order to increase sample sizes within sampling units. For the entire fossil dataset (Table S4.2), carbon and oxygen isotopic composition also did not differ significantly according to tooth position across individuals. These results correspond

with the findings of other small-mammal studies (e.g., Grimes et al. 2004, Kimura et al. 2013), suggesting near contemporaneous growth and mineralization of molars in rodents.

Changes through time in the Crowder Formation

Within the Crowder Formation, the carbon isotopic composition of fossil rodent tooth enamel ranged from -16.44‰ to -9.08‰. These values were adjusted by a diet-enamel enrichment factor of +11.0‰, according to controlled diet experiments conducted on wood-rats (Podlesak et al. 2008) for comparison with the carbon isotopic composition of paleovegetation (Fig. 4.2a). Although sample sizes varied through the section, we found no significant trend in $\delta^{13}C_{en}$ values (Spearman's correlation, $p = 0.67$) or change in variance (Levene's Test, $p = 0.96$) in relation to stratigraphic position. In contrast, the parallel record of $\delta^{13}C$ preserved in soil organic matter (SOM) showed a significant drying trend through time (Smiley et al. *in review*). Crowder $\delta^{13}C_{SOM}$ values were not significantly correlated with the mean $\delta^{13}C_{en}$ values of rodent assemblages from the same paleosol horizons (Spearman's correlation, $p = 0.30$). Phytolith assemblages from this section contained roughly equal proportions of grass and forest morphotypes and documented a minimal contribution of C_4 grasses (1-4%). Fossil rodents provided different information compared to both of these records. Rodent $\delta^{13}C_{en}$ values had greater overall variance than $\delta^{13}C_{SOM}$ values, indicating a contribution of up to 18% of C_4 grasses to the diets of some individuals. This estimate is conservative, since an arid C_3-end-member value was used to construct vegetation mixing lines. However, most individuals in the Crowder Formation indicate a variable, but pure-C_3 diet. The oxygen isotopic composition of rodent enamel ranged from -9.82‰ to -1.17‰, with no significant trend (Spearman's correlation, $p = 0.37$) or change in variance (Levene's test, $p = 0.63$) through time (Fig. 4.2b).

The occlusal surface area and hypsodonty index of rodent dentitions (Fig. 4.2c,d) were also stable over time. Occlusal area differed significantly among families and genera (Kruskal-Wallis test, $p << 0.01$) and among species (Kruskal-Wallis test, $p = 0.01$), primarily due to the occurrence of large-bodied sciurid (squirrel) species. We found marginally significant differences (Kruskal-Wallis test, $p < 0.05$) in hypsodonty index among species and genera. Low hypsodonty values indicate that most taxa were brachydont to mesodont. Because heteromyid specimens form the bulk of the Crowder record, we also evaluated them separately. Heteromyid species differed in hypsodonty index (Kruskal-Wallis test, $p < 0.04$) but not in occlusal area (Kruskal-Wallis test, $p = 0.20$). For the species that occurred at multiple stratigraphic levels (e.g., *Proheteromys sulculus*), we found no significant changes in either isotopic composition or dental traits through time. None of the ecological variables were correlated through the Crowder section, suggesting little correspondence among tooth size, crown height, and diet as inferred from isotopic composition.

Changes through time in the Cajon Valley Formation

Limited stratigraphic coverage of small-mammal fossil localities ($n = 5$) in the Cajon Valley Formation reduced our ability to detect trends in isotopic composition and dental ecomorphology through the MCO. Cajon Valley $\delta^{13}C_{en}$ values ranged from -14.22‰ to -7.46‰ and $\delta^{18}O_{en}$ values ranged from -9.98‰ to -2.90‰ (Fig. 4.3a,b). Two stratigraphic sections in the Cajon Valley Formation were previously analyzed for $\delta^{13}C_{SOM}$ values and phytolith composition (Smiley et al. *in review*). Small-mammal fossil assemblages were recovered primarily from the CV-NW section, with the exception of one assemblage from the CV-SE section (at ~505 meters) composed entirely of *Harrymys maximus* specimens. This unusual assemblage represents the

only occurrence of this large-bodied heteromyid and was found in close stratigraphic association with lignite, freshwater limestone deposits, and forest-dominated phytolith assemblages, indicative of a ponded area surrounded by forest. In contrast, paleoenvironments from the CV-NW section were inferred to be arid shrublands (Smiley et al. *in review*). The phytolith assemblages of both Cajon Valley sections recorded no C_4 grasses. However, $\delta^{13}C_{SOM}$ values in the CV-NW section likely indicate the minor presence of C_4 grasses even under an arid-C_3 mixing model (Fig. 4.3a). After adjusting by a diet-enamel enrichment factor of +11.0‰, the $\delta^{13}C_{en}$ values of Cajon Valley rodents overlapped with the $\delta^{13}C_{SOM}$ record of the arid CV-NW section and also recorded the presence of C_4 grasses on the local landscape. While we infer that some individuals consumed a pure-C_3 diet, most individuals likely incorporated some C_4 vegetation into their diets. The most enriched individuals were inferred to consume up to 34% C_4 grass resources.

Because sample sizes for dental ecomorphology were insufficient at low stratigraphic positions (lack of first and second molars), we did not assess difference in hypsodonty index or occlusal surface through time (Fig. 4.3c,d). The occlusal area of *Harrymus maximus* was significantly larger than that of other species (Kruskal-Wallis test, $p < 0.01$); however, the hypsodonty index did not vary significantly among species (Kruskal-Wallis test, $p = 0.06$) and indicated that all species had brachydont to mesodont dentition. Co-occurring species from the relatively fossil-rich assemblages in Unit 6 overlapped in both hypsodonty index and occlusal area.

Inter-basin comparisons

The Crowder and Cajon Valley rodent assemblages differ significantly in $\delta^{13}C_{en}$ and

$\delta^{18}O_{en}$ values, corresponding with underlying differences in basin environments through the MCO as well as differences in the temporal coverage of these assemblages (Fig. 4.4). The assemblages sampled for isotopic composition span 17.0–15.0 Ma in the Crowder Formation and 15.0–13.0 Ma in the Cajon Valley Formation (with the exception of an early *Cupidinimus* specimen present at 16.0 Ma), representing 'warming phase' and 'cooling phase' faunas, respectively, of the MCO. While total isotopic variance in carbon and oxygen did not differ between the two formations, differences in isotopic composition at all levels of taxonomic organization—family, genus, and species—were more pronounced in the younger Cajon Valley assemblages than in the older Crowder assemblages. The $\delta^{13}C_{en}$ values of rodent families within the Cajon Valley Formation differed significantly ($p < 0.01$), while differences among genera and species approach significance ($p = 0.05$ and $p = 0.06$, respectively). In contrast, no significant differences occurred in the carbon isotopic composition at any taxonomic level within the Crowder Formation. Oxygen isotopic composition was more variable than $\delta^{13}C_{en}$ among species in both formations. We found significant differences in $\delta^{18}O_{en}$ at the family ($p = 0.01$), genus ($p = 0.05$), and species ($p = 0.02$) levels in the Cajon Valley Formation and at the family level ($p < 0.01$) but not at lower taxonomic levels (genus, $p = 0.07$; species, $p = 0.08$) in the Crowder Formation. However, these results should be interpreted cautiously given the lower precision of $\delta^{18}O_{en}$ values due to the laser ablation sampling method.

Within faunal assemblages, differences in isotopic composition could relate to dietary or microhabitat differences among co-occurring species. We found greater inter-specific isotopic differences within individual Cajon Valley assemblages than in Crowder assemblages (Fig. 4.5). However, neither Cajon Valley nor Crowder assemblages exhibited as much isotopic differentiation as species within present-day communities (Table S4.3), represented here by co-

occurring heteromyids from a dry, predominantly C_4-grassland ecosystem (Desert Range, UT) and a mixed C_3-C_4 grassland ecosystem (Beaverdam Wash, UT). For more present-day examples and details on data collection of modern heteromyids, see Smiley et al. (2015). These examples demonstrate differences in species isotopic breadth and overlap between Miocene and present-day assemblages: isotopic differentiation among co-occurring rodents in western ecosystems today is greater than among Crowder and Cajon Valley species during the MCO.

DISCUSSION

Implications for paleoenvironmental reconstruction

As the temporal and spatial distribution of high-resolution terrestrial records during past intervals of climate change increases, examples of asynchronous ecosystem response to the same global driver abound (Strömberg 2011, Cotton et al. 2012, Chen et al. 2015). Multi-proxy approaches and lateral sampling at correlated stratigraphic levels document changes in habitat heterogeneity from local to regional scales (Fox and Koch 2003, Fox et al. 2012). The Crowder and Cajon Valley formations represent two such records with modest environmental change during the last major warming interval of the Neogene and significant spatial variation in vegetation and moisture conditions between basins (over distances of 10s of km) and within each basin (over ~3 km). Paleoenvironmental reconstructions indicate a drying trend, increased grasses in the region during the MCO, and at least three distinct C_3-dominated habitats: a mixed grass and woodland floodplain ecosystem; a poorly-drained, grassy-woodland ecosystem with shallow ponds and swamps; and, an arid shrubland ecosystem (Smiley et al. *in review*). Together, phytoliths and $\delta^{13}C_{SOM}$ reveal the earliest evidence for C_4 grasses in these basins and in the broader Mojave region.

Small-mammal enamel isotopic composition provides unique information for paleoenvironmental reconstruction by reducing the temporal and spatial averaging inherent in phytolith assemblages and paleosol proxies. In the Crowder and Cajon Valley formations, mean $\delta^{13}C_{diet}$ values were similar to $\delta^{13}C_{SOM}$ values for most paleosol units, supporting the reconstructions of primarily-C_3 ecosystems. However, individual rodents were also highly variable around the assemblage mean. For example, in the Cajon Valley Formation, a conservative estimate (assuming an arid-C_3 end-member) for the proportion of C_4 vegetation within the diets of the most enriched *Harrymys maximus* individuals indicated that a third of their diet consisted of C_4 vegetation. This signature of C_4-grass abundance differed strikingly from $\delta^{13}C_{SOM}$ and phytolith-derived estimates, which provided no indication of C_4 vegetation in the associated CV-SE section. The apparent discrepancy between inferred resource availability and resource use implies that rodents record finer-scale variation in vegetation over time or space than do environmental proxies (Hynek et al. 2012). Based on the diet of extant analogues and features of their dental morphology, all of the rodent taxa analyzed here were herbivorous browsers or granivores (Korth 1994, Janis et al. 2008b, Samuels 2009). However, because rodents are often opportunistic feeders, incorporating insects, fungi, and other items into their diet (Reichman and Price 1993), some $\delta^{13}C_{diet}$ variation may result from alternative dietary resources and trophic enrichment (Koch 1998). These alternative explanations should be considered; however, the isotopic variance (up to 7‰) within assemblages is wider than expected based on trophic enrichment alone and likely signifies the consumption of heterogeneous vegetation resources (Smiley et al. 2015).

Evidence for a minor presence of C_4 grasses elsewhere in the Mojave region comes from the isotopic composition of large-mammal tooth enamel from the Barstow Formation between

14.0–13.4 Ma (Feranec and Pagnac 2013). While several ungulate species sampled from the Barstow Formation indicate a pure-C_3 diet, $\delta^{13}C_{en}$ values from equids recorded up to 18% C_4 grass contribution to their diets. Rodent isotopic composition from the Crowder and Cajon Valley formations suggest an earlier presence of C_4 vegetation on the landscape than do large mammals from the Barstow Formation. Because rodents recorded temporal and spatial heterogeneity in vegetation to a greater degree than their large-mammal counterparts and environmental proxies, analyses of their isotopic composition add unique information to the history of C_4-grass presence in the region prior to its expansion and document C_4 grasses as a novel dietary resource for large and small mammals alike. Early and persistent, but spatially-limited, evidence of C_4 grasses from middle Miocene rodents in the Mojave region supports mechanisms for C_4-grass expansion that do not rely on global drivers, such as CO_2 concentration, that would promote simultaneous expansion across regions and continents. Instead, the Crowder and Cajon Valley C_4-grass records correspond with asynchronous and geographically restricted drivers of C_4-grass expansion, such as changes in local aridity or increased fire frequency (Pagani et al. 1999, Keeley and Rundel 2005, Osborne 2008).

Implications for ecological response to the MCO and environmental change

To evaluate whether species dietary ecology and ecomorphology changed through time in relation to corresponding trends in local vegetation and climate, we first consider the Crowder and Cajon Valley records separately and then as a continuous record through the MCO. In the Crowder Formation, faunal assemblages did not differ in $\delta^{13}C_{en}$ values over time, exhibiting no correlation with the increasing $\delta^{13}C_{SOM}$ values inferred to document habitat drying (Fig. 4.2a). While some individuals recorded up to 18% C_4 vegetation in their diet, most rodents had

predominantly C_3 diets through this record. In the Cajon Valley Formation, assemblages from both mesic, C_3-forest ecosystems (CV-SE) and arid, mixed C_3-C_4 ecosystems (CV-NW) recorded a stable range of diets (Fig. 4.3a). Within assemblages, individual diets consistently spanned pure-C_3 resources to mixed C_3-C_4 resources through time.

Oxygen isotopic composition of rodent teeth was also stable over time within each basin (Figs. 4.2b and 4.3b). Mean annual precipitation estimated from the paleosol-derived *CIA-K* proxy was 700-800 mm/yr^{-1} at the base of each section (Smiley et al. *in review*). Subsequent increases in $\delta^{13}C_{SOM}$ values and grass phytolith proportions document a shift in the hydroclimate to more arid local ecosystems by the end of the MCO. The lack of a corresponding trend in $\delta^{18}O_{en}$ values may suggest that changing moisture conditions in the Crowder and Cajon Valley basins did not influence rodent diets. The oxygen isotopic composition of enamel has been used as a proxy for the isotopic composition of meteoric water and the seasonality, aridity, and temperature of past environments (Fricke et al. 1998, Levin et al. 2006, Grimes et al. 2008). However, because many sources contribute to $\delta^{18}O_{en}$ values (e.g., drinking water versus leaf water, metabolic water, atmospheric O_2), detecting and interpreting shifts in $\delta^{18}O_{en}$ values that are related to modest changes in aridity can be difficult (Kohn 1996, Grimes et al. 2008). These challenges are heightened in thermal laser ablation analyses due to the mixing of phosphate- and carbonate-bound oxygen during sampling. Despite these limitations, relative differences in $\delta^{18}O_{en}$ values over time and among species can be useful for inferring water use and moisture conditions (e.g., Smiley et al. 2015). Together, the carbon and oxygen isotopic composition of rodent enamel suggests remarkable ecological stability within each basin in relation to contemporaneous changes in local aridity and vegetation. However, ecological stability may not be the expected response to ongoing rapid climate and environmental change today.

In contrast to the records within basins, differences in small-mammal isotopic composition between basins were pronounced (Fig. 4.4). Younger Cajon Valley faunas had significantly more enriched $\delta^{13}C_{en}$ values and more depleted $\delta^{18}O_{en}$ values than did Crowder faunas. There are three plausible hypotheses for these differences. First, within the context of the MCO, the Crowder assemblages represent 'warming phase' faunas (17.0–15.0 Ma), whereas the Cajon Valley assemblages represent 'cooling phase' faunas (15.0–13.0 Ma). Therefore, differences in isotopic composition between the two formations may reflect ecological responses, such as dietary niche shifts, to vegetation and climate change during the MCO. Second, differences in the isotopic composition of rodent enamel between the basins may correspond with spatial, and not temporal, variation in dietary resources and generalist feeding behavior over a gradient in dietary resources. Third, the taxonomic composition of small-mammal faunas differed between the two formations; therefore, the isotopic differences may reflect distinctive dietary preferences among species assemblages from the Crowder and Cajon Valley basins. The Crowder faunas were dominated by heteromyid and sciurid species, whereas the Cajon Valley faunas comprised mainly heteromyids, geomyids, and cricetids (Table 4.1). Only four small-mammal species were shared between the two basins, despite their relative proximity. Despite low faunal similarity, differences in interspecific dietary preference as an explanation for $\delta^{13}C_{en}$ and $\delta^{18}O_{en}$ differences between the two basins is unlikely given the broad isotopic overlap among species within each individual basin (Fig. 4.4).

Whether the isotopic difference between formations was a response to climate change during the MCO or due to spatial variation in dietary resources and moisture conditions can be tested by documenting changes over time in those species shared between the basins. Two species, *Proheteromys sulculus* and *Perognathus furlongi,* spanned the warming and cooling

phases of the MCO, and both recorded more enriched $\delta^{13}C_{en}$ values in the Cajon Valley Formation than in the Crowder Formation. Although this shift between basins was not significant (Kolmogorov-Smirnov test: $p = 0.11$ for *P. sulculus* and $p = 0.18$ for *P. furlongi*), it suggests a greater reliance on C_4-grass resources over time. While gradients in vegetation structure (e.g., forest-dominated versus grassland ecosystems) and moisture did exist between the basins, major differences in C_4-grass composition were not evident (Smiley et al. *in review*). Therefore, changes in the isotopic composition of *P. sulculus* and *P. furlongi* imply that these rodents consumed a novel and spatially-restricted C_4 dietary resource to a greater degree in the younger Cajon Valley basin than in the older Crowder basin, and support the hypothesis that species underwent shifts in their dietary ecology during the MCO. These alternative explanations for the basin-level differences over time or space are not mutually exclusive. Furthermore, biotic response to the MCO was not restricted to changes in species dietary ecology. Biotic response to climate and vegetation change can also include changes in species richness and composition (e.g., Blois et al. 2010). Indeed, in the Crowder Formation, mammalian species richness declined during the MCO as local ecosystems became increasingly arid (Reynolds et al. 2008, Smiley et al. *in review*).

In contrast to isotopic composition, dental ecomorphology varied little temporally or spatially. Hypsodonty index and occlusal surface area did not change over time within or between the Crowder and Cajon Valley formations during the MCO (Figs. 4.2 and 4.3). Teeth of both relatively large-bodied (e.g., *Harrymys maximus* and sciurid speices) and small-bodied (e.g., *Perognathus furlongi*) rodents remain low-crowned throughout the MCO in both basins. In contrast, large-mammal faunas from the Crowder and Cajon Valley formations comprised both low and high-crowned ungulates that are inferred to range in diet from pure browsers (e.g., the

chalicothere, *Moropus*, and the equid, *Archaeohippus*) to mixed feeders that included browse and grass in their diets (e.g., the equids, *Parapliohippus* and *Scaphohippus*), but no pure grazing taxa were present (Woodburne and Golz 1972, Janis et al. 2008a, Reynolds et al. 2008, Smiley et al. *in review*). Growing evidence suggests that high-crowned teeth are an evolutionary response to the incorporation of grit and soil into the diet in arid ecosystems (Williams and Kay 2001, Damuth and Janis 2011). In the Great Plains, the evolution of high-crowned teeth in rodents preceded the expansion of grassland ecosystems and the appearance of hypsodonty in large mammals (Strömberg 2011, Jardine et al. 2012). However, rodents from the Crowder and Cajon Valley formations appear to have lagged behind the evolution of mesodont and hypsodont dentitions in their contemporaneous Great Plains relatives. This temporal lag may be expected given the delayed rise and dominance of grassland ecosystems in many western regions (Strömberg 2011). Importantly, changes in isotopic composition reflect changes in behavior and dietary ecology over ecological timescales, whereas changes in tooth morphology occur over evolutionary timescales. Therefore, responses to ecosystem changes in isotopic composition should be evident before corresponding changes in ecomorphological traits such as crown height.

Implications for species niches

The isotopic niche concept was applied to the Crowder and Cajon Valley assemblages to assess whether co-occurring species differed in their dietary ecology. The isotopic niche refers to species distributions along an isotopic, or resource-use gradient, in relation to the isotopic composition of available resources, and reflects variation in niche breadth (i.e., generalist or specialist), degree of niche overlap (e.g., shared resources), and differences in dietary preferences (Bearhop et al. 2004, Layman et al. 2007, Newsome et al. 2007). In both Crowder

and Cajon Valley assemblages, there was little evidence for ecological differentiation among co-occurring rodent species based on isotopic composition, thus implying a high degree of niche overlap and shared resources (Fig. 4.5a,b). Species that demonstrated the full isotopic range of the assemblage (e.g., *Paratrogomys whistleri*) may be considered dietary generalists. The ability to differentiate dietary composition based on $\delta^{13}C_{en}$ could be limited in pure or predominantly-C_3 ecosystems like those of the Crowder and Cajon Valley formations. However, variation in $\delta^{13}C_{C3}$ values corresponding with moisture conditions and canopy cover have been utilized to successfully distinguish species ecology in other ecosystems lacking C_4 resources (e.g., Cerling et al. 2004, Kohn 2010, Diefendorf et al. 2010, Domingo et al. 2013). For example, sympatric, herbivorous rodent species from fossil and modern C_3-ecosystems in Europe exhibited non-overlapping $\delta^{13}C$ and $\delta^{18}O$ values, and thus were inferred to differ in their dietary ecology (Grimes et al 2004, Gehler et al. 2012). Given the differences in moisture conditions and vegetation structure within the reconstructed Crowder and Cajon Valley paleoenvironments, it is surprising to find only subtle interspecific differences in the isotopic composition of co-occurring rodent species. Although species may have been distinct in other aspects of their ecology that are not documented by carbon and oxygen isotopes, these results suggest little dietary niche partitioning among rodents inhabiting local ecosystems during the MCO.

The absence of isotopic niche differentiation in these middle Miocene assemblages contrasts with patterns found in present-day communities. Significant differences in $\delta^{13}C_{hair}$ values were found among co-occurring heteromyid species in both mesic and arid ecosystems in Utah (Fig. 4.5c,d) and across a gradient in C_3 and C_4 grass distribution over western North America (Smiley et al. 2015). Differences in the degree of isotopic overlap among fossil and modern species appears to be independent of the total isotopic variation within the community,

which is similar today and during the middle Miocene (~7‰). These results suggest that isotopic niche differentiation in present-day communities is not a consequence of an expanding isotopic breadth of the underlying resource base, but instead may reflect dietary specialization among coexisting species. The lack of ecological differentiation among taxa in the Crowder and Cajon Valley ecosystems suggests that different constraints operated on community assembly during the MCO compared to western ecosystems today. The capacity of warm, mesic middle Miocene ecosystems to accommodate high local species richness without corresponding ecological differentiation may be an important factor contributing to the peak in mammal species richness at broader spatial scales during this time period (e.g., Finarelli and Badgley 2010, Badgley et al. 2014).

The absence of interspecific differences in occlusal area and hypsodonty index among fossil assemblages mirrored isotopic findings. With the exception of large-bodied squirrels, co-occurring fossil species varied little in either dental metric, supporting the inference that species overlapped significantly in their dietary ecology. These findings contrast starkly with patterns found in present-day communities. For example, in modern desert rodent communities, body size differs among coexisting heteromyid species more than would be expected based on random assembly from the regional species pool (Bowers and Brown 1982). Coexisting heteromyid species from different genera also differ in hypsodonty, with larger kangaroo rats exhibiting ever-growing molars and smaller pocket mice exhibiting mesodont molars. Likewise, within genera, quantitative dental measurements accurately distinguish closely related extant *Dipodomys* species (Carrasco 2000). While divergence in size and dentition (and several other features, including locomotion) is pronounced among modern heteromyids, other clades, such as Cricetidae and Sciuridae, exhibit less ecological divergence among co-occurring species within

the same ecosystems (Price and Brown 1982, Zelditch et al. 2015). Therefore, to better elucidate the mechanisms underlying community assembly and the coexistence of ecologically similar small-mammal species during the MCO, groups other than desert-adapted heteromyids (e.g., rodent faunas from subtropical and tropical ecosystems) may be better analogs for the Crowder and Cajon Valley assemblages. However, the focus on heteromyids remains interesting, as shifts in isotopic composition during the MCO may represent an early stage in the ecological differentiation of this diverse and widespread North American clade. The Mojave region contains the most continuous fossil record of small-mammal assemblages in western North America, spanning most of the Neogene from 17.5 to 5.0 Ma (Woodburne et al. 1990, Woodburne 1991, Badgley et al. 2015). Expansion of this research could potentially uncover the history of ecological divergence and community structure among heteromyids in relation to the development of topographic complexity and desert ecosystems in western North America (e.g., Badgley et al. 2014).

CONCLUSIONS

Climate change is a pervasive feature of Earth's dynamic history. Understanding biotic responses to past climate change has taken on new importance given today's accelerating rates of anthropogenic climate change (Walther et al. 2002, Parmesan 2006, Blois and Hadly 2009). Over shallow-time, small-mammal community response to glacial-interglacial climate fluctuations is increasingly well characterized (e.g., Terry et al. 2011, Jezkova et al. 2014, Rowe and Terry 2014). Likewise, ecological inference for large mammals has been an influential component of North American paleontology and paleoenvironmental reconstructions (e.g., Janis et al. 2008a). However, our understanding of small-mammal ecological and evolutionary dynamics over the

Neogene has lagged behind analyses of these important records. This study contributes to filling that gap by focusing on ecological response to local environmental change in the Crowder and Cajon Valley formations during the initiation and termination of the Miocene Climate Optimum warming. Using *in situ* laser ablation sampling approaches, we demonstrated that rodent fossils recorded unique paleoenvironmental information. Specifically, rodents provided estimates of fine-scale variation in vegetation and exhibited dietary preference for spatially or temporally restricted C_4 dietary resources. Changes in rodent dietary ecology did not correspond temporally with underlying changes in vegetation and moisture conditions, suggesting that species response to future climate change may be difficult to predict. The lack of ecological differentiation among co-occurring species in the Crowder and Cajon Valley faunal assemblages illustrates how community assembly may have differed under past, no-analog climate conditions. Small mammals today represent over half of North American diversity. Therefore, gaining insight into their past ecological dynamics is a valuable approach to conserving their future under current climate warming and habitat transformation.

ACKNOWLEDGMENTS

This work was supported by the National Science Foundation (NSF – 1137336, Inter-university Training for Continental-scale Ecology (ITCE)) and a NSF Graduate Research Fellowship for Smiley. Additional support was received from the University of Michigan's Undergraduate Research Opportunity Program Biomedicial and Life Sciences Fellowship and the Ecology and Evolutionary Biology Undergraduate Research Grant for Moroz. We thank Yuri Kimura and Kendra Chritz at the Stable Isotope Ratio Facility for Environmental Research at the University of Utah for their training and assistance with isotopic analyses. We are exceptionally grateful to

Robert E. Reynolds for his guidance with fossil rodents from the Crowder and Cajon Valley formations. Eric Scott and the San Bernardino County Museum provided access to fossil specimens for study and sampling. We also thank Eric Rickart and Cody Thompson for assistance, and the Natural History Museum of Utah and the University of Michigan Museum of Zoology for making modern specimens available for study.

REFERENCES

Alroy, J., 1998. Cope's rule and the dynamics of body mass evolution in North American fossil mammals. Science 280, 731–734.

Badgley, C., Fox, D.L., 2000. Ecological biogeography of North American mammals: species density and ecological structure in relation to environmental gradients. Journal of Biogeography 27, 1437–1467.

Badgley, C., Smiley, T.M., Finarelli, J.A., 2014. Great Basin mammal diversity in relation to landscape history. Journal of Mammalogy 95, 1090–1106.

Badgley, C., Smiley, T.M., Loughney, K., 2015. Miocene mammal diversity of the Mojave region in the context of Great Basin mammal history, in: Mojave Miocene, Desert Symposium Field Guide and Proceedings, pp. 34–43.

Barnosky, A.D., Carrasco, M.A., 2002. Effects of Oligo-Miocene global climate changes on mammalian species richness in the northwestern quarter of the USA. Evolutionary Ecology Research 4, 811–841.

Barnosky, A.D., Hadly, E.A., Bell, C.J., 2003. Mammalian response to global warming on varied temporal scales. Journal of Mammalogy 84, 354–368.

Bearhop, S., Adams, C.E., Waldron, S., 2004. Determining trophic niche width: a novel approach using stable isotope analysis. Journal of Animal Ecology 73, 1007–1012.

Behrensmeyer, A.K., Kidwell, S.M., Gastaldo, R.A., 2000. Taphonomy and paleobiology. Paleobiology 26, 103–147.

Bennington, J.B., Dimichele, W.A., Badgley, C., Bambach, R.K., Barrett, P.M., Behrensmeyer, A.K., Bobe, R., Burnham, R.J., Daeschler, E.B., Dam, J.V., Eronen, J.T., Erwin, D.H., Finnegan, S., Holland, S.M., Hunt, G., Jablonski, D., Jackson, S.T., Jacobs, B.F., Kidwell, S.M., Koch, P.L., Kowalewski, M.J., Labandeira, C.C., Looy, C.V., Lyons, S.K., Novack-Gottshall, P.M., Potts, R., Roopnarine, P.D., Stromberg, C.A.E., Sues, H.D., Wagner, P.J., Wilf, P., Wing, S.L., 2009. Critical issues of scale in paleoecology. PALAIOS 24, 1–4.

Blois, J.L., Hadly, E.A., 2009. Mammalian response to Cenozoic climatic change. Annual Review of Earth and Planetary Science 37, 181–208.

Blois, J.L., McGuire, J.L., Hadly, E.A., 2010. Small mammal diversity loss in response to late-Pleistocene climatic change. Nature 465, 771–774.

Blois, J.L., Zarnetske, P.L., Fitzpatrick, M.C., Finnegan, S., 2013. Climate change and the past, present, and future of biotic interactions. Science 341, 499–504.

Bowers, M.A., Brown, J.H., 1982. Body size and coexistence in desert rodents: chance or community structure? Ecology 63, 391–400.

Brewer, S., Jackson, S.T., Williams, J.W., 2012. Paleoecoinformatics: applying geohistorical data to ecological questions. Trends in Ecology & Evolution 27, 104–112.

Brown, J.H., 1973. Species diversity of seed-eating desert rodents in sand dune habitats. Ecology 54, 775–787.

Brown, J.H., Lieberman, G.A., 1973. Resource utilization and coexistence of seed-eating desert rodents in sand dune habitats. Ecology 54, 788–797.

Carrasco, M.A., 2000. Species discrimination and morphological relationships of kangaroo rats (*Dipodomys*) based on their dentition. Journal of Mammalogy 81, 107–122.

Cerling, T.E., Andanje, S.A., Blumenthal, S.A., Brown, F.H., Chritz, K.L., Harris, J.M., Hart, J.A., Kirera, F.M., Kaleme, P., Leakey, L.N., Leakey, M.G., Levin, N.E., Manthi, F.K., Passey, B.H., Uno, K.T., 2015. Dietary changes of large herbivores in the Turkana Basin, Kenya from 4 to 1 Ma. Proceedings of the National Academy of Sciences 112, 11467–11472.

Cerling, T.E., Harris, J.M., MacFadden, B.J., Leakey, M.G., Quade, J., Eisenmann, V., Ehleringer, J.R., 1997. Global vegetation change through the Miocene/Pliocene boundary. Nature 389, 153–158.

Cerling, T.E., Harris, J.M., Passey, B.H., 2003. Diets of East African Bovidae based on stable isotope analysis. Journal of Mammalogy 84, 456–470.

Cerling, T.E., Hart, J.A., Hart, T.B., 2004. Stable isotope ecology in the Ituri Forest. Oecologia 138, 5–12.

Cerling, T.E., Sharp, Z.D., 1996. Stable carbon and oxygen isotope analysis of fossil tooth enamel using laser ablation. Palaeogeography, Palaeoclimatology, Palaeoecology 126, 173–186.

Chen, S.T., Smith, S.Y., Sheldon, N.D., Strömberg, C.A.E., 2015. Regional-scale variability in the spread of grasslands in the late Miocene. Palaeogeography, Palaeoclimatology, Palaeoecology 437, 42–52.

Cotton, J.M., Sheldon, N.D., Strömberg, C.A.E., 2012. High-resolution isotopic record of C_4 photosynthesis in a Miocene grassland. Palaeogeography, Palaeoclimatology, Palaeoecology 337-338, 88–98.

Damuth, J., and MacFadden, B.J., 1990. Body size in mammalian paleobiology. Cambridge University Press, London.

Damuth, J., Janis, C.M., 2014. A comparison of observed molar wear rates in extant herbivorous mammals. Annales Zoologici Fennici 51, 188–200.

Damuth, J., Janis, C.M., 2011. On the relationship between hypsodonty and feeding ecology in ungulate mammals, and its utility in palaeoecology. Biological Reviews 86, 733–758.

Diefendorf, A.F., Mueller, K.E., Wing, S.L., Koch, P.L., Freeman, K.H., 2010. Global patterns in leaf ^{13}C discrimination and implications for studies of past and future climate. Proceedings of the National Academy of Sciences 107, 5738–5743.

DiMichele, W.A., Behrensmeyer, A.K., Olszewski, T.D., 2004. Long-term stasis in ecological assemblages: evidence from the fossil record. Annual Review of Ecology, Evolution, and Systematics 35, 285–322.

Domingo, M.S., Domingo, L., Badgley, C., Sanisidro, O., Morales, J., 2013. Resource partitioning among top predators in a Miocene food web. Proceedings of the Royal Society B-Biological Sciences 280, 20122138.

Ernest, S., 2005. Body size, energy use, and community structure of small mammals. Ecology 86, 1407–1413.

Farquhar, G.D., Ehleringer, J.R., Hubick, K.T., 1989. Carbon isotope discrimination and photosynthesis. Annual Review of Plant Biology 40, 503–537.

Feranec, R.S., Pagnac, D., 2013. Stable carbon isotope evidence for the abundance of C_4 plants in the middle Miocene of southern California. Palaeogeography, Palaeoclimatology, Palaeoecology 388, 42–47.

Finarelli, J.A., Badgley, C., 2010. Diversity dynamics of Miocene mammals in relation to the history of tectonism and climate. Proceedings of the Royal Society B: Biological Sciences 277, 2721–2726.

Foster, J. F. 1980. Late Cenozoic tectonic evolution of Cajon Valley, Southern California. Ph.D. thesis, University of California Riverside, 238pp.

Fox, B.J., Brown, J.H., 1993. Assembly rules for functional groups in North American desert rodent communities. Oikos 67, 358–370.

Fox, D.L., Honey, J.G., Martin, R.A., Peláez-Campomanes, P., 2012. Pedogenic carbonate stable isotope record of environmental change during the Neogene in the southern Great Plains, southwest Kansas, USA: Carbon isotopes and the evolution of C_4-dominated grasslands. Geological Society of America Bulletin 124, 444–462.

Fox, D.L., Koch, P.L., 2003. Tertiary history of C_4 biomass in the Great Plains, USA. Geology 31, 809–812.

Fricke, H.C., Clyde, W.C., O'Neil, J.R., 1998. Intra-tooth variations in $\delta^{18}O$ (PO_4) of mammalian tooth enamel as a record of seasonal variations in continental climate variables. Geochimica et Cosmochimica Acta 62, 1839–1850.

Gehler, A., Tütken, T., Pack, A., 2012. Oxygen and carbon isotope variations in a modern rodent community – implications for palaeoenvironmental reconstructions. PLoS ONE 7, e49531.

Goldner, A., Herold, N., Huber, M., 2014. The challenge of simulating the warmth of the mid-Miocene climatic optimum in CESM1. Climates of the Past 10, 523–536.

Grimes, S.T., Mattey, D.P., Hooker, J.J., Collinson, M.E., 2003. Paleogene paleoclimate reconstruction using oxygen isotopes from land and freshwater organisms: the use of multiple paleoproxies. Geochimica et Cosmochimica Acta 67, 4033–4047.

Grimes, S.T., Collinson, M.E., Hooker, J.J., Mattey, D.P., Grassineau, N.V., Lowry, D., 2004. Distinguishing the diets of coexisting fossil theridomyid and glirid rodents using carbon isotopes. Palaeogeography, Palaeoclimatology, Palaeoecology 208, 103–119.

Grimes, S.T., Collinson, M.E., Hooker, J.J., Mattey, D.P., 2008. Is small beautiful? A review of the advantages and limitations of using small mammal teeth and the direct laser fluorination analysis technique in the isotope reconstruction of past continental climate change. Palaeogeography, Palaeoclimatology, Palaeoecology 266, 39–50.

Hynek, S.A., Passey, B.H., Prado, J.L., Brown, F.H., Cerling, T.E., Quade, J., 2012. Small mammal carbon isotope ecology across the Miocene–Pliocene boundary, northwestern Argentina. Earth and Planetary Science Letters 321-322, 177–188.

Iacumin, P., Bocherens, H., Mariotti, A., 1996. Oxygen isotope analyses of co-existing carbonate and phosphate in biogenic apatite: a way to monitor diagenetic alteration of bone phosphate? Earth and Planetary Sciences Letters 142, 1–6.

Janis, C.M., Scott, K.M., Jacobs, L.L., (Eds.) 2008a. Evolution of Tertiary mammals of North America Volume 1: Terrestrial carnivores, ungulates and ungulate-like mammals. Cambridge University Press, Cambridge, United Kingdom.

Janis, C.M., Gunnell, G.F., Uhen, M.D., (Eds.) 2008b. Evolution of Tertiary mammals of North America Volume 2: Small mammals, xenarthrans, and marine mammals. Cambridge University Press, Cambridge, United Kingdom.

Jardine, P.E., Janis, C.M., Sahney, S., Benton, M.J., 2012. Grit not grass: concordant patterns of early origin of hypsodonty in Great Plains ungulates and Glires. Palaeogeography, Palaeoclimatology, Palaeoecology 365-366, 1–10.

Jezkova, T., Riddle, B.R., Card, D.C., Schield, D.R., Eckstut, M.E., Castoe, T.A., 2014. Genetic consequences of postglacial range expansion in two codistributed rodents (genus *Dipodomys*) depend on ecology and genetic locus. Molecular Ecology 24, 83–97.

Keeley, J.E., Rundel, P.W., 2005. Fire and the Miocene expansion of C_4 grasslands. Ecology Letters 8, 683–690.

Kelt, D.A., 1999. On the relative importance of history and ecology in structuring communities of desert small animals. Ecography 22, 123–137.

Kidwell, S.M., Flessa, K.W., 1995. The quality of the fossil record: populations, species, and communities. Annual Review of Ecology and Systematics 26, 269–299.

Kidwell, S.M., Tomasovych, A., 2013. Implications of time-averaged death assemblages for ecology and conservation biology. Annual Review of Ecology and Evolutionary Systematics 44, 539–563.

Kimura, Y., Jacobs, L.L., Cerling, T.E., Uno, K.T., Ferguson, K.M., Flynn, L.J., Patnaik, R., 2013. Fossil mice and rats show isotopic evidence of niche partitioning and change in dental ecomorphology related to dietary shift in Late Miocene of Pakistan. PLoS ONE 8, e69308.

Koch, P.L., 1998. Isotopic reconstruction of past continental environments. Annual Review of Earth and Planetary Sciences 26, 573–613.

Kohn, M.J., 1996. Predicting animal $\delta^{18}O$: Accounting for diet and physiological adaptation. Geochimica et Cosmochimica Acta 60, 4811–4829.

Kohn, M.J., 2010. Carbon isotope compositions of terrestrial C_3 plants as indicators of (paleo) ecology and (paleo) climate. Proceedings of the National Academy of Sciences 107, 19691–19695.

Korth, W.K., 1994. The Tertiary record of rodents in North America. Plenum Press, New York, New York.

Kotler, B.P., Brown, J.S., 1988. Environmental heterogeneity and the coexistence of desert rodents. Annual Review of Ecology and Systematics 19, 281–307.

Layman, C.A., Arrington, D.A., Montaña, C.G., Post, D.M., 2007. Can stable isotope ratios provide for community-wide measures of trophic structure? Ecology 88, 42–48.

Levin, N.E., Cerling, T.E., Passey, B.H., Harris, J.M., Ehleringer, J.R., 2006. A stable isotope aridity index for terrestrial environments. Proceedings of the National Academy of Sciences 103, 11201–11205.

Lindsay, E.H., Reynolds, R.E., 2008. Heteromyid rodents from Miocene faunas of the Mojave Desert, Southern California. Science Series 41, 213–235.

MacAvoy, S.E., Arneson, L.S., Bassett, E., 2006. Correlation of metabolism with tissue carbon and nitrogen turnover rate in small mammals. Oecologia 150, 190–201.

McGill, B., Enquist, B., Weiher, E., Westoby, M., 2006. Rebuilding community ecology from functional traits. Trends in Ecology & Evolution 21, 178–185.

Meisling, K.E., Weldon, R.J., 1989. Late Cenozoic tectonics of the northwestern San Bernardino Mountains, southern California. Geological Society of America Bulletin 101, 106–128.

Morton, D.M., Miller, F.K., 2006. Geologic Map of the San Bernardino and Santa Ana 30′ X 60′ Quadrangles, California. US Geological Survey.

Munger, J.C., Brown, J.H., 1981. Competition in desert rodents: an experiment with semipermeable exclosures. Science 211, 510–512.

Newsome, S.D., Martinez del Rio, C., Bearhop, S., Phillips, D.L., 2007. A niche for isotopic ecology. Frontiers in Ecology and the Environment 5, 429–436.

Noble, L.F., 1954. The San Andreas fault zone from Soledad Pass to Cajon Pass, California. Geology of Southern California, California Department of Resources, Division of Mines Bulletin 170, 37-48.

Osborne, C.P., 2008. Atmosphere, ecology and evolution: what drove the Miocene expansion of C_4 grasslands? Journal of Ecology 96, 35–45.

Pagani, M., Freeman, K.H., Arthur, M.A., 1999. Late Miocene atmospheric CO_2 concentrations and the expansion of C_4 grasses. Science 285, 876–879.

Parmesan, C., 2006. Ecological and evolutionary responses to recent climate change. Annual Review of Ecology and Evolutionary Systematics 37, 637–669.

Passey, B.H., Cerling, T.E., 2006. In situ stable isotope analysis ($\delta^{13}C$, $\delta^{18}O$) of very small teeth using laser ablation GC/IRMS. Chemical Geology 235, 238–249.

Passey, B.H., Cerling, T.E., Perkins, M.E., Voorhies, M.R., 2002. Environmental change in the Great Plains: an isotopic record from fossil horses. The Journal of Geology 110, 123–140.

Podlesak, D.W., Torregrossa, A.-M., Ehleringer, J.R., Dearing, M.D., Passey, B.H., Cerling, T.E., 2008. Turnover of oxygen and hydrogen isotopes in the body water, CO_2, hair, and enamel of a small mammal. Geochimica et Cosmochimica Acta 72, 19–35.

Pound, M.J., Haywood, A.M., Salzmann, U., Riding, J.B., 2012. Global vegetation dynamics and latitudinal temperature gradients during the Mid to Late Miocene (15.97–5.33Ma). Earth Science Reviews 112, 1–22.

Price, M.V., 1978. The role of microhabitat in structuring desert rodent communities. Ecology 59, 910–921.

Reichman, O. J., Price, M.V., 1993. Ecological aspects of heteromyid foraging, in: Genoways, H.H. and Brown, J.H. (Eds.), Biology of Heteromyidae. The American Society of Mammalogists, pp. 539–574.

Reynolds, R.E., 1991. Biostratigraphic relationships of Tertiary small vertebrates from Cajon Valley, San Bernardino County, California. San Bernardino County Museum Association Quarterly 38, 54–59.

Reynolds, R.E., Reynolds, R.L., Lindsay, E.H., 2008. Biostratigraphy of the Miocene Crowder Formation, Cajon Pass, southwestern Mojave Desert, California. Natural History Museum of Los Angeles County Science Series 41, 237–253.

Riddle, B.R., Honeycutt, R.L., 1990. Historical biogeography in North American arid regions: an approach using mitochondrial-DNA phylogeny in grasshopper mice (genus *Onychomys*). Evolution 44, 1–15.

Riddle, B.R., Jezkova, T., Hornsby, A.D., Matocq, M.D., 2014a. Assembling the modern Great Basin mammal biota: insights from molecular biogeography and the fossil record. Journal of Mammalogy 95, 1107–1127.

Riddle, B.R., Jezkova, T., Eckstut, M.E., Olah Hemmings, V., Carraway, L.N., 2014b. Cryptic divergence and revised species taxonomy within the Great Basin pocket mouse, *Perognathus parvus* (Peale, 1848), species group. Journal of Mammalogy 95, 9–25.

Rosenzweig, M.L., Winakur, J., 1969. Population ecology of desert rodent communities: habitats and environmental complexity. Ecology 50, 558–572.

Rowe, R.J., Terry, R.C., 2014. Small mammal responses to environmental change: integrating past and present dynamics. Journal of Mammalogy 95, 1157–1174.

Samuels, J.X., 2009. Cranial morphology and dietary habits of rodents. Zoological Journal of the Linnean Society 156, 864–888.

Schoeninger, M.J., Iwaniec, U.T., Nash, L.T., 1998. Ecological attributes recorded in stable isotope ratios of arboreal prosimian hair. Oecologia 113, 222–230.

Shenbrot, G.I., Krasnov, B., Rogovin, K.A., 2012. Spatial ecology of desert rodent communities. Springer Science & Business Media, pp. 292.

Sheldon, N.D., 2006. Using paleosols of the Picture Gorge Basalt to reconstruct the middle Miocene Climatic Optimum. PaleoBios 26, 27–36.

Sheldon, N.D., Retallack, G.J., Tanaka, S., 2002. Geochemical climofunctions from North American soils and application to paleosols across the Eocene–Oligocene Boundary in Oregon. The Journal of Geology 110, 687–696.

Smiley, T.M., Cotton, J.M., Badgley, C., Cerling, T.E., 2015. Small-mammal isotope ecology tracks climate and vegetation gradients across western North America. *Oikos* doi: 10.1111/oik.02722.

Smith, F.A., Brown, J.H., Haskell, J.P., Lyons, S.K., Alroy, J., Charnov, E.L., Dayan, T., Enquist, B.J., Morgan Ernest, S.K., Hadly, E.A., Jones, K.E., Kaufman, D.M., Marquet, P.A., Maurer, B.A., Niklas, K.J., Porter, W.P., Tiffney, B., Willig, M.R., 2004. Similarity of mammalian body size across the taxonomic hierarchy and across space and time. American Naturalist 163, 672–691.

Sokal, R.R., Rohlf, F.J., 2012. Biometry, 4th edn, W.H. Freeman, New York.

Sponheimer, M., Robinson, T., Ayliffe, L., Passey, B., Roeder, B., Shipley, L., Lopez, E., Cerling, T., Dearing, D., Ehleringer, J., 2003. An experimental study of carbon-isotope

fractionation between diet, hair, and feces of mammalian herbivores. Canadian Journal of Zoology 81, 871–876.

Strömberg, C.A., 2005. Decoupled taxonomic radiation and ecological expansion of open-habitat grasses in the Cenozoic of North America. Proceedings of the National Academy of Sciences 102, 11980–11984.

Strömberg, C.A.E., 2011. Evolution of grasses and grassland ecosystems. Annual Review Earth and Planetary Science 39, 517–544.

Strömberg, C.A.E., McInerney, F.A., 2011. The Neogene transition from C_3 to C_4 grasslands in North America: assemblage analysis of fossil phytoliths. Paleobiology 37, 50–71.

Terry, R.C., 2010. The dead do not lie: using skeletal remains for rapid assessment of historical small-mammal community baselines. Proceedings of the Royal Society B: Biological Sciences 277, 1193–1201.

Terry, R.C., Li, C.L., Hadly, E.A., 2011. Predicting small-mammal responses to climatic warming: autecology, geographic range, and the Holocene fossil record. Global Change Biology 17, 3019–3034.

Terry, R.C., Rowe, R.J., 2015. Energy flow and functional compensation in Great Basin small mammals under natural and anthropogenic environmental change. Proceedings of the National Academy of Sciences 112, 9656–9661.

Tipple, B.J., Meyers, S.R., Pagani, M., 2010. Carbon isotope ratio of Cenozoic CO_2: A comparative evaluation of available geochemical proxies. Paleoceanography 25, PA3202.

Wahlert, J.H., 1993. The fossil record, in: Genoways, H.H. and Brown, J.H. (Eds.), Biology of Heteromyidae. The American Society of Mammalogists, pp. 1-37.

Walther, G.R., Post, E., Convey, P., Menzel, A., Parmesan, C., Beebee, T.J., Fromentin, J.-M., Hoegh-Guldberg, O., Bairlein, F., 2002. Ecological responses to recent climate change. Nature 416, 389–395.

Weldon, R.J., 1986. The late Cenozoic geology of Cajon Pass: Implications for tectonics and sedimentation along the San Andreas fault. Ph. D. thesis, California Institute of Technology. 400pp.

Williams, J.W., Jackson, S.T., 2007. Novel climates, no-analog communities, and ecological surprises. Frontiers in Ecology and the Environment 5, 475–482.

Williams, S.H., Kay, R.F., 2001. A comparative test of adaptive explanations for hypsodonty in ungulates and rodents. Journal of Mammalian Evolution 8, 207–229.

Winston, D.S., 1985. The physical and magnetic stratigraphy of the Miocene Crowder Formation, Cajon Valley Pass, Southern California. Masters thesis, University of Southern California. 111pp.

Woodburne, M.O., 1991. The Mojave Desert Province. San Bernardino County Museum Association Quarterly 38, 60–77.

Woodburne, M.O., Golz, D.J., 1972. Stratigraphy of the Punchbowl Formation, Cajon Valley, Southern California. University of California Publications in Geological Sciences 92, 1–73.

Woodburne, M.O., Tedford, R.H., Swisher, C.C., III, 1990. Lithostratigraphy, biostratigraphy, and geochronology of the Barstow Formation, Mojave Desert, southern California. Geological Society of America Bulletin 102, 459–477.

Zachos, J., Pagani, M., Sloan, L., Thomas, E., Billups, K., 2001. Trends, rhythms, and aberrations in global climate 65 Ma to present. Science 292, 686–693.

Zelditch, M.L., Li, J., Tran, L.A.P., Swiderski, D.L., 2015. Relationships of diversity, disparity, and their evolutionary rates in squirrels (Sciuridae). Evolution 69, 1284–1300.

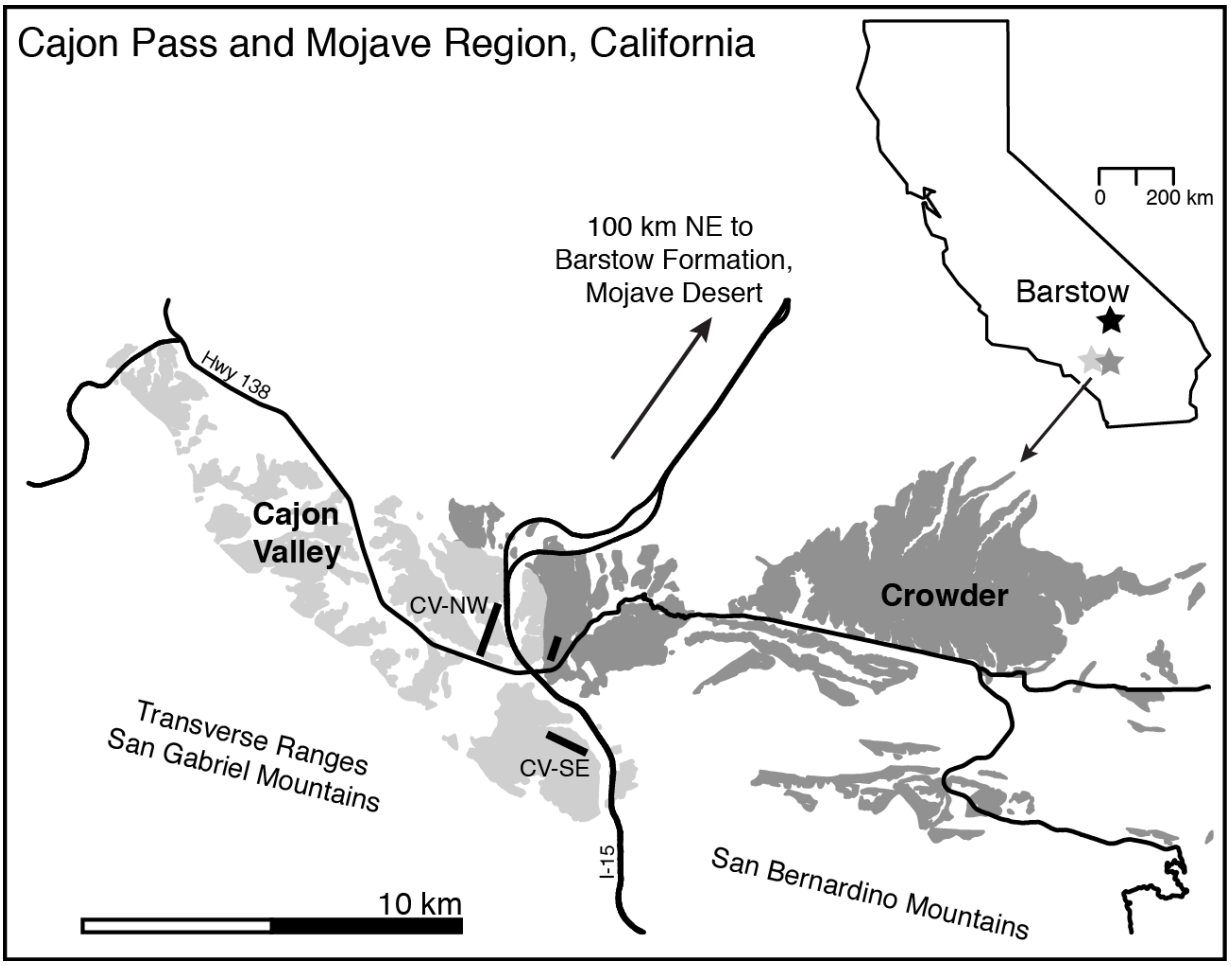

Figure 4.1 Geographic location of the Crowder and Cajon Valley formations in the vicinity of the Cajon Pass and Transverse Ranges, southern California. Thick black bars indicate the position of the previously measured stratigraphic sections where paleosol samples were collected for carbon isotopic composition and phytolith assemblages (Smiley et al. *in review*). CV-NW and CV-SE represent two sections measured within the Cajon Valley Formation. Most fossil localities were at the same stratigraphic level or were closely associated with horizons sampled from the Cajon Valley and Crowder sections. Map inset shows the location of the middle Miocene formations in relation to the Barstow Formation. Geological map data are from Morton and Miller (2006).

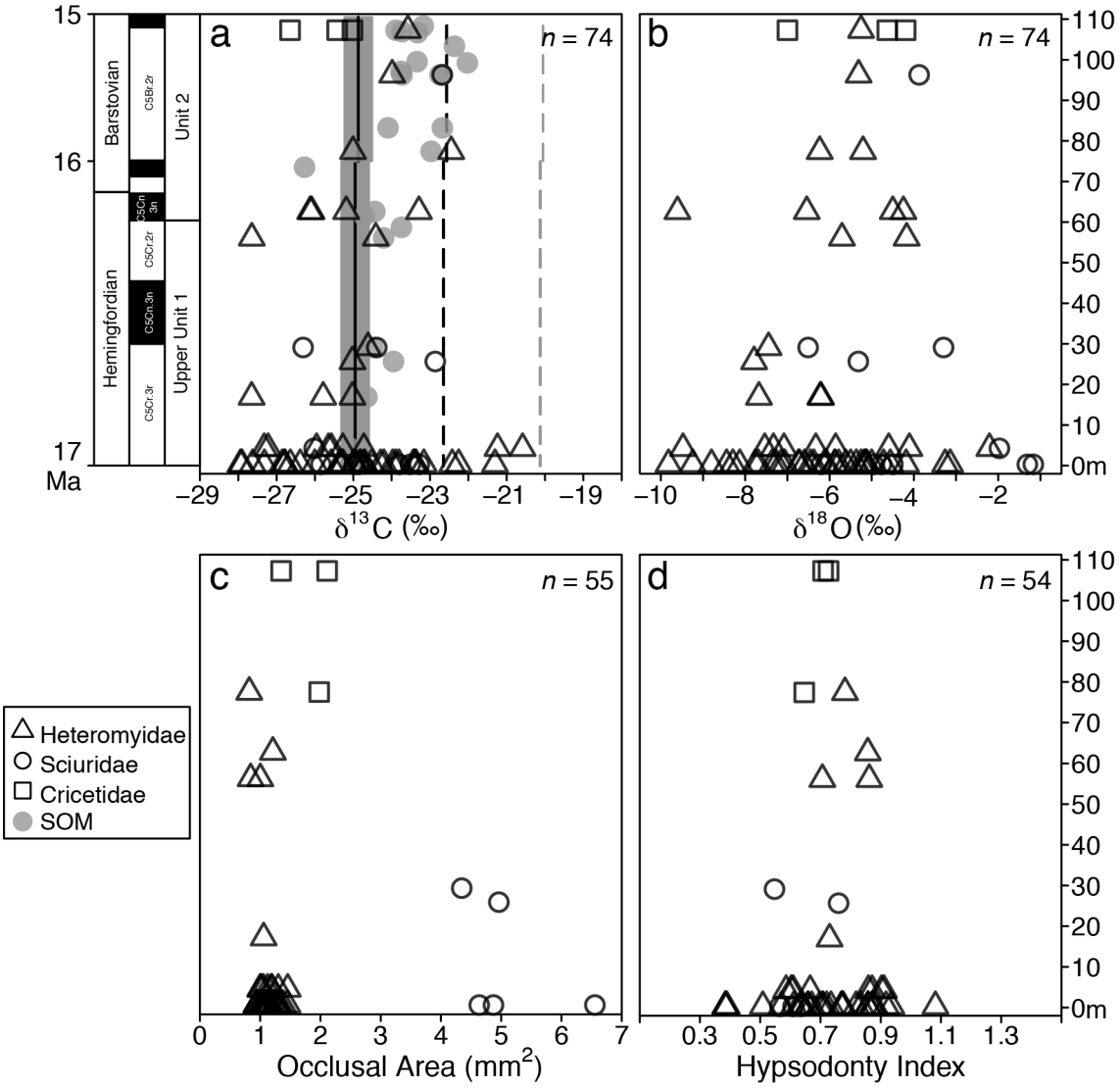

Figure 4.2 Variation in isotopic composition and dental metrics from 17.0–15.0 Ma in the Crowder Formation. Open symbols represent individual specimens and symbol type indicates rodent family (refer to legend). (a) Measured $\delta^{13}C$ values for soil organic matter (solid gray circles) and rodent diet (open symbols). Rodent $\delta^{13}C_{diet}$ values were adjusted by an enrichment factor of +11.0‰ (Podlesak et al. 2008) for comparison with $\delta^{13}C_{SOM}$ and vegetation values. For 1-myr time intervals, the black line indicates mean-C_3 isotopic composition after adjusting for estimated $\delta^{13}C$ of atmospheric CO_2 (with 90% confidence intervals in gray bars) from Tipple et al. (2010). Black and gray dashed lines indicate the arid-C_3 end-member value and estimated 20% C_4 biomass (assuming an arid-C_3 end-member value), respectively. (b) Measured $\delta^{18}O$ values from rodent enamel. (c) Occlusal area (occlusal length multiplied by width) and (d) hypsodonty index, calculated according to Williams and Kay (2001) for complete rodent first and second molars.

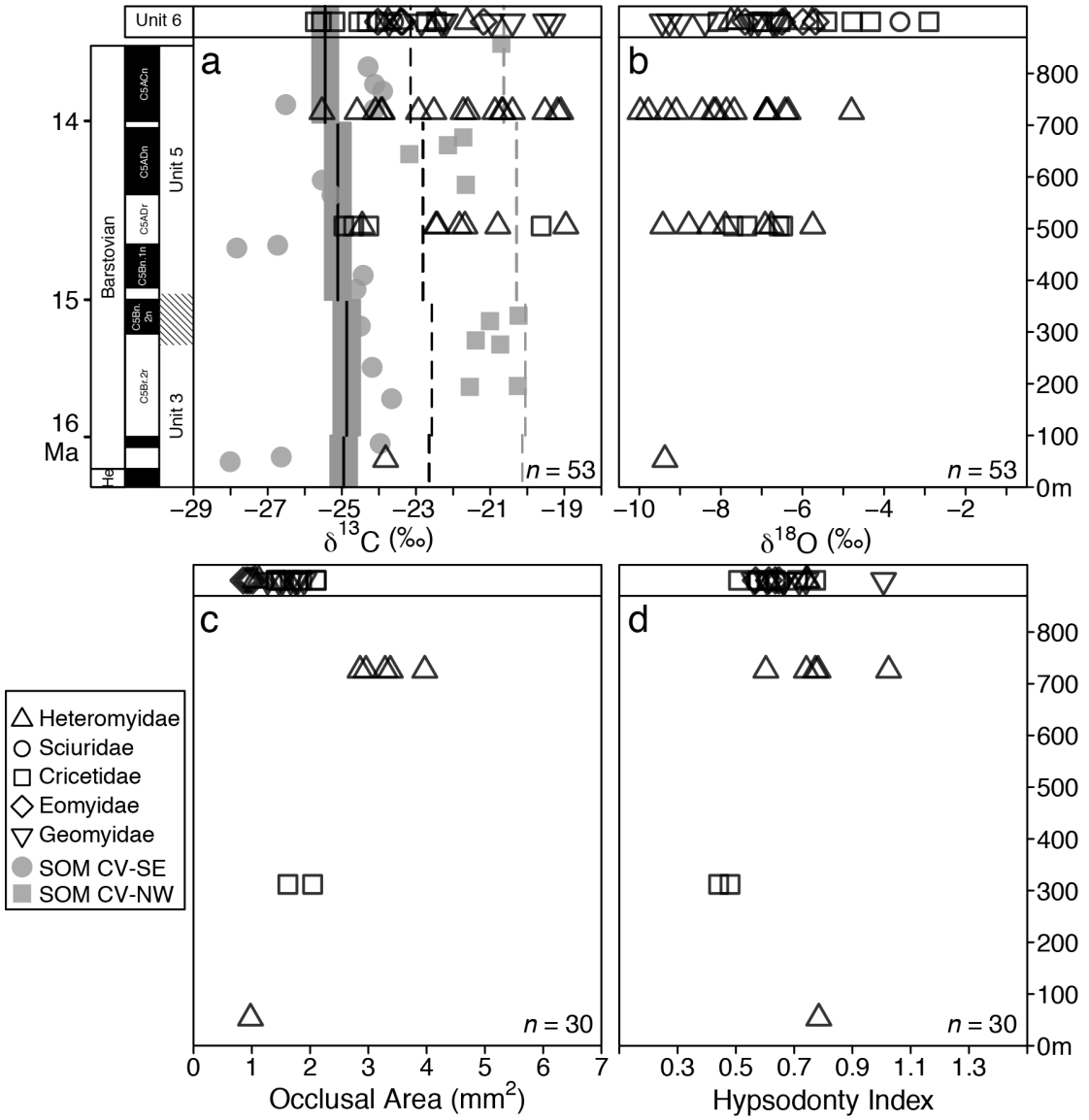

Figure 4.3 Variation in isotopic composition and dental metrics from ~16.5–13.7 Ma in the Cajon Valley Formation. Open symbols represent individual specimens and symbol type indicates rodent family (refer to legend). (a) Measured $\delta^{13}C$ values for soil organic matter for the mesic CV-SE (solid gray circles) and arid CV-NW (solid gray squares) sections. Rodent $\delta^{13}C_{diet}$ values (open symbols) were adjusted by an enrichment factor of +11.0‰ (Podlesak et al. 2008) for comparison with $\delta^{13}C_{SOM}$ and vegetation values. Taxa from Unit 6 represent an important component of the Cajon Valley small-mammal faunas, but were not part of the measured section, therefore do not have corresponding $\delta^{13}C_{SOM}$ or phytolith data. Fossil localities for Unit 6 faunas were proximal to the CV-NW section. For 1-myr time intervals, the black line indicates mean C_3 isotopic composition after adjusting for estimated $\delta^{13}C$ of atmospheric CO_2 (with 90% confidence intervals in gray bars) from Tipple et al. (2010). Black and gray dashed lines indicate the arid-C_3 end-member value and estimated 20% C_4 biomass (assuming an arid-C_3 end-member value), respectively. (b) Measured $\delta^{18}O$ values from rodent enamel. (c) Occlusal area (occlusal length multiplied by width) and (d) hypsodonty index, calculated according to Williams and Kay (2001) for complete rodent first and second molars.

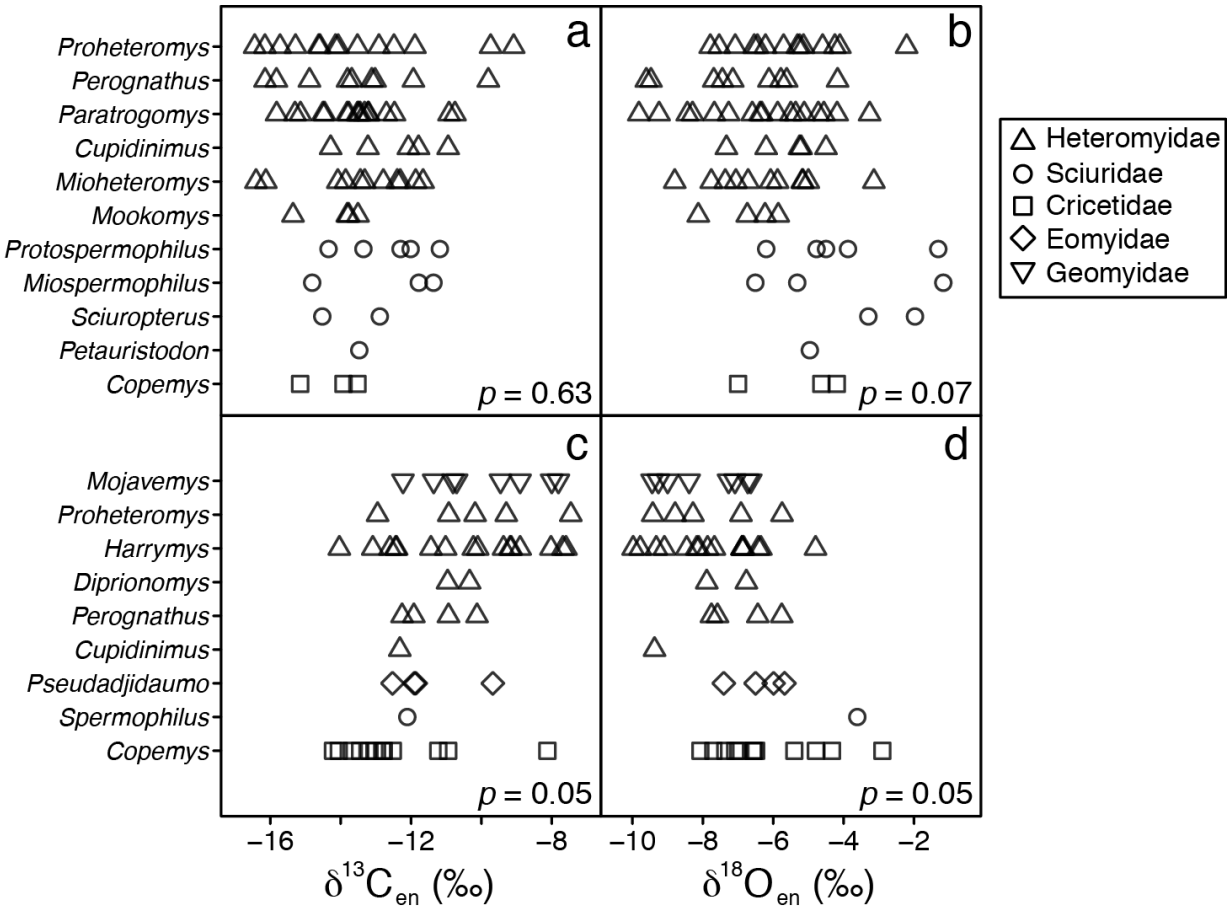

Figure 4.4 $\delta^{13}C_{en}$ and $\delta^{18}O_{en}$ values of individual teeth within each genus for Crowder (a and b) and Cajon Valley (c and d). *P*-values refer to significant differences among genera according to the Kruskal-Wallis analysis of variance for non-parametric data. Comparisons at the species level produced similar results (most genera were monospecific).

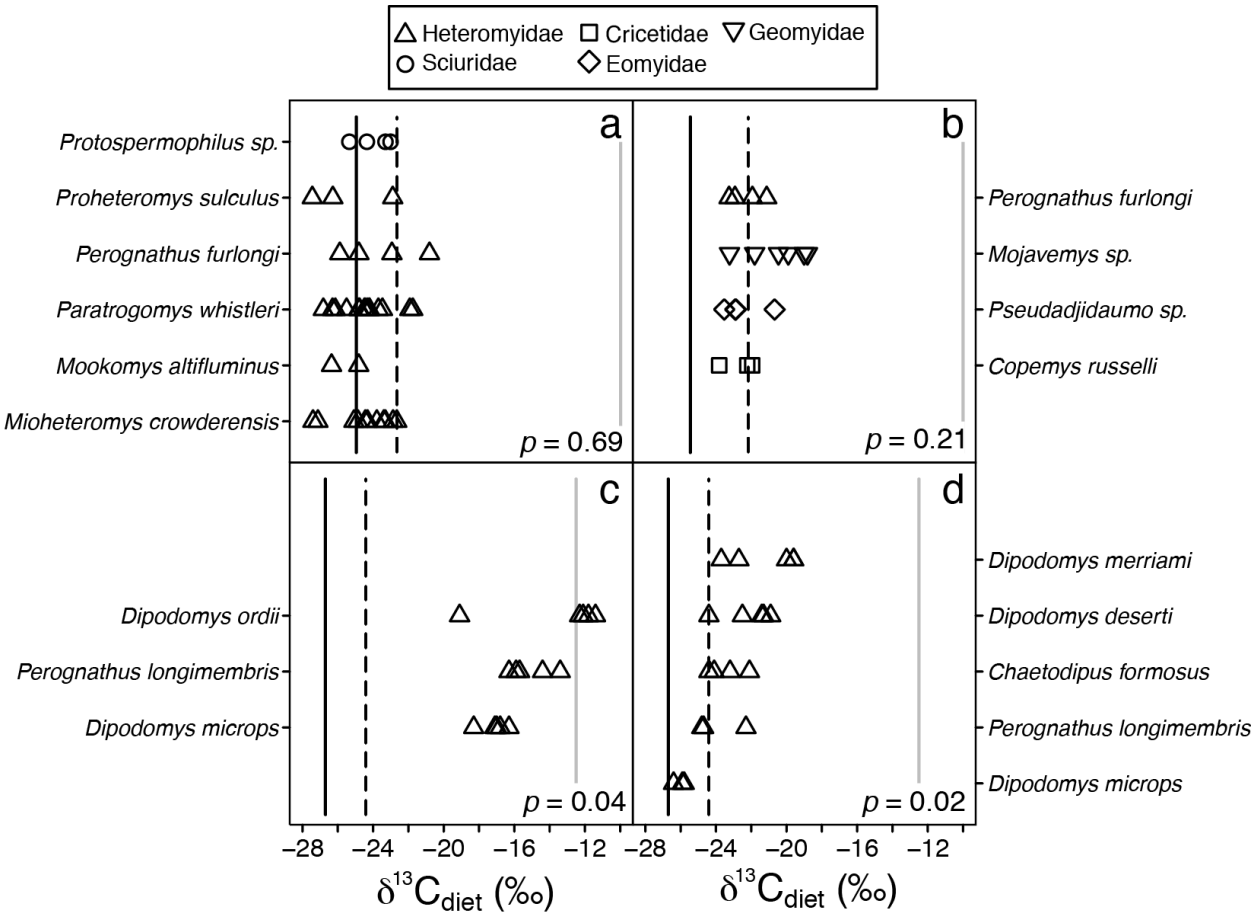

Figure 4.5 Interspecific variation in $\delta^{13}C_{diet}$ values for single Crowder (a) and Cajon Valley (b) fossil assemblages compared to co-occurring heteromyid species in present-day communities. Modern specimens occurred in a dry, predominantly-C_4 ecosystem at Desert Range, UT (c) and a mixed C_3-C_4 grassland ecosystem at Beaverdam Wash, UT (d). Proper enrichment factors for fossil enamel (+11.0‰ from diet; Podlesak et al. 2008) and modern hair (+3.2‰ from diet; Sponheimer et al. 2003) samples were applied for comparison with mean-C_3 (solid black line), arid-C_3 (dashed black line), and mean-C_4 (solid gray line) end-member values. *P*-values refer to significant differences among species according to the Kruskal-Wallis analysis of variance for non-parametric data.

Table 4.1 Small-mammal faunas of the Crowder and Cajon Valley formations sampled for isotopic composition.

Crowder Formation	Cajon Valley Formation
Heteromyidae	Heteromyidae
Cupidinimus halli	*Cupidinimus lindsayi*
Mioheteromys crowderensis	*Diprionomys sp.*
Mookomys "altifluminus"	*Harrymys maximus*
Paratrogomys whistleri	*Perognathus furlongi*
Perognathus furlongi	*Proheteromys sulculus*
Perognathus minutus	Sciuridae
Proheteromys sulculus	*Petauristodon*, large sp.
Sciuridae	*Petauristodon uphami*
Miospermophilus sp.	*Spermophilus primitivus*
Petauristodon sp.	Cricetidae
Protospermophilus sp.	*Copemys longidens*
Sciuropterus sp.	*Copemys sp. cf. C. russelli*
Tamias sp.	*Copemys tenuis*
Cricetidae	Eomyidae
Copemys pagei	*Pseudadjidaumo stirtoni*
Copemys tenuis	Geomyidae
	Mojavemys alexandrae
	Mojavemys lophatus
	Parapliosaccomys sp.

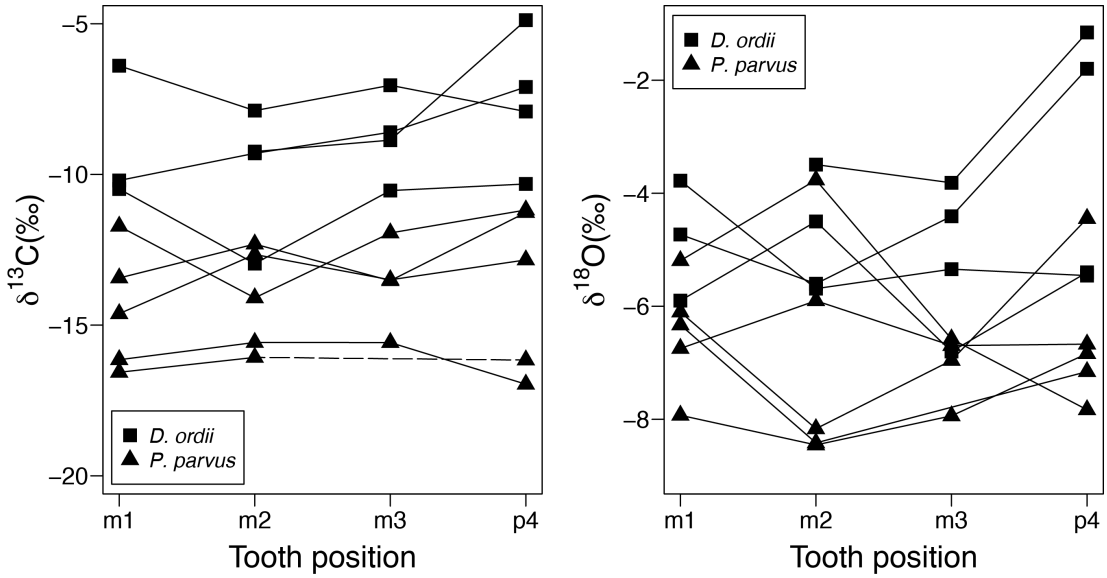

Figure S4.1 Carbon and oxygen isotopic composition (from enamel) of the individual tooth rows in modern *Dipodomys ordii* and *Perognathus parvus* rodents sampled by *in situ* laser ablation mass spectrometry. Although *P. parvus* specimens were systematically more enriched than *D. ordii* specimens (due to differences in dietary preference, see Smiley et al. 2015), there was no systematic variation across individual tooth rows.

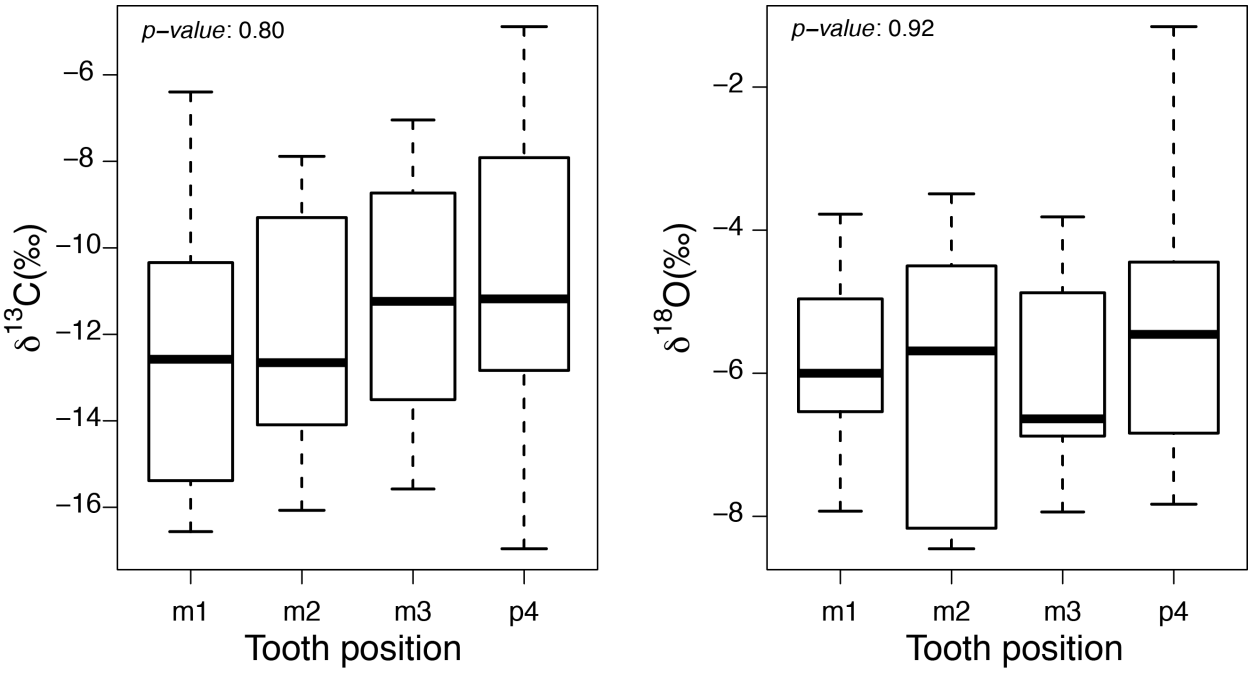

Figure S4.2 Intra-jaw variation for carbon and oxygen isotopic composition (enamel) by tooth position in *Dipodomys ordii* and *Perognathus parvus* rodents sampled by *in situ* laser ablation mass spectrometry. *P*-values refer to the differences among tooth position according to the Kruskal-Wallis analysis of variance for non-parametric data. Among modern *D. ordii* and *P. parvus* specimens, premolars and molars did not vary systematically along the tooth row. There is a modest, but non-significant increase in $\delta^{13}C$ values from the first (m1) to last formed tooth (p4) and no significant difference between tooth positions in $\delta^{18}O$ values.

SUPPLEMENTARY TABLES

Table S4.1 Isotopic composition of modern lower tooth rows for *Perognathus parvus* and *Dipodomys ordii* sampled by *in situ* laser ablation mass spectrometry.

Species	Specimen	Tooth Position	Voltage (mV)	$\delta^{13}C_{en}$ (‰) corrected	$\delta^{18}O_{en}$ (‰) corrected	Location
P. parvus	11429	m1	1654	-13.4	-7.9	Stansbury, UT
P. parvus	11429	m2	1734	-12.3	-8.5	Stansbury, UT
P. parvus	11429	m3	1556	-13.5	-7.9	Stansbury, UT
P. parvus	11429	p4	1229	-11.3	-6.8	Stansbury, UT
P. parvus	13524	m1	1111	-14.6	-5.2	Stansbury, UT
P. parvus	13524	m2	1102	-12.7	-3.8	Stansbury, UT
P. parvus	13524	m3	1648	-13.5	-6.6	Stansbury, UT
P. parvus	13524	p4	1009	-12.8	-7.8	Stansbury, UT
P. parvus	68045	m1	1952	-11.7	-6.1	Okanogan, WA
P. parvus	68045	m2	1703	-14.1	-8.2	Okanogan, WA
P. parvus	68045	m3	1589	-11.9	-7.0	Okanogan, WA
P. parvus	68045	p4	1706	-11.2	-4.4	Okanogan, WA
P. parvus	68056	m1	1926	-16.6	-6.3	Okanogan, WA
P. parvus	68056	m2	978	-16.1	-8.4	Okanogan, WA
P. parvus	68056	p4	2389	-16.2	-7.2	Okanogan, WA
P. parvus	68057	m1	2109	-16.1	-6.7	Okanogan, WA
P. parvus	68057	m2	1003	-15.6	-5.9	Okanogan, WA
P. parvus	68057	m3	604	-15.6	-6.7	Okanogan, WA
P. parvus	68057	p4	1370	-17.0	-6.7	Okanogan, WA
D. ordii	68239	m1	1213	-6.4	-3.8	Hackberry, NE
D. ordii	68239	m2	1269	-7.9	-5.7	Hackberry, NE
D. ordii	68239	m3	3154	-7.0	-5.3	Hackberry, NE
D. ordii	68239	p4	1281	-7.9	-5.5	Hackberry, NE
D. ordii	68242	m1	778	-10.2	-5.9	Hackberry, NE
D. ordii	68242	m2	692	-9.3	-4.5	Hackberry, NE
D. ordii	68242	m3	1201	-8.6	-6.8	Hackberry, NE
D. ordii	68242	p4	813	-7.1	-5.4	Hackberry, NE
D. ordii	58361	m2	542	-9.2	-3.5	Otero, NM
D. ordii	58361	m3	786	-8.9	-3.8	Otero, NM
D. ordii	58361	p4	977	-4.9	-1.2	Otero, NM
D. ordii	58377	m1	748	-10.5	-4.7	Otero, NM
D. ordii	58377	m2	893	-13.0	-5.6	Otero, NM
D. ordii	58377	m3	960	-10.5	-4.4	Otero, NM
D. ordii	58377	p4	855	-10.3	-1.8	Otero, NM

Table S4.2 Isotopic composition and dental measurements of fossil rodent teeth from the Crowder and Cajon Valley formations. Lower and upper cases refer to lower and upper, respectively, molar (m or M) and premolar (p or P) tooth positions.

Formation	Field Number	Specimen Number	Family	Species	Tooth Position	Strat. Ht (m)	$\delta^{13}C_{en}$ (‰) corrected	$\delta^{18}O_{en}$ (‰) corrected	Occlusal Area (mm^2)	Hypsodonty Index
Crowder	1.103.125/6	1354	Sciuridae	*Petauristodon sp.*	?M1	0.30	-13.47	-4.96	-	-
Crowder	1.103.125/6	1356	Sciuridae	*Miospermophilus wyomingensis*	M2	0.30	-11.78	-1.17	4.87	0.61
Crowder	1.103.125/6	1358	Sciuridae	*Protospermophilus sp.*	M1 or M2	0.30	-14.34	-1.31	4.82	0.59
Crowder	1.103.125/6	1359	Sciuridae	*Protospermophilus sp.*	m2	0.30	-13.35	-4.50	4.64	0.57
Crowder	1.103.125/6	1360	Sciuridae	*Protospermophilus sp.*	m2	0.30	-12.01	-6.20	6.56	0.63
Crowder	1.103.125/6	1361	Sciuridae	*Protospermophilus sp.*	m3	0.30	-	-	4.61	0.45
Crowder	1.103.125/6	1362	Sciuridae	*Protospermophilus sp.*	m3	0.30	-12.30	-4.77	7.02	0.64
Crowder	1.103.125/6	1368	Heteromyidae	*Mookomys altifluminus*	p4	0.30	-	-	0.45	0.91
Crowder	1.103.125/6	1371	Heteromyidae	*Mookomys altifluminus*	m1	0.30	-	-	0.94	0.71
Crowder	1.103.125/6	1372	Heteromyidae	*Mookomys altifluminus*	m1	0.30	-15.35	-8.13	1.13	0.71
Crowder	1.103.125/6	1373	Heteromyidae	*Mookomys altifluminus*	m1	0.30	-	-	1.11	0.51
Crowder	1.103.125/6	1374	Heteromyidae	*Mookomys altifluminus*	m1	0.30	-13.81	-6.74	0.94	0.86
Crowder	1.103.125/6	1375	Heteromyidae	*Mookomys altifluminus*	m3	0.30	-	-	0.68	0.69
Crowder	1.103.125/6	1392	Heteromyidae	*Perognathus furlongi*	p4	0.30	-13.80	-5.62	0.78	1.06
Crowder	1.103.125/6	1395	Heteromyidae	*Perognathus furlongi*	m1	0.30	-9.80	-6.12	1.25	0.57
Crowder	1.103.125/6	1396	Heteromyidae	*Perognathus furlongi*	m1	0.30	-11.93	-5.78	1.16	0.87
Crowder	1.103.125/6	1398	Heteromyidae	*Perognathus furlongi*	m2	0.30	-14.89	-7.69	1.16	0.64
Crowder	1.103.125/6	1403	Heteromyidae	*Proheteromys sulculus*	m3	0.30	-15.28	-5.25	0.75	0.84
Crowder	1.103.125/6	1404	Heteromyidae	*Perognathus furlongi*	m3	0.30	-	-	0.79	0.55
Crowder	1.103.125/6	1409	Heteromyidae	*Perognathus furlongi*	m2	0.30	-	-	0.94	0.64
Crowder	1.103.125/6	1411	Heteromyidae	*Perognathus minutus*	p4	0.30	-13.02	-7.15	-	-
Crowder	1.103.125/6	1413	Heteromyidae	*Paratrogomys whistleri*	m1	0.30	-12.70	-5.36	0.99	0.87
Crowder	1.103.125/6	1432	Heteromyidae	*Paratrogomys whistleri*	m1	0.30	-	-	1.09	0.83
Crowder	1.103.125/6	1443	Heteromyidae	*Mookomys sp.*	m2	0.30	-	-	1.01	0.39
Crowder	1.103.125/6	1444	Heteromyidae	*Paratrogomys whistleri*	M1	0.30	-10.75	-8.44	1.15	0.73
Crowder	1.103.125/6	1457	Heteromyidae	*Proheteromys sulculus*	p4	0.30	-	-	0.93	0.83
Crowder	1.103.125/6	1462	Heteromyidae	*Paratrogomys whistleri*	p4	0.30	-15.30	-5.12	-	-
Crowder	1.103.125/6	1463	Heteromyidae	*Proheteromys sulculus*	p4	0.30	-11.89	-5.14	0.85	1.09
Crowder	1.103.125/6	1465	Heteromyidae	*Paratrogomys whistleri*	m1	0.30	-13.77	-4.56	1.38	0.78
Crowder	1.103.125/6	1467	Heteromyidae	*Paratrogomys whistleri*	m1	0.30	-14.50	-6.59	1.07	0.66
Crowder	1.103.125/6	1468	Heteromyidae	*Paratrogomys whistleri*	m1	0.30	-	-	1.28	0.77
Crowder	1.103.125/6	1468	Heteromyidae	*Paratrogomys whistleri*	m1	0.30	-	-	1.28	0.77
Crowder	1.103.125/6	1469	Heteromyidae	*Paratrogomys whistleri*	m1	0.30	-15.82	-9.82	1.04	0.67
Crowder	1.103.125/6	1470	Heteromyidae	*Paratrogomys whistleri*	m2	0.30	-	-	1.22	0.88
Crowder	1.103.125/6	1471	Heteromyidae	*Paratrogomys whistleri*	m1	0.30	-13.81	-5.50	1.17	-
Crowder	1.103.125/6	1472	Heteromyidae	*Paratrogomys whistleri*	m2	0.30	-13.32	-7.27	-	-
Crowder	1.103.125/6	1473	Heteromyidae	*Paratrogomys whistleri*	m2	0.30	-13.45	-6.37	1.05	0.92
Crowder	1.103.125/6	1474	Heteromyidae	*Paratrogomys whistleri*	m2	0.30	-15.14	-8.29	1.04	0.87
Crowder	1.103.125/6	1475	Heteromyidae	*Paratrogomys whistleri*	m2	0.30	-10.92	-4.18	1.29	0.94
Crowder	1.103.125/6	1476	Heteromyidae	*Paratrogomys whistleri*	m2	0.30	-12.47	-3.26	1.15	0.82
Crowder	1.103.125/6	1477	Heteromyidae	*Paratrogomys whistleri*	m2	0.30	-13.49	-4.72	1.09	0.72
Crowder	1.103.125/6	1478	Heteromyidae	*Paratrogomys whistleri*	m2	0.30	-13.22	-5.87	1.09	0.77
Crowder	1.103.125/6	1487	Heteromyidae	*Proheteromys sulculus*	m2	0.30	-	-	1.11	0.86

Crowder	1.103.125/6	1489	Heteromyidae	*Proheteromys sulculus*	m2	0.30	-	-	1.11	0.86
Crowder	1.103.125/6	1488	Heteromyidae	*Proheteromys sulculus*	m2	0.30	-16.44	-6.45	1.00	0.88
Crowder	1.103.125/6	1503	Heteromyidae	*Mioheteromys crowderensis*	m1	0.30	-16.41	-8.80	1.08	0.61
Crowder	1.103.125/6	1503	Heteromyidae	*Mioheteromys crowderensis*	m2	0.30	-14.08	-7.06	1.13	0.66
Crowder	1.103.125/6	1508	Heteromyidae	*Paratrogomys whistleri*	p4	0.30	-13.20	-9.24	0.90	0.48
Crowder	1.103.125/6	1520	Heteromyidae	*Mioheteromys crowderensis*	m1	0.30	-13.32	-6.71	1.32	0.63
Crowder	1.103.125/6	1525	Heteromyidae	*Mioheteromys crowderensis*	m1	0.30	-13.44	-5.16	0.95	0.38
Crowder	1.103.125/6	1525	Heteromyidae	*Mioheteromys crowderensis*	m2	0.30	-13.86	-5.00	0.95	0.38
Crowder	1.103.125/6	1528	Heteromyidae	*Mioheteromys crowderensis*	p4	0.30	-12.39	-7.36	0.88	1.22
Crowder	1.103.125/6	1530	Heteromyidae	*Mioheteromys crowderensis*	p4	0.30	-	-	1.10	0.79
Crowder	1.103.125/6	1531	Heteromyidae	*Mioheteromys crowderensis*	p4	0.30	-11.87	-5.18	0.80	0.71
Crowder	1.103.125/6	1532	Heteromyidae	*Mioheteromys crowderensis*	p4	0.30	-12.31	-5.88	1.07	0.88
Crowder	1.103.125/6	1535	Heteromyidae	*Mioheteromys crowderensis*	m1	0.30	-12.79	-6.07	1.30	0.70
Crowder	1.103.125/6	1537	Heteromyidae	*Mioheteromys crowderensis*	m1	0.30	-16.13	-7.76	1.45	1.08
Crowder	1.103.125/6	1540	Heteromyidae	*Mioheteromys crowderensis*	m3	0.30	-11.66	-3.14	0.87	0.94
Crowder	1.103.125/6	1542	Zapodidae	*Megasminthus sp.*	m3	0.30	-	-	3.30	0.65
Crowder	1.103.53	135	Heteromyidae	*Proheteromys sulculus*	m3	4.25	-15.72	-7.54	0.77	0.80
Crowder	1.103.53	147	Heteromyidae	*Proheteromys sulculus*	p4	4.25	-14.15	-4.60	1.03	0.93
Crowder	1.103.53	150	Heteromyidae	*Proheteromys sulculus*	m3	4.25	-9.74	-2.21	1.03	0.86
Crowder	1.103.53	280	Sciuridae	*Sciuropterus sp.*	p4	4.25	-14.52	-1.97	-	-
Crowder	1.103.53	307	Heteromyidae	*Perognathus sp.*	m1	4.25	-15.82	-9.47	1.00	0.61
Crowder	1.103.53	308	Heteromyidae	*Mookomys altifluminus*	m1	4.25	-13.77	-5.86	1.20	0.67
Crowder	1.103.53	312	Heteromyidae	*Proheteromys sulculus*	M2	4.25	-	-	1.12	0.91
Crowder	1.103.53	313	Heteromyidae	*Cupidinimus sp.*	M1	4.25	-13.23	-7.33	1.18	0.90
Crowder	1.103.53	315	Heteromyidae	*Proheteromys sulculus*	m1	4.25	-9.08	-7.08	1.30	0.59
Crowder	1.103.53	316	Heteromyidae	*Proheteromys sulculus*	m1	4.25	-14.07	-4.11	1.01	0.87
Crowder	1.103.53	317	Heteromyidae	*Paratrogomys whistleri*	m2	4.25	-14.46	-6.32	1.05	0.86
Crowder	1.103.53	318	Heteromyidae	*Cupidinimus sp.*	m1	4.25	-	-	1.46	0.60
Crowder	1.103.53	393	Heteromyidae	*Paratrogomys whistleri*	m3	16.90	-13.52	-7.67	0.67	0.75
Crowder	1.103.53	397	Heteromyidae	*Cupidinimus sp.*	M3	16.90	-14.29	-6.20	0.64	0.61
Crowder	1.103.53	398	Heteromyidae	*Proheteromys sulculus*	m1	16.90	-16.15	-6.22	1.06	0.73
Crowder	1.103.53	490	Sciuridae	*Miospermophilus sp.*	M2	25.65	-11.36	-5.32	4.96	0.76
Crowder	1.103.53	491	Sciuridae	*Miospermophilus sp.*	M1 or M2	25.65	-	-	3.55	0.58
Crowder	1.103.53	497	Heteromyidae	*Proheteromys sulculus*	p4	25.65	-13.52	-7.79	1.04	0.99
Crowder	1.103.53	539	Sciuridae	*Miospermophilus sp.*	p4	29.10	-14.81	-6.51	-	-
Crowder	1.103.53	541	Sciuridae	*Sciuropterus sp.*	m2	29.10	-12.89	-3.30	4.35	0.55
Crowder	1.103.53	553	Heteromyidae	*Perognathus furlongi*	P4	29.10	-13.12	-7.45	1.05	0.72
Crowder	1.103.53	582	Heteromyidae	*Perognathus furlongi*	P4	56.10	-16.15	-4.17	0.90	0.49
Crowder	1.103.53	582	Heteromyidae	*Perognathus furlongi*	M2	56.10	-	-	0.84	0.71
Crowder	1.103.53	583	Heteromyidae	*Proheteromys sulculus*	m1	56.10	-12.91	-5.70	1.00	0.86
Crowder	1.103.53	734	Heteromyidae	*Perognathus sp.*	P4	62.63	-13.69	-9.60	-	-
Crowder	1.103.53	742	Heteromyidae	*Proheteromys sulculus*	M1	62.63	-14.59	-4.25	-	-
Crowder	1.103.53	744	Heteromyidae	*Proheteromys sulculus*	m1	62.63	-14.63	-6.54	-	-
Crowder	1.103.53	746	Heteromyidae	*Cupidinimus sp.*	m2	62.63	-11.79	-4.50	1.21	0.86
Crowder	1.103.137	1137	Heteromyidae	*Mookomys altifluminus*	m2	77.43	-13.51	-6.23	0.82	0.78
Crowder	1.103.137	1141	Heteromyidae	*Cupidinimus halli*	m1	77.43	-10.95	-5.20	-	-
Crowder	1.103.137	1145	Cricetidae	*Copemys tenuis*	M2	77.43	-	-	1.98	0.65
Crowder	1.103.139	1169	Sciuridae	*Miospermophilus sp.*	M1 or M2	96.28	-	-	4.61	0.56
Crowder	1.103.139	1170	Sciuridae	*Protospermophilus sp.*	m1 or m2	96.28	-11.18	-3.87	-	-
Crowder	1.103.139	1171	Heteromyidae	*Proheteromys sulculus*	?	96.28	-12.49	-5.31	0.79	0.98

Crowder	1.103.144	1233	Sciuridae	*Protospermophilus sp.*	?	107.28	-	-	6.94	0.50
Crowder	1.103.144	1235	Heteromyidae	*Cupidinimus sp.*	?	107.28	-12.08	-5.25	-	-
Crowder	1.103.144	1236	Heteromyidae	*Cupidinimus sp.*	?	107.28	-	-	1.40	0.95
Crowder	1.103.144	1242	Cricetidae	*Copemys tenuis*	M1	107.28	-13.52	-4.19	2.11	0.73
Crowder	1.103.144	1243	Cricetidae	*Copemys tenuis*	m3	107.28	-13.92	-7.00	1.31	0.64
Crowder	1.103.144	1244	Cricetidae	*Copemys pagei*	m1	107.28	-15.15	-4.63	1.35	0.71
Cajon	1.103.62/63	836	Heteromyidae	*Cupidinimus sp.*	?	53.34	-12.32	-9.37	0.98	0.78
Cajon	1.103.105/106	174	Cricetidae	*Copemys sp.*	?m2	505.00	-13.18	-7.70	-	-
Cajon	1.103.105/106	173	Cricetidae	*Copemys sp.*	m2	505.00	-12.77	-6.57	-	-
Cajon	1.103.105/106	172	Cricetidae	*Copemys longidens*	m2	505.00	-8.13	-6.48	1.62	0.44
Cajon	1.103.105/106	171	Cricetidae	*Copemys tenuis*	M1	505.00	-17.68	-7.71	2.04	0.48
Cajon	1.103.105/106	165	Heteromyidae	*Proheteromys sulculus*	m2	505.00	-10.93	-6.92	-	-
Cajon	1.103.105/106	164	Heteromyidae	*Proheteromys sulculus*	m2	505.00	-10.18	-9.42	-	-
Cajon	1.103.105/106	158	Heteromyidae	*Proheteromys sulculus*	M2	505.00	-12.95	-8.79	-	-
Cajon	1.103.105/106	157	Heteromyidae	*Proheteromys sulculus*	M2	505.00	-9.29	-8.28	-	-
Cajon	1.103.105/106	154	Heteromyidae	*Diprionomys sp.*	p4	505.00	-10.96	-6.76	0.62	0.93
Cajon	1.103.105/106	152	Heteromyidae	*Diprionomys sp.*	p4	505.00	-10.34	-7.89	0.72	0.94
Cajon	1.103.105/106	143	Cricetidae	*Copemys sp.*	m2	505.00	-13.45	-7.36	-	-
Cajon	1.103.105/106	141	Heteromyidae	*Proheteromys sp.*	m3	505.00	-7.46	-5.75	0.72	0.88
Cajon	1.103.40	1937	Heteromyidae	*Harrymys maximus*	m3	726.03	-8.02	-6.42	2.02	0.66
Cajon	1.103.40	1936	Heteromyidae	*Harrymys maximus*	m3	726.03	-8.90	-8.12	3.42	0.78
Cajon	1.103.40	1934	Heteromyidae	*Harrymys maximus*	m2	726.03	-9.15	-6.88	-	-
Cajon	1.103.40	1933	Heteromyidae	*Harrymys maximus*	?m1	726.03	-14.04	-8.17	-	-
Cajon	1.103.40	1932	Heteromyidae	*Harrymys maximus*	m1	726.03	-11.43	-9.78	3.29	0.77
Cajon	1.103.40	1929	Heteromyidae	*Harrymys maximus*	m2	726.03	-11.02	-7.87	2.96	1.02
Cajon	1.103.40	1928	Heteromyidae	*Harrymys maximus*	m1	726.03	-10.11	-6.84	3.38	0.60
Cajon	1.103.40	1927	Heteromyidae	*Harrymys maximus*	m1	726.03	-7.68	-6.88	-	-
Cajon	1.103.40	1925	Heteromyidae	*Harrymys maximus*	m2	726.03	-9.37	-7.67	2.86	0.78
Cajon	1.103.40	1921	Heteromyidae	*Harrymys maximus*	p4	726.03	-12.41	-9.32	2.32	0.61
Cajon	1.103.40	1920	Heteromyidae	*Harrymys maximus*	p4	726.03	-7.60	-4.80	2.92	0.96
Cajon	1.103.40	1915	Heteromyidae	*Harrymys maximus*	dp4	726.03	-13.09	-8.46	2.44	0.68
Cajon	1.103.40	1914	Heteromyidae	*Harrymys maximus*	p4	726.03	-9.19	-6.35	2.36	1.17
Cajon	1.103.40	1913	Heteromyidae	*Harrymys maximus*	p4	726.03	-12.44	-9.09	2.82	1.08
Cajon	1.103.40	1912	Heteromyidae	*Harrymys maximus*	p4	726.03	-12.60	-9.98	-	-
Cajon	1.103.40	1907	Heteromyidae	*Harrymys maximus*	M1	726.03	-10.23	-6.88	3.97	0.74
Cajon	1.103.171	79	Heteromyidae	*Perognathus furlongi*	m1	Unit 6	-12.26	-5.76	1.05	0.75
Cajon	1.103.171	78	Heteromyidae	*Perognathus furlongi*	m3	Unit 6	-10.13	-6.44	0.75	0.77
Cajon	1.103.171	77	Heteromyidae	*Perognathus furlongi*	m1	Unit 6	-11.92	-7.75	1.12	0.74
Cajon	1.103.171	76	Heteromyidae	*Perognathus furlongi*	m1	Unit 6	-10.94	-7.58	-	-
Cajon	1.103.171	65	Geomyidae	*Mojavemys sp.*	m2	Unit 6	-8.90	-9.26	1.46	0.67
Cajon	1.103.171	64	Geomyidae	*Mojavemys sp.*	m1	Unit 6	-7.81	-6.64	1.79	0.61
Cajon	1.103.171	63	Geomyidae	*Mojavemys sp.*	m1	Unit 6	-12.23	-9.44	1.67	0.74
Cajon	1.103.171	62	Geomyidae	*Mojavemys sp.*	M2	Unit 6	-9.46	-7.09	1.27	1.01
Cajon	1.103.171	61	Geomyidae	*Mojavemys sp.*	M2	Unit 6	-10.81	-8.39	1.52	0.66
Cajon	1.103.171	59	Geomyidae	*Mojavemys sp.*	M1	Unit 6	-8.00	-6.72	1.75	0.56
Cajon	1.103.171	39	Sciuridae	*Spermophilus sp.*	P4	Unit 6	-12.11	-3.61	3.81	0.59
Cajon	1.103.171	194	Cricetidae	*Copemys sp.*	M1	Unit 6	-14.22	-6.55	2.11	0.58
Cajon	1.103.171	2989-125	Eomyidae	*Leptodontomys sp.*	m1	Unit 6	-12.53	-5.68	1.01	0.61
Cajon	1.103.171	2989-124	Eomyidae	*Leptodontomys sp.*	M1	Unit 6	-11.90	-6.50	0.91	0.57
Cajon	1.103.171	2989-123	Eomyidae	*Leptodontomys sp.*	m1	Unit 6	-11.87	-7.40	0.86	0.64

Cajon	1.103.171	122	Eomyidae	*Leptodontomys sp.*	m1	Unit 6	-9.68	-5.99	0.96	0.65
Cajon	1.103.171	110	Cricetidae	*Copemys russelli*	m2	Unit 6	-11.22	-4.33	1.42	0.71
Cajon	1.103.171	108	Cricetidae	*Copemys russelli*	m2	Unit 6	-10.95	-5.40	1.42	0.77
Cajon	1.103.171	105	Cricetidae	*Copemys russelli*	m2	Unit 6	-12.82	-2.90	1.51	0.61
Cajon	1.103.99/101/102	202	Cricetidae	*Copemys longidens*	m2	Unit 6	-13.69	-4.79	1.66	0.51
Cajon	1.103.99/101/102	201	Cricetidae	*Copemys sp.*	M3	Unit 6	-14.05	-7.08	0.98	0.49
Cajon	1.103.99/101/102	199	Cricetidae	*Copemys tenuis*	M2	Unit 6	-	-	1.79	0.64
Cajon	1.103.99/101/102	198	Cricetidae	*Copemys tenuis*	M1	Unit 6	-13.04	-8.07	2.11	0.58
Cajon	1.103.99/101/102	131	Cricetidae	*Copemys tenuis*	M1	Unit 6	-12.52	-6.99	1.86	0.61
Cajon	1.103.99/101/102	121	Geomyidae	*Mojavemys alexandrae*	m3	Unit 6	-10.71	-7.27	1.55	0.74
Cajon	1.103.99/101/102	120	Geomyidae	*Mojavemys alexandrae*	m2	Unit 6	-11.36	-9.00	1.90	0.72
Cajon	1.103.99/101/102	119	Eomyidae	*Leptodontomys sp.*	p4	Unit 6	-	-	0.63	1.01

Table S4.3 Isotopic composition of modern heteromyids (*Dipodomys*, *Chaetodipus*, *Perognathus*) from Beaverdam Wash, UT and Desert Range, UT. Isotopic composition was measured from the hair of museum specimens.

Species	Specimen	$\delta^{13}C_{hair}$ (‰)	Location
P. longimembris	4064	-21.6	Beaverdam Wash, UT
P. longimembris	4065	-19.1	Beaverdam Wash, UT
P. longimembris	4066	-21.5	Beaverdam Wash, UT
C. formosus	4067	-21.2	Beaverdam Wash, UT
C. formosus	4068	-20.0	Beaverdam Wash, UT
C. formosus	4069	-18.9	Beaverdam Wash, UT
C. formosus	4070	-20.9	Beaverdam Wash, UT
D. microps	4001	-22.6	Beaverdam Wash, UT
D. microps	4080	-22.7	Beaverdam Wash, UT
D. microps	4082	-23.2	Beaverdam Wash, UT
D. deserti	4015	-18.1	Beaverdam Wash, UT
D. deserti	4100	-18.2	Beaverdam Wash, UT
D. deserti	4101	-17.7	Beaverdam Wash, UT
D. deserti	4102	-19.3	Beaverdam Wash, UT
D. deserti	4103	-21.2	Beaverdam Wash, UT
D. merriami	4053	-19.5	Beaverdam Wash, UT
D. merriami	4110	-16.8	Beaverdam Wash, UT
D. merriami	4111	-20.5	Beaverdam Wash, UT
D. merriami	4112	-16.4	Beaverdam Wash, UT
D. merriami	4114	-16.4	Beaverdam Wash, UT
D. ordii	3834	-8.6	Desert Range, UT
D. ordii	3863	-8.2	Desert Range, UT
D. ordii	3894	-9.1	Desert Range, UT
D. ordii	3905	-15.9	Desert Range, UT
D. ordii	3918	-8.9	Desert Range, UT
D. microps	3869	-13.9	Desert Range, UT
D. microps	3872	-13.6	Desert Range, UT
D. microps	3874	-13.1	Desert Range, UT
D. microps	3897	-15.1	Desert Range, UT
D. microps	3907	-13.8	Desert Range, UT
P. longimembris	3902	-11.2	Desert Range, UT
P. longimembris	3903	-12.7	Desert Range, UT
P. longimembris	3904	-10.2	Desert Range, UT
P. longimembris	3914	-13.1	Desert Range, UT
P. longimembris	3915	-12.5	Desert Range, UT

CHAPTER 5

Detecting diversification processes in relation to tectonic history from an incomplete fossil record

ABSTRACT

For mammals, mountains are among the most diverse ecosystems globally. However, the strong relationship between species richness and topographic complexity observed today is not a persistent feature of the fossil record through deep time. Reshaping of the topographic landscape during tectonic activity can have a strong influence on diversification processes, and indeed peak mammal diversity and elevated diversification rates in western North America occurred during an interval of intense Basin and Range tectonic extension. However, our ability to infer origination and extinction rates reliably from the fossil record is hampered by variation in preservation history. Herein, I used information from fossil rodents and the continental rock record of western North America to evaluate theoretically plausible diversification histories in relation to tectonic activity and demonstrate the influence of variable preservation probability on the fidelity of the fossil record. I converted phylogenies generated from birth-death models to simulated fossil records by removing phylogenetic information and recording species durations over 1-myr time intervals. I then degraded the simulated fossil records according to five preservation scenarios, based on common trends (e.g., increasing rock record towards the present) or derived from fossil occurrences and rock area. For each scenario, I estimated origination, extinction, and diversification rates and evaluated the ability of the degraded fossil

records to accurately recover the underlying diversification scenarios. Despite variable and low preservation probabilities, the simulated fossil record retained the signal of diversification dynamics in most scenarios. Large increases or decreases in preservation probability between temporal bins resulted in the largest deviations from expectations, although the effect was restricted to those particular intervals. A consistent bias towards higher speciation, extinction, and diversification rates under certain preservation scenarios distorted the absolute rate values; however, relative differences in rates were correctly inferred, especially when the record was binned into broad temporal intervals corresponding to distinct diversification regimes. Results from these simulations indicate that elevated diversification rates in relation to tectonic activity during the middle Miocene are likely to be evident in the fossil record, even if preservation rates in the North American fossil record were highly variable. Despite challenges in reading the fossil record, input from the past is necessary in order to evaluate the ultimate mechanisms underlying speciation and extinction dynamics.

INTRODUCTION

One of the outstanding questions in biology remains, how do patterns in species diversity arise and persist over space and time? Explanations for diversity gradients have frequently emphasized regional or temporal differences in diversification rates (e.g., Jablonski et al. 2006, Weir and Schluter 2007, Mittelbach et al. 2007, Rolland et al. 2014). One hypothesized mechanism for long-term variation in speciation and extinction rates is the influence of tectonic activity and broad-scale landscape changes on species geographic ranges and diversification dynamics (Cracraft 1985, Badgley 2010, Hoorn et al. 2010, Moen and Morlon 2014). The generation of topographic complexity and geographic barriers during tectonic activity reduces

habitat continuity while increasing environmental heterogeneity along elevational gradients (e.g., Mulch 2016). These landscape changes can isolate populations, thereby promoting population divergence, allopatric speciation, and high species turnover at the regional scale (e.g., Coblentz and Riitter 2004, Renema et al. 2008, Moen and Morlon 2014). The present-day biogeographic pattern resulting from these evolutionary, ecological, and historical processes has been termed the topographic diversity gradient, or TDG (Badgley et al. *in review*). Examples of the TDG in birds, plants, and mammals have been found on all continents where gradients in topographic complexity result from contrasting tectonic regimes and histories (Badgley and Fox 2000, Barthlott et al. 2005, Ruggiero and Hawkins 2008, Badgley 2010).

Approaches for investigating macroevolutionary processes governing diversity patterns such as the TDG have traditionally relied on inference from the fossil record, using occurrence data, to quantify speciation and extinction over time and space (e.g., Stanley 1979, Sepkoski et al. 1981, Foote 2000, Alroy 2009). In recent years, phylogenetically-based methods have been developed that utilize relationships among extant taxa to reconstruct the tempo and mode of diversification through time (e.g., Ricklefs 2007, Stadler 2011, Rabosky 2014). These approaches have also been employed to quantify regional differences in diversification rates and explain broad-scale diversity gradients (e.g., Weir and Schulter 2007, Rolland et al. 2014). Both phylogenetic and fossil-occurrence-based approaches have their strengths and limitations, and a growing number of studies demonstrate the advantages of integrating molecular and fossil data into diversification analyses (Purvis et al. 2009, Liow et al. 2010, Quental and Marshall 2010, Fritz et al. 2013). An advantage of the fossil record is that knowledge of past diversity allows rates to be estimated directly rather than inferred from tree topology and model assumptions (Foote 2000, Rabosky 2009). However, incomplete preservation and sampling can dampen,

accentuate, or even erase patterns in the fossil record (Raup 1979, Foote and Raup 1996, Smith et al. 2012). In response to this challenge, numerous methods have been developed that subsample or standardize fossil datasets (e.g., rarefaction, capture-mark-recapture, shareholder quorum subsampling) in order to assess the robustness of observed patterns to sampling processes (Raup 1975, Alroy et al. 2001, Connolly and Miller 2001, Alroy 2010).

Various diversification analyses and subsampling techniques have been applied to the North American fossil record in order to evaluate the history of the strong TDG found in mammals (Barnosky and Carrasco 2002, Kohn and Fremd 2008, Finarelli and Badgley 2010, Badgley and Finarelli 2013). Today, mammals are twice as diverse within the topographically complex western region compared to the low-relief Great Plains (Badgley and Fox 2000, Badgley 2010). Multiple lines of evidence suggest that the evolution of extant rodent clades was closely linked with the Neogene history of tectonic activity in western geological provinces (e.g., Riddle 1996, Hafner et al. 2007, Riddle et al. 2014). In particular, landscape relief increased significantly during tectonic extension and the development of the Basin and Range Province over the last 30 myr (Horton and Chamberlain 2004, McQuarrie and Wernicke 2005, Dickinson 2006). The most intense interval of landscape change occurred from ~18 to 14 Ma in response to the subduction of the spreading margin between the Farallon and Pacific tectonic plates (Atwater and Stock 1998, Sonder and Jones 1999). Diversification analyses of the mammalian fossil record show a consistent pattern: diversity was higher in the tectonically active region than in the quiescent region during this interval of intense extension and increased landscape relief (Barnosky and Carrasco 2002, Kohn and Fremd 2008, Finarelli and Badgley 2010).

Additionally, the TDG was not persistent through time and may have emerged when interactions between topographic complexity and climate warming (i.e., the middle Miocene

Climatic Optimum; Zachos et al. 2008) facilitated elevated species richness. The middle Miocene peak in mammal diversity occurred across taxonomic groups, but in particular among rodents (Fig. 5.1, Badgley and Finarelli 2013, Badgley et al. 2014). For example, the fossil record of heteromyid rodents (kangaroo rats and pocket mice) documents a dynamic history over space and time with elevated diversity and fossil occurrences within the Basin and Range Province from ~17 to 13 Ma (Fig. 5.2). The heteromyid fossil record is notable for its excellent geographic coverage; however, large gaps in the small-mammal fossil record do exist, especially within the Basin and Range Province prior to ~18 Ma (Barnosky et al. 2007, Badgley et al. 2015).

Given the concurrent, dynamic histories of tectonic activity, mammal diversification, and fossil preservation, the aim of this study was to utilize simulations of the fossil record to evaluate the reciprocal impacts of variability across these records. To do so, I first developed theoretically plausible diversification models for the origin of the TDG in relation to tectonic history and simulated fossil records based on those models. Then, I imposed various preservation scenarios on the simulated fossil records and used standard methods to quantify diversification rates. Finally, I examined to what degree different and variable preservation scenarios limit our ability to correctly infer underlying dynamics. Specifically, I utilized standard birth-death models (Kendall 1948) to generate simulated fossil records for four diversification models that varied in terms of speciation rates (Fig. 5.3a). In these stochastic models, species from one time step give rise to species in the following time step with a per-lineage rate, λ, or go extinct with a per-lineage rate, μ.

Within the context of tectonic activity and development of topographic complexity, four plausible diversification hypotheses for the generation of the TDG gradient are as follows. The

first model is akin to a mountains-as-cradle model, where time-invariant but elevated speciation rates generate high species richness in the region of tectonic activity. This *Constant* model also represents a scenario in which variation in diversification rates derived from the fossil record arises only from stochastic processes or changes in preservation probability through time. In contrast, two alternative models incorporate variation in speciation rates through time. The *Tectonic-pulse* model has two shifts in speciation rate over the history of the record, an instantaneous increase that coincides with the onset of intensified tectonic extension (18 Ma) and an instantaneous decrease at the end of this interval (14 Ma). The *Tectonic-constraint* model is a more complex version of the *Tectonic-pulse* model and assumes five different rate regimes. In this model, speciation rate through time is determined as a function of the area gained over 6-myr time intervals during tectonic extension in the southern Basin and Range Province (McQuarrie and Wernicke 2005). A 50-200% increase in land area in different regions of western North America resulted from the rotation and displacement of fault-bounded blocks during Neogene extension and increased large-scale basin-and-range relief as the landscape broadened (e.g., Snow and Wernicke 2000, Horton and Chamberlain 2006). Quantifying relief remains a difficult problem in the geologic past (Clark 2007, Mulch 2016); therefore, I used area gained as a proxy for change in topographic complexity over the Neogene. For example, the interval of greatest block faulting was also the interval that experienced the largest increase in land area (McQuarrie and Wernicke 2005). Because speciation rates are higher than extinction rates in each of these scenarios, species richness increases through time in an exponential or episodic manner.

The final model assumes a different history of diversity over the Neogene. In the *Diversity-dependent* model, the speciation rate initially exceeds the extinction rate, and then

changes linearly as a function of the number of species. While extinction rate remains constant through time, the speciation rate 'slows down' until an equilibrium number of species is maintained and the speciation rate remains constant and equal to the extinction rate. In this diversification scenario, I focus on the diversification dynamics after species equilibrium has been reached, as the ability of the fossil record to capture the initial diversity-dependent slow-down in speciation rates has already been evaluated elsewhere (Liow et al. 2010). Although I do not specify the underlying mechanism for diversity-dependent diversification, this model could generate the TDG if the species carrying capacity in mountainous regions exceeded that of nearby low-relief regions, and if diversification declined over time. Diversification rates may decrease due to 'filling up' of ecological space or less opportunity for allopatric speciation over time in relation to increasingly finer subdivision of the available land area during to tectonic activity (Moen and Morlon 2014).

In contrast to varying speciation rates, extinction rate is held constant in each of the four models. This simplifying assumption enables the direct assessment of how variable preservation impacts our ability to identify changes in speciation rates, without the influence of simultaneous changes in extinction rates. However, it should be noted that tectonically-driven landscape changes likely also influenced extinction rates. Therefore, these four scenarios are not the only possible models for generating the TDG, and a fuller suite of models and parameter settings that includes variation in extinction rates could be tested in the future.

Preservation and sampling biases are a pervasive challenge and can affect estimates of diversity for reasons ranging from a heterogeneous rock record through time to non-uniform sampling effort by researchers (Raup 1975, Foote and Raup 1996, Peters and Heim 2010, Smith et al. 2013). For the Neogene mammal record, an unconformity in the rock record over most of

western North America represents a significant gap in our knowledge from ~23 to 18 Ma (e.g., Barnosky et al. 2007, Badgley et al. 2014). For these reasons, I evaluate the fidelity of the simulated diversification records under different preservation scenarios that are either predetermined or empirically derived from the fossil and rock records (Fig. 5.3b). Preservation can distort estimates of diversity and diversification rates, and even diversification metrics that are robust to several different sampling biases remain sensitive to variable preservation rates through time (Alroy 1996, Foote 2000, Peters and Foote 2001). Comparing simulated fossil records degraded under alternative preservation scenarios, I assess how well the observed variation in speciation and extinction rates reproduces the 'true' underlying diversification dynamics and how much variation should be attributed to differences in preservation probability (e.g., Liow et al. 2010). This comparison can have important implications for accounting for preservation probability through time in complex modeling approaches that jointly infer speciation, extinction, and preservation rates (e.g., Silvestro et al. 2014). While it is not the goal of this paper to reproduce the TDG over time—to do so would require extensive consideration of variation in speciation, extinction, immigration, and preservation rates through time—I aim to demonstrate how variation in one parameter—speciation—could contribute to this distinctive pattern in the fossil record. Additionally, I demonstrate how the inferred record of speciation rates may become altered due to variation in fossil preservation.

METHODS

Determining model parameter values

Three parameters potentially influence the simulated fossil record: speciation rate (λ), extinction rate (μ), and preservation probability (R) through time. In order to choose biologically

realistic values for extinction and speciation, I conducted a survivorship analysis to estimate extinction rates. Using the MIOMAP database of North American mammals (Carrasco et al. 2007), I compiled data for all Neogene rodent taxa, including first and last occurrences at the genus and species levels and geographic location of fossil occurrences (e.g., Fig. 5.2). Based on observed lineage durations, cohort analysis produced a best-fit extinction rate to describe the resulting survivorship curve (Raup 1978, Baumiller 1993). To simplify the diversification modeling process, I assumed that this extinction rate was constant throughout the simulated record. Then, I tested various λ values to determine a range of possible speciation rates that yielded, on average, approximately the same number of species present in the tectonically-active region of North America today (n = ~160; Wilson and Reeder 2005). For the *Constant* model, one speciation rate was applied. For the *Tectonic-pulse* model, two speciation rates were applied as I increased the speciation rate for a 4-myr interval corresponding with elevated tectonic activity in the geologic record (Fig. 5.3a).

For the *Tectonic-constraint* model, variation in speciation rate through time was determined as a function of the area gained over 6-myr intervals during tectonic extension in the southern Basin and Range Province. To estimate area gained over geologic time, I used the output from the kinematic models of McQuarrie and Wernicke (2005). Specifically, I calculated the area of the tectonic reconstructions (bounded by the geographic distribution of fossil localities) and assessed changes in total area for successive time intervals. Thus, area gained serves as proxy for tectonic activity and the development of topographic complexity, and was directly correlated with speciation rates in this simulation. For the *Diversity-dependent* model, the speciation rate was initially similar to that of the *Constant* model, but decreased over time as a function of the number of species in the clade. In this logistic-growth model, the equilibrium

number of species, or species carrying capacity, was 160 species, at which point the speciation and extinction rates varied stochastically around a single value ($\lambda = \mu$). The window of analysis was restricted to this equilibrium period of diversification.

I imposed five preservation scenarios (Fig. 5.3b) to remove species randomly from the simulated fossil record under each diversification model (removal process described below). Two of the preservation scenarios represent general patterns in the fossil and rock records. In the first scenario, preservation probability was generally low across the fossil record, with estimates for Cenozoic mammal species ranging from 25-37% (Foote 1997, Foote et al. 1999). Therefore I applied a constant preservation probability of 30% throughout the record (R30%). In the second scenario, fossil preservation improved linearly from 10% to 50% within progressively younger rocks (Raup 1979, Kidwell and Holland 2002), resulting in increasing preservation probability through time (IncR). The third preservation scenario was based on the idea that relief, and therefore sediment accumulation and preservation probability, were highest during the interval of intense faulting and extension, and declined subsequently (PulseR). Two additional scenarios were derived from gap analysis of fossil-rodent occurrence data (Foote and Raup 1996, Foote 2000) and from the number and duration of rock-unit packages in western North America (Peters 2008). Gap analysis refers to an approach for estimating variation in preservation probability based on the temporal distribution of fossil occurrences compared to lineage durations, assuming that species range through their first and last occurrences in the fossil record (e.g., range-frequency ratio, or FreqRat, of Foote and Raup 1996). The ratio of species-level occurrences to tallied diversity per interval in the North American rodent record provided a frequency-based approach to estimating preservation probability (FreqR). It is also possible to derive an independent estimate of preservation potential based on the geographic and temporal distribution

of the rock record (e.g., Smith et al. 2012). For the fifth scenario, I used the Macrostrat database (Version 0.3) to assess the maximum possible extent of non-marine rock units for 1-myr intervals over the Neogene (StratR). The geospatial analysis was restricted to the tectonically-active region only, and the proportional area of rock of a given age was used to estimate preservation probability through the Neogene. This estimate served as a rough first approximation, however, and more precise filtering of the rock record (e.g., fluvial, fossiliferous sediments) may produce a different preservation curve. I compared results from all preservation scenarios to the full simulated record with no loss of fossil occurrences due to preservation (R100%).

Simulating diversification and preservation scenarios

Using a birth-death process, I simulated 1000 phylogenetic trees per diversification model (e.g., Fig 5.4a). Extinction rate was constant in all simulations. These trees were then transformed to represent a simulated fossil record following procedures implemented by Liow et al. (2010). Specifically, for each simulation, I removed branching relationships and determined taxon duration for each tip taxon (including extinct taxa). Taxon duration extended from the interval of first appearance—including the internal branch for one lineage per branching event—to the interval of last appearance (Fig. 5.4b). Therefore, in these simulations, first appearances were treated as speciation events and not as immigration events. Time was divided into discrete, 1-myr intervals to match previous analyses of the North American fossil mammal record over the Cenozoic (e.g., Finarelli and Badgley 2010). Simulations were run for 40 myr, but results of downstream analyses were retained for the middle 30 myr to avoid significant edge effects (Foote 2000) and to correspond temporally with the interval of tectonic extension in western

North America (30 Ma to present; McQuarrie and Wernicke 2005). The *Diversity-dependent* model was evaluated for longer than 40 myr, in order to ensure that the model would reach equilibrium (constant diversity through time, with approximately 160 species within each 1-myr time bin). The initial period of decreasing speciation rates, or 'slow-down,' was removed prior to diversification analyses, as were 5-myr intervals on either end of the analysis window to avoid edge effects and match the methods implemented in the prior three models.

I imposed the five different preservation scenarios described above (Fig. 5.3b) on the simulated fossil records. Taxa present within a 1-myr window were randomly sampled according to the corresponding preservation probability, R, for that interval. In this way, lineage first (FAD) or last (LAD) appearance data or any of the intervening 1-myr intervals could be lost from the record. Importantly, because I utilized lineage range-through assumptions, if an occurrence of a lineage was lost between the FAD and LAD, it was still considered present through sampling gaps and thereby contributed to the diversity count and diversification rate analysis of those intervening intervals.

Evaluating diversification rates

For each simulated record, I calculated the instantaneous per-capita speciation ($\hat{p}$) and extinction ($\hat{q}$) rates under different preservation scenarios, according to the following equations (Foote 2000):

$$\hat{p} = \ln\left(\frac{N_{\mathrm{t}}}{N_{\mathrm{bt}}}\right)/\Delta\, t, \quad (1)$$

$$\hat{q} = \ln\left(\frac{N_{\mathrm{b}}}{N_{\mathrm{bt}}}\right)/\Delta\, t, \quad (2)$$

where N_{t} is the number of taxa that cross the top of the interval only (i.e., FAD), N_{b} is the number of taxa that cross the bottom of the interval only (i.e., LAD), N_{bt} is the number of taxa

that cross both the top and the bottom of the time interval, and the time interval, Δt, is 1-myr for these analyses. Taxa that occurred in one time interval only were considered singleton taxa and removed from rate calculations. Singleton taxa can represent either poorly sampled faunas or, if concentrated in one temporal bin, a disproportionately well-sampled interval. They can thus generate spurious results that are dominated by variable preservation rather than accurate changes in diversification rates (Foote 2000). Diversification rate ($\hat{d}$) represents the net change in diversity as extinction rates are subtracted from speciation rates:

$$\widehat{d} = \hat{p} - \hat{q}, \text{ or} \quad (3)$$

$$\widehat{d} = \ln\left(\frac{N_t}{N_b}\right)/\Delta t \quad (4)$$

Alternative methods for calculating diversification rates exist (e.g, Alroy 2014, Silvestro et al. 2014). However, since the per-capita rate method features prominently in the existing literature for the North American record of rodent diversity (Finarelli and Badgley 2010, Badgley and Finarelli 2014, Badgley et al. 2015), I retain its usage here. For consistency, I refer to the model parameters as λ (speciation rate) and μ (extinction rate) and the estimated rates from the simulated fossil record as $\hat{p}$ (per-capita origination rate) and $\hat{q}$ (pre-capita extinction rate) through the paper. Trees were generated, converted, and analyzed using R packages 'APE' (Paradis et al. 2004), 'TreeSim' (Stadler 2011), and 'phytools' (Revell 2012), with modified and newly generated functions for the purposes of this study.

Evaluating fidelity of the fossil record

Beyond visual inspection of rate variation through time, I also examined how well the simulated fossil record retained the original diversification pattern under each preservation scenario by two primary tests. First, although rates calculated using the per-capita approach were

not expected to reproduce the exact model parameter values (e.g., Alroy 2014), trends in both should be strongly correlated. To investigate whether the simulated fossil record provided a reliable signal of temporal variation in underlying diversification rates, I applied Spearman's rank correlation analysis to test for significant, positive correlations between the model λ and calculated $\hat{p}$ speciation rates for the simulated and degraded records (n = 1000). Next, I divided each simulated record into different 'diversification regimes' based on variation in λ and time since the root of the tree. For example, the *Tectonic-pulse* model was divided into three regimes: pre-pulse from 30 to 18 Ma (λ = 0.2), the pulse interval from 18 to 14 Ma (λ = 0.3), and post-pulse from 14 Ma to present (λ = 0.2). Within each regime, using a Wilcoxon-signed ranks test, I evaluated the mean and distribution of $\hat{p}$, $\hat{q}$, and $\hat{d}$ values calculated across all simulations for 100% preservation probability (R100%) compared to the distribution of values under the five incomplete preservation scenarios.

RESULTS

In this section, I first discuss the parameter estimates that were utilized in the modeling framework. I then present results from four diversification models under five different preservation scenarios compared to those parameter estimates and to the simulated, complete fossil record.

Parameter estimates

Based on survivorship analysis, the Neogene extinction rate (species extinctions per lineage-million-years, or extinctions/LMA) for rodents in the tectonically active, western region of North America exceeded the rate for North American rodents as a whole. The best-fit μ value

estimated from lineage durations was 0.12 ± 0.01 extinctions/LMA for all North American extinct genera (n = 166), compared to 0.14 ± 0.01 extinctions/LMA for western genera (n = 115; standard deviations obtained from 500 bootstrap replicates). These results suggest that species durations in western lineages were 15% shorter than lineage durations estimated from the entire North American rodent dataset (rodents from the tectonically active and passive regions combined). Compared to the survivorship curve generated from the best-fit μ value, the empirical data showed a bias towards more short-lived genera than expected and conversely, fewer long-lived genera than expected under a homogeneous branching model with constant λ and μ values. Assuming an extinction rate of 0.14 extinctions/LMA, speciation rates ranged from just above 0.14 to 0.30 speciation events/LMA (Fig. 5.3a) in order to produce the observed number of extant species for the region (n = ~160; Wilson and Reeder 2005) at the end of each diversification model run.

In addition to λ and μ values, estimates of preservation probabilities, R, through time were derived from gap analysis of the actual fossil record (e.g., Fig. 5.2) and from rock area extracted from the Macrostrat database (Version 0.3, Peters 2008). Fossil-based preservation probability (FreqR) was highly variable through time (Fig. 5.3b). A weak but significant relationship was found between diversity and FreqR preservation probability (Spearman's r = 0.45, *p-value* = 0.02), suggesting that variability in preservation may be contributing to the volatile pattern of Neogene rodent diversity in western North America. However, because these curves were derived from the same underlying data, gap analysis may not represent a fully independent measure of preservation probability. These findings contrast with previous studies assessing the North American rodent diversity record, which did not find significant sampling biases based on the correlation between the number of fossil localities and diversity or through

shareholder quorum subsampling (Alroy 2010, Finarelli and Badgley 2010, Badgley et al. 2014). The areal extent of the rock record may be a better independent measure of preservation probability (e.g., Smith et al. 2012), and data from Macrostrat reflected the common trend of increasing rock area towards the present (Fig. 5.3b). Somewhat surprisingly, this rock record did not signal a pulse in the area of sediment accumulation associated with tectonic activity and basin development in western North America during the middle Miocene. This finding may be a result of the coarse geographic and lithological resolution of this analysis.

Simulated diversification

The five different preservation scenarios had different effects on diversification dynamics inferred from simulated, degraded fossil records. The simulated fossil records based on phylogenetic histories with no preservation filter accurately reproduced diversity patterns through time (Fig. 5.4c). For the *Constant*, *Tectonic-pulse*, and *Tectonic-constraint* models, diversity increased through time to the present-day rodent species richness (n = 160), while for the *Diversity-dependent* model, diversity varied stocastically around the target number of species (n = 160) through the duration of the analysis. Short-term variation documented in lineage-through-time plots may be smeared across the 1-myr temporal bins used for tallying fossil diversity, resulting in slightly inflated richness towards the present. However, edge effects on diversity and diversification rate calculations at the root and tip of simulated trees were avoided by running the simulations over 40 million years (or longer to reach equilibrium for the *Diversity-dependent* model), and then removing the initial and final five-million years of results. Per-capita $\hat{p}$ and $\hat{q}$ rate estimates were similar, but non-identical to model λ and μ values, as expected (e.g., Alroy 2014).

Although per-capita $\hat{p}$ and $\hat{q}$ rate estimates from simulations were systematically higher than model parameter values, the temporal variation in rates (or lack thereof) was reflected by the simulated fossil record with perfect preservation (R100%). Therefore, record fidelity under different preservation scenarios was compared to the distribution of per-capita rates derived from the non-degraded fossil record. Results from 1000 simulated records per diversification model for each preservation scenario are presented in Figures 5.5-5.8. For diversification scenarios with increasing diversity through time, one common feature of these simulations is that the 95% confidence intervals around rate estimates narrow towards the present, indicating that lower overall diversity at the root of the simulated histories leads to slightly more variable rates within this modeling scheme. With constant, high diversity (n = 160) through time, the *Diversity-dependent* model does not exhibit this behavior, suggesting that the number of species present within a given time bin may influence simulated diversification dynamics and model uncertainity. To demonstrate the effects of preservation probability on the absolute value of rate estimates under different speciation regimes, kernel-density plots of rate distributions are presented in Figures 5.9-5.12. These plots demonstrate how rate estimates were systematically higher for most preservation scenarios. According to Wilcoxon-signed ranks test, the mean and distribution of $\hat{p}$, $\hat{q}$, and $\hat{d}$ estimates for all preservation scenarios differed significantly (*p-values* < 0.01) from those of the non-degraded record (R100%). However, the estimated rate distributions under the *Diversity-dependent* model were less variable around the mean value and closer to the non-degraded record overall (Fig. 5.12).

Under the *Constant* diversification model, both mean speciation and mean extinction rates were time-invariant throughout the Neogene, a pattern that remained consistent in three of the five preservation scenarios (Fig. 5.5). Surprisingly, variable preservation rates (e.g., IncR,

StratR) alone were not responsible for notable deviations from the 'true' diversification dynamics. Only large jumps in preservation rate, such as those imposed by the PulseR and FreqR scenarios, seriously compromised the fidelity of the simulated fossil record. Even then, the effect was relatively short-lived. The effects of preservation impacted all diversification metrics; however, the net diversification rate, $\hat{d}$, exhibited the least amount of variability. Although λ and μ were time-invariant within this model, I evaluated two separate diversification regimes to account for greater variability around mean $\hat{p}$ and $\hat{q}$ estimates early in the clade history (Fig. 5.9). Mean estimates of origination, extinction, and diversification rates were the same for both regimes; however, there was greater variation in the rate distributions and larger deviations in rate estimates under all preservation scenarios before 18 Ma. After 18 Ma, 95% confidence intervals around the mean values narrowed (Fig. 5.5) and mean $\hat{p}$ and $\hat{q}$ estimates approached the 'true' value under 100% preservation (Fig. 5.9). Notably, all preservation scenarios produced similar estimates of mean origination, extinction, and diversification rates in these broad time bins.

In contrast, increased speciation rates over a 4-myr interval can be detected under all preservation scenarios (Fig. 5.6). In the *Tectonic-pulse* diversification model, the origination pulse was present, albeit dampened (R30%, IncR, StratR) or accentuated (PulseR, FreqR), depending on the preservation dynamics. In the FreqR preservation scenario, spurious origination and extinction rate peaks also arose. In all scenarios except for FreqR, a significant, positive correlation between λ and mean $\hat{p}$ was found (via Spearman's rank correlation coefficient, *p-values* < 0.01), indicating that underlying diversification dynamics could be recovered despite variation in preservation probability. Kernel-density plots differ among the three diversification regimes (Fig. 5.10). Greater variation around the mean estimates occurred

early in the clade history, with considerable increase in falsely identified elevated rates under all of the preservation scenarios. Surprisingly, the PulseR scenario had the least impact on rate estimates possibly due to a rate-dampening effect under low preservation probability (R = 10%) prior to the pulse (Fig. 5.10, *Pre-18 Ma*). During the tectonic pulse, mean speciation rates were elevated and as they declined after the pulse, rate distributions tightened around the mean (Fig. 5.10). Although the FreqR preservation scenario distorted temporal diversity dynamics across 1-myr time bins (Fig. 5.6), within broader diversification regimes, mean origination, extinction, and diversification rates were similar for all preservation scenarios (Fig. 5.10).

The *Tectonic-constraint* model—based on area change during Neogene extension in western North America as a proxy for tectonic activity and corresponding temporal variation in λ—had more complex behavior under the different diversification scenarios (Fig. 5.7) than the previous two diversification models. Subtle variation in origination rates was observed, but notably dampened, in the R30%, IncR, and StratR scenarios and was distorted in the PulseR and FreqR scenarios. A significant positive correlation between λ and the mean origination value for 1000 simulations was found (via Spearman's rank correlation coefficient, *p-values* < 0.01) for all preservation scenarios except FreqR. These results suggest that diversification histories with several rate shifts may be difficult to detect in the fossil record regardless of preservation probabilities through time. Larger rate shifts than those modeled here may be easier to detect. Rate estimates under all diversification scenarios improved during younger diversification regimes (Fig. 5.11), again suggesting a bias towards false high rates during intervals when diversity is low. The similarity of these findings across all three models may reflect an artifact of the birth-death modeling process and its transformation to a simulated fossil record. Early in the clade history, diversification dynamics are more volatile, and the addition or loss of species

appears to have a greater proportional impact, even on per-capita rates. This may or may not be an issue for the actual fossil record due to the asynchronous presence, proliferation, and decline of several different rodent clades, instead of the singular 'rodent' clade modeled here.

Finally, the *Diversity-dependent* model exhibited behavior distinct from the previous three models, in part due to a different underlying diversity pattern (Fig. 5.8). Because the total number of species in sequential 1-myr time bins remained roughly constant (n = 160), the *Diversity-dependent* model represented an equilibrium diversification scenario, with $\lambda = \mu$, and a net diversification rate of approximately zero. When preservation probability was constant through time (e.g., R30%), equilibrium diversity was reduced, but preserved. Not surprisingly, simulated diversity dynamics under variable preservation scenarios closely matched preservation probability through the Neogene, with false peaks in species richness occurring during intervals of elevated preservation. Despite this, simulated origination and extinction rates remained roughly constant and equal under all but two of the preservation scenarios, PulseR and FreqR (Fig. 5.8). Similarly to the previous three diversification models, under the variable PulseR and FreqR preservation scenarios, the degraded record inaccurately reflected the 'true' underlying rates, and could lead to the misidentification of significant changes in speciation and extinction rates through time. However, preservation effects on speciation and extinction rates tended to cancel out, and diversification rates under all scenarios remained tightly clustered around zero, as expected during the maintenance of equilibrium diversity (Fig. 5.8). The *Diversity-dependent* model was evaluated as a single diversification regime, with the mean and distribution of estimated rates remaining remarkably similar under all preservation scenarios (Fig. 5.12). The primary exception is a notable increase in net diversification rates under the PulseR preservation

scenario, implying that a steep, but short-term increase in preservation could indeed appear as a diversification event.

DISCUSSION

Simulating the imperfect fossil record

Findings from these simulations emphasize the insight that can be gained from investigating not only diversity patterns through time, but also teasing apart the mechanisms driving those patterns. The fossil record provides a crucial but incomplete picture of diversification dynamics in the past and leading to present-day diversity gradients. The origin of the topographic diversity gradient, or TDG, is explored here, with a focus on the exceptional rodent record of western North America. In particular, I examined how changes in tectonic activity during basin extension may have promoted speciation events and thus contributed to variability in diversification rate throughout the evolutionary history of mammalian faunas in this region (e.g., Barnosky and Carrasco 2002, Kohn and Fremd 2008, Badgley 2010). However, the diversity trend of the fossil record must be balanced with an appreciation of preservation and sampling biases. The range of speciation rates (λ = 0.14-0.30 species/LMA) employed in these simulations is representative of rates yielded by previous fossil and some molecular analyses. For example, Alroy (2009) found an origination rate of 0.23 species/LMA for North American fossil mammals, while Zelditch et al. (2015) utilized the BAMM program (Bayesian Analysis of Macroevolutionary Mixtures; Rabosky 2014) to infer variation in lineage diversification rates centered around ~0.20 species/myr for Sciuridae (squirrels) from a consensus tree derived from molecular data (Fabre et al. 2012). However, our ability to accurately recover those rates, and in particular rate shifts through time, is compromised by incomplete preservation in the fossil

record (Holland 2016). To simulate the impact of preservation on diversification models, I employed both idealized preservation probabilities and empirically-derived preservation curves. Therefore, the parameter values used are plausible if basic.

Under most preservation scenarios, the simulated fossil records reflected the temporal variation in the true underlying diversification dynamics. Stability in speciation and extinction rates was recovered for the *Constant* and *Diversity-dependent* diversification models, while variation in speciation rates was evident for the *Tectonic-pulse* and *Tectonic-constraint* models, despite low constant (R30%) and variable, but increasing (IncR, StratR) preservation probabilities (Figs. 5.5-5.8). However, preservation scenarios with large jumps in preservation probability from one temporal bin to the next (PulseR, FreqR) generated false peaks in speciation and extinction rates. Importantly, deviations from the original model were limited to the intervals of pronounced preservation change and did not impact the record more broadly. These results are summarized by the distribution of rates recovered during different diversification 'regimes,' or time intervals with a common history spanning more than two million years (Figs. 5.9-5.12). Broadening the temporal window of rate evaluation served to minimize the impact of different preservation scenarios, especially those with large and sporadic variation in R. Under this approach, speciation and extinction rates were elevated to a similar degree compared to the original fossil record (R100%) and still retained relative rate shifts between diversification regimes regardless of the preservation mode (Figs. 5.9-5.11). The absolute values for estimated per-capita speciation and extinction rates compared to the original fossil record (R100%) were often recovered for the *Diversity-dependent* model, for which rates did not vary substantially among differing preservation scenarios (Fig. 5.12). While grouping data into regimes may mask considerable underlying variation in diversification rates, it may be an appropriate strategy for

trying to discern rate shifts in relation to significant and temporally constrained changes in abiotic or biotic conditions.

Preservation probability varies not only over time, but also over space, physical environments, and across clades. These preservation issues were avoided in the record simulated here; for instance, small-mammal teeth have similar taphonomic properties (Hibbard 1941) and with the exception of Quaternary cave deposits (e.g., Terry 2010), small-mammal fossils are typically found by screen-washing retrieval methods that are frequently applied to alluvial sediments (e.g., Lindsay 1972, Badgley et al. 1998). How to reconcile variability in diversification rates with heterogeneous preservation remains a challenging but important problem in paleoecology and macroevolution (e.g., Foote 2000), especially given that preservation rates are often treated as time-invariant or assumed to follow a common trajectory with respect to lineage duration across the history of a clade (e.g., Liow et al. 2010, Silvestro et al. 2014a). Some of this simplification occurs so as to avoid over-parameterization of complex models (Silvestro et al. 2014b). However, if preservation parameters that are independent from lineage history (e.g., based on rock-record estimates from Macrostrat) are applied, some of these simplifying assumptions can be reconciled, thus enhancing our capability to recover the actual dynamics underpinning diversity patterns over time (e.g., Smith et al. 2012).

Alternative diversification models and approaches

The modeling framework presented here is simplified in order to distinguish the impacts of variation in two model parameters. Several other diversification processes are not only plausible, but also necessary to produce the diversity patterns we observe through time. For small-mammal species richness to rise and fall over the Neogene within the two regions of North

America (Fig. 5.1) requires that extinction rates vary and even exceed origination rates at times (Alroy 2009, Finarelli and Badgley 2010, Badgley et al. 2014). Alternatively, under a *Diversity-dependent* model, once an equilibrium number of species has been reached, large-scale variation in preservation alone could produce a highly variable species richness pattern through the Cenozoic. Evidence for exponential species increase, as modeled in the *Constant*, *Tectonic-pulse* and *Tectonic-constraint* diversification scenarios, is not typically recovered from the fossil record (e.g., Alroy et al. 2000). Fossil and molecular records alike support the concept of diversification slowdowns over time (Alroy 2009, Morlon 2010, Rabosky 2013). The mechanisms for these slowdowns, or *Diversity-dependent* diversification as modeled here, remain controversial; however, factors related to both biotic interactions and changes in the geographic template are likely to play an important role in limiting the total number of species that a region can both generate and support (Moen and Morlon 2014, Rabosky and Hurlbert 2015). Importantly, Neogene tectonic activity in western North America led to increased topographic complexity regionally and substantial gains in land area, both of which could have promoted elevated species richness (Cracraft 1985, Rosenzweig 1995).

Diversity-dependent diversification can be a compelling mechanism for explaining diversity patterns over space and time; however, the volatile record of North American rodent diversity is not necessarily consistent with this process. Depending on the spatial and temporal scale of the analysis, the North American mammal record has been used to infer both diversity-dependent dynamics (e.g., driven by biotic interactions) and landscape-driven dynamics (Alroy et al. 2000, Barnosky 2001). In the second case, various analyses have coupled variation in diversity and diversification rates with changes in tectonic activity (e.g., extension), climate (e.g., the Miocene Climatic Optimum), and vegetation heterogeneity (e.g., Vrba 1992, Barnosky and

Carrasco 2002, Kohn and Fremd 2008, Finarelli and Badgely 2010, Eronen et al. 2015). These different mechanisms are not mutually exclusive, and the changing nature of species ecology, geographic distributions, and community assembly over a topographically and environmentally complex and dynamic landscape is likely to be a product of the interactions between biotic and abiotic factors (Badgley 2010, Blois and Hadly 2009, Hoorn et al. 2010). For example, diversification dynamics in mountainous regions may follow a diversity-dependent pattern during the development of topographic complexity as 1) species diversify to fill up ecological space along elevational gradients, and 2) geographic opportunities for vicariance decline through time in response to finer subdivision of the available landscape (Moen and Morlon, 2014). However, even under a diversity-dependent scenario, one might expect dynamic species richness and not equilibrium-diversity from the fossil record during an interval of intense tectonic activity. In addition to evidence from the fossil record, quantifying rate variation from comparative phylogenetic methods may illuminate underlying diversification mechanisms (e.g., Stadler 2011, Zelditch et al. 2015). For example, approaches such as BAMM (Rabosky 2014) could be implemented for North American rodents and may yield interesting differences in speciation and extinction rates between clades found predominantly in the tectonically active or passive regions. Ideally, fossil data can be integrated as tip taxa or direct ancestors (e.g., via BioGeoBEARS, Matzke 2013) into such comparative methods (Quental and Marshall 2010, Liow et al. 2010).

A vital biogeographic process governing species distributions and diversity patterns is absent from the modeling framework of this study. In addition to *in situ* speciation, immigration and geographic-range expansions are major processes that add new species to a region (Jablonski et al. 2006, Martin et al. 2008, Riddle et al. 2014). Examples of speciation, extinction, and

immigration feature prominently in the North American record throughout the Neogene, influencing regional diversification, faunal composition, and turnover (e.g., Davis 2005, Alroy 2009, DeSantis et al. 2012, Badgley and Finarelli 2013, Badgley et al. 2015). At regional spatial scales, the origination metric, $\hat{p}$, includes both speciation and immigration (Finarelli and Badgley 2010), but distinguishing these two processes in the fossil record is challenging. Given high-resolution temporal and spatial coverage of fossil occurrences, it is possible to track the geographic distribution of lineages throughout their history to identify immigration events and range shifts over regional scales (Jablonski et al. 2006, Stigall and Lieberman 2006, Maguire and Stigall 2008, Terry et al. 2011). Alternatively, state-dependent modeling approaches (e.g., geographic-state speciation and extinction models, or GeoSSE) have been developed to jointly infer speciation, extinction, and immigration rates between regions (e.g., Goldberg et al. 2011, FitzJohn 2012, Rolland et al. 2014). These GeoSSE-type models do not currently include fossil taxa and demonstrate potential challenges in their implementation (Rabosky and Goldberg 2015); however, the prospect of distinguishing speciation from immigration events between regions makes future development of these approaches compelling (e.g., Van Dam and Matzke 2016).

Tectonics and diversification

The fossil record provides evidence of past diversity beyond what we would be able to retrieve from molecular phylogenies alone (e.g., Quental and Marshall 2010). However, dynamics from the fossil record, such as the strengthening and weakening of the TDG, can be distorted by preservation bias (e.g., Foote 2000). Despite the imperfect nature of the fossil record, qualitative inspection of the empirically-derived preservation scenarios through time

(Fig. 5.3b) indicates that the Neogene mammal diversity curve in North America (Fig. 5.1) is not a direct product of frequency-based fossil occurrences or the temporal distribution of the rock record. Likewise, the middle Miocene diversity peak is not correlated with the number of localities in the fossil record nor lost when subsampled (Badgley et al. 2014). Therefore, the elevated species richness west of the Rocky Mountains during this interval remains a pattern demanding explanation. The fact that we do not find a corresponding peak in the adjacent, but tectonically quiescent Great Plains region would suggest that tectonic activity plays a role in promoting species diversity, possibly through increased speciation rates (Cracraft 1985, Renema et al. 2008, Badgley 2010). Under this scenario, elevated speciation rates due to geographic isolation and limited range size across a topographically complex landscape are likely to be coupled with higher extinction rates. Indeed, a higher extinction rate was estimated for western lineages compared to the North American rodent record as a whole, aligning with these expectations. Short lineage durations, especially in the Basin and Range Province during the middle Miocene, are demonstrated in the fossil record of heteromyids, indicating that the generation of topographic complexity may have promoted both origination and extinction dynamics in this and other rodent clades (Fig. 5.2). This hypothesis is supported by the pattern of high species turnover recorded from the fossil record in association with the interval of greatest tectonic activity (Finarelli and Badgley 2010, Badgley et al. 2014). High turnover rates are unlikely to be explained by variation in preservation. Therefore, variable speciation and extinction rates through time (e.g., *Tectonic-pulse* and *Tectonic-constraint* scenarios) should play a role in small-mammal diversification in western North America through time, and especially in the development of the TDG during the middle Miocene. Concurrent global warming during the

Miocene Climatic Optimum may have facilitated range shifts into intermontane regions, further contributing to the peak in diversity during this time.

Rate analyses using the Foote metrics employed in these simulations did find elevated origination and extinction rates during the middle Miocene in the Great Basin (e.g., Badgley et al. 2014). However, these rates were highly variable through time. If variable preservation contributed to the apparent diversification signal, then it may be advisable to look at rate distributions in coarser temporal bins, and instead identify the direction and magnitude of shifts in diversification regimes in relation to major transitions in tectonic, climate, or other environmental factors. Given the modeling framework provided here, it would be useful to consider what combination of model parameter values could potentially produce the diversification record observed in North American rodents. Tectonic activity may underpin variation in origination, extinction, and preservation (i.e., by enhancing sediment accumulation), leading to positive correlations among all three factors (e.g., Peters 2008). Results from this study suggest that, although the nature of these correlations may differ across time periods and geographic regions, underlying diversification dynamics for the most part can be correctly inferred. In the future, Bayesian modeling approaches in which different hypotheses for diversification in relation to tectonic regimes are tested against fossil-occurrence data or the timing of major divergences inferred from molecular or full-evidence phylogenies may prove particularly illuminating (e.g., Rabosky 2014, Silvestro et al. 2014). Likewise, explicit consideration of both the temporal and geographic distribution of the sedimentary record in relation to fossil localities is critical to better understand the influence of preservation on our reading of diversity patterns from the fossil record (Holland 2016).

Throughout these investigations, however, origination has included both *in situ* speciation and immigration. Geographic-range shifts from the passive to the active region during the middle Miocene remain difficult to track (Finarelli and Badgley 2010). However, an increase in faunal similarity across spatial scales in the active region from 17 to 14 Ma suggests that range shifts were contributing to species richness patterns (Badgley et al. 2015). Spatially-explicit modeling approaches that can incorporate species exchange between the tectonically active and passive regions—for instance, due to climate warming and range shifts to higher elevations—may elucidate the biogeographic processes contributing to the strengthening and weakening of the TDG gradient over geologic time. Although different factors may drive the TDG diversity gradient at different times, topographic and climate interactions are likely to remain an important influence on diversification dynamics. Preservation bias potentially limits our ability to read this record through time, but together, expanding fossil collections and enhanced analytical techniques are increasingly filling these gaps.

CONCLUSIONS

Despite preservation and sampling biases in the fossil record through time, the fossil record can be used to infer robustly shifts in diversification rates. Rate estimates from simulated, degraded fossil records reliably reflected the underlying origination pulse under a variety of preservation scenarios. However, caution should be applied when estimating diversification rates during periods when preservation probability is considered to be highly variable between sequential time bins. Increased origination rates in relation to tectonic extension are hypothesized to have contributed to elevated mammal richness in western North America during the middle Miocene. While new species can be added to the region by speciation and immigration, basic

models such as those explored herein can help constrain the processes that influence diversity patterns over geologic time. Ultimately, integration of data from fossil and molecular records combined with approaches that consider diversification (i.e., speciation and extinction) and biogeographic (i.e., immigration and geographic-range shifts) processes jointly will be necessary to understand the mechanistic underpinnings of diversity gradients such as the topographic diversity gradient.

ACKNOWLEDGMENTS

This work was supported by the University of Michigan Rackham Predoctoral Fellowship. I thank Jonathan Mitchell and Tomasz Baumiller for very helpful discussion of the concepts in this manuscript and for sharing useful analytical code. I also thank Catherine Badgley for thoughtful editing of this manuscript. Finally, I am especially grateful to Pascal Title for valuable R tutorials and his enthusiastic guidance with phylogenetic simulations.

REFERENCES

Alroy, J., 1996. Constant extinction, constrained diversification, and uncoordinated stasis in North American mammals. Palaeogeography, Palaeoclimatology, Palaeoecology 127, 285–311.

Alroy, J., 2009. Speciation and extinction in the fossil record of North American mammals, in: Butlin, R.K., Bridle, J.R., Schuler, D. (Eds.), Speciation and Patterns of Diversity. Cambridge University Press, pp. 301–323.

Alroy, J., 2010. Fair sampling of taxonomic richness and unbiased estimation of origination and extinction rates. Quantitative Methods in Paleobiology. Paleontological Society Papers. 16, 55–80.

Alroy, J., 2014. Accurate and precise estimates of origination and extinction rates. Paleobiology 40, 374–397.

Alroy, J., Koch, P.L., Zachos, J.C., 2000. Global climate change and North American mammalian evolution. Paleobiology 26, 259–288.

Alroy, J., Marshall, C.R., Bambach, R.K., Bezusko, K., Foote, M., Fursich, F.T., Hansen, T.A., Holland, S.M., Ivany, L.C., Jablonski, D., Jacobs, D.K., Jones, D.C., Kosnik, M.A., Lidgard, S., Low, S., Miller, A.I., Novack-Gottshall, P.M., Olszewski, T.D., Patzkowsky, M.E., Raup, D.M., Roy, K., Sepkoski, J.J., Sommers, M.G., Wagner, P.J., Webber, A., 2001. Effects of sampling standardization on estimates of Phanerozoic marine diversification. Proceedings of the National Academy of Sciences 98, 6261–6266.

Atwater, T., Stock, J., 1998. Pacific-North America Plate Tectonics of the Neogene Southwestern United States: An Update. International Geology Review 40, 375–402.

Badgley, C., 2010. Tectonics, topography, and mammalian diversity. Ecography 33, 220–231.

Badgley, C., Downs, W., Flynn, L.J., 1998. Taphonomy of small-mammal fossil assemblages from the middle Miocene Chinji formation, Siwalik group, Pakistan. National Science Museum monographs 14, 145–166.

Badgley, C., Fox, D.L., 2000. Ecological biogeography of North American mammals: species density and ecological structure in relation to environmental gradients. Journal of Biogeography 27, 1437–1467.

Badgley, C., Finarelli, J.A., 2013. Diversity dynamics of mammals in relation to tectonic and climatic history: comparison of three Neogene records from North America. Paleobiology 39, 373–399.

Badgley, C., Smiley, T.M., Finarelli, J.A., 2014. Great Basin mammal diversity in relation to landscape history. Journal of Mammalogy 95, 1090–1106.

Badgley, C., Smiley, T.M., Loughney, K., 2015. Miocene mammal diversity of the Mojave region in the context of Great Basin mammal history, in: Mojave Miocene, Desert Symposium Field Guide and Proceedings, pp. 34–43.

Barnosky, A.D., 2001. Distinguishing the effects of the Red Queen and Court Jester on Miocene mammal evolution in the northern Rocky Mountains. Journal of Vertebrate Paleontology 21, 172–185.

Barnosky, A.D., Carrasco, M.A., 2002. Effects of Oligo-Miocene global climate changes on mammalian species richness in the northwestern quarter of the USA. Evolutionary Ecology Research 4, 811–841.

Barnosky, A.D., Bibi, F., Hopkins, S.S.B., Nichols, R., 2007. Biostratigraphy and magnetostratigraphy of the mid-Miocene Railroad Canyon Sequence, Montana and Idaho, and age of the mid-Tertiary unconformity west of the continental divide. Journal of Vertebrate Paleontology 27, 204–224.

Barthlott, W., Mutke, J., Rafiqpoor, D., Kier, G., Kreft, H., 2005. Global centers of vascular plant diversity. Nova Acta Leopoldina NF 92, 61–83.

Baumiller, T.K., 1993. Survivorship analysis of Paleozoic Crinoidea - Effect of filter morphology on evolutionary rates. Paleobiology 19, 304–321.

Blois, J.L., Hadly, E.A., 2009. Mammalian response to cenozoic climatic change. Annual Reviews in Earth and Planetary Sciences 37, 181–208.

Carrasco, M.A., Barnosky, A.D., Kraatz, B.P., Davis, E.B., 2007. The Miocene Mammal Mapping Project (MIOMAP): An online database of Arikareean through Hemphillian fossil mammals. Bulletin of Carnegie Museum of Natural History 1–5.

Clark, M.K., 2007. The significance of paleotopography. Reviews in Mineralogy and Geochemistry 66, 1–21.

Coblentz, D.D., Riitters, K.H., 2004. Topographic controls on the regional-scale biodiversity of the south-western USA. Journal of Biogeography 31, 1125–1138.

Connolly, S.R., Miller, A.I., 2001. Joint estimation of sampling and turnover rates from fossil databases: capture-mark-recapture methods revisited. Paleobiology 27, 751–767.

Cracraft, J., 1985. Biological diversification and its causes. Annals of the Missouri Botanical Garden, 794–822.

Davis, E.B., 2005. Mammalian beta diversity in the Great Basin, western USA: palaeontological data suggest deep origin of modern macroecological structure. Global Ecology and Biogeography 14, 479–490.

DeSantis, L.R.G., Beavins Tracy, R.A., Koontz, C.S., Roseberry, J.C., Velasco, M.C., 2012. Mammalian niche conservation through deep time. PLoS ONE 7, e35624.

Dickinson, W.R., 2006. Geotectonic evolution of the Great Basin. Geosphere 2, 353.

Eronen, J.T., Janis, C.M., Chamberlain, C.P., Mulch, A., 2015. Mountain uplift explains differences in Palaeogene patterns of mammalian evolution and extinction between North America and Europe. Proceedings of the Royal Society-B 282, 20150136.

Fabre, P.-H., Hautier, L., Dimitrov, D., Douzery, E.J.P., 2012. A glimpse on the pattern of rodent diversification: a phylogenetic approach. Bmc Evolutionary Biology 12, 88.

Finarelli, J.A., Badgley, C., 2010. Diversity dynamics of Miocene mammals in relation to the history of tectonism and climate. Proceedings of the Royal Society B: Biological Sciences 277, 2721–2726.

FitzJohn, R.G., 2012. Diversitree: comparative phylogenetic analyses of diversification in R. Methods in Ecology and Evolution 3, 1084–1092.

Foote, M., 1997. Estimating taxonomic durations and preservation probability. Paleobiology 23, 278–300.

Foote, M., 2000. Origination and extinction components of taxonomic diversity: general problems. Paleobiology 26, 74–102.

Foote, M., Raup, D.M., 1996. Fossil preservation and the stratigraphic ranges of taxa. Paleobiology 22, 121–140.

Foote, M., Hunter, J.P., Janis, C.M., Sepkoski, J.J., 1999. Evolutionary and preservational constraints on origins of biologic groups: divergence times of eutherian mammals. Science 283, 1310–1314.

Fritz, S.A., Schnitzler, J., Eronen, J.T., Hof, C., Böhning-Gaese, K., Graham, C.H., 2013. Diversity in time and space: wanted dead and alive. Trends in Ecology & Evolution 28, 509–516.

Goldberg, E.E., Lancaster, L.T., Ree, R.H., 2011. Phylogenetic inference of reciprocal effects between geographic range evolution and diversification. Systematic Biology 60, 451–465.

Hafner, J.C., Light, J.E., Hafner, D.J., Hafner, M.S., Reddington, E., Rogers, D.S., Riddle, B.R., 2007. Basal clades and molecular systematics of heteromyid rodents. Journal of Mammalogy 88, 1129–1145.

Hibbard, C.W., 1941. New mammals from the Rexroad fauna, upper Pliocene of Kansas. American Midland Naturalist 26, 337–368.

Holland, S.M., 2016. The non-uniformity of fossil preservation. Philosophical Transactions of the Royal Society B 371, 20150130.

Hoorn, C., Wesselingh, F.P., ter Steege, H., Bermudez, M.A., Mora, A., Sevink, J., Sanmartin, I., Sanchez-Meseguer, A., Anderson, C.L., Figueiredo, J.P., Jaramillo, C., Riff, D., Negri, F.R., Hooghiemstra, H., Lundberg, J., Stadler, T., Sarkinen, T., Antonelli, A., 2010. Amazonia through time: Andean uplift, climate change, landscape evolution, and biodiversity. Science 330, 927–931.

Horton, T.W., Sjostrom, D.J., Abruzzese, M.J., Poage, M.A., Waldbauer, J.R., Hren, M., Wooden, J., Chamberlain, C.P., 2004. Spatial and temporal variation of Cenozoic surface elevation in the Great Basin and Sierra Nevada. American Journal of Science 304, 862–888.

Horton, T.W., Chamberlain, C.P., 2006. Stable isotopic evidence for Neogene surface downdrop in the central Basin and Range Province. Geological Society of America Bulletin 118, 475–490.

Jablonski, D., Roy, K., Valentine, J.W., 2006. Out of the tropics: evolutionary dynamics of the latitudinal diversity gradient. Science 314, 102–106.

Kendall, D.G., 1948. On the generalized "birth-and-death" process. The Annals of Mathematical Statistics 1–15.

Kidwell, S.M., Holland, S.M., 2002. The quality of the fossil record: implications for evolutionary analyses. Annual Review Ecology and Systematics 33, 561–588.

Kohn, M.J., Fremd, T.J., 2008. Miocene tectonics and climate forcing of biodiversity, western United States. Geology 36, 783–786.

Lindsay, E.H., 1972. Small mammal fossils from the Barstow Formation. California. University of California Publications in Geological Sciences, 93, 1–104.

Liow, L.H., Quental, T.B., Marshall, C.R., 2010. When can decreasing diversification rates be detected with molecular phylogenies and the fossil record? Systematic Biology 59, 646–659.

Maguire, K.C., Stigall, A.L., 2008. Paleobiogeography of Miocene Equinae of North America: a phylogenetic biogeographic analysis of the relative roles of climate, vicariance, and dispersal. Palaeogeography, Palaeoclimatology, Palaeoecology 267, 175–184.

Martin, R.A., Peláez-Campomanes, P., Honey, J.G., Fox, D.L., Zakrzewski, R.J., Albright, L.B., Lindsay, E.H., Opdyke, N.D., Goodwin, H.T., 2008. Rodent community change at the Pliocene–Pleistocene transition in southwestern Kansas and identification of the Microtus immigration event on the Central Great Plains. Palaeogeography, Palaeoclimatology, Palaeoecology 267, 196–207.

Matzke, N.J., 2013. BioGeoBEARS: biogeography with Bayesian (and likelihood) evolutionary analysis in R scripts. R package, version 0.2.

McQuarrie, N., Wernicke, B.P., 2005. An animated tectonic reconstruction of southwestern North America since 36 Ma. Geosphere 1, 147–172.

Mittelbach, G.G., Schemske, D.W., Cornell, H.V., Allen, A.P., Brown, J.M., Bush, M.B., Harrison, S.P., Hurlbert, A.H., Knowlton, N., Lessios, H.A., McCain, C.M., McCune, A.R., McDade, L.A., McPeek, M.A., Near, T.J., Price, T.D., Ricklefs, R.E., Roy, K., Sax, D.F., Schluter, D., Sobel, J.M., Turelli, M., 2007. Evolution and the latitudinal diversity gradient: speciation, extinction and biogeography. Ecology Letters 10, 315–331.

Moen, D., Morlon, H., 2014. Why does diversification slow down? Trends in Ecology & Evolution 29, 190–197.

Morlon, H., Potts, M.D., Plotkin, J.B., 2010. Inferring the dynamics of diversification: a coalescent approach. Plos Biology 8, e1000493.

Mulch, A., 2016. Stable isotope paleoaltimetry and the evolution of landscapes and life. Earth and Planetary Science Letters 433, 180–191.

Paradis, E., Claude J., Strimmer, K. 2004. APE: analyses of phylogenetics and evolution in R language. Bioinformatics 20, 289–290.

Peters, S.E., 2008. Macrostratigraphy and its promise for paleobiology, in: Kelley, P.H., Bambach, R.K. (Eds.), From evolution to geobiology: research questions driving paleontology at the start of a new century. Paleontological Society Papers 14, 205–232.

Peters, S.E., Foote, M., 2001. Biodiversity in the Phanerozoic: a reinterpretation. Paleobiology 27, 583–601.

Peters, S.E., Heim, N.A., 2010. The geological completeness of paleontological sampling in North America. Paleobiology 36, 61–79.

Purvis, A., Orme, C., 2009. Temporal patterns in diversification rates, in: Butlin, R.K., Bridle, J.R., Schuler, D. (Eds.), Speciation and Patterns of Diversity. Cambridge University Press, pp. 278–300.

Quental, T.B., Marshall, C.R., 2010. Diversity dynamics: molecular phylogenies need the fossil record. Trends in Ecology & Evolution 25, 434–441.

Rabosky, D.L., 2009. Extinction rates should not be estimated from molecular phylogenies. Evolution 64, 1816–1824.

Rabosky, D.L., 2013. Diversity-dependence, ecological speciation, and the role of competition in macroevolution. Annual Reviews in Ecology and Evolution and Systematics. 44, 481–502.

Rabosky, D.L., 2014. Automatic detection of key innovations, rate shifts, and diversity-dependence on phylogenetic trees. PLoS ONE 9, e89543.

Rabosky, D.L., Goldberg, E.E., 2015. Model inadequacy and mistaken inferences of trait-dependent speciation. Systematic Biology 64, 340–355.

Rabosky, D.L., Hurlbert, A.H., 2015. Species Richness at Continental Scales Is Dominated by Ecological Limits. American Naturalist 185, 572–583.

Raup, D.M., 1975. Taxonomic diversity estimation using rarefaction. Paleobiology 1, 333–342.

Raup, D.M., 1978. Cohort analysis of generic survivorship. Paleobiology 4, 1–15.

Raup, D.M., 1979. Biases in the fossil record of species and genera. Bulletin of the Carnegie Museum of Natural History 13, 85–91.

Renema, W., Bellwood, D.R., Braga, J.C., Bromfield, K., 2008. Hopping hotspots: global shifts in marine biodiversity. Science 321, 654–657.

Revell, L.J., 2012 phytools: an R package for phylogenetic comparative biology (and other things). Methods Ecology and Evolution 3, 217–223.

Ricklefs, R.E., 2007. Estimating diversification rates from phylogenetic information. Trends in Ecology & Evolution 22, 601–610.

Riddle, B.R., 1996. The molecular phylogeographic bridge between deep and shallow history in continental biotas. Trends in Ecology & Evolution 11, 207–211.

Riddle, B.R., Jezkova, T., Hornsby, A.D., Matocq, M.D., 2014. Assembling the modern Great Basin mammal biota: insights from molecular biogeography and the fossil record. Journal of Mammalogy 95, 1107–1127.

Rolland, J., Condamine, F.L., Jiguet, F., Morlon, H., 2014. Faster speciation and reduced extinction in the tropics contribute to the mammalian latitudinal diversity gradient. Plos Biol 12, e1001775.

Rosenzweig, M.L., 1995. Species diversity in space and time. Cambridge University Press.

Ruggiero, A., Hawkins, B.A., 2008. Why do mountains support so many species of birds? Ecography 31, 306–315.

Sepkoski, J.J., Bambach, R.K., Raup, D.M., Valentine, J.W., 1981. Phanerozoic marine diversity and the fossil record. Nature 293, 435–437.

Silvestro, D., Schnitzler, J., Liow, L.H., Antonelli, A., Salamin, N., 2014a. Bayesian estimation of speciation and extinction from incomplete fossil occurrence data. Systematic Biology 63, 349–367.

Silvestro, D., Salamin, N., Schnitzler, J., 2014b. PyRate: a new program to estimate speciation and extinction rates from incomplete fossil data. Methods in Ecology and Evolution 5, 1126–1131.

Smith, A.B., Lloyd, G.T., McGowan, A.J., 2012. Phanerozoic marine diversity: rock record modeling provides an independent test of large-scale trends. Proceedings of the Royal Society B: Biological Sciences 279, 4489–4495.

Snow, J.K., Wernicke, B.P., 2000. Cenozoic tectonism, in the Central Basin and Range: magnitude, rate, and distribution of upper crustal strain. American Journal of Science 300, 659–719.

Sonder, L.J., Jones, C.H., 1999. Western United States extension: How the west was widened. Annual Reviews in Earth and Planetary Sciences 27, 417–462.

Stadler, T., 2011. Mammalian phylogeny reveals recent diversification rate shifts. Proceedings of the National Academy of Sciences 108, 6187–6192.

Stadler, T., 2011. Simulating trees on a fixed number of extant species. Systematic Biology 60, 676–684.

Stanley, S.M., 1979. Macroevolution: pattern and process. Freeman, San Francisco, California, USA.

Stigall, A.L., Lieberman, B.S., 2006. Quantitative palaeobiogeography: GIS, phylogenetic biogeographical analysis, and conservation insights. Journal of Biogeography 33, 2051–2060.

Terry, R.C., 2010. The dead do not lie: using skeletal remains for rapid assessment of historical small-mammal community baselines. Proceedings of the Royal Society B: Biological Sciences 277, 1193–1201.

Terry, R.C., Li, C.L., Hadly, E.A., 2011. Predicting small-mammal responses to climatic warming: autecology, geographic range, and the Holocene fossil record. Global Change Biology 17, 3019–3034.

Van Dam, M.H., Matzke, N.J., 2016. Evaluating the influence of connectivity and distance on biogeographical patterns in the south-western deserts of North America. Journal of Biogeography, online view.

Vrba, E.S., 1992. Mammals as a key to evolutionary theory. Journal of Mammalogy 73, 1–28.

Weir, J.T., Schluter, D., 2007. The latitudinal gradient in recent speciation and extinction rates of birds and mammals. Science 315, 1574–1576.

Wilson, D.E., Reeder, D.M., (Eds.) 2005. Mammal species of the world: a taxonomic and geographic reference (Third Ed.). Johns Hopkins University Press, Baltimore, Maryland, USA.

Zachos, J.C., Dickens, G.R., Zeebe, R.E., 2008. An early Cenozoic perspective on greenhouse warming and carbon-cycle dynamics. Nature 451, 279–283.

Zelditch, M.L., Li, J., Tran, L.A.P., Swiderski, D.L., 2015. Relationships of diversity, disparity, and their evolutionary rates in squirrels (Sciuridae). Evolution 69, 1284–1300.

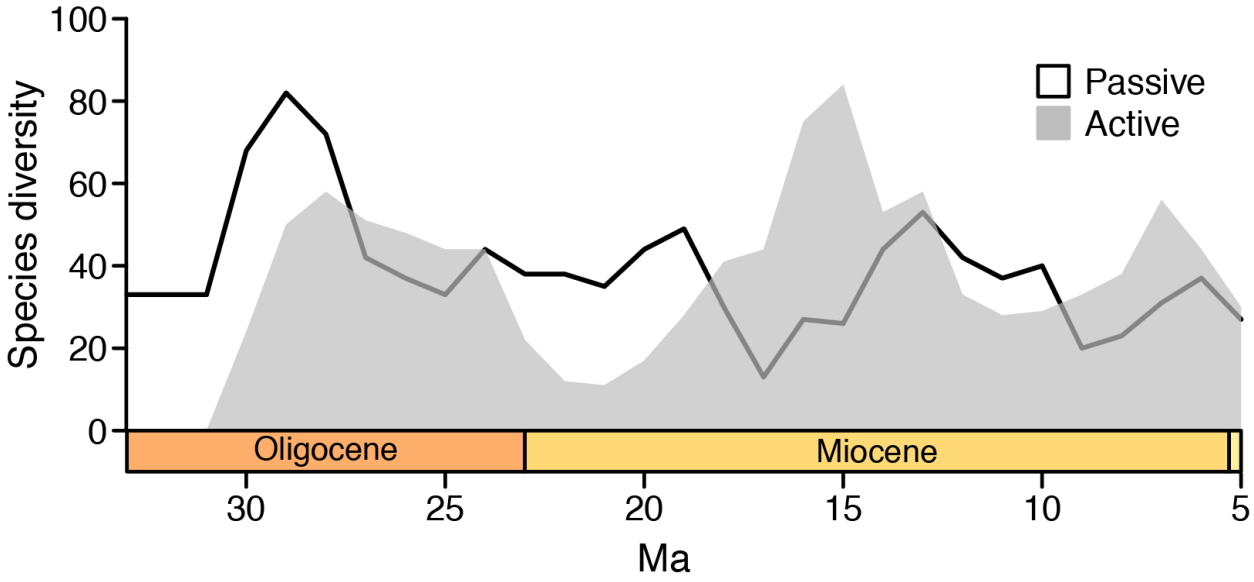

Figure 5.1 Rodent species diversity through time for 1-myr time bins for the Active Region (west of the Rocky Mountain Front Range) in transparent gray and for the Passive Region (Great Plains and east) outlined in black. Peak mammal diversity for the Active Region coincided with intense tectonic extension and global warming during the middle Miocene. The Passive Region did not show a corresponding peak during that interval. Both records were dynamic through time, and the TDG was only intermittently present. Species diversity was calculated assuming that species ranged through first and last occurrences within a region and using the methods of Finarelli and Badgley (2010). Fossil-occurrence data were obtained from the MIOMAP database for North American fossil mammals (Carrasco et al. 2007).

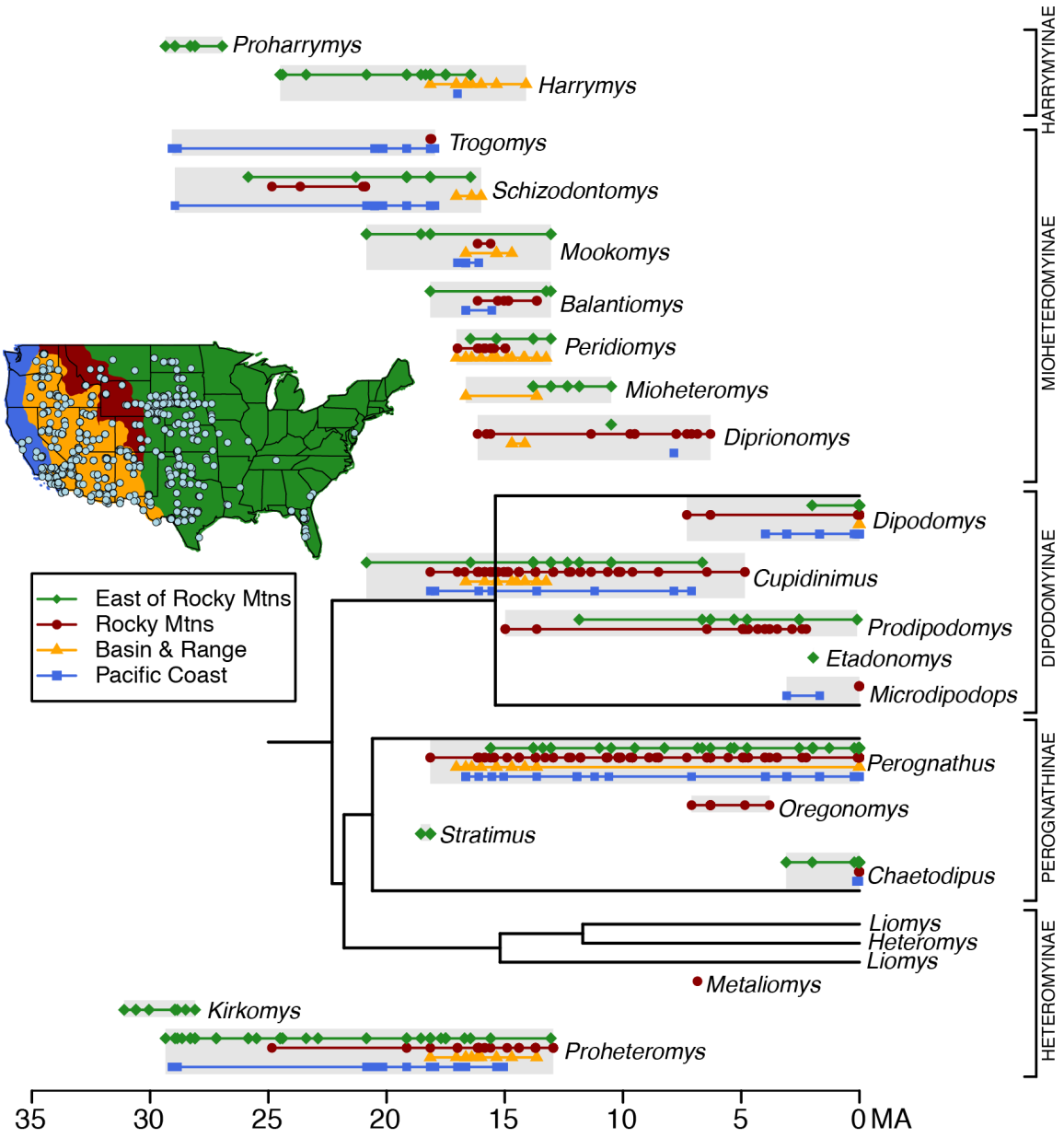

Figure 5.2 The geographic and temporal distribution of heteromyid lineages from the North American fossil record (data extracted from MIOMAP; Carrasco et al. 2007). The black lines represent a time-calibrated molecular phylogeny of extant genera (Hafner et al. 2007). Extinct heteromyid genera and families were placed onto and adjacent to this phylogenetic scaffolding. Gray bars represent the temporal duration of lineages across all regions of North America, while color lines indicate temporal durations of genera across four major tectonic provinces. Color symbols along these lines refer to fossil occurrences within each genus, and pale blue circles in the accompanying map demonstrate the geographic distribution of fossil occurrences. In the figure and map inset, green refers to the 'Passive Region' east of the Rocky Mountains and includes the extensive fossil record from the Great Plains. The 'Active Regions' are as follows: red corresponds with the Rocky Mountain province, yellow corresponds with the Basin and Range extensional tectonic province, and blue corresponds with the Pacific Coast province.

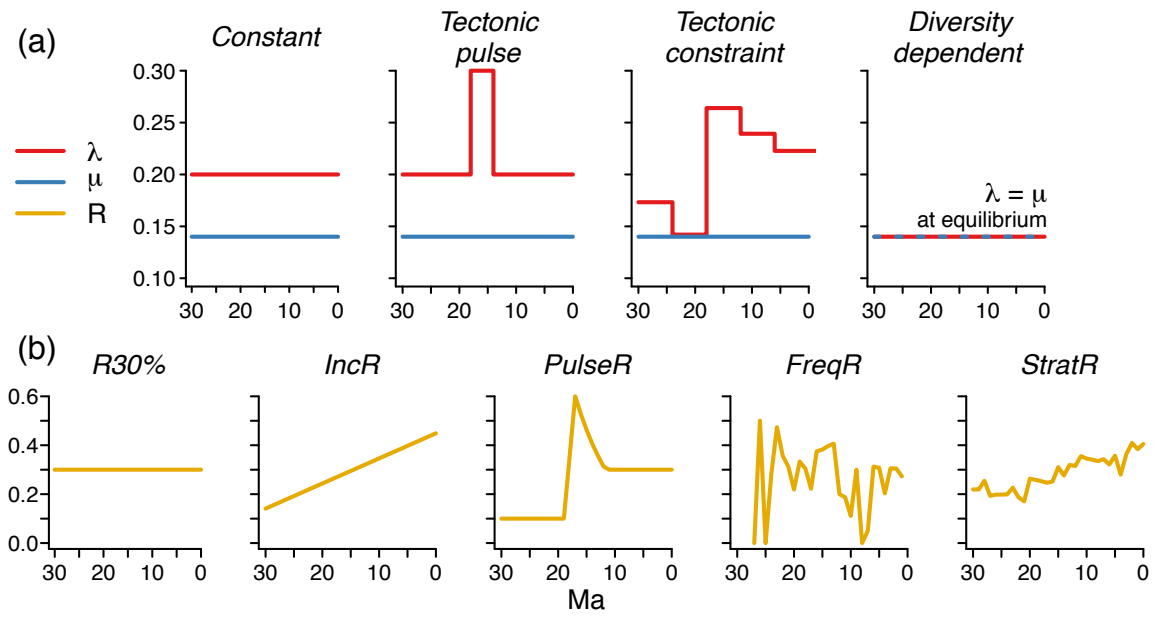

Figure 5.3 (a) Theoretically plausible diversification models for generating the topographic diversity gradient. The *Constant* model refers to time-invariant but elevated speciation rate, λ, through the Neogene. The *Tectonic-pulse* model simulated a single interval of elevated speciation rates in relation to intense block-faulting and tectonic activity in the Basin and Range province from 18 to14 Ma, while the *Tectonic-constraint* model utilized the area change over 6-myr intervals in the Basin and Range province to derive a variable speciation rate curve through time. Each of these three models results in exponentially increasing diversity patterns through time. In contrast, the *Diversity-dependent* model experiences logistic growth through time, and speciation and extinction rates are equal once the species carrying capacity is reached. Diversification analyses were carrying out during this equilibrium phase, in which species richness does not change (unless due to preservation). (b) Each diversification model was degraded according to five preservation scenarios to simulate the imperfect fossil record. Constant, low preservation probability (R30%), increasing preservation probability (IncR), and pulsed preservation probability related to tectonically-driven basin development (PulseR) are hypothetical preservation scenarios. FreqR refers to preservation probability derived from fossil rodent occurrences and StratR refers to preservation probability based on the area of the rock record in the active region extracted from the Macrostrat database (Peters 2008).

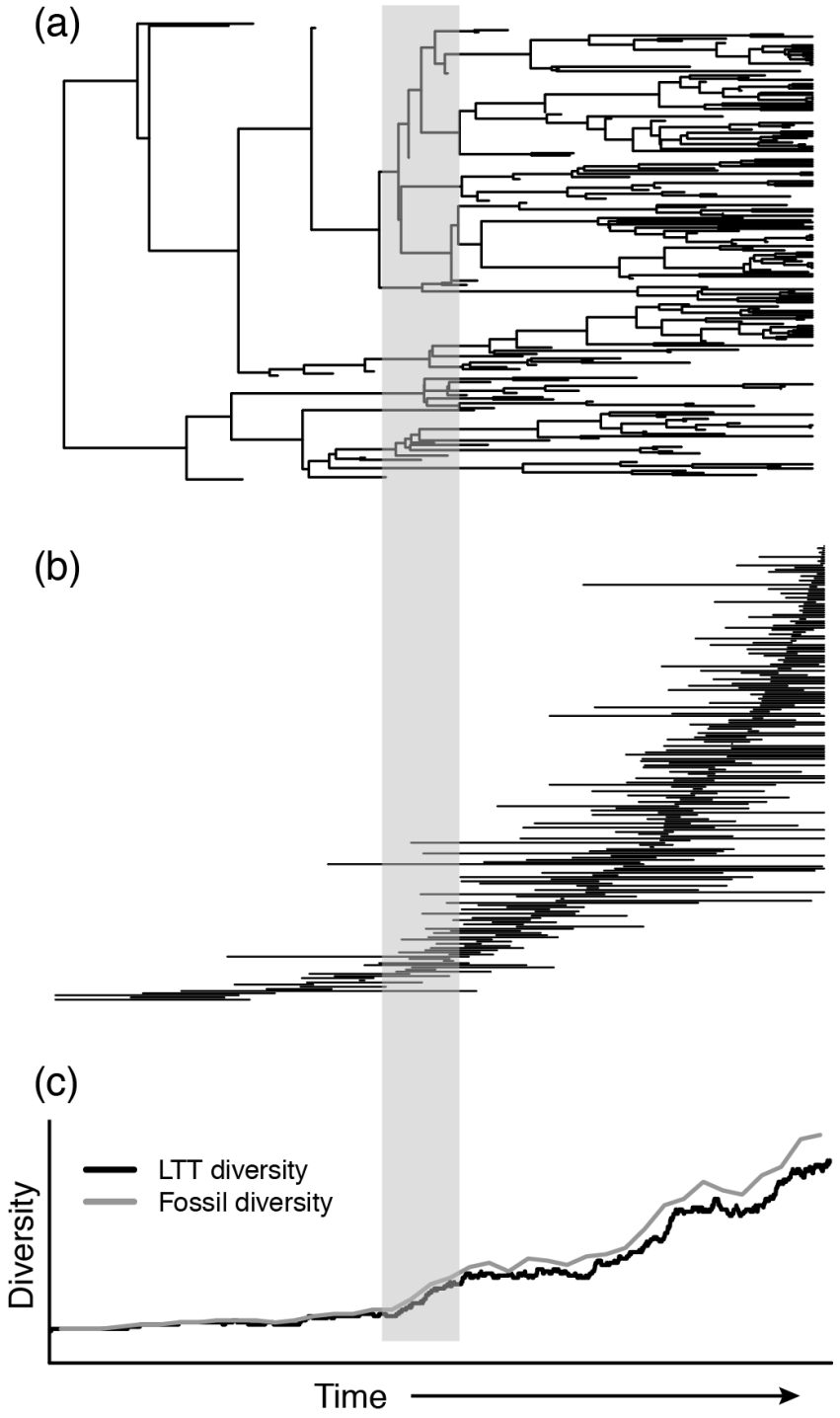

Figure 5.4 (a) Exemplar phylogeny, including extinct species, generated under the *Tectonic-pulse* diversification model. The gray bar indicates the interval of elevated speciation rates. (b) The temporal duration of each lineage was extracted from the phylogeny to produce a simulated fossil record. (c) Diversity from the fossil record was compiled in 1-myr temporal bins and with full preservation (gray curve) tracks lineage-through-time (LTT) diversity generated from the molecular phylogeny (black curve).

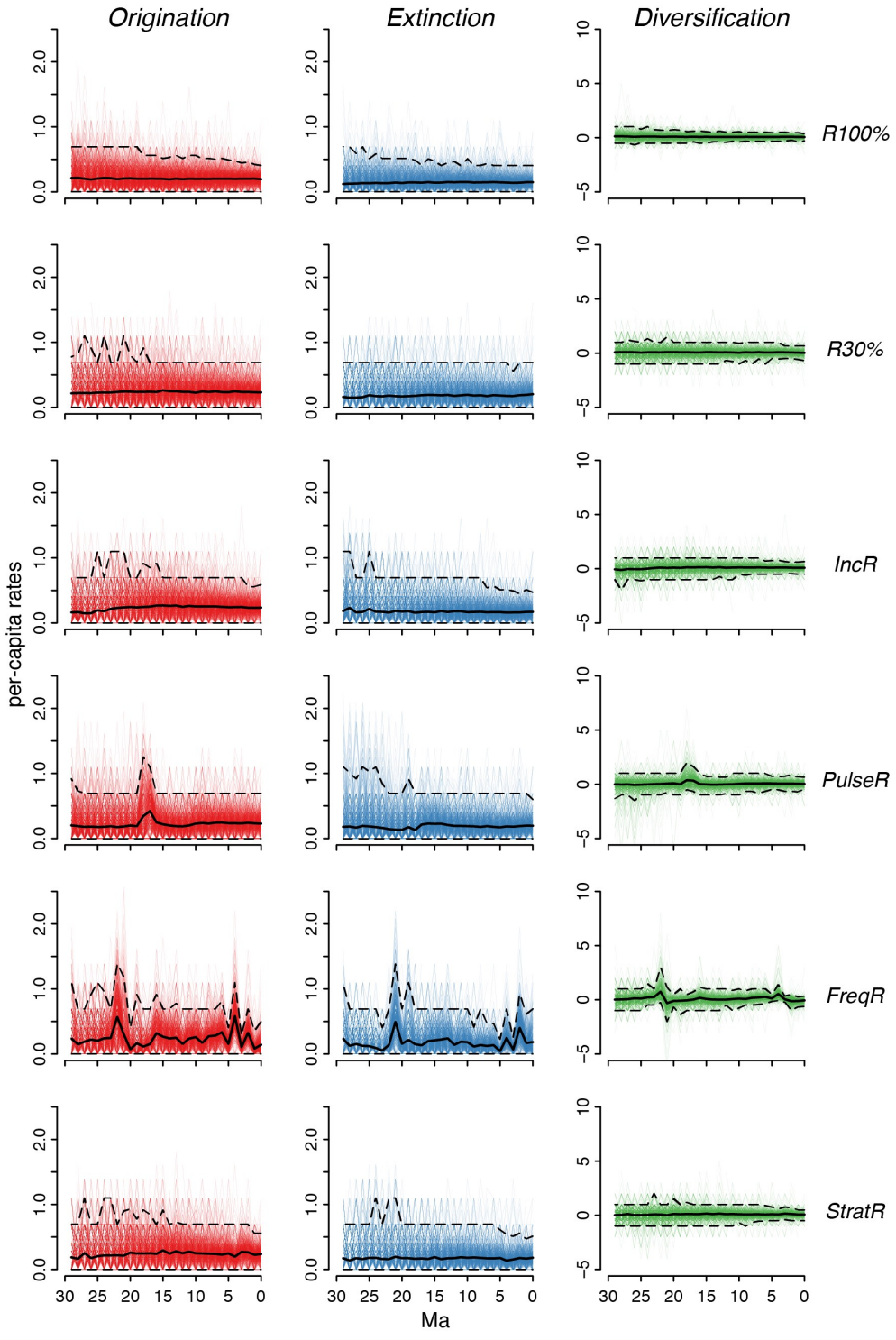

Figure 5.5 Results from 1000 simulated fossil records under the *Constant* diversification model. Per-capita rates of origination, extinction, and diversification per 1-myr time intervals were calculated according to Foote (2000) for the complete fossil record (R100%) and five degraded records. Color lines represent each simulation, while the solid black line represents the mean rate across simulations. Black dashed lines are 95% confidence intervals around the mean.

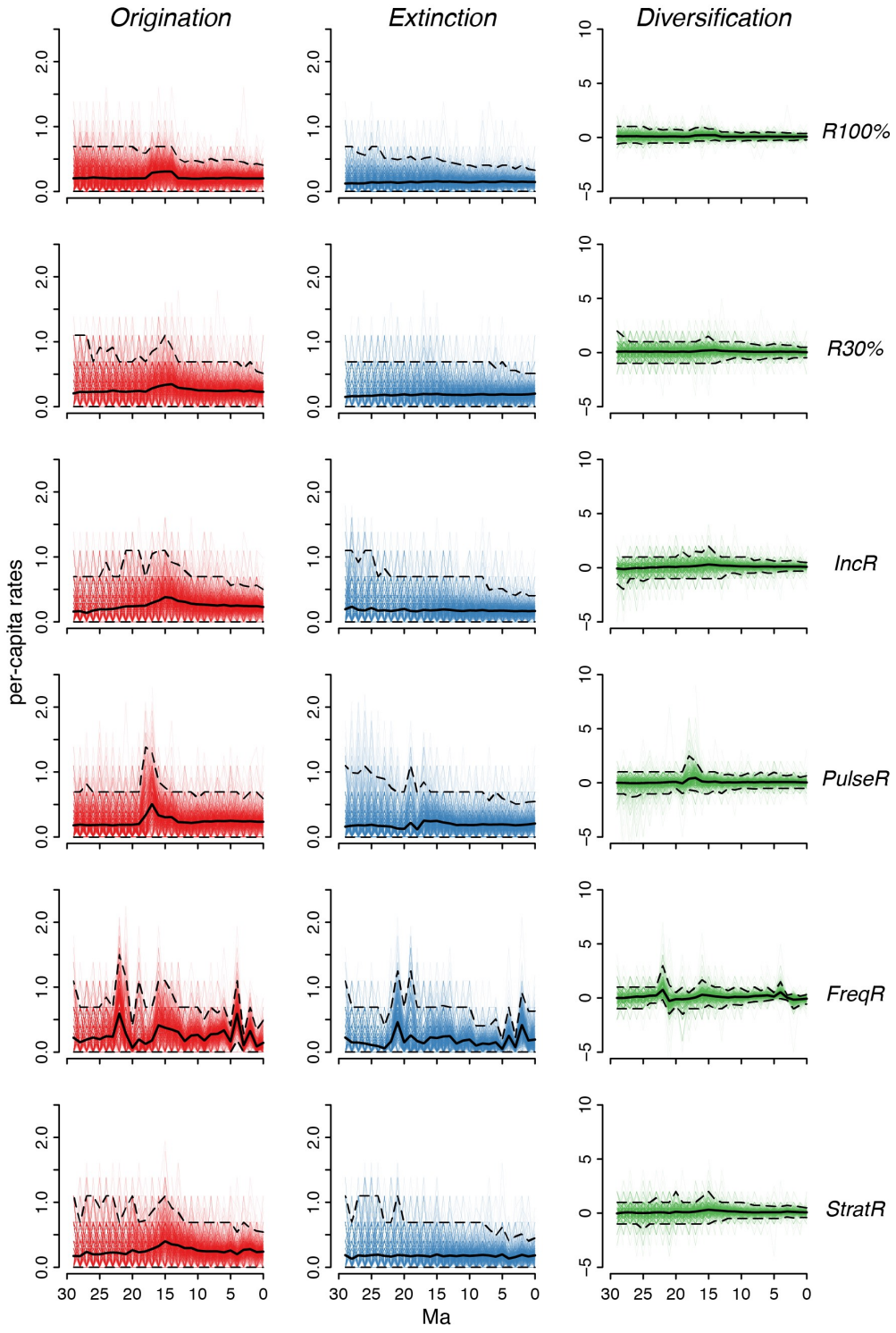

Figure 5.6 Results from 1000 simulated fossil records under the *Tectonic-pulse* diversification model. Per-capita rates of origination, extinction, and diversification per 1-myr time intervals were calculated according to Foote (2000) for the complete fossil record (R100%) and five degraded records. Color lines represent each simulation, while the solid black line represents the mean rate across simulations. Black dashed lines are 95% confidence intervals around the mean.

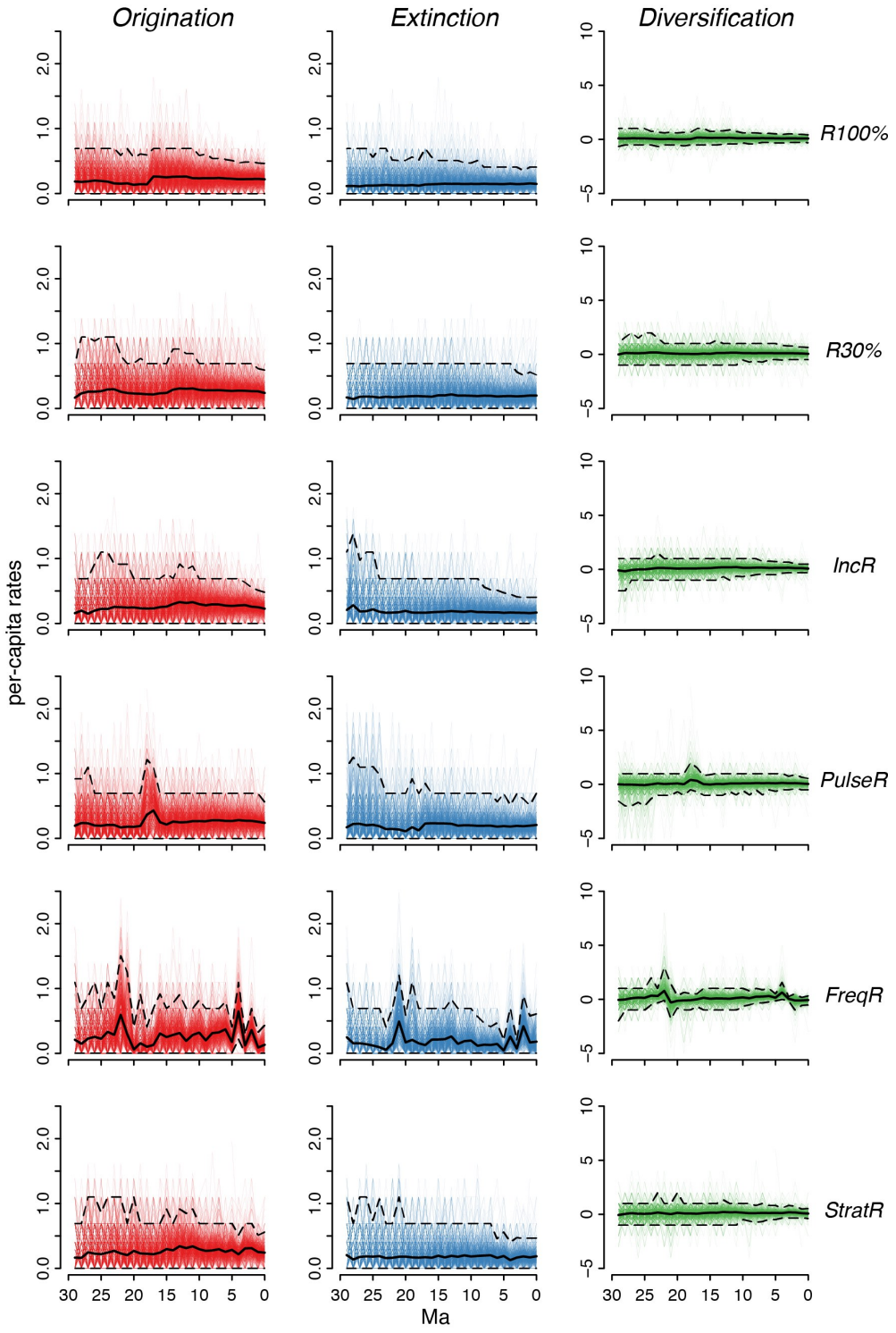

Figure 5.7 Results from 1000 simulated fossil records under the *Tectonic-constraint* diversification model. Per-capita rates of origination, extinction, and diversification per 1-myr time intervals were calculated according to Foote (2000) for the complete fossil record (R100%) and five degraded records. Color lines represent each simulation, while the solid black line represents the mean rate across simulations. Black dashed lines are 95% confidence intervals around the mean.

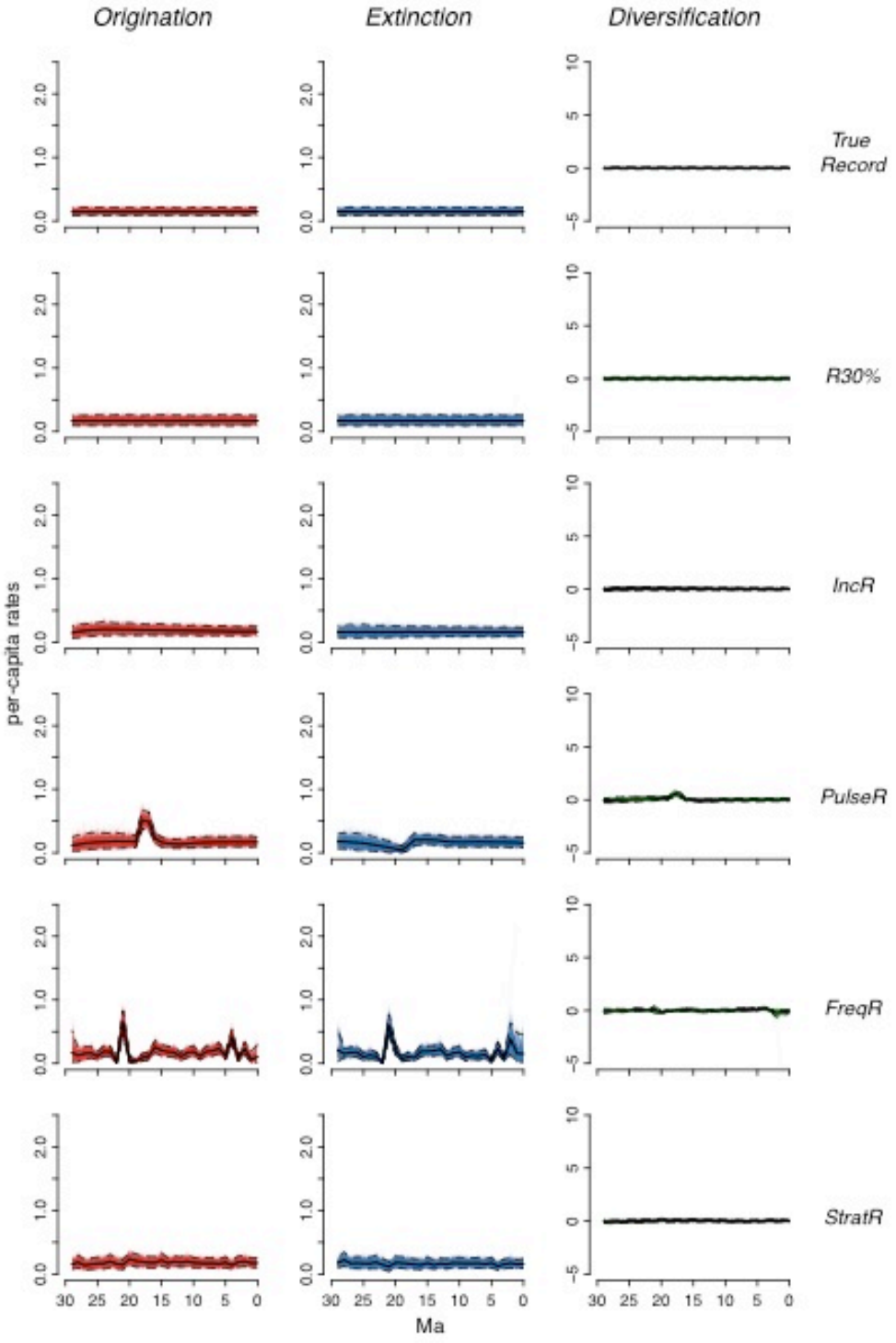

Figure 5.8 Results from 1000 simulated fossil records under the *Diversity-dependent* diversification model. Per-capita rates of origination, extinction, and diversification per 1-myr time intervals were calculated according to Foote (2000) for the complete fossil record (R100%) and five degraded records. Color lines represent each simulation, while the solid black line represents the mean rate across simulations. Black dashed lines are 95% confidence intervals around the mean.

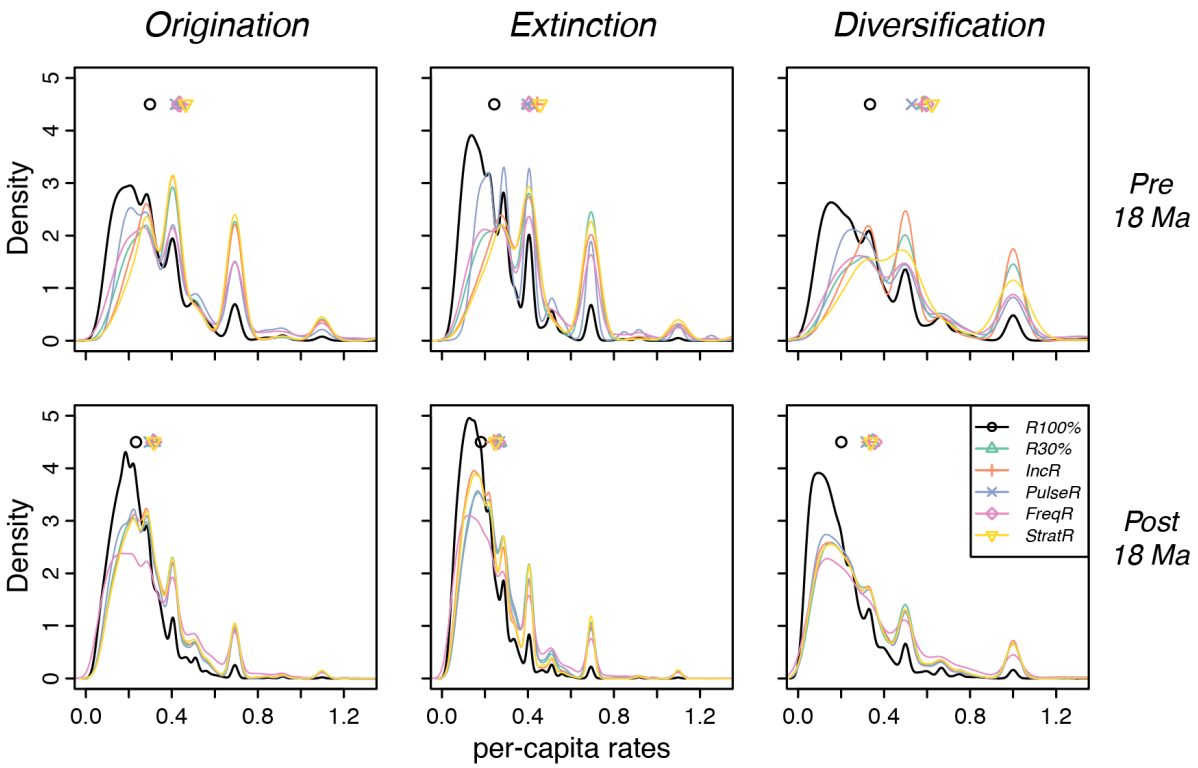

Figure 5.9 Kernel-density plots (lines) and mean rates (symbols) under the *Constant* diversification model. Despite the constant underlying diversification dynamics, the distribution of rates derived from the complete fossil record (black line and circle) and degraded fossil records (color lines and symbols) were evaluated before and after 18 Ma in order to examine differences in confidence intervals at the base of the record compared to younger time intervals.

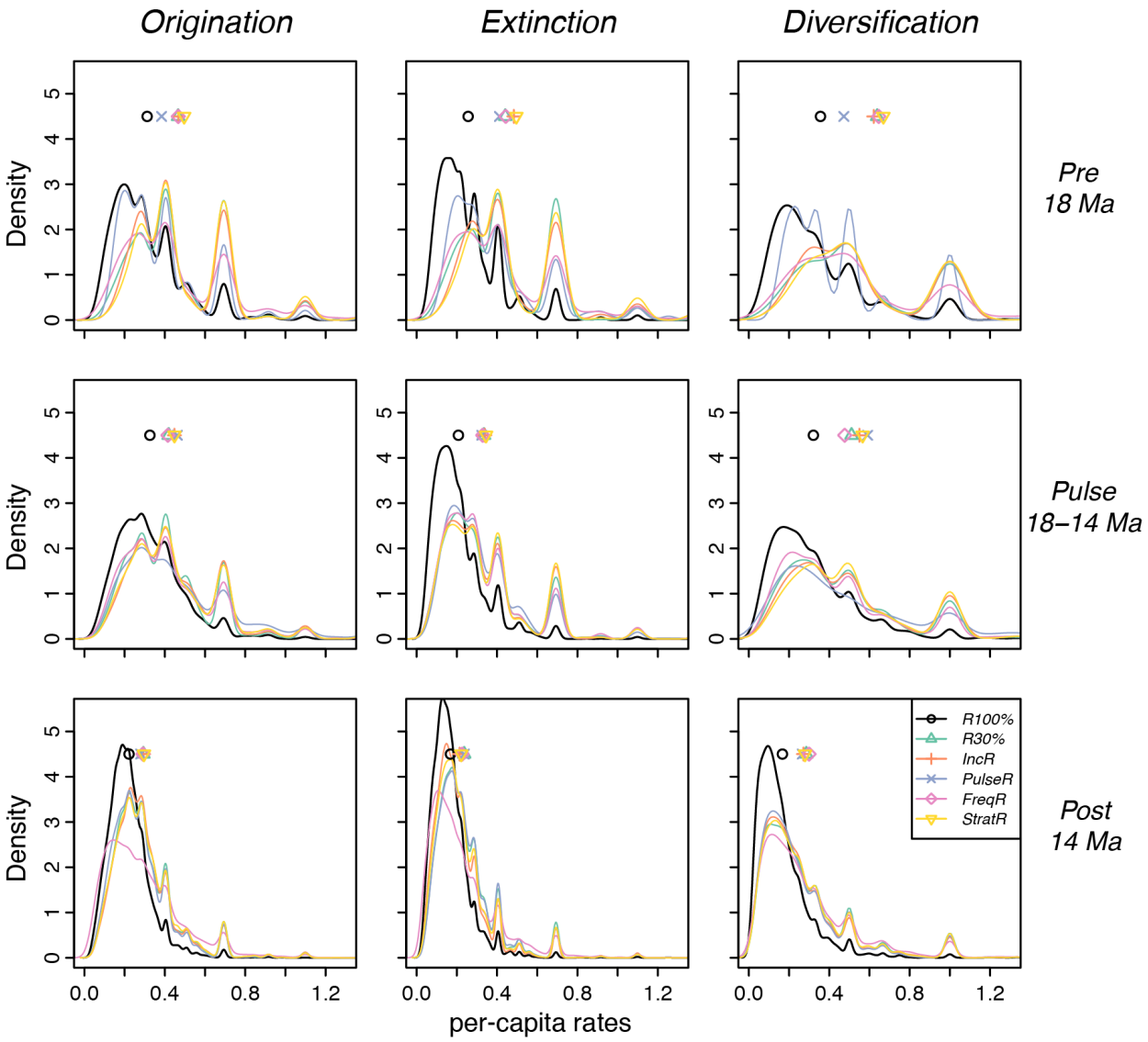

Figure 5.10 Kernel-density plots (lines) and mean rates (symbols) under the *Tectonic-pulse* diversification model. The distribution of rates derived from the complete fossil record (black line and circle) and degraded fossil records (color lines and symbols) were evaluated during three diversification regimes, with an elevated speciation rate in the middle interval from 18 to 14 Ma.

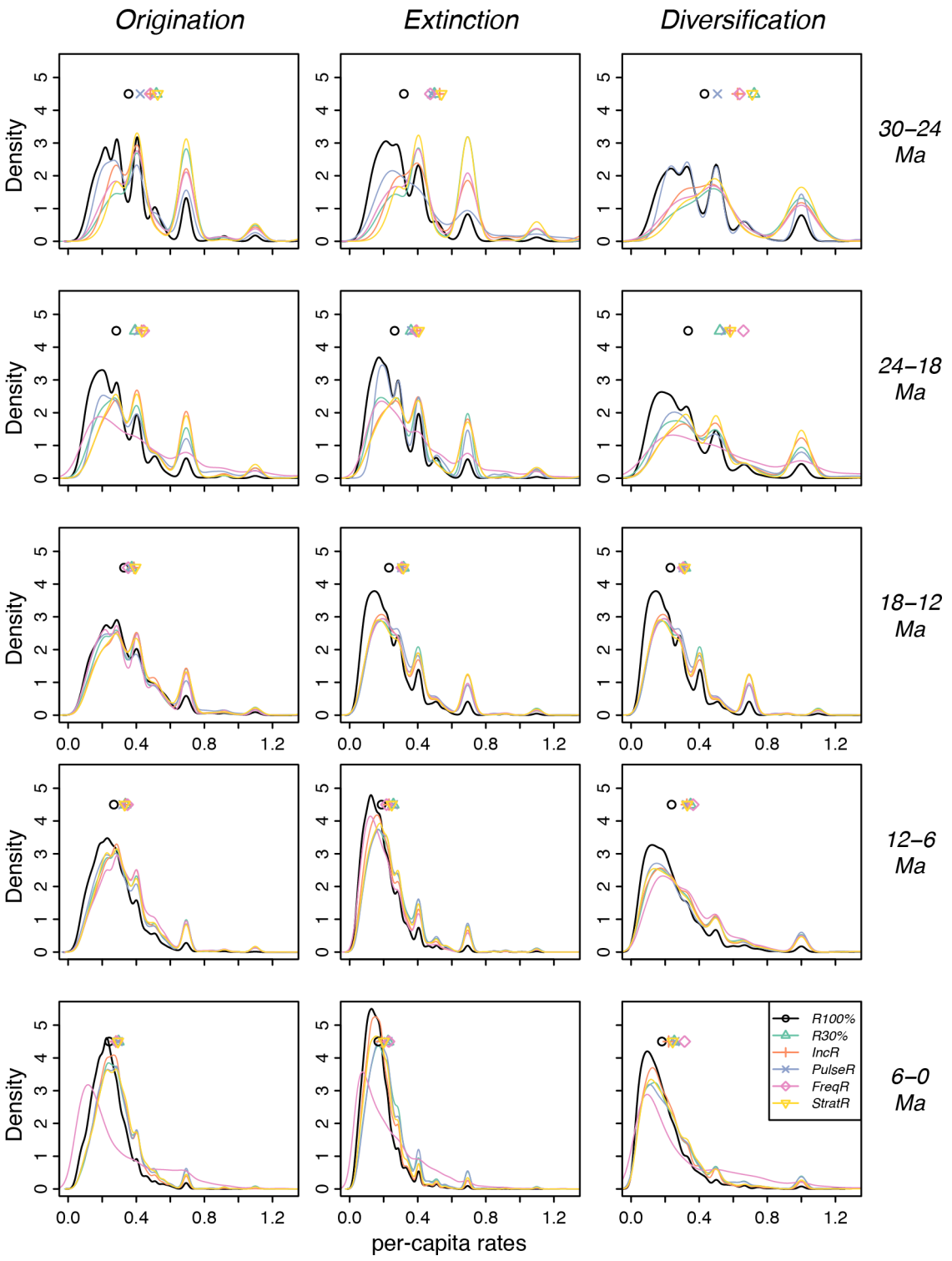

Figure 5.11 Kernel-density plots (lines) and mean rates (symbols) under the *Tectonic-pulse* diversification model. The distribution of rates derived from the complete fossil record (black line and circle) and degraded fossil records (color lines and symbols) were evaluated during five distinct diversification regimes in relation to changes in area during tectonic extension in the Basin and Range province through the Neogene.

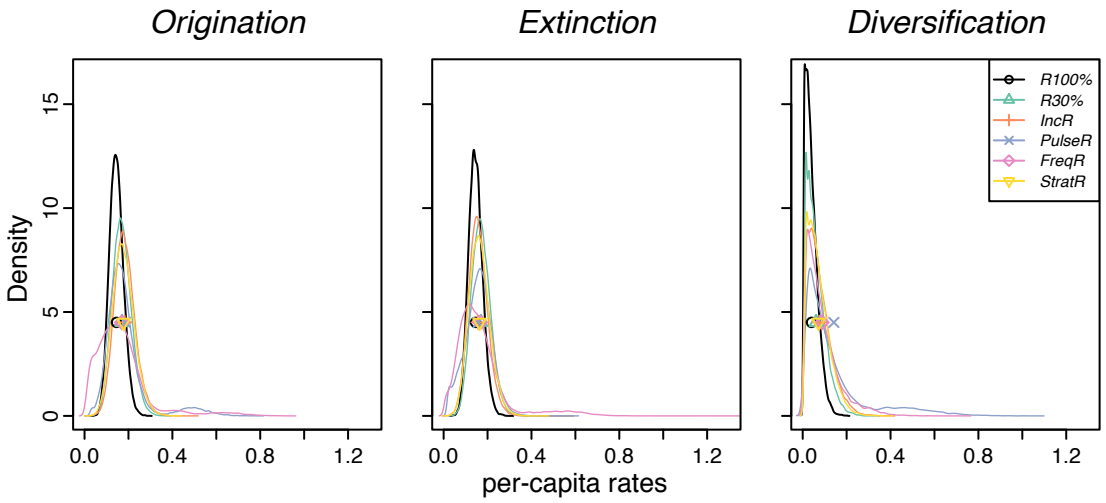

Figure 5.12 Kernel-density plots (lines) and mean rates (symbols) under the *Diversity-dependent* diversification model over 30 million years. The distribution of rates derived from the complete fossil record (black line and circle) is remarkably similar to the distribution of rates recovered from the degraded fossil records (color lines and symbols) throughout the record. Note the change in scale on the y-axis (3x) to accommodate these high levels of congruence in rate estimation under each of the preservation scenarios.

CHAPTER 6

Conclusion

A central question linking geological and biological processes is the influence of landscape history on diversification dynamics and the assembly of regional faunas. The evolution of western North American mammal faunas has a complex history intimately linked with tectonic activity, climate change, and the development of topographically complex and environmentally heterogeneous habitats over the last 30 million years (e.g., Badgley et al. 2014, Riddle et al. 2014). Gradients in mammal diversity in relation to mountains occur from local to continental scales in North America today. Along elevational gradients, strong ecotones influence the distribution of organisms according to their physiological tolerances and habitat preferences (Brown 2001, McCain 2005, Rowe et al. 2015). At broader spatial scales, complex topographic fabric affects climate patterns, influences vegetation composition, and facilitates high regional turnover in species composition (Simpson 1964, Kerr and Packer 1997, Badgley and Fox 2000, Coblentz and Riitter 2004). The history of landscape change, barrier formation, and species dispersal influences the production, accommodation, and extinction of species within the region over geologic time (Cracraft 1985, Hoorn et al. 2010, Badgley 2010). At the continental scale, a striking biodiversity gradient for North American mammals emerges: areas of higher elevation and greater topographic complexity (e.g., Basin and Range Province) have higher species richness than areas of low topographic relief (e.g., Great Plains). This topographic

diversity gradient (TDG) is the outcome of ecological, evolutionary, and biogeographic processes operating over a dynamic landscape and climate history.

Perspectives from the mammal fossil record of North America support the assertion that tectonic activity and corresponding changes in topographic complexity and habitat heterogeneity have promoted speciation, extinction, and high faunal turnover through time (Barnosky and Carrasco 2002, Davis 2005, Kohn and Fremd 2008). However, the record of elevated diversity in topographically complex regions is not a persistent feature over geologic time (Finarelli and Badgley 2010). Peak mammal diversity in western North America and a strong topographic diversity gradient occurred in the middle Miocene (Badgley et al. 2014), during an interval of intense tectonic activity that generated the alternating isolated mountain ranges and basins that characterize the Basin and Range Province today (Dickinson 2006, McQuarrie and Wernicke 2005). While barrier formation during this time likely promoted allopatric speciation, concurrent global warming during the Miocene Climatic Optimum (MCO) also likely promoted geographic-range shifts into and across the intermontane western region, increasing regional diversity and influencing faunal composition across spatial scales. Conclusions from this dissertation shed light on how interactions between tectonic and climate change during the MCO influenced species richness and ecology from local to regional scales.

The call for a conceptual framework linking local ecological processes with regional diversification processes requires a synthetic approach that integrates data from the fossil and extant records (Ricklefs 1987, Mittelbach and Schmenske 2015). The rich Cenozoic fossil record of mammalian faunas in North America presents an opportunity to test hypotheses about species responses to abiotic changes over a range of temporal and spatial scales relevant to both the assembly of local communities and the formation of regional species pools (Blois and Hadly

2009, Brewer et al. 2012, Fritz et al. 2013). Differences in the magnitude, direction, and rate of landscape and climate change in the geological record act as naturally occurring 'experiments' in which we can indirectly observe biotic response to different combinations of abiotic drivers through the lens of fossil preservation. The work summarized herein coupled analyses of basin-level environmental change and small-mammal ecological response with regional patterns in small-mammal composition and diversification during the MCO. My work enhances our understanding of the processes underpinning the TDG in deep time, and in particular demonstrates how elevated diversity during this time is accommodated across spatial scales.

Summary of key findings

Approaches for assessing species ecology in the past have expanded rapidly over the past few decades, including stable isotope analysis and metrics that quantify dental properties and morphological traits in relation to dietary ecology (Passey and Cerling 2006, Eronen et al. 2010, Evans 2013). In particular, small-mammal datasets are increasingly accessible through novel analytical techniques, such as *in situ* laser ablation mass spectrometry and μCT scanning of minute fossil teeth (e.g., Evans et al. 2007, Grimes et al. 2008, Hynek et al. 2012, Kimura et al. 2013). A critical step in applying these tools to the fossil record is understanding how they depict species diets and ecological interactions today. To address whether species ecology varies predictably across climate and vegetation gradients, I sampled the isotopic composition of heteromyids across their geographic distribution to generate rodent diet isoscape models—or 'mice-oscapes'—in relation to climatic and vegetation gradients. Findings described in Chapter 2 demonstrate that small-mammal isotopic composition can be used reliably to infer vegetation, and in particular spatial and temporal heterogeneity in C_3 and C_4 grass resources (Smiley et al.

2015). Furthermore, stable isotopes can distinguish small-mammal dietary ecology, even among closely related herbivorous species, and guide our understanding of differences in resource use that may facilitate species coexistence.

Armed with a framework for applying stable isotope approaches to small-mammal assemblages from the fossil record, I assessed how species ecology—and diversity—responded to basin-scale climate and vegetation changes during the MCO. I focused on the Crowder and Cajon Valley formations in southern California, two of the few fossil records to span this critical interval from 17 to 14 Ma in the Basin and Range Province. In Chapter 3, I first developed a multi-proxy record of paleoenvironmental conditions from each formation, based on paleosol elemental geochemistry, carbon isotopic composition of preserved soil organic matter, and phytolith assemblages (e.g., Hyland et al. 2013, Cotton et al. 2014). Together, these proxies demonstrated that C_4 grasses were a stable but minor component of the local vegetation, that high habitat heterogeneity characterized ecosystems within and across basins, and that aridity and grass composition increased locally during the MCO (Smiley et al. *in review*). Mammal species diversity declined during this aridity shift in the Crowder Formation, and faunal dissimilarity between the two basins was high, suggesting high species turnover across space and over time.

In Chapter 4, I utilized *in situ* laser ablation stable isotopic analysis and dental morphology to assess whether concurrent changes in rodent dietary ecology in the Crowder and Cajon Valley small-mammal faunas were evident. Ecological stability over time characterized faunas within each basin; however, significant isotopic differences between the older Crowder and younger Cajon Valley assemblages indicate a shift in dietary ecology over longer timescales during the MCO. Rodents recorded finer-scale variation in vegetation than did environmental

proxies and documented an increase in C_4-grass consumption despite little apparent change in the availability of this resource on the local landscape. This work also allowed me to gain insight into past ecological interactions and dietary niche partitioning. Contrary to the prediction that ecological niche differentiation should be necessary to support high species diversity within these assemblages, I found significant overlap in both stable isotopic composition and dental morphology among co-occurring species. Interspecific overlap in dietary ecology during the MCO contrasts with rodent communities in present-day western ecosystems, which exhibit substantial interspecific differences in both isotopic composition and dental properties. This work contributes to filling a gap in our knowledge of small-mammal paleoecology and community assembly during past climate and habitat change, specifically during a critical time in the formation of the faunal assemblages that characterize the Basin and Range Province today (Riddle et al. 2014).

While focus on the Mojave region helps to elucidate local-scale dynamics, a gap in the fossil record prior to the MCO over much of western North America, including southern California, limits our ability to evaluate regional changes in diversity over longer timescales. In particular, the early rise in species richness during the onset of intense tectonic extension may co-vary with preservation probability (e.g., Badgley et al. 2015). For these reasons, my final research chapter utilized simulations to examine how changes in preservation probability impact our ability to reliably infer diversification dynamics over the Neogene (e.g., Foote 2000, Liow et al. 2010). I developed three diversification hypotheses for increasing species richness in relation to tectonic activity and increased topographic complexity during the middle Miocene, and tested the fidelity of simulated, degraded fossil records across a range of preservation scenarios. Despite variable preservation, most degraded records were able to recover the underlying

diversification dynamics, indicating that elevated diversification rates in relation to tectonic activity during the middle Miocene are likely to be evident in the fossil record. Expections to this general finding include intervals when preservation rate changes substantially (e.g., from 10% to 50% between consecutive 1-myr time bins), which may impart a temporary, false signal of elevated speciation or extinction rates. In these cases, estimated diversification rates are more reliable indicators of underlying dynamics than independent estimates of speciation or extinction.

Tectonic and climate drivers of small-mammal diversity during the MCO

A major motivation of my dissertation research has been to increase understanding of the ecological, evolutionary, and biogeographic processes that operate across spatial scales and in relation to landscape and climate change to ultimately generate the middle Miocene peak in mammal species richness. The Mojave region, in particular, stands out in the tectonically active and topographically complex Basin and Range Province for its long, continuous, and fossil-rich record through the MCO. Dissertation research focused on this region, and specifically small-mammal faunas from the Crowder and Cajon Valley formations, has enabled me to elucidate local-scale processes that contributed to the regional diversity peak and influenced species richness and paleoecological response to warming and landscape change during the middle Miocene. Comparisons between local- and regional-scale diversity, as evaluated by alpha, beta and gamma diversity measures, have shed light on historical and geographic processes influencing diversification, immigration, and ecological diversity of species in the Mojave and across the Basin and Range Province (Badgley et al. 2014, Badgley et al. 2015, Smiley and Badgley 2015).

The Crowder and Cajon Valley assemblages record high alpha-diversity (e.g., up to seven co-occurring, ecologically similar rodent species). The highest species richness in the Crowder and Cajon Valley formations occurred at ~17–16 Ma, indicating that local-scale diversity contributed to the MCO diversity peak. These ecosystems—prior to regional aridification and grassland expansion—could have supported higher species diversity with less ecological divergence than in present-day western ecosystems due to increased productivity or greater habitat heterogeneity during the globally warm and regionally mesic middle Miocene interval. Global climate cooled rapidly following the MCO (Zachos et al. 2008) and a corresponding decline in species richness is documented regionally (Finarelli and Badgley 2010). Local records from the Mojave region record a hint of this decline in small-mammal diversity in response to increased aridity and grass composition. Likewise, substantial faunal turnover across stratigraphic levels within the Crowder and Cajon Valley basins (Smiley et al. *in review*) reflects the dynamic record of faunal turnover (e.g., Badgley et al. 2014) and short species durations recorded at broader spatial scales during the MCO (e.g., Figure 5.2).

Expanding the spatial scope of my analysis, I found that mammalian assemblages in the Crowder and Cajon Valley formations exhibited notably low faunal similarity despite geographic proximity. The nearby Barstow Formation represents an important and roughly contemporaneous fossil record in the Mojave Region, and also shared few mammal species, large or small, with either the Crowder or the Cajon Valley formations (Smiley et al. *in review*). Low faunal similarity from 17 to 13 Ma at the scale of the Mojave supports the idea that elevated species richness during the MCO also resulted from pronounced spatial turnover in species composition, or high beta-diversity. Faunal exchange across alternating basins and ranges, even within a single

region, may have been reduced during the tumultuous history of tectonic activity and landscape change during this time, leading to high faunal provinciality in western North America.

Studies beyond this dissertation, conducted by myself and others, have evaluated diversity patterns and faunal similarity at even broader spatial scales—over subregions of the Basin and Range Province, including records from Nevada, Oregon, Idaho, and Utah—finding that diversity increased simultaneously within subregions during the MCO (Badgley et al. 2015). Whether the source of new species in these regions was primarily *in situ* speciation or immigration remains unresolved. Thus far, both processes are evident (Badgley et al. 2015, Smiley and Badgley 2015). Faunal similarity was low during the MCO compared to equivalently scaled comparisons of modern faunas. However, increased similarity across Basin and Range subregions and among formations within the Mojave, including the Crowder, Cajon Valley, and Barstow formations, during the MCO compared to the subsequent cooling interval suggests that geographic-range shifts contributed to the peak in species richness. Additionally, these studies found higher species similarity between formations within the Mojave than between subregions and greater similarity between subregions that are geographically close (Smiley and Badgley 2015). This geographically nested pattern of faunal similarity and high spatial turnover in mammal species composition implies that geographic barriers, environmental heterogeneity, and *in situ* speciation all contributed to elevated mammalian diversity during middle Miocene global warming and tectonic mountain building. Thus, multiple biogeographic processes contribute to the TDG when it is present.

By studying species richness and composition from local to regional scales, this body of work provides insight into the processes shaping the peak in mammal species richness during the MCO and reveals the influence of climate and vegetation change on species ecology. While

sampling effects may also play a role in shaping the Miocene diversity pattern, fossil-record simulations suggest that the species richness peak during the MCO is not due solely to the effects of preservation. From both paleontological and molecular perspectives, the middle Miocene was a critical interval in the assembly of western small-mammal faunas (e.g., Riddle et al. 2014). Understanding the influence of landscape and climate change on local-scale ecological interactions, community assembly, and regional species-pool dynamics remains a critical research goal for illuminating the history of Basin and Range faunas further (Ricklefs 1987, Gilman et al. 2010, Blois et al. 2013, Mittelbach and Schemske 2015).

More research is needed to fully characterize the mechanistic underpinnings of the topographic diversity gradient today and in the past. This work, along with the work of others, strengthens the call to link local and regional biogeographic processes into a single framework in order to better understand the dynamic nature of species diversity in the Basin and Range over the Neogene. These studies also highlight the reciprocal insights achieved from integration of data from fossil and modern records. The fossil record provides our most direct link to ecosystem dynamics during substantial climate and environmental change in the past. And in today's world, information from the past is critically important to strengthening our predictions of how ecosystems are likely to change in the coming centuries (Fritz et al. 2013, Finnegan et al. 2015). This research contributes an important paleoecological perspective on the topographic diversity gradient during the middle Miocene interval of climate warming and landscape transformation.

REFERENCES

Badgley, C., 2010. Tectonics, topography, and mammalian diversity. Ecography 33, 220–231.

Badgley, C., Fox, D.L., 2000. Ecological biogeography of North American mammals: species density and ecological structure in relation to environmental gradients. Journal of Biogeography 27, 1437–1467.

Badgley, C., Smiley, T.M., Finarelli, J.A., 2014. Great Basin mammal diversity in relation to landscape history. Journal of Mammalogy 95, 1090–1106.

Badgley, C., Smiley, T.M., Loughney, K., 2015. Miocene mammal diversity of the Mojave region in the context of Great Basin mammal history, in: Mojave Miocene, Desert Symposium Field Guide and Proceedings, pp. 34–43.

Barnosky, A.D., Carrasco, M.A., 2002. Effects of Oligo-Miocene global climate changes on mammalian species richness in the northwestern quarter of the USA. Evolutionary Ecology Research 4, 811–841.

Blois, J.L., Hadly, E.A., 2009. Mammalian response to Cenozoic climatic change. Annual Review of Earth and Planetary Science 37, 181–208.

Blois, J.L., Zarnetske, P.L., Fitzpatrick, M.C., Finnegan, S., 2013. Climate change and the past, present, and future of biotic interactions. Science 341, 499–504.

Brewer, S., Jackson, S.T., Williams, J.W., 2012. Paleoecoinformatics: applying geohistorical data to ecological questions. Trends in Ecology & Evolution 27, 104–112.

Brown, J.H., 2001. Mammals on mountainsides: elevational patterns of diversity. Global Ecology and Biogeography 10, 101–109.

Coblentz, D.D., Riitters, K.H., 2004. Topographic controls on the regional-scale biodiversity of the south-western USA. Journal of Biogeography 31, 1125–1138.

Cotton, J.M., Hyland, E.G., Sheldon, N.D., 2014. Multi-proxy evidence for tectonic control on the expansion of C_4 grasses in northwest Argentina. Earth and Planetary Science Letters 395, 41–50.

Cracraft, J., 1985. Biological diversification and its causes. Annals of the Missouri Botanical Garden 72, 794–822.

Davis, E.B., 2005. Mammalian beta diversity in the Great Basin, western USA: Palaeontological data suggest deep origin of modern macroecological structure. Global Ecology and Biogeography 14, 479–490.

Dickinson, W.R., 2006. Geotectonic evolution of the Great Basin. Geosphere 2, 353–368.

Eronen, J.T., Polly, P.D., Fred, M., Damuth, J., Frank, D.C., Mosbrugger, V., Scheidegger, C., Stenseth, N.C., Fortelius, M., 2010. Ecometrics: The traits that bind the past and present together. Integrative Zoology 5, 88–101.

Evans, A.R., 2013. Shape descriptors as ecometrics in dental ecology. Hystrix, the Italian Journal of Mammalogy 24, 133–140.

Evans, A.R., Wilson, G.P., Fortelius, M., Jernvall, J., 2007. High-level similarity of dentitions in carnivorans and rodents. Nature 445, 78–81.

Finarelli, J.A., Badgley, C., 2010. Diversity dynamics of Miocene mammals in relation to the history of tectonism and climate. Proceedings of the Royal Society B: Biological Sciences 277, 2721–2726.

Finnegan, S., Anderson, S.C., Harnik, P.G., Simpson, C., 2015. Paleontological baselines for evaluating extinction risk in the modern oceans. Science 348, 567–570.

Foote, M., 2000. Origination and extinction components of taxonomic diversity: general problems. Paleobiology 26, 74–102.

Fritz, S.A., Schnitzler, J., Eronen, J.T., Hof, C., Böhning-Gaese, K., Graham, C.H., 2013. Diversity in time and space: wanted dead and alive. Trends in Ecology & Evolution 28, 509–516.

Gilman, S.E., Urban, M.C., Tewksbury, J., Gilchrist, G.W., Holt, R.D., 2010. A framework for community interactions under climate change. Trends in Ecology & Evolution 25, 325–331.

Grimes, S.T., Collinson, M.E., Hooker, J.J., Mattey, D.P., 2008. Is small beautiful? A review of the advantages and limitations of using small mammal teeth and the direct laser fluorination analysis technique in the isotope reconstruction of past continental climate change. Palaeogeography, Palaeoclimatology, Palaeoecology 266, 39–50.

Hoorn, C., Wesselingh, F.P., ter Steege, H., Bermudez, M.A., Mora, A., Sevink, J., Sanmartin, I., Sanchez-Meseguer, A., Anderson, C.L., Figueiredo, J.P., Jaramillo, C., Riff, D., Negri, F.R., Hooghiemstra, H., Lundberg, J., Stadler, T., Sarkinen, T., Antonelli, A., 2010. Amazonia through time: Andean uplift, climate change, landscape evolution, and biodiversity. Science 330, 927–931.

Hyland, E., Sheldon, N.D., Fan, M., 2013. Terrestrial paleoenvironmental reconstructions indicate transient peak warming during the early Eocene climatic optimum. Geological Society of America Bulletin 125, 1338–1348.

Hynek, S.A., Passey, B.H., Prado, J.L., Brown, F.H., Cerling, T.E., Quade, J., 2012. Small mammal carbon isotope ecology across the Miocene–Pliocene boundary, northwestern Argentina. Earth and Planetary Science Letters 321-322, 177–188.

Kerr, J.T., Packer, L., 1997. Habitat heterogeneity as a determinant of mammal species richness

in high-energy regions. Nature 385, 252–254.

Kimura, Y., Jacobs, L.L., Cerling, T.E., Uno, K.T., Ferguson, K.M., Flynn, L.J., Patnaik, R., 2013. Fossil mice and rats show isotopic evidence of niche partitioning and change in dental ecomorphology related to dietary shift in Late Miocene of Pakistan. PLoS ONE 8, e69308.

Kohn, M.J., Fremd, T.J., 2008. Miocene tectonics and climate forcing of biodiversity, western United States. Geology 36, 783–786.

Liow, L.H., Quental, T.B., Marshall, C.R., 2010. When can decreasing diversification rates be detected with molecular phylogenies and the fossil record? Systematic Biology 59, 646–659.

McCain, C.M., 2005. Elevational gradients in diversity of small mammals. Ecology 86, 366–372.

McQuarrie, N., Wernicke, B.P., 2005. An animated tectonic reconstruction of southwestern North America since 36 Ma. Geosphere 1, 147–172.

Mittelbach, G.G., Schemske, D.W., 2015. Ecological and evolutionary perspectives on community assembly. Trends in Ecology & Evolution 30, 241–247.

Passey, B.H., Cerling, T.E., 2006. In situ stable isotope analysis ($\delta^{13}C$, $\delta^{18}O$) of very small teeth using laser ablation GC/IRMS. Chemical Geology 235, 238–249.

Ricklefs, R.E., 1987. Community diversity: relative roles of local and regional processes. Science 235, 167–171.

Riddle, B.R., Jezkova, T., Hornsby, A.D., Matocq, M.D., 2014. Assembling the modern Great Basin mammal biota: insights from molecular biogeography and the fossil record. Journal of Mammalogy 95, 1107–1127.

Rowe, R.J., Heaney, L.R., Rickart, E.A., 2015. Scale effects on the pattern and predictors of small mammal diversity along a local elevational gradient in the Great Basin. Journal of Biogeography 42, 1964–1974.

Simpson, G. G., 1964. Species density of North American recent mammals. Systematic Zoology 13, 57–73.

Smiley, T. M., Badgley, C., 2015. Patterns of Miocene mammalian diversity across spatial scales in the Great Basin of western North America. Journal of Vertebrate Paleontology, Program and Abstracts.

Smiley, T.M., Cotton, J.M., Badgley, C., Cerling, T.E., 2015. Small-mammal isotope ecology tracks climate and vegetation gradients across western North America. *Oikos* doi: 10.1111/oik.02722.

Smiley, T.M., Hyland, E.G., Cotton, J.M., Reynolds, R.E., *in review*. Early evidence of C_4 grasses, precipitation variability, and faunal response during the Miocene Climatic Optimum in the Mojave region.

Zachos, J.C., Dickens, G.R., Zeebe, R.E., 2008. An early Cenozoic perspective on greenhouse warming and carbon-cycle dynamics. Nature 451, 279–283.